MARTIN MARIETTA ENERGY SYSTEMS LIBRARIES
3 4456 0360703 2

CENTRAL RESEARCH LIBRARY
DOCUMENT COLLECTION
Reference

AEC RESEARCH AND DEVELOPMENT REPORT

ORNL-1729
Progress

DECLASSIFIED
Classification Changed to ... By Authority of ... AEC-1-25-54
By ... 7-11-62

LABORATORY RECORDS
1954

AIRCRAFT NUCLEAR PROPULSION PROJECT

QUARTERLY PROGRESS REPORT

FOR PERIOD ENDING JUNE 10, 1954

CENTRAL RESEARCH LIBRARY
DOCUMENT COLLECTION

LIBRARY LOAN COPY

DO NOT TRANSFER TO ANOTHER PERSON

If you wish someone else to see this document, send in name with document and the library will arrange a loan.

OAK RIDGE NATIONAL LABORATORY
OPERATED BY
CARBIDE AND CARBON CHEMICALS COMPANY
A DIVISION OF UNION CARBIDE AND CARBON CORPORATION
POST OFFICE BOX P
OAK RIDGE, TENNESSEE

[redacted]

ORNL-1729

This document consists of 155 pages.

Copy 95 of 255 copies. Series A.

Contract No. W-7405-eng-26

AIRCRAFT NUCLEAR PROPULSION PROJECT

QUARTERLY PROGRESS REPORT

For Period Ending June 10, 1954

W. H. Jordan, Director
A. J. Miller, Assistant Director
A. W. Savolainen, Editor

DATE ISSUED

JUL 20 1954

OAK RIDGE NATIONAL LABORATORY
Operated by
CARBIDE AND CARBON CHEMICALS COMPANY
A Division of Union Carbide and Carbon Corporation
Post Office Box P
Oak Ridge, Tennessee

[redacted]

MARTIN MARIETTA ENERGY SYSTEMS LIBRARIES

3 4456 0360703 2

INTERNAL DISTRIBUTION

1. G. M. Adamson
2. R. G. Affel
3. C. R. Baldock
4. C. J. Barton
5. E. S. Bettis
6. D. S. Billington
7. F. F. Blankenship
8. E. P. Blizard
9. M. A. Bredig
10. F. R. Bruce
11. A. D. Callihan
12. D. W. Cardwell
13. C. E. Center
14. R. A. Charpie
15. G. H. Clewett
16. C. E. Clifford
17. W. B. Cottrell
18. R. G. Cochran
19. D. D. Cowen
20. S. Cromer
21. F. L. Culler
22. L. B. Emlet (K-25)
23. W. K. Ergen
24. A. P. Fraas
25. W. R. Grimes
26. E. E. Hoffman
27. A. Hollaender
28. A. S. Householder
29. J. T. Howe
30. R. W. Johnson
31. W. H. Jordan
32. G. W. Keilholtz
33. C. P. Keim
34. M. T. Kelley
35. F. Kertesz
36. E. M. King
37. J. A. Lane
38. C. E. Larson
39. R. S. Livingston
40. R. N. Lyon
41. W. D. Manly
42. L. A. Mann
43. W. B. McDonald
44. J. L. Meem
45. A. J. Miller
46. K. Z. Morgan
47. E. J. Murphy
48. J. P. Murray (Y-12)
49. G. J. Nessle
50. P. Patriarca
51. H. F. Poppendiek
52. P. M. Reyling
53. H. W. Savage
54. A. W. Savolainen
55. E. D. Shipley
56. O. Sisman
57. G. P. Smith
58. L. P. Smith (consultant)
59. A. H. Snell
60. C. L. Storrs
61. C. D. Susano
62. J. A. Swartout
63. E. H. Taylor
64. J. B. Trice
65. E. R. Van Artsdalen
66. F. C. VonderLage
67. J. M. Warde
68. A. M. Weinberg
69. J. C. White
70. G. D. Whitman
71. E. P. Wigner (consultant)
72. G. C. Williams
73. J. C. Wilson
74. C. E. Winters
75-84. ANP Library
85. Biology Library
86-90. Laboratory Records Department
91. Laboratory Records, ORNL R.C.
92. Health Physics Library
93. Metallurgy Library
94. Reactor Experimental Engineering Library
95-97. Central Research Library

[redacted]

EXTERNAL DISTRIBUTION

98. Air Force Engineering Office, Oak Ridge
99. Air Force Plant Representative, Burbank
100. Air Force Plant Representative, Seattle
101. Air Force Plant Representative, Wood-Ridge
102. American Machine and Foundry Company
103. ANP Project Office, Fort Worth
104-115. Argonne National Laboratory (1 copy to Kermit Anderson)
116. Armed Forces Special Weapons Project (Sandia)
117. Armed Forces Special Weapons Project, Washington (Gertrude Camp)
118-122. Atomic Energy Commission, Washington (Lt. Col. M. J. Nielsen)
123. Babcock and Wilcox Company
124. Battelle Memorial Institute
125. Bendix Aviation Corporation
126-128. Brookhaven National Laboratory
129. Bureau of Aernautics (Grant)
130. Bureau of Ships
131-136. Carbide and Carbon Chemicals Company (Y-12 Plant)
137. Chicago Patent Group
138. Chief of Naval Research
139. Commonwealth Edison Company
140. Convair, San Diego (C. H. Helms)
141. Curtiss-Wright Corporation, Wright Aeronautical Division (K. Campbell)
142. Department of the Navy – Op-362
143. Detroit Edison Company
144. Division of Research and Medicine, AEC, ORO
145-149. duPont Company, Augusta
150. duPont Company, Wilmington
151. Duquesne Light Company
152. Foster Wheeler Corporation
153-155. General Electric Company, ANPD
156-163. General Electric Company, APS, Richland
164. Glen L. Martin Company (T. F. Nagey)
165. Hanford Operations Office
166. Iowa State College
167-170. Knolls Atomic Power Laboratory
171-172. Lockland Area Office
173-174. Los Alamos Scientific Laboratory
175. Materials Laboratory (WADC) (Col. P. L. Hill)
176. Metallurgical Project
177. Monsanto Chemical Company
178. Mound Laboratory
179-182. National Advisory Committee for Aeronautics, Cleveland (A. Silverstein)
183. National Advisory Committee for Aeronautics, Washington
184-185. Naval Research Laboratory
186. Newport News Shipbuilding and Dry Dock Company
187. New York Operations Office
188-189. North American Aviation, Inc.
190. Nuclear Development Associates, Inc.
191. Pacific Northwest Power Group

[redacted]

[redacted]

192. Patent Branch, Washington
193-199. Phillips Petroleum Company (NRTS)
200-201. Powerplant Laboratory (WADC) (A. M. Nelson)
202-211. Pratt and Whitney Aircraft Division (Fox Project)
212-213. Rand Corporation (1 copy to V. G. Henning)
214. San Francisco Field Office
215. Sylvania Electric Products, Inc.
216. Tennessee Valley Authority (Dean)
217. USAF Headquarters
218. U.S. Naval Radiological Defense Laboratory
219-220. University of California Radiation Laboratory, Berkeley
221-222. University of California Radiation Laboratory, Livermore
223. Walter Kidde Nuclear Laboratories, Inc.
224-229. Westinghouse Electric Corporation
230-240. Wright Air Development Center (WCSNS, Col. J. R. Hood, Jr.)
241-255. Technical Information Service, Oak Ridge

[redacted]

Reports previously issued in this series are as follows:

ORNL-528	Period Ending November 30, 1949
ORNL-629	Period Ending February 28, 1950
ORNL-768	Period Ending May 31, 1950
ORNL-858	Period Ending August 31, 1950
ORNL-919	Period Ending December 10, 1950
ANP-60	Period Ending March 10, 1951
ANP-65	Period Ending June 10, 1951
ORNL-1154	Period Ending September 10, 1951
ORNL-1170	Period Ending December 10, 1951
ORNL-1227	Period Ending March 10, 1952
ORNL-1294	Period Ending June 10, 1952
ORNL-1375	Period Ending September 10, 1952
ORNL-1439	Period Ending December 10, 1952
ORNL-1515	Period Ending March 10, 1953
ORNL-1556	Period Ending June 10, 1953
ORNL-1609	Period Ending September 10, 1953
ORNL-1649	Period Ending December 10, 1953
ORNL-1692	Period Ending March 10, 1954

FOREWORD

This quarterly progress report of the Aircraft Nuclear Propulsion Project at ORNL records the technical progress of the research on the Circulating-Fuel Reactor and all other ANP research at the Laboratory under its Contract W-7405-eng-26. The report is divided into three major parts: I. Reactor Theory and Design, II. Materials Research, and III. Shielding Research.

The ANP Project is comprised of about 300 technical and scientific personnel engaged in many phases of research directed toward the achievement of nuclear propulsion of aircraft. A considerable portion of this research is performed in support of the work of other organizations participating in the national ANP effort. However, the bulk of the ANP research at ORNL is directed toward the development of a circulating-fuel type of reactor.

The nucleus of the effort on circulating-fuel reactors is now centered upon the Aircraft Reactor Experiment – a high-temperature prototype of a circulating-fuel reactor for the propulsion of aircraft. The equipment for this reactor experiment is now being assembled; the current status of the experiment is summarized in Section 1 of Part I. The supporting research on materials and problems peculiar to the ARE – previously included in the subject sections – is now included in this ARE section, where convenient. The few exceptions are referenced to the specific section of the report where more detailed information may be found.

The ANP research, in addition to that for the Aircraft Reactor Experiment, falls into three general categories: (1) studies of aircraft-size circulating-fuel reactors, (2) materials problems associated with advanced reactor designs, and (3) studies of shields for nuclear aircraft. These phases of research are covered in Parts I, II, and III, respectively, of this report.

[redacted]

CONTENTS

FOREWORD vii

SUMMARY 1

PART I. REACTOR THEORY AND DESIGN

1. CIRCULATING-FUEL AIRCRAFT REACTOR EXPERIMENT 7

The Experimental Reactor System 7
Pumps 7
Heat exchangers 7
Fluid circuits 8
Fuel-enrichment system 8
Loading facilities 8
Fuel-sampling facility 9
Fuel-unloading facility 10
Reactor control 10
Fuel System Mock-up Tests 10
Operation of the Fuel System 10
Cleaning 11
Pressure filling 11
Pressure and flow characteristics 11
Functional tests 11
Hot-gas test 12
Pump Fabrication and Tests 12
Reactor System Component Loop 14
Fuel Recovery and Reprocessing 14

2. EXPERIMENTAL REACTOR ENGINEERING 18

In-Pile Loop Component Development 18
Centrifugally sealed pump 18
Horizontal-shaft sump pump 19
Vertical-shaft sump pump 19
Hydraulic pump drives 21
Fluoride-to-water heat exchanger 21
Forced-Circulation Corrosion Loops 21
Sodium-Beryllium-Inconel Mass-Transfer Test 22
Fluoride-to-Sodium Heat-Exchanger Test 22
Gas-Furnace Heat-Source Development 23
Sodium Sampler 24
Removal of Fluoride Mixtures from Equipment 24
Bearing-Materials Tests 24
Rotary-Shaft Seals 26

3. REFLECTOR-MODERATED REACTOR 28

A Comparison of Lithium- and Zirconium-Base Fluoride Fuels 28
Reactor Physics 32
Reactor Calculations 32

[redacted]

[redacted]

PART II. MATERIALS RESEARCH

4. CHEMISTRY OF MOLTEN MATERIALS 39

Quenching Experiments with Fluoride Systems 39
$NaF-ZrF_4$ 39
$NaF-UF_4$ 41
Visual Observation of Melting Temperatures 42
Differential Thermal Analysis of the $NaF-ZrF_4$ System 42
Filtration Analysis of Fluoride Systems 42
$NaF-ZrF_4$ 42
$NaF-LiF-RbF-UF_4$ 42
Thermal Analysis of Fluoride Systems 43
$LiF-UF_3$ 43
$NaF-UF_3$ 43
$RbF-UF_3$ 43
$KF-LiF-UF_3$ 43
$RbF-LiF-UF_3$ 44
$NaF-ZrF_4-UF_4-UF_3$ 44
$NaF-ThF_4$ 44
$LiF-BeF_2-ThF_4-UF_4$ 45
$NaF-CrF_3$ 45
Thermal Analysis of Chloride and Mixed Chloride-Fluoride Systems 45
UCl_3-UCl_4 45
UCl_4-UF_4 46
UCl_3-UF_3 46
$KCl-UCl_4$ 46
$RbCl-UCl_4$ 47
$KCl-CuCl-UCl_3$ 47
X-Ray Diffraction Studies of the $NaF-ZrF_4$ System 47
Chemical Reactions in Molten Salts 50
Chemical equilibria in molten fluorides 50
Solubility of UF_3 in $NaF-ZrF_4$ mixtures 51
Solubility of UF_3 in NaF-KF-LiF mixtures 52
Solubility of UF_3 in NaF-RbF-LiF mixtures 53
Chlorination of UF_3 54
Preparation of $UF_3 \cdot 2ZrF_4$ 54
Preparation of various fluorides 54
Fundamental Chemistry of Fused Salts 55
EMF measurements 55
Physical chemistry 57
Chemical Effects of Fission Products 57
Quantity of fission products 57
Separation of solid phases 57
Effects on viscosity and heat capacity 58
Effects on corrosion 58
Purification and Properties of Alkali Hydroxides 59
Purification of hydroxides 59
Reaction of sodium hydroxide with metals 59
Production of Purified Molten Fluorides 60
Laboratory-scale production 60
Experimental production 60

[redacted]

Large-scale production 61
Production of enriched fuel for in-pile loop 61

5. CORROSION RESEARCH 62

Fluoride Corrosion of Inconel in Static and Seesaw Tests 63
Effect of chromium addition to fluoride melt 63
Effect of temperature 63
Effect of surface area 64
Effect of reduced phases in fluoride melt 65
Effect of fission products 65
Static and Seesaw Tests of Various Materials in Fluoride Mixtures and Liquid Metals 66
Dissimilar metals in $NaF-ZrF_4-UF_4$ 66
Molybdenum-coated Inconel in $NaF-ZrF_4-UF_4$ 66
Stainless steel in lithium with lithium nitride added 66
Chromalloyed steels in liquid metals 66
Cermets in $NaF-ZrF_4-UF_4$ 68
Graphite in $NaF-ZrF_4-UF_4$ and in sodium 70
Fluoride Corrosion of Inconel in Thermal-Convection Loops 72
Effects of UF_3 and mixtures of UF_3 and UF_4 in fluoride fuels 72
Effect of hydrogen fluoride 74
Effect of temperature 74
Effect of exposure time 76
Thermal-Convection-Loop Tests of Various Materials 77
$NaF-ZrF_4-UF_4$ in special Inconel 77
$NaF-ZrF_4-UF_4$ in Hastelloy B 77
$NaF-ZrF_4-UF_4$ in stainless steel 77
$NaF-ZrF_4-UF_4$ in Inconel with stainless steel or nickel inserts 77
Sodium in Inconel with beryllium inserts 79
Lithium in stainless steel 79
Fundamental Corrosion Research 79
Mass transfer in liquid lead 79
Products of hydroxide-metal reactions 81
Dehydration of sodium hydroxide 84
Color changes in fused hydroxides 85

6. METALLURGY 88

Stress-Rupture Tests of Inconel 89
High-Conductivity Metals for Radiator Fins 91
Special Materials Research 91
Hastelloys B and C 91
Nickel-molybdenum alloys 93
Stainless-steel-clad molybdenum and columbium 93
Columbium 93
Boron carbide 93
Welding and Brazing 94
Brazing alloy development 94
Beryllium test assembly 97

7. HEAT TRANSFER AND PHYSICAL PROPERTIES 99

Physical Properties Measurements 99
Heat capacity 99

Density and viscosity 99
Thermal conductivity 100
Electrical conductivity 100
Vapor pressures 101
Fused-Salt Heat Transfer 101
Reactor Hydrodynamics 102
Heat-Removal Study of BSF Reactor 102
Heat Transfer in Circulating-Fuel Reflector-Moderated Reactor 103
Heat Transfer in NaOH-Moderated Circulating Fuel Reactor 103

8. RADIATION DAMAGE 105

Radiation Stability of Fluoride Fuels 105
LITR Fluoride-Fuel Loop 107
In-Pile Stress Corrosion and Creep 107
Remote Metallography 107

9. ANALYTICAL STUDIES OF REACTOR MATERIALS 109

Analytical Chemistry of Reactor Materials 109
Oxidation states of chromium and uranium in $NaZrF_5$-base fuels 109
Determination of oxygen in $NaZrF_5$-base fuels 110
Oxidation of trivalent uranium by hexavalent uranium 111
Stability of trivalent uranium in hydrochloric acid solutions 111
Removal of film from Inconel tubing 111
Determination of sulfur in natural gas 112
Petrographic Investigations of Fluoride Fuels 112
Summary of Sercvie Analyses 112

PART III. SHIELDING RESEARCH

10. LID TANK FACILITY 117

Slant Penetrations of Neutrons Through Water 117
Secondary Gamma-Ray Study 118

11. BULK SHIELDING FACILITY 121

Gamma-Ray Air-Scattering Calculations 121
Thermal-Neutron-Flux Perturbation by Gold Foils in Water 128
Reactor Power Calibration Techniques 128
Leakage-Flux Changes Due to Control-Rod Settings 135

12. TOWER SHIELDING FACILITY 136

Experimental Program 136
Operation of the Reactor 136

PART IV. APPENDIX

13. LIST OF REPORTS ISSUED DURING THE QUARTER 141

[redacted]

ANP PROJECT QUARTERLY PROGRESS REPORT

SUMMARY

PART I. REACTOR THEORY AND DESIGN

The main pump for the fuel system of the Aircraft Reactor Experiment was installed, and it was therefore possible to start the first operational phase of the experiment – the water test of the fuel system (Sec. 1). The objectives of the water test are, in addition to cleaning of the system, determining effectiveness of the pressure fill of the system, checking tightness of the valves, determining the flow characteristics of the system, ascertaining the helium consumption rate, checking ability to transfer liquid (from one fill tank to another) while holding a fixed level in the pump tank, determining operability of the fuel enrichment system, and checking process instrumentation. The main sodium pump has also been installed and the stand-by fuel and sodium pumps will be installed soon. The fuel-to-helium and sodium-to-helium heat exchangers which had faulty welds have been refabricated and reinstalled. Facilities for loading the sodium, fuel carrier, and fuel concentrate, for sampling the fuel, and for unloading the fuel after the experiment have been or are being constructed. Operation of a large-scale test loop for circulating fluoride mixtures to test corrosion and structural stability of ARE components started June 5, 1954; the duration aim of the test is 2000 hr. The loop contains an ARE-type pump, a fuel-to-helium heat exchanger, and two reactor-core hairpin tubes.

The experimental reactor engineering program (Sec. 2) has included the development of components for in-pile loops, the design of forced-circulation corrosion-testing loops, and the construction of a unit for testing the mass-transfer characteristics of a sodium-beryllium-Inconel system. In addition a sodium-sampling device was developed, and a method for removing fluoride mixtures from equipment to be salvaged was devised. Further tests of bearing and shaft-seal materials were also made. Development and hot testing of the vertical-shaft, down-flow sump pump for operation of the initial in-pile loop in the LITR were completed, and a model of an air-driven horizontal-shaft sump pump was fabricated. In additional development work on the centrifugally sealed pump, it was found to be possible to decrease the size with no sacrifice in pump performance. A compact heat exchanger for the removal of fission heat from in-pile loops is being fabricated. An Inconel corrosion-testing loop is being designed for circulating fluoride mixtures that will provide high-velocity turbulent flow and large temperature differentials. The tests of the 1-Mw, regenerative fluoride-to-sodium heat exchanger were terminated and the test unit is being dismantled for examination. A 100-kw gas-fired furnace is being fabricated to determine its suitability as a heat source for future heat-exchanger tests. If tests indicate that a heat source of this type will be satisfactory, a 1-Mw furnace will be developed.

Components of the proposed 60-Mw Circulating-Fuel Reactor Experiment (CFRE) are now being designed and constructed and are to be tested to determine operational characteristics (Sec. 3). Detailed designs will be prepared from the data thus obtained. A stress analysis of the reactor is being prepared, and a series of charts has been constructed for use in determining temperature distribution and thermal stress. A comparative analysis of lithium- and zirconium-base fuels was made that indicates the superiority of the lithium-base fuels for reflector-moderated reactors. Estimates of the xenon-poisoning effect in the Reflector-Moderated Reactor have emphasized the need for removing the xenon during operation. An experiment is being planned to determine whether adequate purging of the xenon can be obtained. Calculations of a set of 48 reactors are being made that evaluate the effect of reactor dimensions on concentration of U^{235} in the fuel, on total U^{235} investment, on peak-to-average power density in the core, and on the fraction of thermal fissions in the core.

PART II. MATERIALS RESEARCH

The intensive studies of the fluoride systems of interest as reactor fuels were continued with particular emphasis on systems in which the uranium-bearing component is the less corrosive UF_3 or a mixture of UF_3 and UF_4 rather than UF_4 alone (Sec. 4). It appears that attainable concentrations of UF_3 in ZrF_4-based fuels are insufficient to fuel aircraft reactors; however, the use of UF_3 in addition to UF_4 in such mixtures appears to be promising. The UF_3 is apparently sufficiently

[redacted]

soluble in NaF-KF-LiF mixtures (which would require Li^7 for utilization) to make such fuels attractive; the use of NaF-RbF-LiF mixtures as solvents for UF_3 (without UF_4) has not yet been shown to be possible. The elucidation of the complex NaF-ZrF_4 system has virtually been completed, and exploratory phase-equilibrium studies of the chloride-fluoride systems are under way. An apparatus for the visual observation of liquidus temperatures has been tested and found to be satisfactory. The chemical effects of fission products on aircraft reactor fuels are being explored.

The static, seesaw, and thermal-convection loop facilities were used extensively to further test the corrosion resistance of various materials in fluoride mixtures and in liquid metals (Sec. 5). It has been demonstrated in both seesaw and thermal-convection-loop tests that Inconel is not attacked by ZrF_4-based fuels containing UF_3 instead of the customary UF_4. Since UF_3 is not sufficiently soluble in NaF-ZrF_4 and several other fluoride mixtures of interest, tests are under way for determining the amount of UF_3 required to eliminate corrosive attack on Inconel by a fuel which contains UF_3 and UF_4.

The effects of temperature and exposure time have been investigated further and additional confirmation of the relationship of these variables to mass transfer in fluoride-Inconel systems was obtained. The amount of mass transfer increases with an increase in temperature or an increase in temperature difference between the hot and cold legs of a thermal-convection loop. The previously reported rapid initial attack and slower secondary attack after 250 hr of exposure of Inconel to NaF-ZrF_4-UF_4 were again demonstrated in a loop operated for 5000 hr. The depth of attack increases about 4 mils for each 1000 hr of exposure.

Reductions in depth of attack by UF_4-bearing fluoride mixtures, in comparison with the attack on standard Inconel, were found in loops constructed of Hastelloy B and of a special Inconel with a portion of the chromium replaced by molybdenum. In both seesaw and thermal-convection-loop tests it was shown that, when Inconel and type 316 stainless steel are exposed in the same system to a fluoride mixture, the steel is inferior to Inconel in its resistivity to attack. Two type 316 stainless steel thermal-convection loops filled with high-purity lithium operated for 1000 hr with only small amounts of mass transfer and no indication of plugging, in contrast to those operated previously, which plugged in 200 to 300 hr. The increased life was probably due to the higher purity of the lithium and, especially, to the decrease in the lithium nitride content. In the study of corrosion and mass-transfer characteristics of materials in contact with liquid lead, it was found that quartz thermal-convection loops which contained types 410 and 446 stainless steel specimens had much longer life prior to plugging than similar loops which contained pure iron and chromium or one of the 300-series stainless steels. Studies are continuing on the identification of compounds produced by hydroxide-metal reactions.

The metallurgical research effort has been devoted to studies of the mechanical properties of Inconel in contact with fluoride mixtures, to investigations of materials suitable for high-thermal-conductivity fins, to searches for container materials other than Inconel for fluoride mixtures, and to the development of fabricational techniques (Sec. 6). Tests have shown that Inconel exposed to fluoride mixtures has a much longer rupture life when stressed under uniaxial conditions than when stressed under the multiaxial conditions that will prevail in reactor applications. Therefore tube-burst or other multiaxial-stress tests are to be emphasized in further studies.

In previous investigations of materials suitable for high-thermal-conductivity fins for radiators, it was found that copper fins clad with types 310, 446, or 430 stainless steel or with Inconel were quite satisfactory in the unstressed condition if a suitable diffusion barrier was provided; however, in oxidation tests under stress it was found that high stresses greatly increased the oxidation of the fin material. Experimental work was started on the preparation of high-boron-content material for use as shielding between the moderator and the heat exchanger and between the heat exchanger and the pressure shell of the Reflector-Moderated Reactor.

High-temperature oxidation tests of several brazing alloys have shown that the majority of the nickel-chromium-base alloys are suitable for service in an oxidizing atmosphere at 1500°F and that several of the alloys retain this resistance at 1700°F. A new semiautomatic heliarc-welding process for the production of tube-to-header joints is described and its use in the construction of a

prototype sodium-to-air radiator is illustrated. An assembly has been fabricated for use in determining the effect of thermal stresses and thermal cycling on beryllium metal and for studying the compatibility of sodium and beryllium.

The physical properties of several fluoride mixtures and other materials of interest to aircraft reactor technology were determined, and the heat-transfer characteristics of reactor fluids were studied (Sec. 7). The enthalpies and heat capacities of the ARE fuel (NaF-ZrF_4-UF_4, 53.5-40.0-6.5 mole %) and of K_3CrF_6 were determined. Density and viscosity measurements were made for molten RbF-LiF (57-43 mole %), and thermal conductivities were measured for molten RbF-LiF and solid NaF-KF-LiF (11.5-42.0-46.5 mole %). Electrical conductivity measurements were obtained on molten NaOH over the temperature range of 625 to 1490°F. A Lucite model of the circulating-fuel Reflector-Moderated Reactor was fabricated and is to be used to study the hydrodynamic structure in that system. The results of a mathematical analysis of convection are presented for the case of forced flow between parallel plates of fluids with volume-heat sources; this analysis is useful in estimating the temperature structure in the flow annuli of reflector-moderated reactor cores. A study has been initiated to investigate the heat-transfer and fluid-flow characteristics of a NaOH-moderated circulating-fuel reactor system.

The radiation damage program included additional irradiations in the MTR of fluoride mixtures in Inconel capsules, construction of in-pile circulating-fuel loops, and development of creep-testing equipment for use in the MTR (Sec. 8). The Inconel capsules now being irradiated in the MTR contain UF_3- or UF_4-bearing fluoride mixtures so that additional comparative data can be obtained on the effect of UF_3 in decreasing the corrosiveness of fluoride mixtures. Temperatures of the capsules are being carefully controlled so that the Inconel-fuel interface temperature will remain approximately 1500°F throughout each test. A re-examination of a group of Inconel capsules from the earlier irradiations showed that previously reported excessive grain growth and deep penetration of the Inconel had occurred in only a few capsules and in those capsules the Inconel-fuel interface had been heated to temperatures much higher than the desired 1500°F.

The analytical studies of reactor materials included the problems of separating UF_3 from UF_4 in $NaZrF_5$-base fuels and fuel solvents, the formulation of a method for determining oxygen in these mixtures, stability tests of trivalent uranium in hydrochloric acid solutions, and petrographic examinations of ZrF_4-based fuels (Sec. 9). In the studies of the separation of UF_3 from UF_4, methods were investigated for the conversion of the fluorides to chloride salts and the simultaneous extraction of the chlorides into non-aqueous solutions. Petrographic examination of NaF-ZrF_4-UF_4 fuels reduced with metallic zirconium, with metallic uranium, or with hydrogen has shown that the predominant phase in the reduction complexes obtained is always a solid solution of U^{4+} and U^{3+} in $Na_9Zr_8F_{41}$.

PART III. SHIELDING RESEARCH

The Lid Tank Facility has been used primarily for studying special attenuation problems which arise in aircraft shield design (Sec. 10). The crew-shield plastic sides attenuate neutrons which arrive at slant incidence, and therefore experiments are being carried out to measure the effect of slant incidence on the attenuation. At 60 deg to the normal, the short-circuiting effect becomes quite important. The gamma-ray attenuations in lead and bismuth have been compared as a function of the neutron flux at the metal in a metal-water shield. A first study of the data shows little difference between the two materials, but more work is to be done to clarify this point.

The work at the Bulk Shielding Facility has included gamma-ray air-scattering calculations, the determination of the thermal-neutron-flux perturbation by gold foils in water, a study of reactor power calibration techniques, and a determination of the effect of control-rod settings on leakage flux (Sec. 11). The calculation of air scattering for the divided shield with a lead shadow shield was carried out some time ago for gamma rays by using the spectral data obtained on the reactor shield mock-up at the Bulk Shielding Facility. The data have now been extended to include attenuation by the crew shield so that a direct comparison is possible with earlier Shielding Board calculations. For scattered radiation there is good agreement, but the leakage around the shadow shield was badly underestimated in the

early work. This will require redesign of the shield configuration but will not introduce an excessive weight penalty. The correction for flux depression by detector foils is known for indium foils, but since much work is done with gold foils, the determination of flux depression in water has been extended to this element. In connection with intercalibration of the several shielding reactors (Bulk Shielding Facility and Tower Shielding Facility reactors at ORNL and a reactor at Convair), it has been demonstrated that bare-foil activation gives a reliable measure of reactor power density. The effect of safety and control-rod positions on fast-neutron leakage from the reactor has been determined experimentally for use in correlating data taken on two otherwise similar reactors. Fortunately, the effect appears to be small, as is the effect of small changes in fuel loading.

The Tower Shielding Facility reactor was made critical for the first time at the site on March 12 (Sec. 12). Since that date much time has been spent in determining the operational characteristics of the equipment, and the reactor now operates regularly in the air at powers of up to 4 kw. It will soon be operated at up to 100 kw, the design maximum power level.

Part I

REACTOR THEORY AND DESIGN

1. CIRCULATING-FUEL AIRCRAFT REACTOR EXPERIMENT

E. S. Bettis J. L. Meem
ANP Division

The first operational phase of the Aircraft Reactor Experiment is now under way. With the installation of the main fuel pump, it was possible to start the water test of the fuel system. The water was charged to a fill tank and then forced by gas pressure into the system. Subsequent circulation of the water by the fuel pump carried the gas from pockets in the system, which will not pressure fill, to the pump tank where the water degassed. The system probably became gas free, that is, full of liquid, but since there is no positive indication of fullness, vacuum filling of the system is being considered. Data on the pressure and flow characteristics of the system are being obtained.

The main sodium pump has also been installed and the stand-by fuel and sodium pumps will be installed soon. The fuel-to-helium and sodium-to-helium heat exchangers which had faulty welds have been refabricated and reinstalled. Minor modifications were made during refabrication that are expected to improve the performance of these heat exchangers. The thermal-barrier doors, which are lowered to permit preheating of the heat exchangers to above the melting point of the fuel or the sodium, were modified to eliminate thermal buckling. Operation of the helium supply was checked, and the arrangements were made for assuring an adequate supply of helium for operation. The original fuel-injection system, which was dependent on the operation of valves, was modified to permit injection of the fuel concentrate by a more reliable gas-pressure equalization technique. Facilities for loading the sodium, fuel carrier, and fuel concentrate, for sampling the fuel, and for unloading the fuel after the experiment have been or are being constructed. Plans have been made for a leak check of the fuel system at operating temperature. Helium spiked with krypton will be introduced into the fuel system and the helium in the annulus around the fuel piping will be checked for krypton.

A large-scale test loop for circulating fluoride mixtures is being operated to test corrosion and structural stability of ARE components. The loop contains an ARE-type pump, a fuel-to-helium heat exchanger rebuilt from one originally purchased for the ARE, and two hairpin tubes purchased as spares for the ARE reactor core. The system is operating isothermally at about 1375°F with a flow rate of 20 gpm. The duration aim of the test, which started June 5, 1954, is 2000 hr.

THE EXPERIMENTAL REACTOR SYSTEM

W. B. Cottrell J. Y. Estabrook
J. K. Leslie
ANP Division

G. J. Nessle J. E. Eorgan
Materials Chemistry Division

G. A. Cristy E. Wischhusen
Engineering and Mechanical Division

Pumps

The main fuel pump and the main sodium pump have been installed in their respective systems. The stand-by sodium pump, which is on hand, and the stand-by fuel pump will be installed in the immediate future. All these pumps have been satisfactorily hot checked with sodium at 1300°F for 100 hr.

Operation of the main fuel pump with water revealed that the maximum oil flow in the lubricating system was too low (~ 2 gpm) at high pump speeds (~ 1800 rpm). Consequently, the auxiliary lubricating pump, now a single-phase Chempump, will be paralleled with a three-phase Chempump, and the single-phase pump will be held in reserve. Tests with the three-phase Chempump show that the oil flow is ample (>3 gpm) at all speeds of the primary pump.

Heat Exchangers

Disassembly, refabrication, and reinstallation of the fuel-to-helium heat exchangers and the sodium-to-helium heat exchangers which had faulty welds have been completed. The welding was completed by the two qualified ARE welders ahead of schedule. There were two significant design changes in the fuel heat exchangers as refabricated. Each fuel heat exchanger now has three parallel passes, rather than two, in series with

three similar parallel passes. Also, a small bypass line was eliminated to simplify fabrication of the fuel heat exchangers. Without the bypass lines, however, the heat exchangers are not completely drainable.

Two insulated and heated barrier doors are provided for each heat exchanger to permit preheating of the heat exchanger to above the melting point of the fuel or the sodium before these liquids are loaded into their respective systems. These doors, which are lowered within the closed duct to block the flow of helium through the heat exchangers, were tested at operating temperature (1300°F) before the heat exchangers were removed for refabrication. The doors stuck at temperatures above 900°F, and therefore they have been modified to eliminate thermal buckling. These doors have not yet been retested at operating temperature because of the water tests now in progress.

Fluid Circuits

The major fluid circuits (fuel and sodium) have been virtually completed for some time. The rewelding of some pipe lines necessitated by the removal and reinstallation of the heat exchangers has been completed. Except for the bypass around the reactor in the sodium system, all fuel and sodium piping is completely welded, instrumented (thermocouples located every 3 ft), heated, and insulated. The heater electrical connections are essentially complete, but a substantial number of thermocouple connections remain to be made.

An operational check of the helium supply system disclosed a few leaks which have been repaired. The helium supply problem has been resolved. Three railroad tank cars have been allocated for ARE use so that a helium tank car should be on hand at all times. Arrangements have been effected to have two helium trailer trucks (capacity 20,200 scf) on hand at all times to transport the helium from the tank cars to the ARE building. The bank of 12 helium cylinders (capacity 2640 scf) held in reserve at the experiment will be supplemented by a bank of 15 larger cylinders (capacity 16,000 scf), which are now being fabricated.

Fuel-Enrichment System

The original fuel-enrichment system provided for the injection of the fuel concentrate into the system below the liquid-gas interface in the pump tank. Since such an arrangement is inherently dependent upon the operation of the system valves, freeze valves were inserted in the $\frac{3}{8}$-in. transfer lines to back up the bellows valves in the system, which are of questionable reliability at the temperatures involved (1300 to 1400°F). These freeze valves were merely sections of tubing from which the heat could be removed so that the liquid fuel inside the tubing would freeze. However, in tests of similar freeze sections the $\frac{3}{8}$-in. tubing frequently ruptured upon thawing, and this injection technique could not be considered sufficiently reliable.

It was therefore decided to effect transfer of the fuel concentrate into the fuel system by a gas-pressure equalization technique. In order to employ this technique, only two modifications to the existing system were necessary. First, the transfer line had to be installed so that the fuel concentrate would be injected in the pump above the liquid-gas interface, and second, gas equalizer lines, both with gas valves, had to be provided from the storage tank to the transfer tank and from the transfer tank to the pump. The concentrate will now be injected through the pump flange into the pump tank. Since the pump flange is maintained at 600°F, it was necessary to develop a special resistance-heated annular fitting which could attain a temperature of 1400°F in the center fuel passage.

The transfer tank, originally fabricated of type 316 stainless steel, has been refabricated of Inconel to conform to the rest of the system. The fuel-enrichment system will be tested with water as soon as the transfer tank is installed and connected.

Loading Facilities

Facilities for loading the sodium, fuel carrier, and fuel concentrate into their respective containers have been, or are being, fabricated. Each of these facilities will effect transfer of the liquid from a portable container into the tank provided for it at the ARE. The transfer will be effected by gas pressure in each case.

The sodium, which will assay less than 0.02 wt % oxygen, will be received in four 55-gal drums. The fuel carrier, $NaZrF_4$, will be received in 13 cylinders, each containing approximately 250 lb of the fluoride. The fuel concentrate, Na_2UF_6, will be received in 15 cylinders, each

weighing approximately 75 lb. All these materials are on hand. In all cases the fluid to be transferred will be maintained under helium pressure. The transfer temperatures are 600, 1200, and 1300°F for the sodium, carrier, and concentrate, respectively.

Fuel-Sampling Facility

It is anticipated that from 5 to 10 samples of fuel will be drawn from the ARE between the time the fuel system is filled with fuel carrier and the time the reactor is operated at an appreciable power level. For the chemical analyses to be performed on these samples, only 10 to 20 g of material are required; however, to ensure that the sample is actually representative of the flowing fuel, at least 300 to 400 g of material must be withdrawn. Equipment for accomplishing this sampling operation has been designed, fabricated, and successfully tested.

The sampling apparatus consists, as shown in Fig. 1.1, of a nickel pot containing a machined graphite liner and a flanged top through which pass the fluoride entrance tube, three electrical contacts, the gas manifold connection, and a lever for moving the graphite-lined sample cup under the fluoride entrance tube. This apparatus will be connected to the system by a heated $\frac{3}{8}$-in. Inconel line containing a bellows valve and will be placed in the reactor pit at a level 4 to 8 ft above the highest fuel level in the ARE system. With the sampling cup out of the fuel delivery stream, a vacuum will be drawn on the nickel pot; when sufficient fuel has been drawn into the graphite liner to contact the lowest probe, the sample cup will be swung under the delivery stream. When the sample cup has overflowed sufficient fuel to contact the second probe, an atmosphere of helium will be admitted to stop the flow of fuel. As soon as the apparatus is sufficiently cool to handle, it will be disconnected and replaced by an identical apparatus. It is anticipated that sampling can be accomplished without closing the valve in the sample line and without resorting to the use of freeze valves in the delivery lines.

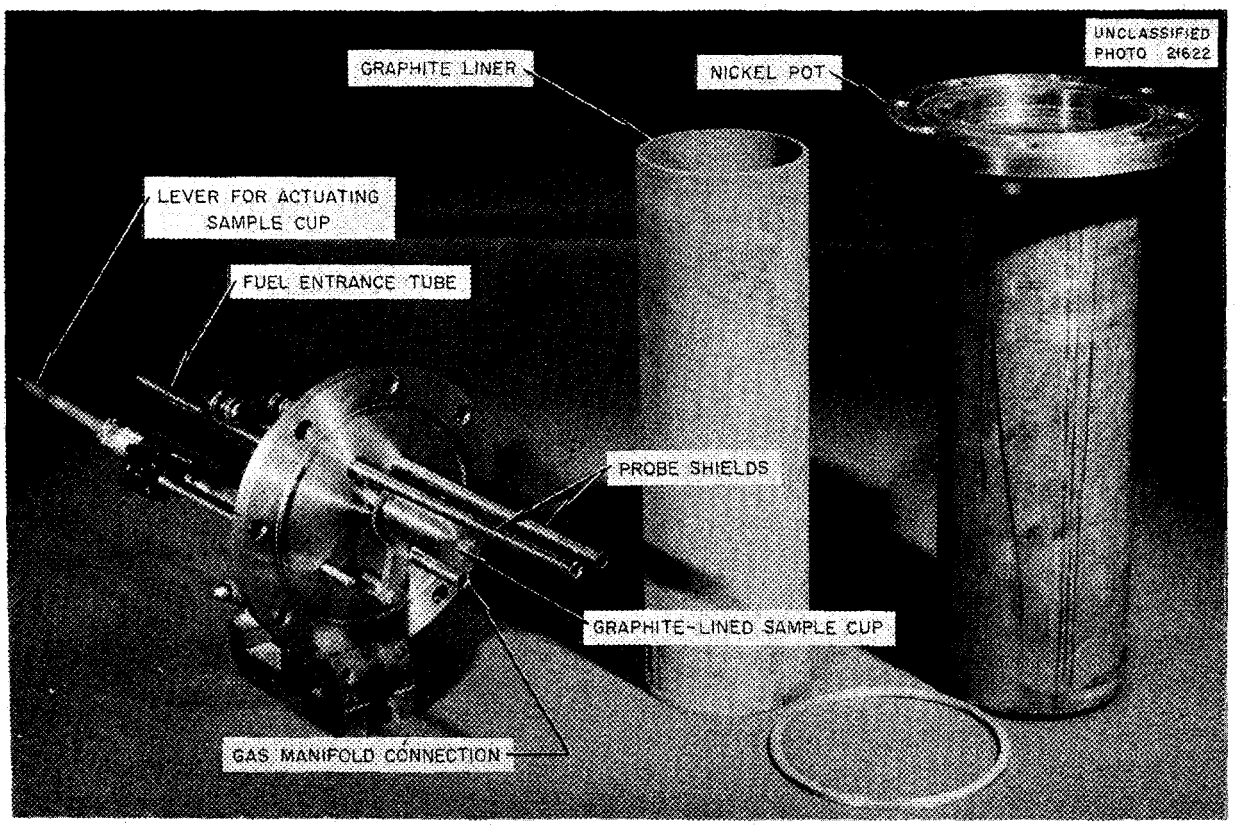

Fig. 1.1. Fuel-Sampling Apparatus.

Four complete tests of the apparatus have been made with four different values for pressure above the fuel and inside the sampling apparatus. These tests, in which the sampling apparatus was not heated, were satisfactory; it is anticipated that, barring unforeseen complications in the ARE, sampling of the fuel circuit should proceed smoothly.

Fuel-Unloading Facility

The radioactive fuel mixture will be discharged from the hot-fuel dump tank through a 1-in. pipe to aluminum cans for removal to fuel recovery and reprocessing equipment. A mock-up of the unloading equipment was constructed and tested with the fuel carrier $NaZrF_5$. The feasibility of unloading the ARE with equipment of this type has been satisfactorily demonstrated.

Reactor Control

The control actuator assembly has been mounted over the reactor, and the shim and control rods have been installed above the reactor. Accurate measurements have been made from the bottom of the reactor to assure proper location of the rods. The fission-chamber circuits have been checked, and the chambers are now being installed. In order to prevent a chamber from catching where the sleeve changes from 3 in. to $2\frac{1}{2}$ in. in diameter, a tapered transition section will be provided. Except for the final check on the ion chambers, the nuclear instrumentation has been completely checked. The actual installation of the ion chambers and shielding plugs will be accomplished just before the fuel carrier is loaded into the system.

FUEL SYSTEM MOCK-UP TESTS

H. W. Savage A. G. Grindell
W. G. Cobb W. R. Huntley
ANP Division

The complete filling of the ARE fuel system would be most easily accomplished with the system under vacuum, but the problems involved in obtaining and holding vacuum are formidable. Therefore, a mock-up was constructed and operated to test filling and degassing characteristics under a helium pressure greater than atmospheric. The mock-up was also used to test the drainability of the circuit.

The test unit was an essentially full-scale mock-up of the ARE fuel system without the heat exchangers. Included were a reactor core, a pump, a fill tank, piping, and valves with which to duplicate ARE pressure drops. The fill tank, core, and pump were set at levels corresponding to the respective levels in the ARE building. The working fluid used was tetrabromoethane because its room temperature density and viscosity (sp gr = 2.95, μ = 9.3 cp at 77°F) are similar to those of the fluoride fuel at operating temperature. A helium blanket at 20 to 30 psig was maintained in all tests.

The primary objective of the tests was to quantitatively determine the flow rate required to completely fill the reactor core and sweep all gas bubbles from it. A secondary objective was a determination of the degassing and self-priming characteristics of the pump.

In all the tests, flow rates of 60 to 64 gpm were required for filling all six parallel circuits in the core and sweeping out all gas bubbles. Since the tubes in the mock-up were 1.00 in. in inside diameter and the ARE core tubes are 1.115 in. in inside diameter, it is estimated that flows of 85 gpm may be required for filling the ARE. In the mock-up it could be ascertained by visual observation that all gas had been removed from the core, but visual observation will not be possible in the ARE.

The pump degassed well in all tests. In no case was there sufficient surface turbulence to endanger the probes or gas lines by splashing (the liquid surface was visible through glass portholes in the pump casing). In each filling operation, the pump lost its prime several times but regained it each time without adjustments of the controls.

In the drainability tests, gravity draining unassisted by gas pressure resulted in approximately 25% removal of liquid from the reactor core. Helium-pressure-assisted drainage (15 psi differential between pump and dump-tank pressures) resulted in a maximum of approximately 60% removal.

OPERATION OF THE FUEL SYSTEM

R. G. Affel W. B. Cottrell
G. D. Whitman
ANP Division

The installation of the main fuel pump essentially completed the fuel system, and the water test of the system is now under way. While this represents attainment of the first operational phase

described in the "ARE Operating Procedures,"[1] the immediate objectives of the water test are (1) cleaning of the system, (2) determining effectiveness of the pressure fill of the system, (3) checking tightness of the valves, (4) determining the flow characteristics of the system, (5) ascertaining the helium consumption rate, (6) checking ability to transfer liquid (from one fill tank to another) while holding a fixed level in the pump tank, (7) determining operability of the fuel-enrichment system, and (8) checking process instrumentation.

Cleaning

In order to remove the scale of calcium metasilicate now deposited throughout the system as a result of previous tests with water and Conklene (a detergent – sodium metasilicate), the system will be washed with a 1% solution of the tetrasodium salt of ethylenediaminetetraacetic acid in water. According to the analytical results (cf. Sec. 9, "Analytical Studies of Reactor Materials"), this solution will dissolve the calcium deposits and leave no residue when it, in turn, is flushed out of the system. It was recommended that the solution be circulated for 4 hr in the system at 170°F. Furthermore, because of the significant holdup volume of the system (about 1 cu ft of each 6 cu ft), the rinsing step should be repeated six or seven times to ensure complete removal of the washing agent. To date, the initial cleaning and two rinses have been effected, and the water shows the expected decreasing concentration of impurities. The water for the second rinse is being used in the operational tests described above.

Pressure Filling

The water was first charged to the fill tank and then forced into the system by gas pressure. Although the system (reactor and heat exchanger) contained gas pockets which would not pressure fill, subsequent circulation of the water by the fuel pump carried the gas pockets around to the pump tank where the water degassed. Although it is probable that the system thus became gas free (full of liquid), there does not appear to be any positive indication available. The gas remaining in the system is of little consequence in water operation, but it would be intolerable in operation with fuel. Unless operational parameters permit a more positive determination of the extent of filling, it may be necessary to vacuum fill the system. Vacuum filling of the system has thus far been avoided because oxygen could conceivably enter from the vent system and contaminate the hot fuel.

Pressure and Flow Characteristics

Many data have been taken on the pressure and flow characteristics of the fuel system. It is apparent that the flow through the bypass (in parallel with the heat exchangers) is less than that through the heat exchangers. This is undoubtedly caused by the pressure drop across the bypass throttling valve being greater than anticipated and that across the heat exchanger being less. The pump speed and system pressure-drop data do not check with the system flow data. It is most probable that the flowmeter (a Rotameter which transmits a signal from a coil within which moves a tapered iron core attached to the Rotameter bob) is not calibrated correctly. This possibility is being checked. The Rotameter has shown a tendency to drift, and it has not been possible therefore to make accurate measurements of the system flow characteristics.

Functional Tests

In the operation of the system to date, the dump-line valves appear to be tight, although there is some indication that the valves to individual tanks leak slightly under pressure. Such slight leaks are tolerable, although not desirable, and the leak tightness of the valves may improve upon repeated operation.

The helium consumption rate during the test with water in the fuel system has been about 3 cfm. It is therefore probable that the maximum helium consumption at any time during the experiment will be about 10 cfm.

It was found to be possible to transfer water from one fill tank to another through the system and to maintain a fixed liquid level in the pump. This operation could be of significance should it be desirable to replace the initial batch of carrier and/or to replace the hot fuel at the conclusion of the test.[1]

[1] W. B. Cottrell, *ARE Operating Procedures, Parts I, II, and III*, ORNL CF-54-2-68 (Feb. 11, 1954).

Hot-Gas Test

Although it would be desirable to leak-check both the fuel and the sodium systems at operating temperature, there is no completely satisfactory method for doing this except with fuel and sodium because the systems are not completely drainable. However, the inadequacy of a cold check in comparison with a hot check is so apparent that a gas check of the fuel system at the operating temperature will be effected. Basically this test will consist of heating the system to 1200°F, filling the fuel system with one gas under pressure, filling the fuel-system annulus with another gas at lower pressure, and spectrographically analyzing the gas in the annulus for the presence of the gas from the fuel system. Although in principle any two gases would suffice for this test, it would be impossible, for example, to detect a small leak of helium into nitrogen because of the background of air in the annulus system. Accordingly, helium spiked with krypton will be used in the fuel system, and the helium in the annulus will be examined for krypton.

PUMP FABRICATION AND TESTS

H. W. Savage W. G. Cobb
A. G. Grindell W. R. Huntley
R. E. MacPherson
ANP Division

P. Patriarca G. M. Slaughter
Metallurgy Division

All six ARE-pump rotary elements have been assembled and were found to meet hot-test requirements in tests made by using the two impellers which have been accepted. Four of the six rotary elements have passed all acceptance tests.[2] The other two rotary assemblies were rejected because of unsatisfactory upper seals which permitted excessive gas leakage. Relapping of the seals resulted in no improvement because the lapped surfaces were scored in subsequent testing. It was thought that the lapping abrasives (1500-grit diamond dust, and others) were not being completely removed from the soft nose of the upper seal. As a check on this possibility, the adequacy of lapping with water-soluble scouring compounds (for example, Bon Ami) is being evaluated.

One of the accepted elements, with a cast impeller (to be exchanged for a fabricated impeller before start-up of ARE), has been installed in the fuel system, and one was installed in the sodium system. One accepted element has been assigned to K-25 for use in a heat-exchanger test. One unaccepted element is installed in the cold shakedown test unit for seal tests. The other unaccepted element is being used in the hot shakedown test unit for hot-testing fabricated impellers. Two fabricated impellers have passed all acceptance tests,[3] and one has been furnished to K-25 for the heat-exchanger test.

Shorting of the probes used for liquid-level indication in the sodium pump has shown the clearance between the riser wall and probe to be inadequate. The original design called for a $\frac{3}{8}$-in. schedule-40 pipe riser which allowed bridging of sodium condensate between the inner pipe wall and the $\frac{3}{32}$-in.-dia probe. The size of the riser was increased to $\frac{1}{2}$ in. and no shorting of the probes occurred during subsequent testing. All the sodium pumps have been modified to utilize $\frac{1}{2}$-in. risers.

The operation of an ARE-type d-c pump drive motor in a dry helium atmosphere continued uneventfully during the quarter. Approximately 3500 hr of operating time have been accumulated at a test temperature of 130 to 140°F. This test will be terminated at 4000 hr.

The detail and assembly drawings of the pumps, made in the fall of 1953, are being revised to incorporate the modifications in the pump cooling and lubricating systems and other modifications.

The fabrication of five Inconel impellers for ARE pumps by machining and welding has been completed. The rough-machined parts are shown in Fig. 1.2. These parts, except the vanes, were subjected to a stress-relief annealing heat treatment so that precise dimensional tolerances could be maintained during subsequent machining. The stress-relief thermal cycle consisted of heating at 125°C/hr to a temperature of 1000°C, maintaining this temperature for $\frac{1}{2}$ hr, and cooling at 125°C/hr to room temperature.

The drive-shaft hub was then tack welded to a carbon steel strong-back to prevent warping during welding, and the vanes were heliarc welded

[2] H. W. Savage *et al.*, *ANP Quar. Prog. Rep. Mar. 10, 1954*, ORNL-1692, p 10.

[3] *Ibid.*, p 11.

into place, as shown in Fig. 1.3. The stress-relief heat treatment was then repeated. After the vanes had been machine finished, the fluid-entrance hub was heliarc plug-welded into position, and the joints between the hub and the vanes were heliarc welded as far as they were accessible, as shown in Fig. 1.4. The stress-relief heat treatment was again repeated. The

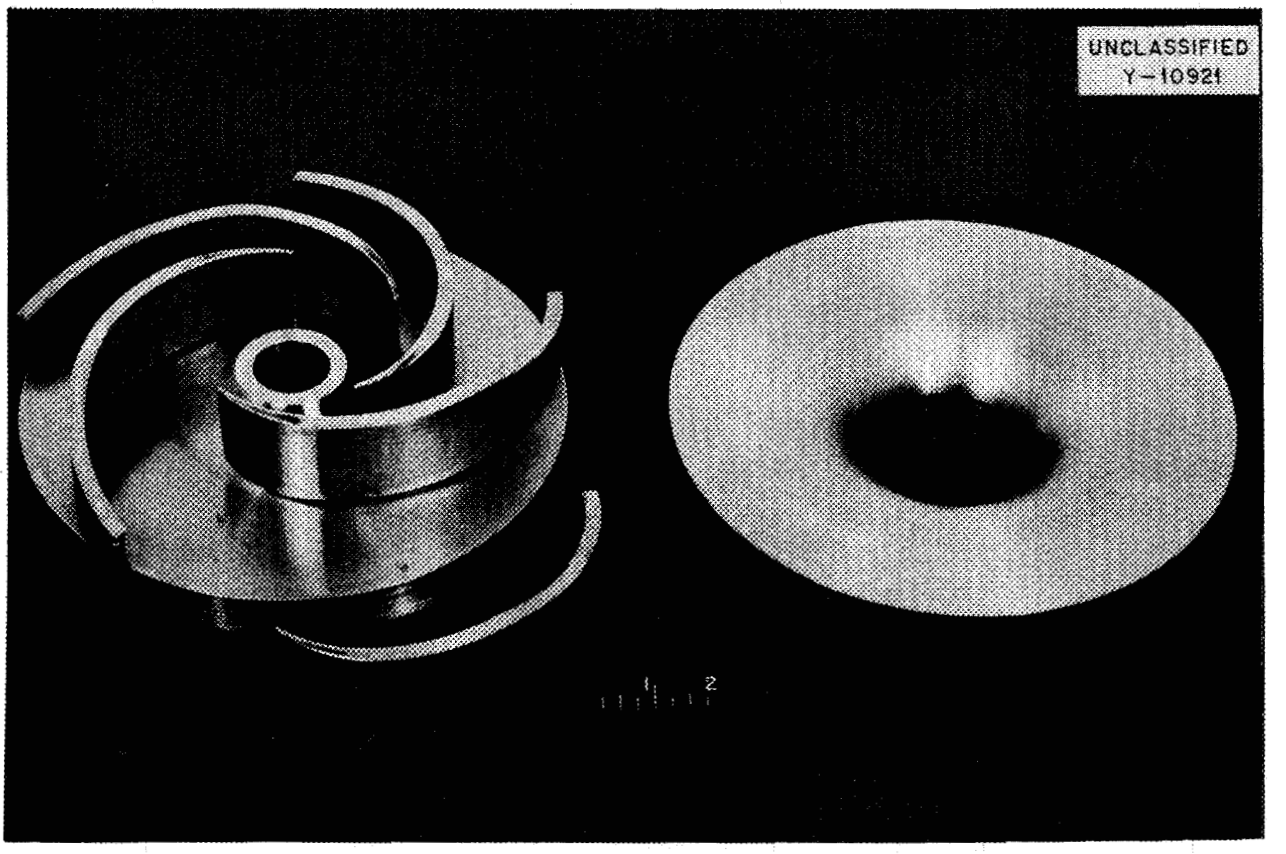

Fig. 1.2. Rough-Machined Parts of Inconel Impeller.

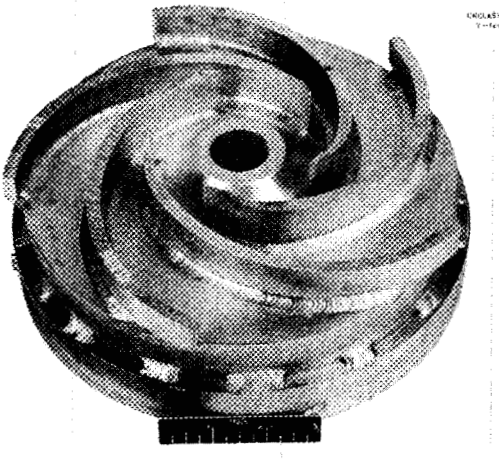

Fig. 1.3. Impeller After Heliarc Welding of Vanes to Drive-Shaft Hub. Impeller is tack welded to carbon steel strong-back.

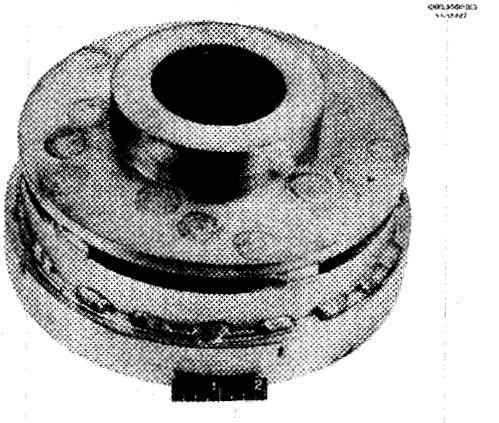

Fig. 1.4. Impeller with Fluid-Entrance Hub Plug-Welded into Position.

welded impeller was then removed from the strongback and machine finished. The completed assembly is shown in Fig. 1.5.

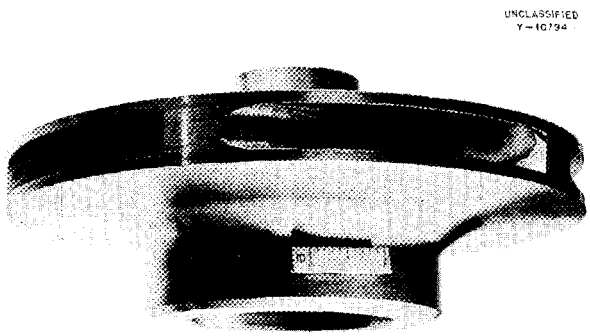

Fig. 1.5. Completed Impeller.

REACTOR SYSTEM COMPONENT LOOP

H. W. Savage A. G. Grindell
W. G. Cobb W. R. Huntley
ANP Division

The services of the K-25 Technical Division have been secured for constructing a large-scale system for circulating fluoride mixtures and testing reactor-system components. The major components of the system are the pump (mentioned above), a fuel-to-helium heat exchanger rebuilt from one originally purchased for the ARE, and two hairpin tubes purchased as spares for the ARE reactor core (Fig. 1.6). The system is operating isothermally at 1375 ± 25°F, with a flow rate of 20 gpm. The duration aim of the test, which started June 5, 1954, is 2000 hr. When the operation is terminated, the heat exchanger and hairpin tubes will be examined and evaluated in terms of corrosion, structural stability, etc.

FUEL RECOVERY AND REPROCESSING

D. E. Ferguson G. I. Cathers
Chemical Technology Division

The chemical process currently being considered[4] for recovery and decontamination of U^{235} from the ARE fuel mixture NaF-ZrF_4-UF_4 consists of dissolution of the fuel in an aqueous aluminum nitrate–nitric acid solution, solvent extraction with 5% tributyl phosphate in a kerosene diluent, and isolation on an ion-exchange resin column. In one solvent-extraction cycle a gross beta-decontamination factor of greater than 10^4 and uranium recovery of greater than 99.9% will be obtained.

Additional work has now been completed on dilute-TBP extraction of uranium solutions having high nitrate-salting strength. In batch countercurrent extraction experiments with six TBP concentrations in the range 1 to 30 vol %, with feed nitric acid concentrations of 0.5 and 3 M, ruthenium and total-rare-earth beta-activity decontamination factors improved with decreasing TBP concentration in the solvent (Fig. 1.7). The anomalous zirconium and niobium beta decontaminations obtained affected somewhat the gross-beta decontamination factor determinations in the low TBP concentration range. However, the best gross beta decontamination was obtained at a TBP concentration of 7.5% or less regardless of acidity. There was some evidence of a maximum in gross beta decontamination at 5 to 7.5 vol % TBP with a feed acidity of 0.5 M. Maximums were also observed in the zirconium and niobium decontamination factors at a low acid concentration.

Three extraction and scrub stages were used, with stoichiometrically neutral aluminum nitrate solution as the scrubbing agent. The salting strength was controlled by varying the aluminum nitrate content to obtain a uranium distribution coefficient of about 4 at the feed plate and 0.5 at the last scrub stage. Figure 1.8 is a plot of the distribution coefficients of the various activities at the feed plate. These data could be correlated, in general, with the conclusions drawn from Fig. 1.7.

Testing of the data by log-log plots (Figs. 1.9 and 1.10) showed that the ruthenium and total-rare-earth distribution coefficients have close to second-order dependence on TBP concentration at constant uranium distribution. The equilibrium constant for this case is represented by the equation

$$K = \frac{\text{D.C.}_{(\text{Ru } \beta \text{ or TRE } \beta)}}{(\text{TBP conc})^n}$$

where n, the dependence, is equal to 2. A least-squares analysis showed the average dependence for all data in the case of ruthenium activity to be 2.10 and in the case of total rare earths to be 1.95.

[4] D. E. Ferguson, G. I. Cathers, and O. K. Tallent, *ANP Quar. Prog. Rep. June 10, 1953*, ORNL-1556, p 101.

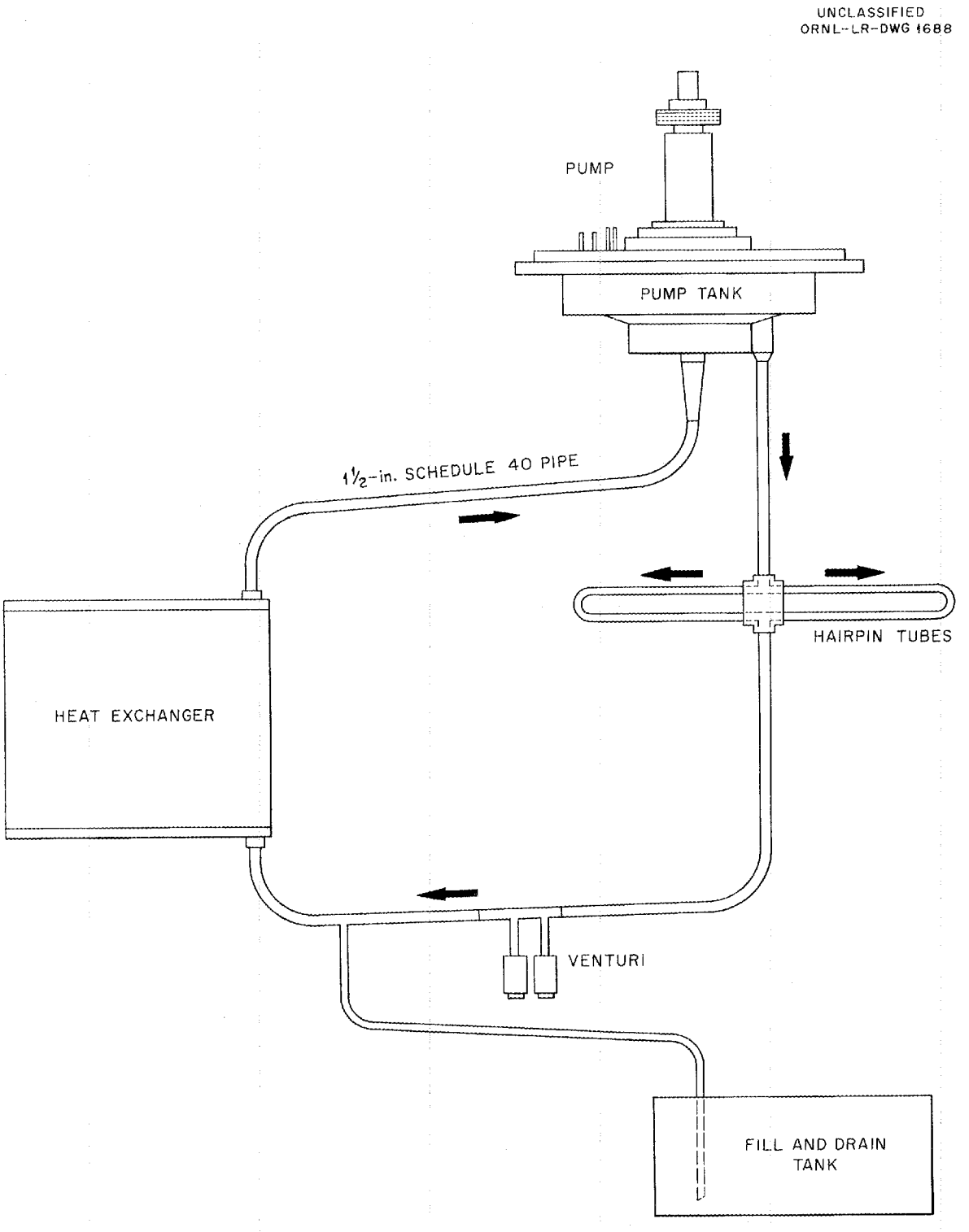

Fig. 1.6. Fuel-to-Helium Heat-Exchanger Test Loop.

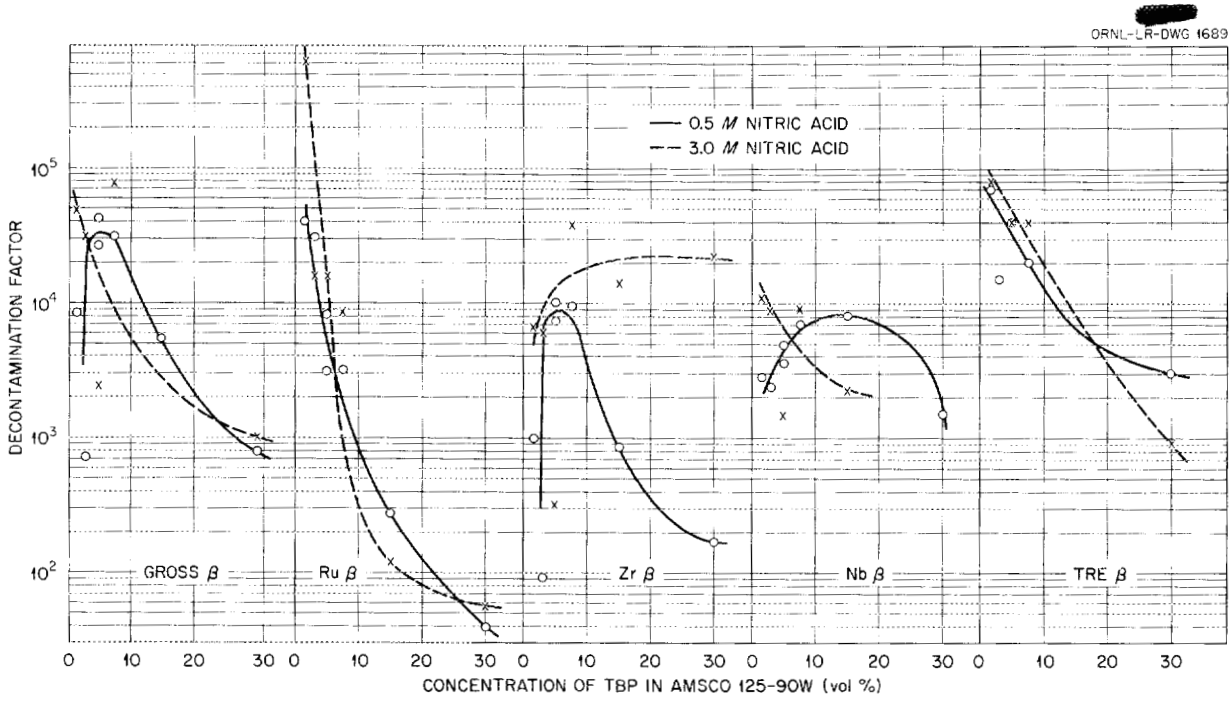

Fig. 1.7. Decontamination vs TBP Concentration in Solvent Extraction.

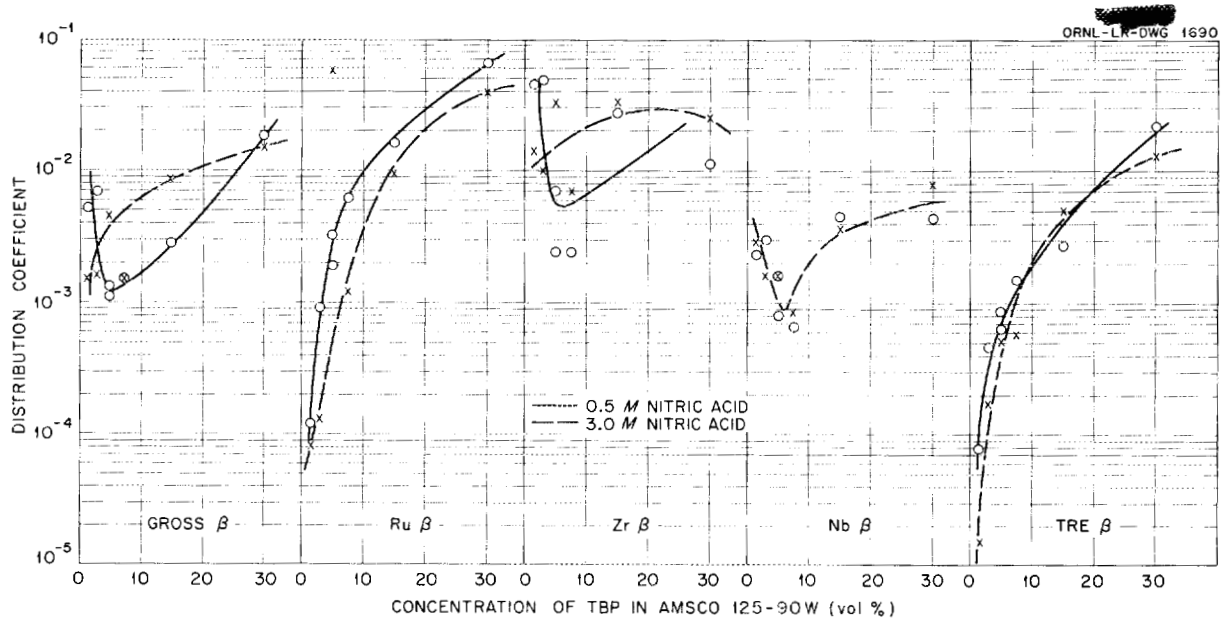

Fig. 1.8. Activity Distribution Coefficients at Feed Plate vs TBP Concentration in Solvent Extraction.

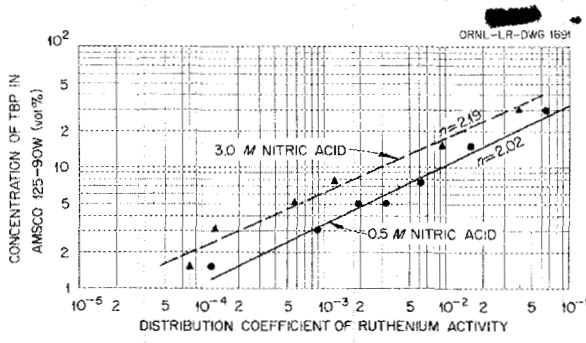

Fig. 1.9. Dependence of Ruthenium Activity on TBP Concentration.

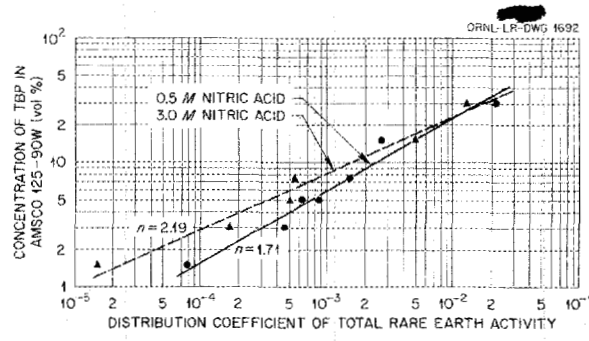

Fig. 1.10. Dependence of Total-Rare-Earth Activity on TBP Concentration.

2. EXPERIMENTAL REACTOR ENGINEERING

H. W. Savage
ANP Division

Development of components for in-pile radiation-damage test loops has continued. Major emphasis was placed on completing development and hot testing of the vertical-shaft, down-flow sump pump for operation of the initial in-pile loop in the LITR and on the design and fabrication of the first hot-test model of an air-driven horizontal-shaft sump pump. Further development work has been done on the centrifugally sealed pump, and it has been possible to decrease the size with no sacrifice in pump performance. Tests of hydraulic motors for driving in-pile pumps are being conducted. A compact heat exchanger has been designed for removal of fission heat from in-pile loops. Fabrication of the first exchanger is in progress.

Forced-circulation corrosion-testing loops are being designed for obtaining information on the corrosion of Inconel in high-velocity turbulent fluoride mixtures with large temperature differentials in the system. A test unit for ascertaining the mass-transfer characteristics of a sodium-beryllium-Inconel system was constructed and is now operating with turbulently flowing sodium and a high temperature differential.

Tests of the 1-Mw, regenerative fluoride-to-sodium heat exchanger were terminated and the test unit is being dismantled for examination. A 100-kw gas-fired furnace is being fabricated for testing to determine its suitability as a heat source for future heat-exchanger tests. If tests indicate that a heat source of this type will be satisfactory, a 1-Mw furnace will be developed.

A sampling device for taking an unrestricted number of samples of molten sodium from high-temperature systems was completed and several samples were successfully taken. Also, a satisfactory solvent for removing fluoride mixtures from Inconel was developed, tested, and put into general use.

Several bearing-material combinations were tested in molten fluorides under strictly controlled conditions. It was found possible to screen out some combinations, while others showed sufficient promise for further testing.

IN-PILE LOOP COMPONENT DEVELOPMENT

W. B. McDonald
ANP Division

Centrifugally Sealed Pump

J. A. Conlin
ANP Division

The deaeration and filling problems encountered with the previously described[1] centrifugally sealed pump have been essentially solved, and a series of modifications have been made for increasing pump performance and decreasing the over-all pump dimensions. Some success in reducing pump dimensions has been achieved, but no change in head and flow characteristics has been obtained.

A satisfactory method of deaeration was established by bleeding off 5 to 10% of the total pump flow from the pump discharge and returning it to the centrifugal-seal cavity. The centrifugal-seal cavity acts as a centrifuge for removing the gas from the fluid and replacing the bleed-off with clear fluid from the seal cavity. Deaeration at a low developed head is, as far as can be determined, complete. However, as the developed head is increased by increasing pump speed, deaeration becomes less satisfactory; in fact, some aeration occurs slowly when the pump speed is increased after complete deaeration at low speed. At high speed the gas pressure in the seal cavity is above the pump suction pressure by about 65% of the developed head. After an investigation it was concluded that gas (in this case, air) is dissolved in the fluid (water) under pressure in the seal cavity and then comes out of solution in the form of small bubbles at the low pressure (pump suction) portion of the loop. However, the mechanism of aeration of the water is not definitely known. It is possible that the turbulent surface of the liquid in the seal cavity at high pump speed may increase the rate of solution of the air in the water or even entrap air in the form of bubbles which then pass into the system through the seal. The precise degree of aeration has not been measured, but it is not very great, and, of course, the extent of aeration which would occur

[1] W. B. McDonald *et al.*, *ANP Quar. Prog. Rep. Mar. 10, 1954*, ORNL-1692, p 15.

with fluoride mixtures under a helium gas is not known.

The introduction of the deaeration bleed into the seal cavity caused the seal to leak when fluid was added to the system. This seal leakage was corrected by the addition of a deflector to keep the bypass fluid away from the junction between the inner tube in the seal cavity and the pump impeller.

In its present state, the pump may be started empty in a horizontal position and filled by simply adding water to the system, with care being taken not to overfill the system. A series of tests is now under way for developing filling and operating techniques that will be satisfactory for operation of the pump with fluoride mixtures.

In an attempt to improve pump performance, an impeller that had been modified by drilling the flow ports tangentially to the core was tested. However, the resulting performance was somewhat worse instead of better.

A pump casing with an unconventional discharge passage was tested in an attempt to reduce the over-all diameter of this or any similar pump. The modified casing (Fig. 2.1) has a narrow annular passage around the outside diameter of the impeller and a volute-like passage formed in an axial direction from the annulus. The volute turns, at the water deflector (cut-water), into a passage which discharges in an axial direction parallel to the pump inlet at a maximum distance from the axis of the pump no greater than the outside diameter of the annulus around the impeller.

Performance of this casing was slightly better than that of the casing used previously which had a conventional annular collector ring and a tangential discharge nozzle. However, the results were inconsistent because of the aeration conditions, and it is believed that under identical conditions an equally well-designed conventional casing would show slightly better performance than that of the modified casing. The principal advantage in the axial-discharge design is that the discharge nozzle does not extend radially beyond the pump casing. However, this advantage must be balanced by the greater difficulty of fabricating such a casing. The velocity-to-head conversion could probably be improved by modifying the cut-water to extend over the impeller and thereby obtain more benefit from the high fluid velocity in the annulus.

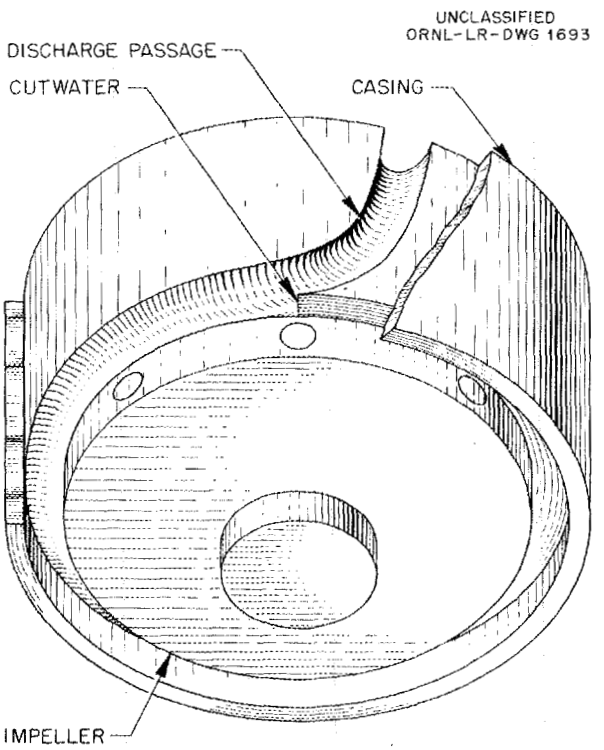

Fig. 2.1. Modified Axial-Discharge Pump Casing.

Horizontal-Shaft Sump Pump

D. F. Salmon
ANP Division

A horizontal-shaft air-driven sump pump for hot testing with a fluoride mixture is being assembled (Fig. 2.2). A plastic model of the pump was tested with 1-1,2-2 tetrabromoethane (sp gr ~ 3, $\mu \sim 9$ cp). Priming was accomplished by periodic sudden applications of pressure in the sump to force slugs of liquid into the pump inlet. A longer time was required to degas this liquid than water. For faster degassing, part or all of the flow was directed through the sump instead of directly into the pump inlet.

Vertical-Shaft Sump Pump

D. R. Ward
ANP Division

Two vertical-shaft sump pumps[1] were tested with sodium at 1500°F and delivered to the Solid State Division for operation in in-pile loop tests. Two identical pumps are being retained for more testing

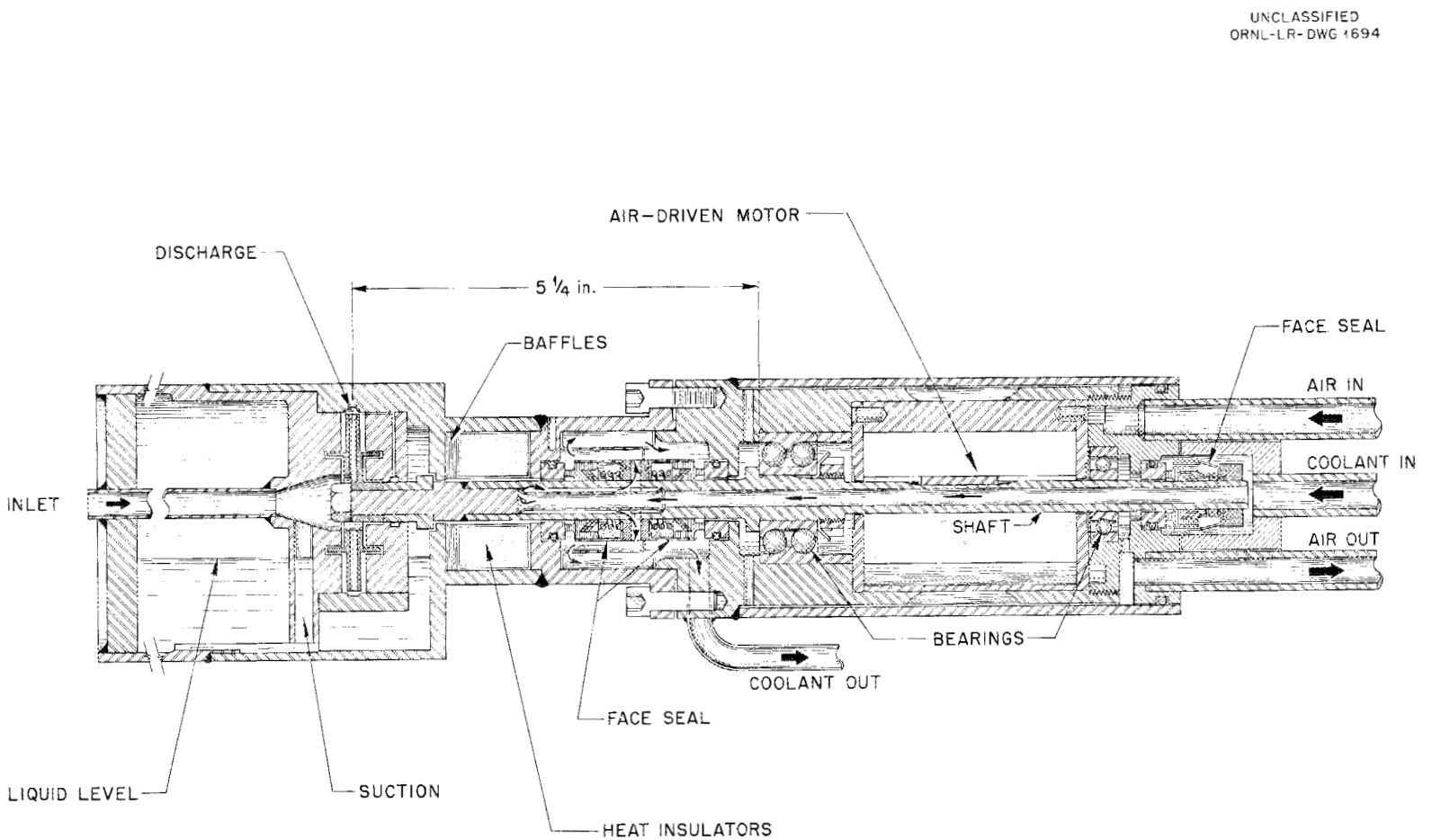

Fig. 2.2. Horizontal-Shaft Air-Driven Sump Pump for an In-Pile Loop.

and development aimed at simplifying fabrication and increasing pump capacity in anticipation of more severe requirements, both in experimental test loops and in other in-pile loop tests.

Hydraulic Pump Drives

J. A. Conlin
ANP Division

Hydraulic motors are being considered as possible in-pile pump drives because they have high starting torque and high power output from a very small unit, and there might be a possibility of using the hydraulic oil both as a power source and as a coolant. Two commercially available motors were ordered – a gear type and an axial-piston type. Since neither of these was immediately available, an axial-piston motor similar in design but of much larger capacity than the one ordered was put on a no-load duration test to determine its operating characteristics. The normal maximum operating speed of this motor is 3600 rpm; however, the test was run at the approximate in-pile pump speed of 5000 rpm.

The motor completed a 500-hr test with no indication of trouble except for a constant shaft oil-seal leak of 0.47 cc/hr. The seal leakage was aggravated by two things. First, during initial tests the shaft, for reasons unknown, became excessively hot. Second, it was necessary to bypass about 0.5 gpm of oil through the motor casing and bearings to prevent excessive motor temperatures at the high speed. This caused a 0.7- to 1.0-psig back pressure against the seal, which was a rubber-lip type that was not intended for use under pressure. An operating oil temperature of between 100 and 120°F was maintained during the test.

Fluoride-to-Water Heat Exchanger

D. F. Salmon
ANP Division

A heat-extraction unit is needed for in-pile test loops which is small enough to be inserted in the reactor hole and does not require a complicated external circuit of auxiliaries, since shielding for external apparatus is cumbersome and expensive. A concentric-tube double-wall heat exchanger has been designed that has a stagnant annulus of fluoride mixture between circulating streams of molten fluoride mixture on one side and cooling water on the other. The stagnant mixture will be solid at the water wall and molten at the circulating-fluoride-mixture wall, and there will be a temperature drop of approximately 1000°F radially across the annulus. The circulating cooling water will either be dumped or cooled outside the reactor.

The exchanger is designed around an Inconel-sheathed electrical tubular heater for preheating the unit prior to starting circulation of the fluoride mixture stream. The hairpin design to permit differential thermal expansion is shown in Fig. 2.3. With the fluoride mixture NaF-KF-LiF [11.5-42.0-46.5 mole %, K (solid) $\simeq$ 3.5 Btu/hr·sq ft (°F/ft) and K (liquid) $\simeq$ 2.6 Btu/hr·sq ft (°F/ft)] in the annulus, approximately 12 kw/ft can be removed from a 1500°F stream of fluoride mixture $NaF\text{-}ZrF_4\text{-}UF_4$ (50-46-4 mole %) and adsorbed by the water stream.

FORCED-CIRCULATION CORROSION LOOPS

W. C. Tunnell
ANP Division
W. K. Stair, Consultant
J. F. Bailey, Consultant
University of Tennessee

Previous attempts to circulate fluoride mixtures at simultaneously high velocities and large temperature differentials were only partially successful.[2] Therefore a small loop is being built that is designed to have a temperature differential of about 135°F, with a maximum temperature of 1500°F, and a Reynolds number of about 4500. Electrical resistance heating of the 0.300-in.-OD, 0.025-in.-wall container tube will be used, but the power consumption will be larger than in the previous apparatus. This loop will be used to confirm engineering design estimates of performance, but it may not yield significant metallurgical information.

The Metallurgy Division has provided specifications for six additional loops. Three loops are to have maximum Reynolds numbers of 10,000 and temperature differentials of 100, 200, and 300°F, and the other three loops are to have temperature differentials of 200°F and Reynolds numbers of 1,000, 3,000, and 15,000. Heat economizers will

[2] D. F. Salmon, *ANP Quar. Prog. Rep. Mar. 10, 1954*, ORNL-1692, p 19.

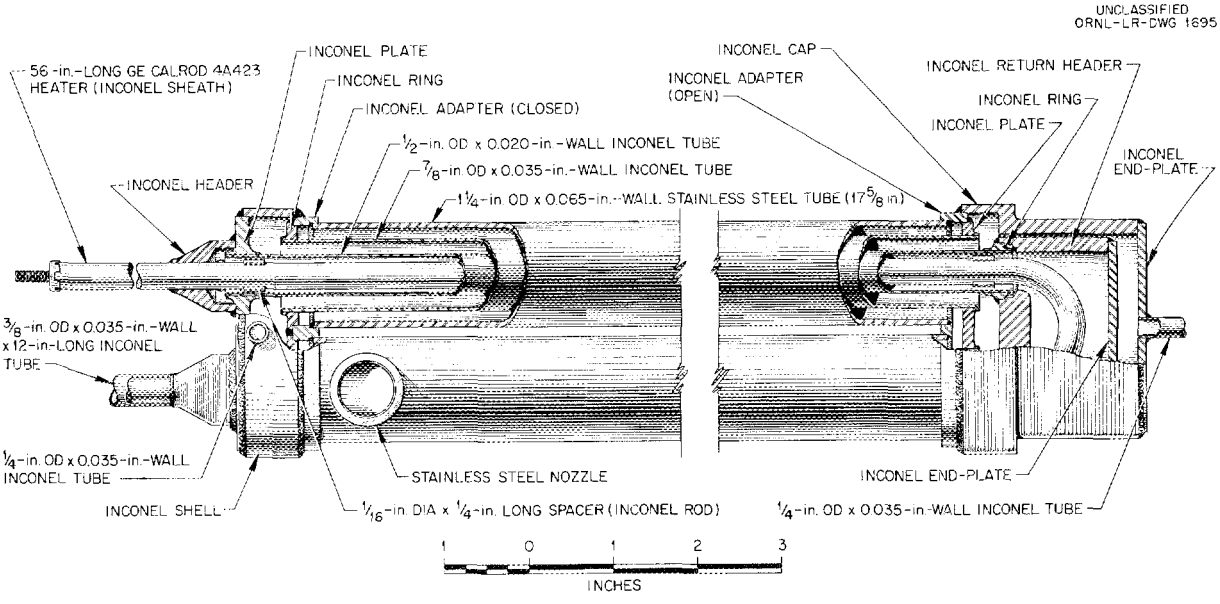

Fig. 2.3. Concentric-Tube Double-Wall Heat Exchanger for Use Inside a Reactor Hole.

be used, in at least the first three units, to conserve electric power, space, and fabrication costs.

The unit with a 300°F ΔT and a Reynolds number of 10,000 is designed to dissipate 80 kw of heat to air and therefore to have an 80-kw reheating capacity; resistance heating will be used. The unit will also include a vertical-shaft sump pump[3] for circulating the molten fluoride mixture at 5000 lb/hr.

SODIUM-BERYLLIUM-INCONEL MASS-TRANSFER TEST

L. A. Mann
ANP Division

A test unit has been constructed for investigating mass transfer of beryllium to Inconel in a flowing sodium system under conditions which approach those proposed for the Reflector-Moderated Reactor. A series of tests will be run to determine whether it will be necessary to protect the beryllium reflector-moderator from the sodium coolant during operation of the reactor.

The test unit is designed to operate with a sodium flow of 3 gpm through a venturi-shaped beryllium insert with a minor diameter of about 0.25 in. The sodium temperature will range from 1200°F maximum (at the beryllium) to less than 900°F minimum. The Reynolds number will be about 100,000 at the beryllium minor diameter and about 50,000 at the coldest section of the loop.

FLUORIDE-TO-SODIUM HEAT-EXCHANGER TEST

A. P. Fraas R. W. Bussard
R. E. MacPherson
ANP Division

As was previously reported,[4] test operations on the 1-Mw regenerative fluoride-to-sodium heat exchanger were interrupted by failure of the sodium heater coil. The coil was replaced and an attempt was made to continue operation of the equipment to obtain endurance information. However, a leak developed from the sodium side of the heat exchanger into the fluoride side, and the unit has been shut down for dismantling. The heat exchanger will be delivered to the Metallurgy Division for examination.

[3] W. B. McDonald *et al.*, *ANP Quar. Prog. Rep. Mar. 10, 1954*, ORNL-1692, p 15.

[4] R. E. MacPherson, H. J. Stumpf, and J. G. Gallagher, *ANP Quar. Prog. Rep. Mar. 10, 1954*, ORNL-1692, p 18.

GAS-FURNACE HEAT-SOURCE DEVELOPMENT

A. P. Fraas R. W. Bussard
R. E. MacPherson
ANP Division

Past experience and future plans for the testing of prototypes of the Reflector-Moderated Reactor intermediate heat exchanger have indicated a need for high-capacity, compact heat sources. As a step in this direction, a loop is currently being assembled to check the operating characteristics of a 100-kw gas-fired furnace. This unit, if operable, will provide a basic design capable of being enlarged to accommodate the large heat loads which will be demanded in the near future. The furnace, as shown in Fig. 2.4, is a drastic departure from conventional furnace design. It employs natural gas and pressurized air feed, the air being preheated to 1000°F before entry into the combustion zone, by a countercurrent heat exchanger, with flue gases. The flame temperature is expected to approach 4000°F. No ceramic lining is utilized in the combustion chamber; instead, the design provides for cooling of all exposed metal surfaces by the normal sodium flow through the furnace. The combustion chamber is a cylindrical opening 6 in. in length and 5 in. in diameter. The sides of the chamber are formed by sodium coils and the ends by the gas and air inlet arrangements. After combustion, the flue gas passes over the coils to give up its heat to sodium and is then channeled into a spiral discharge duct where it flows countercurrent to feed air to provide an economizer arrangement.

If operability is proved in this test, it is planned to construct a 1-Mw furnace employing the same basic design. This furnace will serve as the heat source for tests of the second prototype of the

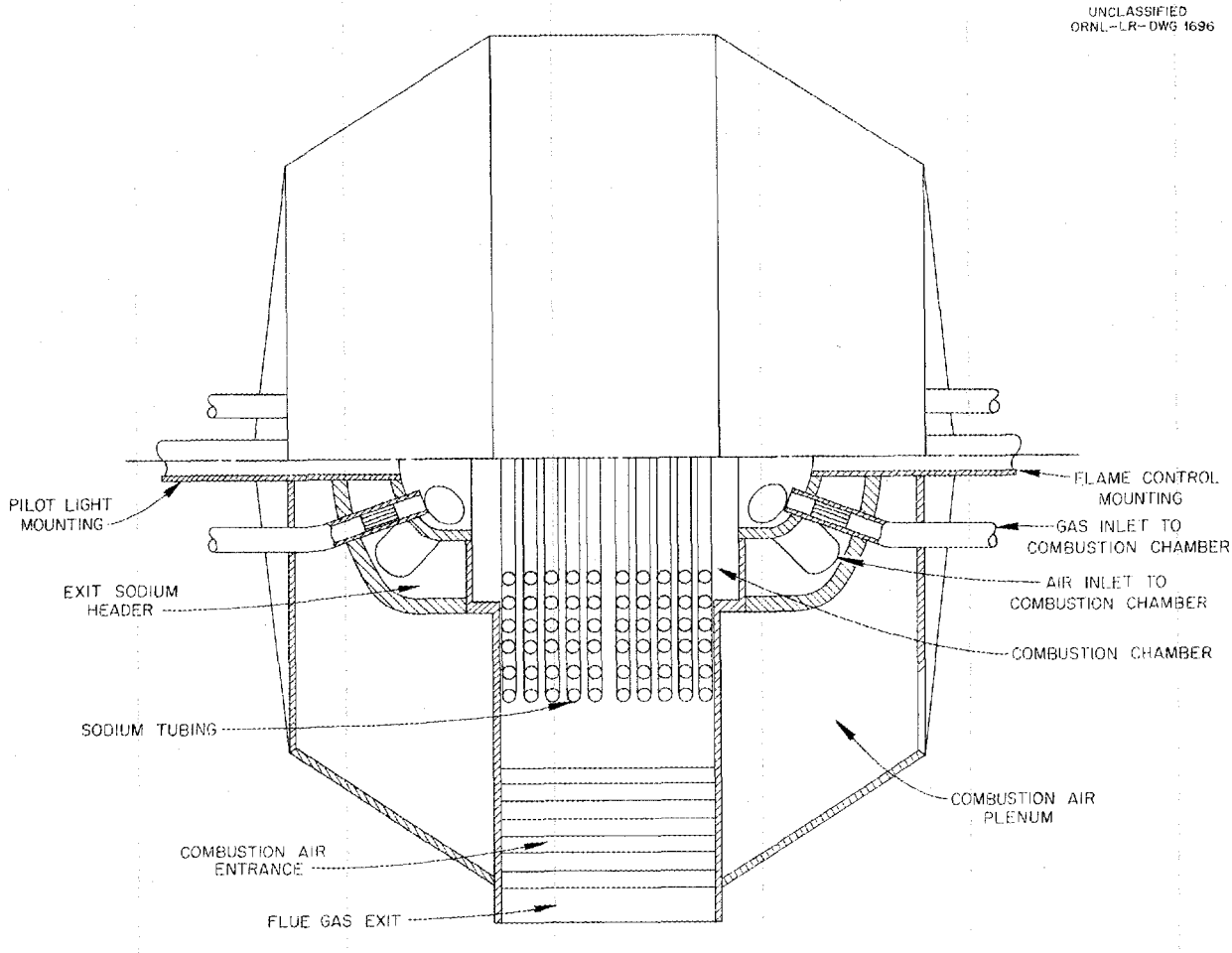

Fig. 2.4. 100-kw Gas-Fired Furnace.

Reflector-Moderated Reactor intermediate heat exchanger.

SODIUM SAMPLER

L. A. Mann
ANP Division

A unit has been designed, constructed, and test-operated for repetitive sampling of molten sodium at temperatures of up to 1500°F. A device is included in the unit for separating the sodium from its oxide by flotation in mercury and for furnishing the sodium and oxide in separate flasks for titration. The basic method reported by Pepkowitz and Judd[5] for analyzing Na_2O in Na is used, and the sampler is a simplified adaptation of a similar device developed at KAPL.

REMOVAL OF FLUORIDE MIXTURES FROM EQUIPMENT

L. A. Mann
ANP Division

A solvent for $NaF\text{-}ZrF_4$ and $NaF\text{-}ZrF_4\text{-}UF_4$ mixtures has been developed, tested, and put into general use. The solution has the composition (by weight): 15% HNO_3, 5% H_2BO_3, 4% $Pb(NO_3)_2$, 76% H_2O. It is used at a temperature of 180 to 200°F, with the solution either flowing or being stirred. A hood is required because of the NO_2 fumes evolved. An approximately $\frac{1}{8}$-in. coating of $NaF\text{-}ZrF_4\text{-}UF_4$ on Inconel was completely removed (visual inspection) in 2 hr, with an Inconel corrosion rate of approximately 1 mg/sq in. hr. In further tests, $NaF\text{-}ZrF_4$ was completely removed in 10 min except from very small openings which took longer to clean. This cleaning method is, of course, not recommended for thin-walled tubing or for equipment to be subsequently tested or examined for corrosion.

BEARING-MATERIALS TESTS

W. C. Tunnell
ANP Division

Tests have continued, with the equipment previously described,[6] in attempts to find combinations of materials usable for journal bearings in high-temperature fluoride mixtures. The early tests showed metal build-up between the test specimens. It is believed that the build-up material was the product of corrosion of the stainless steel containers. Recent tests have been conducted in Inconel containers, and although there is still some evidence of metal build-up, the specimens remain sufficiently clean during the test period so that wear patterns can be obtained. Figures 2.5 and 2.6 are photographic records of some of the test results; Fig. 2.5 shows the wear that resulted in operating a tungsten carbide pin against a tungsten carbide plate, and Fig. 2.6 shows the comparatively little wear that results when a tungsten carbide pin was tested against a titanium carbide plate. Additional records that are made of each test include the surface finish, flatness, and hardness values of each specimen, before and after each run, and a Faxfilm replica of the surface condition of the pin and of a typical section of the plate. (Faxfilm is a surface evaluation process furnished by the Brush Development Company. A clear solvent is applied to the surface to be reproduced. A clear plastic film is then pressed against the surface and solvent, and after a few seconds for drying, the duplicate surface is lifted off with the plastic film. This film is then mounted on a slide and can be projected.) The fluoride mixture is analyzed after each run for corrosion products to determine whether constituents of the specimens have been introduced into the fluoride mixture. No corrosion products have yet been found in the fluoride mixtures analyzed.

The materials tested and the test results are shown in Table 2.1, which lists all the combinations tested to date. Of the materials tested, Cr_3C_2 appears to be a poor possibility for use as a bearing material because it shows excessive wear. Hot-pressed beryllium oxide and Al_2O_3 have been eliminated as possible bearing materials because of excessive corrosion and/or erosion. Tungsten carbide and Kennametal titanium carbide appear to be possible bearing materials; both materials showed very little wear and very little corrosion in the tests. These materials also showed good wear resistance when tested in sodium, as reported by Vail.[7] Boron carbide also indicated promise in wear and corrosion resistance.

[5] L. P. Pepkowitz and W. C. Judd, *Determination of Sodium Monoxide in Sodium*, KAPL-P-452 (Oct. 1952); L. P. Pepkowitz, W. C. Judd, and R. Downer, *Determination of Sodium Monoxide in Sodium, An Addendum*, KAPL-972 (Aug. 5, 1953).

[6] W. C. Tunnell *et al.*, *ANP Quar. Prog. Rep. Mar. 10, 1954*, ORNL-1692, p 22.

[7] D. B. Vail, *Compatibility of Materials in Liquid Metals*, KAPL-589 (Aug. 18, 1951).

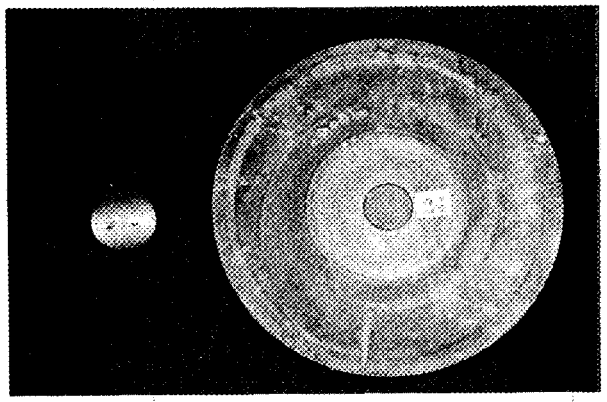

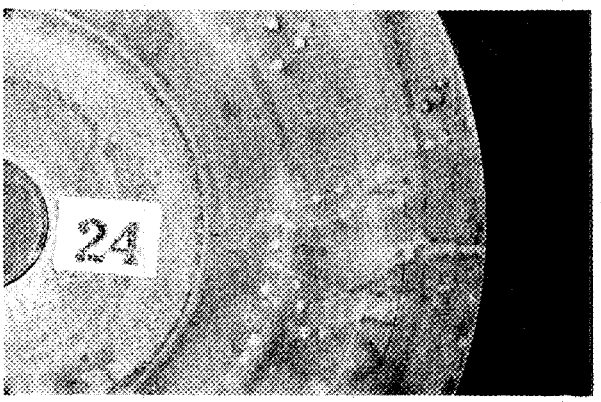

Fig. 2.5. Tungsten Carbide Pin Operated Against a Tungsten Carbide Plate in Contact with a Fluoride Mixture in an Inconel Container at 1200°F for 2 hr.

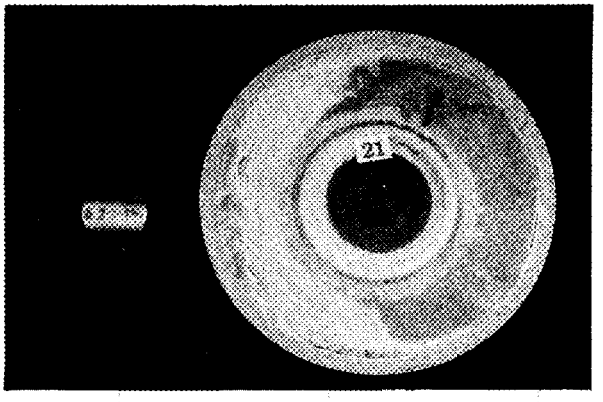

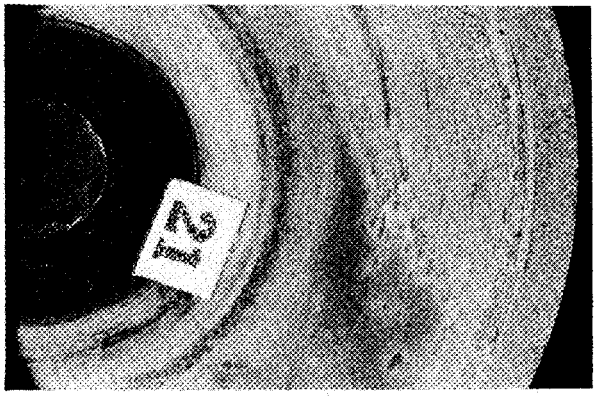

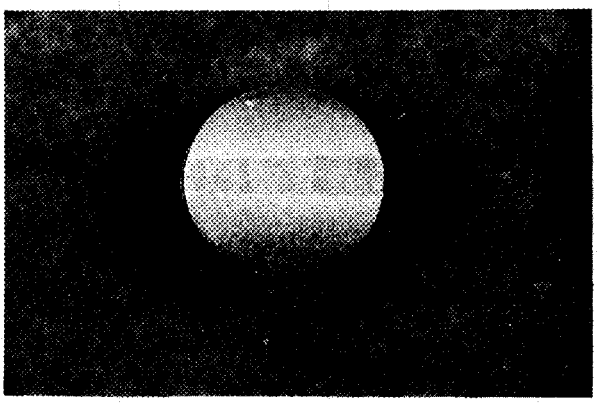

Fig. 2.6. Tungsten Carbide Pin Operated Against a Titanium Carbide Plate in Contact with a Fluoride Mixture in an Inconel Container at 1200°F for 2 hr.

TABLE 2.1. RESULTS OF TESTS OF BEARING-MATERIALS COMBINATIONS EXPOSED TO $NaF-ZrF_4-UF_4$ AT 1200°F FOR 2 hr IN BEARING-MATERIALS TESTER*

PIN MATERIAL	PLATE MATERIAL											RESULTS
	Hot-Pressed BeO	BeO-Ni	WC	Al_2O_3	Al_2O_3-MgO	B_4C	Cr_3C_2	TiC-Ni	TiC-Co	Graphitar	High-Density Graphite	
Hot-pressed BeO	29		27	X								Eliminated
BeO-Ni	X			X								
WC	X		21	30		25		23	24	31	28	
Al_2O_3	X			X								Eliminated
Al_2O_3-MgO	X			X								
B_4C	X			X								
Cr_3C_2	X		22	X		33		18 19				
TiC-Ni	X		20	X					26			
TiC-Co	X			X								
Graphitar	X			X								
High-density graphite	X			X								

*The numbers are test serial numbers. The notation X indicates unsatisfactory combinations. Blank spaces mean not yet tested or results not yet available.

ROTARY-SHAFT SEALS

W. C. Tunnell P. G. Smith
ANP Division

Tests are under way to determine the feasibility of sealing fluoride mixtures in an in-pile pump with a packed seal on a horizontal shaft. One packing that was tested consisted of a mixture of 95 wt % Asbury Graphite and 5 wt % MoS_2 retained by bronze wool at each end of a stuffing box. The stuffing box was $3\frac{1}{2}$ in. long with a $\frac{1}{4}$-in. annulus. For this test, the apparatus was operated for a total of 382 hr, and the test was then terminated because a heater burned out as a result of leakage of the fluoride mixture. Leakage from this seal (test No. 33)[8] was at the rate of 0.7 cc/day throughout the test. Postrun examination revealed only slight shaft wear at regions where the packing retainers were located and in the gland region. The pot showed no sign of packing leakage from the hot end of the seal.

In another test of the same packing material (test No. 35), an inert blanket was installed on the cold end of the seal to protect the section of the shaft under the gland from wear by oxidation products. A pillow-block bearing was installed on

[8]W. C. Tunnell *et al.*, *ANP Quar. Prog. Rep. Mar. 10, 1954*, ORNL-1692, p 26.

the ½-in. shaft to improve alignment. The type 316 stainless steel shaft was coated with 1/16-in.-thick Colmonoy ground to a 20-μin. finish. The test apparatus was operated for 603 hr with NaF-ZrF_4-UF_4 at a temperature of 1250 to 1300°F and with a pressure of 2 psi on the seal. The leakage rate from the seal was about 0.5 cc/day and appeared to be mostly packing material. The power requirement of the seal varied from 100 to 200 watts. Termination was caused by shaft seizure.

Postrun examination revealed shaft wear of about the same magnitude as in test No. 33. A section of the shaft surface at the hot end appeared to have peeled off or to have corroded slightly. Analysis of a sample from the pot showed that an unsatisfactorily large amount of the packing material had leaked into the pot. There was evidence of corrosion on the hot end of the gland, which indicates a need for an inert-gas blanket between the gland and the stuffing box, as well as between the gland and the shaft. Another test is planned for the near future with an improved inert-gas blanket and improved gland alignment.

Seal test No. 31 was the same as seal test No. 28,[8] except that Asbury Graphite was substituted for the National Carbon Graphite in the 10 wt % BaF_2–90 wt % graphite packing material. The results obtained were very similar to those for test No. 28 in that excessive leakage occurred. The duration of the test was 165 hr.

3. REFLECTOR-MODERATED REACTOR

A. P. Fraas
ANP Division

Components of the proposed 60-Mw Circulating-Fuel Reactor Experiment (CFRE) are now being designed and constructed and are to be tested to determine operational characteristics. Plans are being made for tests of full-scale fuel pumps and of elements of full-scale heat exchangers. Also, thermal-stress cycling tests for both Inconel and beryllium are to be performed. A fairly complete detailed stress analysis of the reactor is well under way. A series of charts was prepared to facilitate the determination of the temperature distribution and thermal stresses in media having uniformly distributed volume-heat sources.[1] Also, a comparison of lithium- and zirconium-base fluoride fuels for aircraft reactors was made that indicates the definite advantages to be gained through the use of the lithium-base fuel.

Estimates of the xenon-poisoning effect in the Reflector-Moderated Reactor have confirmed the great incentive for removing the xenon during operation. Therefore an experiment is being planned to determine whether the xenon can be adequately purged. Studies of reactor dynamics indicate that the design of the Reflector-Moderated Reactor precludes the possibility of the coupling of mechanical oscillations with nuclear oscillations to create antidamped oscillations that would destroy the reactor.

Calculations of a set of 48 related reactors are well under way. The effects of reactor dimensions on concentration of U^{235} in the fuel, on total U^{235} investment, on outside peak-to-average power density in the core, and on the per cent thermal fissions in the core are presented.

A COMPARISON OF LITHIUM- AND ZIRCONIUM-BASE FLUORIDE FUELS

A key decision in the design of a circulating-fuel reactor is the choice of the fluoride fuel to be employed. Of the fuels that currently seem most promising, the sodium-zirconium-uranium fluoride fuel has the poorest physical properties but would be the easiest and cheapest to prepare, while the sodium-lithium-potassium-uranium fluoride fuel has the best physical properties but would require Li^7 – an expensive material. The properties of greatest interest for these two fuels for uranium concentrations of 25 lb/cu ft are given in Table 3.1.

In a comparison of the two fuels it is evident that the lithium-base mixture has both a lower melting point and a much lower vapor pressure. The lower vapor pressure is particularly advantageous in that it should eliminate the many troubles experienced with sublimation of ZrF_4

[1] F. A. Field, *Temperature Gradient and Thermal Stresses in Heat Generating Bodies*, ORNL CF-54-5-196 (May 21, 1954).

TABLE 3.1. PHYSICAL PROPERTIES OF TWO FLUORIDE FUELS CONTAINING 25 lb OF U^{235} PER CUBIC FEET OF FLUORIDE MIXTURE AT 1472°F

PHYSICAL PROPERTIES	$NaF\text{-}ZrF_4\text{-}UF_4$ (50-44.5-5.5 mole %)	$NaF\text{-}LiF\text{-}KF\text{-}UF_4$ (11-45-41-3 mole %)
Melting point, °F	970	850
Vapor pressure at 1500°F, mm Hg	8	<1
Prandtl number, $C_p\mu/K$	3.71	1.24
Viscosity,* cp	6.5	2.5
Thermal conductivity,* Btu/hr·sq ft (°F/ft)	1.25	1.95
Specific heat,* Btu/lb	0.295	0.40
Density,* lb/cu ft	203	132

*Data supplied by H. F. Poppendiek.

and the formation of high-melting-point deposits on the roofs of expansion tanks, in pressure gage lines, etc. The higher viscosity of the zirconium-base fuel gives a lower Reynolds number in the reactor core and hence a more severe boundary-layer heating problem; the temperature differential between the peak temperature in the boundary layer and the mean fuel temperature is about 50% greater than that for the lithium-base fuel.[2] Thus the zirconium-base fuel, with its higher viscosity and its much higher vapor pressure, would be more likely to give trouble with boiling in local hot spots and hence, conceivably, violent fluctuations in power.

Recent multigroup calculations show that for a representative core geometry the critical mass for a lithium-base fuel will be about 16% greater than that for a zirconium-base fuel because of thermal-neutron absorption in the potassium. The reactor under consideration had an 18-in.-dia core with a 12-in.-thick reflector and a 4-in.-thick fuel annulus, and the beryllium in the island and reflector was canned in 0.010-in.-thick Inconel. The core shells were $\frac{1}{8}$-in.-thick Inconel.

A further consideration in favor of the alkali-metal fluoride fuels is based on radiation damage; the alkali-metal fluorides are very stable compounds, and their recombination rate can be expected to be larger than that for ZrF_4.

One of the most important design criteria is the effect of the physical properties of the fuel on the heat exchanger. While many design compromises are possible, the most important of these can be deduced from Fig. 3.1, which was prepared for a series of fuel-to-NaK heat exchangers. The pressure-stress limitations are usually controlling, and if the same allowable stresses are to be used, the pressure drop must be held constant. The designs represented by Fig. 3.1 were prepared by determining the number of tubes required for each tube length to give a 50-psi pressure drop through the tubes in the NaK circuit. The tube spacing was then adjusted to give a 40-psi drop in the fuel passages. As shown in Fig. 3.1, the number of tubes in the heat exchanger must be increased to provide more flow passage area as the tube length is increased.

The curves for the temperature differential between the fuel and NaK are instructive. If the temperature difference for the zirconium-base fuel is to be the same as that for the lithium-base fuel, the tube length must be increased, for example, from 6.0 to 7.6 ft if the temperature difference is kept at 91°F. This would require a 15% increase in the number of tubes. The Reynolds number would drop from 4850 to 2100, that is, from a value well within the turbulent range to one likely to give laminar flow and hence even poorer heat transfer than that estimated. If the same tube spacing were used and a higher pressure drop accepted, the comparison would be less unfavorable in most respects. However, the pumping horsepower would need to be increased by 50% with the zirconium-base fuel, and many stresses, such as those in the NaK outlet header sheets, would be more than doubled.

The effects of heat-exchanger volume on both shield weight and the activation of the NaK in the secondary circuit are vitally important. The weight of the reactor, heat exchanger, and reactor shield assembly, together with the radiation dose from the NaK in the secondary circuit at a point 50 ft from the engines, is given in Fig. 3.2 as a function of the temperature loss in the fuel-to-NaK heat exchanger. The data are for a 200-Mw reactor with a shield designed to give 10 r/hr at 50 ft from the reactor at full power. It can be seen that for a given design temperature loss the lithium-base fuel is markedly superior to the zirconium-base fuel in that it gives one-half the radiation dose and a 6000-lb saving in shield assembly weight.

The limitations on high-temperature heat-exchanger design imposed by pressure stresses merit further explanation. The many closely spaced holes in the header sheets generally make the header sheets much less strong than the thin tube walls. In the spherical-shell heat exchanger for the Reflector-Moderated Reactor, the NaK must enter the heat exchanger at about 100 psi to take care of the roughly 50-psi pressure loss in the heat exchanger, the 40-psi loss in the radiators, and the 10-psi loss in the connecting lines. Most of the estimated 50-psi pressure drop in the fuel system occurs in the heat exchanger. On this basis the pressure difference across the header sheet at the hot end is less than 10 psi, while that at the cold end is about 100 psi. Fortunately, the strength of Inconel is about five times greater

[2] H. F. Poppendiek and L. D. Palmer, *Forced Convection Heat Transfer in Pipes with Volume Heat Sources Within the Fluids*, ORNL-1395 (Dec. 2, 1952).

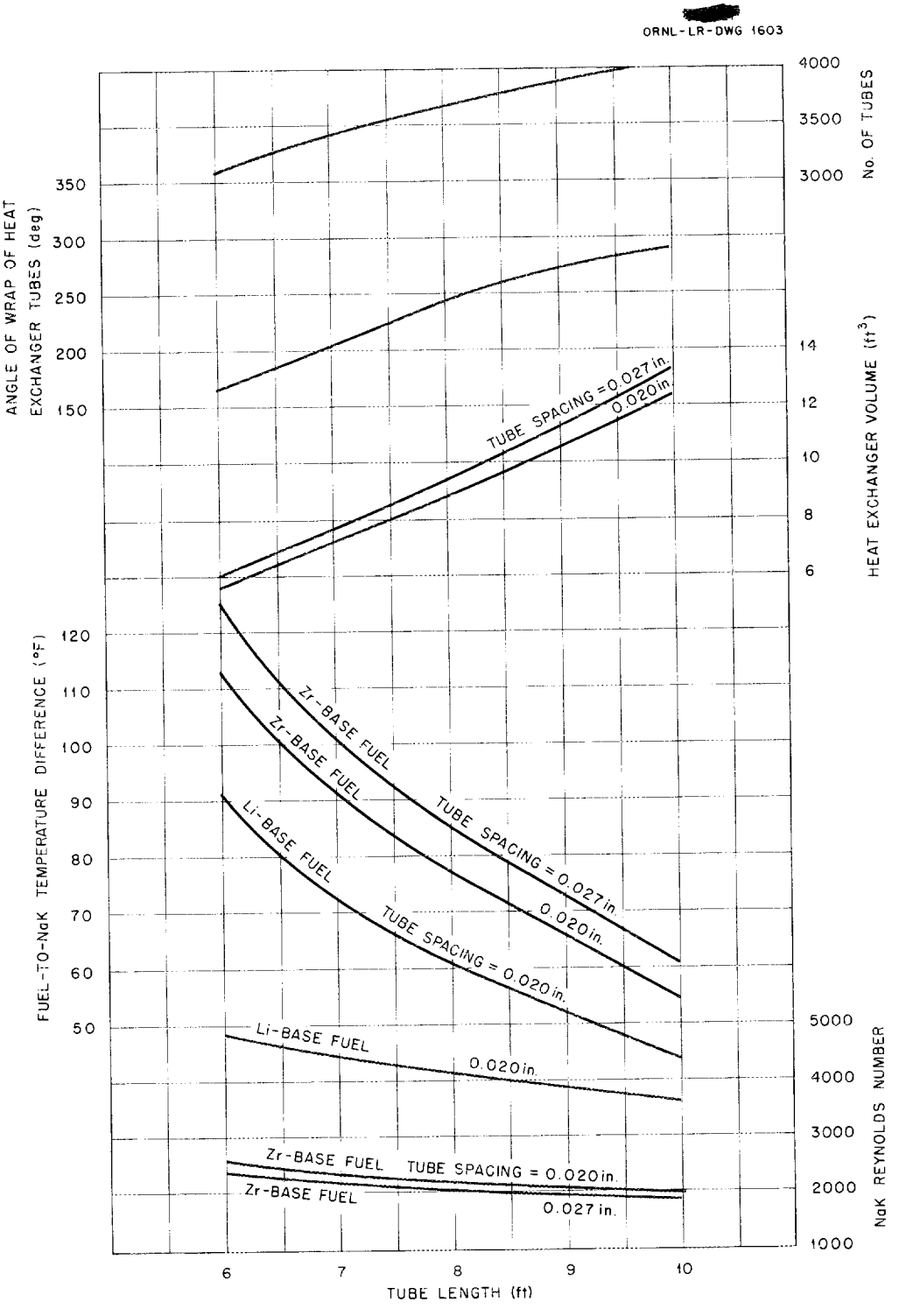

Fig. 3.1. Effects of Tube Length on Design Variables for a 60-Mw Fuel-to-NaK Heat Exchanger for 50-psi Pressure Drop in the NaK Circuit.

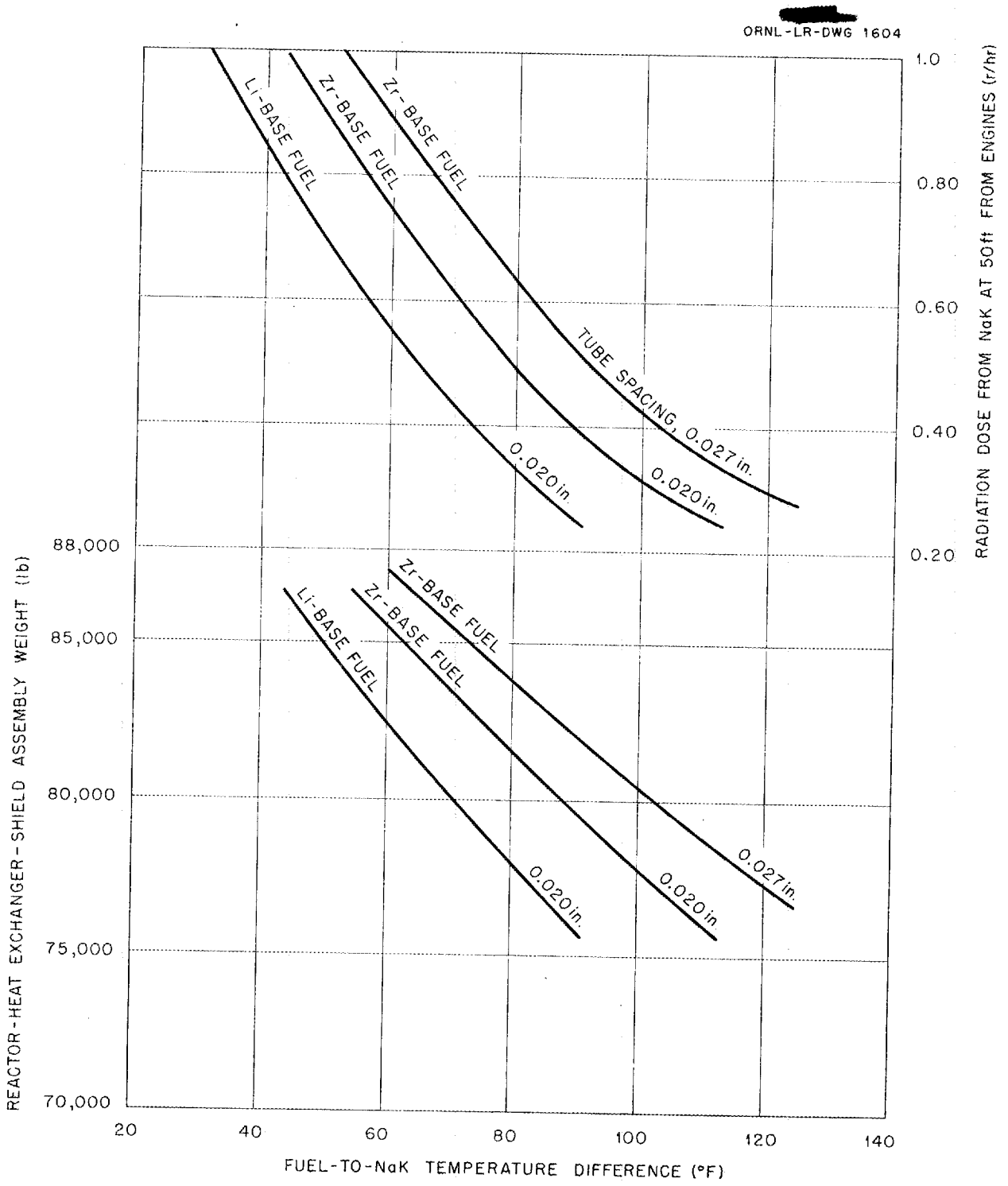

Fig. 3.2. Weight of Reactor, Heat Exchanger, and Reactor-Shield Assembly and Radiation Dose from the NaK in the Secondary Circuit at a Point 50 ft from the Engines as a Function of the Temperature Loss in the Fuel-to-NaK Heat Exchanger.

at the cold end than at the hot end. It has been shown[3] that the optimum tube diameter is close to $\frac{3}{16}$ in. and that the minimum thickness of ligament between holes in the header sheet should be at least 0.10 in. for satisfactory welding. If an essentially cylindrical header sheet, such as that shown in Fig. 3.3, is used to minimize the stresses, the ligaments between the tubes will be in tension. If allowances are made for both the cross-sectional area lost in the holes and the increases in the stresses around the holes that arise from geometric effects, the maximum tensile stress in the ligaments will be about five times that for a simple cylindrical shell of the same wall thickness with no perforations. The 1000-hr rupture strength for Inconel at 1200°F is 12,000 psi, and therefore the allowable stress should not exceed 6000 psi to give some factor of safety. If the header-sheet thickness were arbitrarily chosen as 0.25 in., its radius of curvature would be 3 in. (The allowable stress from simple loop tension considerations is 60 times the pressure differential for the unperforated cylinder, or 12 times that for the perforated cylinder. Thus the ratio of header-sheet thickness to radius of curvature becomes 1:12.) While other plausible designs can be evolved on a similar basis, that illustrated in Fig. 3.3 appears to be about the best devised to date.

[3] A. P. Fraas and M. E. LaVerne, *Heat Exchanger Design Charts*, ORNL-1330 (Dec. 7, 1952).

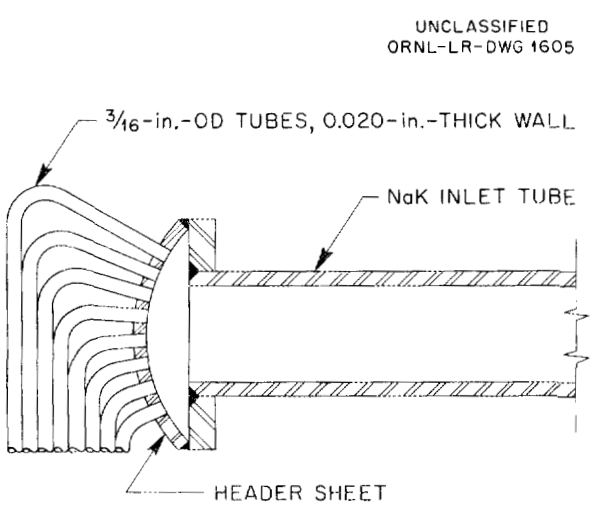

Fig. 3.3. Section Through Header Region of a Tube Bundle for a 60-Mw Heat Exchanger.

REACTOR PHYSICS

W. K. Ergen
ANP Division

Estimates of the xenon poisoning[4] of the 60-Mw Reflector-Moderated Reactor (power density 1.35 kw/cc) indicate that unless the xenon is rather rapidly purged from the fuel during operation a reactivity loss of the order of a few per cent will occur. Also, the maximum xenon concentration after shutdown would give a reactivity loss of about 10% or more. A control mechanism capable of compensating for such reactivity losses would be rather complicated, and the added uranium concentration would be highly undesirable. Therefore, an experiment is now being planned to determine whether the xenon can be adequately purged.

The elaborate coding of the multigroup calculations, mentioned in the previous report,[5] has temporarily been set aside. Instead, a three-group three-region code is being prepared which does not exceed the present capabilities of the ORACLE. This code is adequate for a variety of problems, and the use of the ORACLE is far more convenient than the use of an out-of-town machine.

The possibility of the coupling of mechanical oscillations with nuclear-power oscillations in the Reflector-Moderated Reactor was studied, since such coupling is known[6] to be capable, in principle, of creating antidamped oscillations. In particular, the possibility of the reactor oscillating mechanically like a Helmholtz resonator was investigated. The antidamped oscillations cannot occur if the frequency of the mechanical oscillations is very much higher than the frequency of the nuclear-power oscillations, as will be the case in the 60-Mw CFRE.

REACTOR CALCULATIONS

M. E. LaVerne
ANP Division

C. S. Burtnette
United States Air Force

Core radii of 20, 30, 40, and 60 cm, fuel thicknesses of 5, 10, 15, and 20 cm, and extrapolated

[4] J. L. Meem, *The Xenon Problem in the ART*, ORNL CF-54-5-1 (May 3, 1954).

[5] R. R. Coveyou and R. B. Bate, *ANP Quar. Prog. Rep. Mar. 10, 1954*, ORNL-1692, p 40.

[6] P. R. Kasten, *Linearized Stability Criteria for HRT Type Reactors*, ORNL CF-54-4-183 (Apr. 21, 1954).

reflector thicknesses of 20, 30, and 40 cm were selected for calculations of the set of related reactors referred to previously.[7] Poison (sodium and Inconel) distributions in the reflector and island were obtained from a previous study.[8] The fluoride fuel NaF-ZrF_4-UF_4 (53.5-40.0-6.5 mole %) was used for the entire set of calculations. From the set of 48 reactors determined by the specified independent parameters, it was found possible to select 30 reactors that would give results that could be used to cross-plot and interpolate the properties of the 18 omitted reactors to an accuracy sufficient for this survey. The results obtained are summarized in Figs. 3.4, 3.5, 3.6, and 3.7.

[7] M. E. LaVerne and C. S. Burtnette, *ANP Quar. Prog. Rep. Mar. 10, 1954*, ORNL-1692, p 39.

[8] R. W. Bussard *et al.*, *Moderator Cooling System for the Reflector-Moderated Reactor*, ORNL-1517 (Jan. 22, 1954).

ORNL-LR-DWG 1177

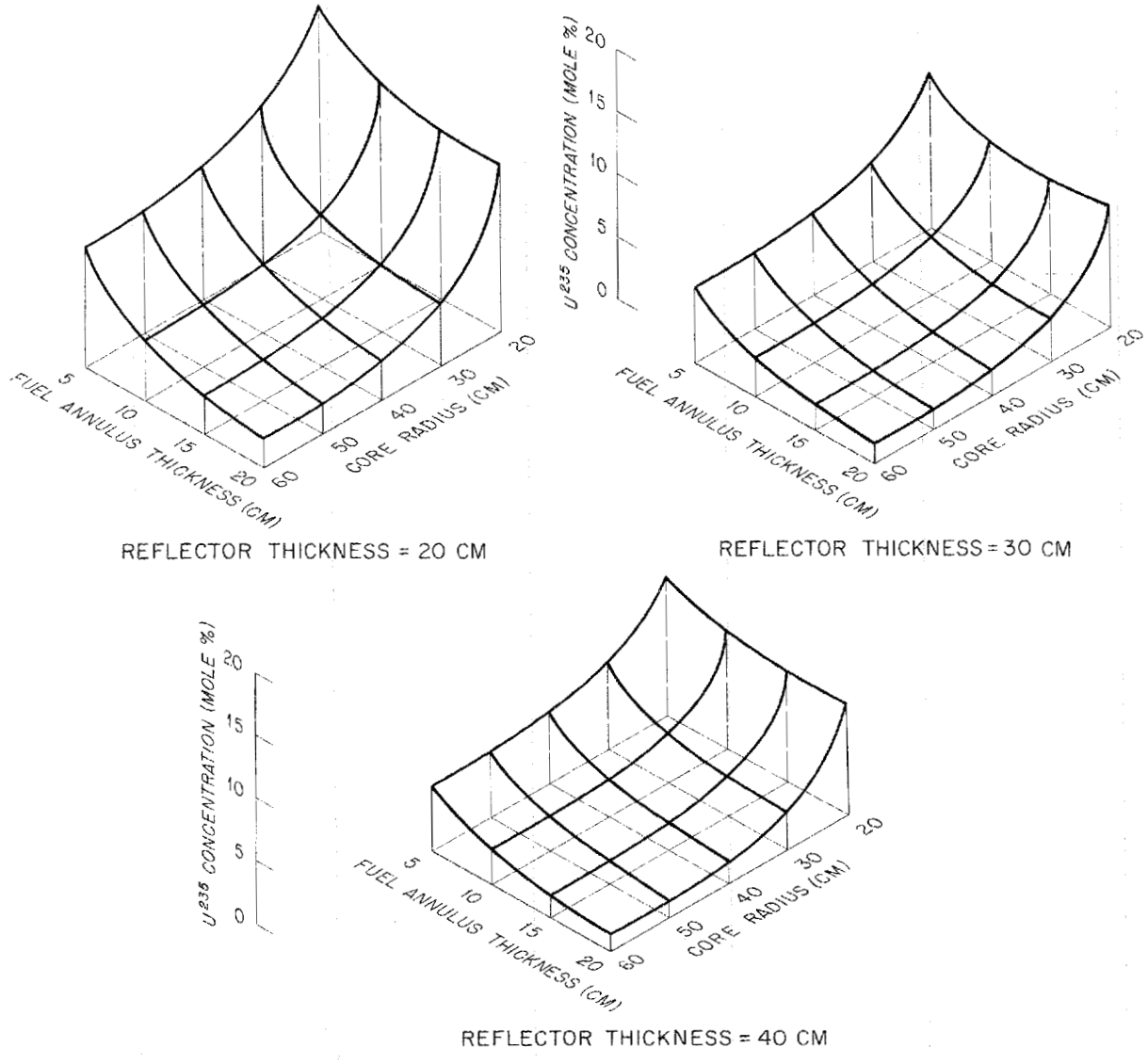

Fig. 3.4. Effect of Reactor Dimensions on Concentration of U^{235} in Fuel.

In view of stringent limitations on permissible uranium concentrations in the fuel, it is clear from Fig. 3.4 that there exists a considerable advantage in increasing reflector thickness from 20 to 30 cm but exceedingly little advantage in a further increase to 40 cm. The remaining figures have, therefore, been restricted to a 30-cm reflector thickness.

The effect on total uranium investment of the reactor dimensions and the external fuel volume, such as would exist in a heat exchanger external to the core, is shown in Fig. 3.5. The surface shown for zero external volume is, of course, simply that for critical mass. At a core radius of 30 cm the critical mass is virtually independent of fuel thickness. In the surfaces for both the

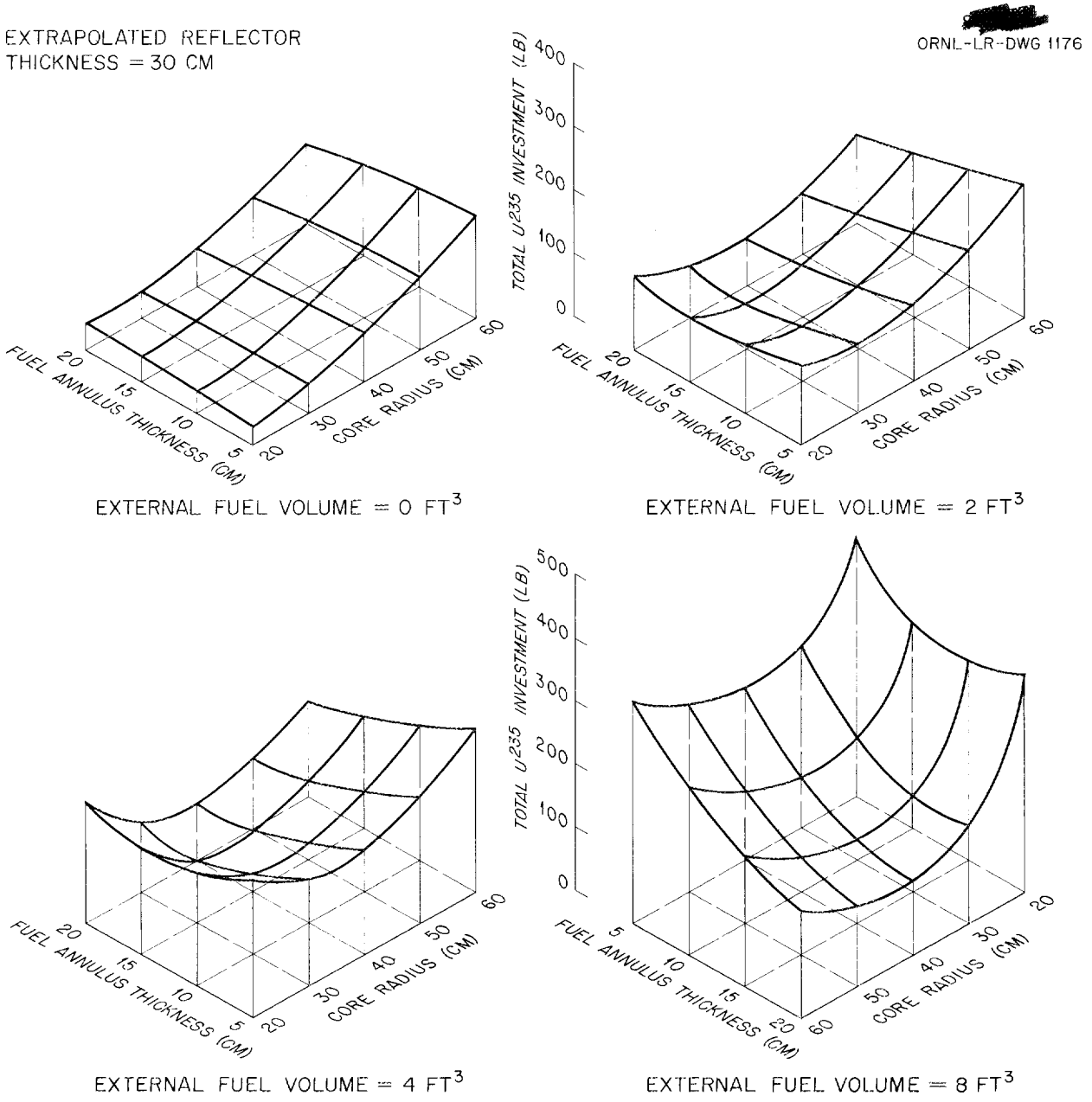

Fig. 3.5. Effect of Reactor Dimensions and External Fuel Volume on Total U^{235} Investment.

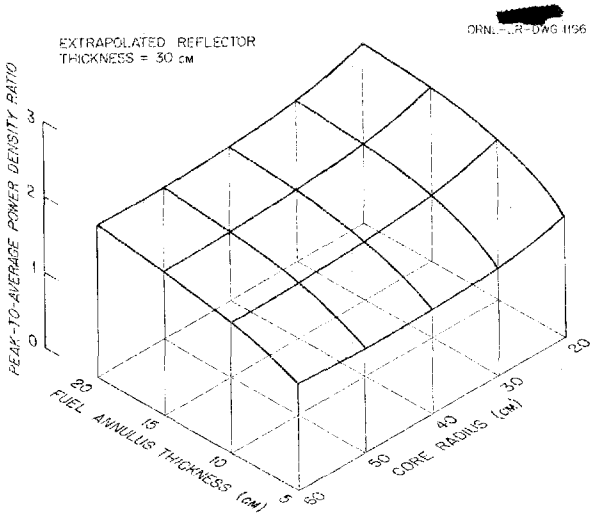

Fig. 3.6. Effect of Reactor Dimensions on Outside Peak-to-Average Power-Density Ratio in Core of Reflector-Moderated Reactor.

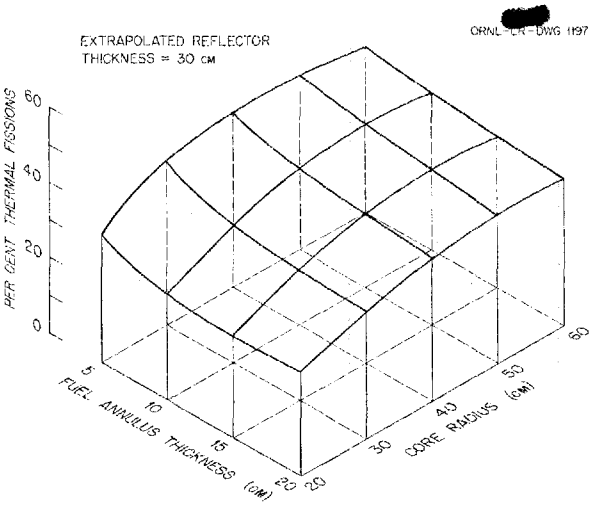

Fig. 3.7. Effect of Reactor Dimensions on Per Cent Thermal Fissions in Core of Reflector-Moderated Reactor.

2- and 4-cu ft external volumes, simple visual examination indicates the probable existence of an optimum set of proportions. Whether any closed contours (as required for an absolute minimum) actually exist has not yet been determined. The reversal of scales for the 8-cu ft surface was necessitated by the existence of an extreme peak at what was the front corner.

The effect of reactor dimensions on outside peak-to-average power-density ratio is shown in Fig. 3.6. The effects here are not large; an increase in core radius from 20 to 60 cm at a constant fuel thickness gives a decrease in the ratio of about 20%, while an increase in the fuel thickness from 5 to 20 cm at a constant core radius results in an increase in the ratio of about 33%.

The per cent thermal fissions as a function of reactor dimensions is shown in Fig. 3.7. The least-thermal reactor (28%) has the thickest fuel layer and the smallest core, while the most-thermal reactor (45%) has the thinnest fuel layer and the largest core.

When the 60-Mw design reactor[7] was modified by deleting the Inconel tubes and their surrounding stagnant sodium and fitting the resulting voids with beryllium, the critical mass decreased by 29%, that is, from an original value of 40.7 lb to 29.0 lb. This percentage decrease was duplicated by NDA[9] in a calculation on a 300-Mw reflector-moderated reactor for which the same method of poison reduction was employed.

The Curtiss-Wright Corporation, under contract to USAF, is performing an extensive series of multigroup, multiregion calculations on the IBM-701 for the ORNL-ANP Project. Specifications for these calculations are being prepared by the ORNL-ANP General Design and Reactor Physics Groups in cooperation with Curtiss-Wright.

Critical mass limits computed by Curtiss-Wright for the two-region, Teflon-uranium foil core, beryllium-reflected critical experiment as affected by foil thickness and space-point interval are listed in Table 3.2. These results agree quite well with the UNIVAC calculation previously reported.[7]

[9] M. R. Adolph, R. C. Ross, and M. S. Silberstein, *Circulating-Fuel Reactor Studies, Part I*, NDA 10-122 (Apr. 4, 1954).

TABLE 3.2. CRITICAL MASS LIMITS FOR RHOMBICUBOCTAHEDRON CRITICAL EXPERIMENTS

FOIL THICKNESS (mils)	Δr (cm)	CRITICAL MASS (lb of U^{235})
0*	1.828	14
10	0.457	18

*Homogeneous mixture.

Part II

MATERIALS RESEARCH

4. CHEMISTRY OF MOLTEN MATERIALS

W. R. Grimes
Materials Chemistry Division

The experimental studies of the chemistry of molten materials have been devoted almost exclusively to fluoride systems of interest as fuels. Considerable attention has been paid, during the quarter, to systems in which the uraniferous material consists wholly or in part of UF_3.

Studies of phase equilibrium by the method of thermal analysis have been continued. This technique has been applied to exploratory studies in mixed chloride-fluoride systems. Quenching techniques have been significantly improved and have been used, with petrographic and x-ray examination of the melts so produced, to virtually finish the elucidation of the complex NaF-ZrF_4 system. Differential thermal analysis and filtration techniques have been used in several phase-equilibrium experiments, and an apparatus for visual observation of liquidus temperatures has been tested and found to be satisfactory.

The solubility of UF_3 in several molten-salt systems has been examined experimentally. It appears that attainable concentrations of UF_3 in ZrF_4-based fuels are insufficient to fuel aircraft reactors; however, use of UF_3 and UF_4 in such mixtures appears to be promising. The UF_3 compound is apparently sufficiently soluble in NaF-LiF-KF mixtures (which would require Li^7 for utilization) to make such fuels attractive; the use of NaF-RbF-LiF mixtures as solvents for UF_3 (without UF_4) has not yet been shown to be possible.

The large-scale (250-lb-capacity) equipment for the production of fluoride mixtures has been reactivated and is now in three-shift five-day operation for furnishing the ZrF_4-based materials required for large-scale testing at ORNL and other installations.

QUENCHING EXPERIMENTS WITH FLUORIDE SYSTEMS

R. E. Thoma R. E. Moore
M. S. Grim C. J. Barton
Materials Chemistry Division
G. D. White H. Insley, Consultant
Metallurgy Division

The major part of the quenching work with compositions in the NaF-ZrF_4 system has been completed and a revised diagram for the system is presented. Work on the NaF-UF_4 system continued, but further work will be required before a revised diagram can be completed. It is anticipated that attention will shift from the binary system to the NaF-ZrF_4-UF_4 system and possibly the NaF-ZrF_4-UF_3 system in the near future.

NaF-ZrF_4

The methods and apparatus for performing quenching experiments were described previously.[1] During this quarter, all the quenching experiments were made by heating the sample up to, but not above, the quenching temperature.

The incongruent melting point of the compound $Na_3Zr_4F_{19}$ was established as 538°C by quenching mixtures with 57 and 60 mole % ZrF_4. The liquidus temperatures of mixtures with 57 and 60 mole % ZrF_4 were found to be 546 ± 5°C and 609 ± 5°C, respectively. The 57 mole % ZrF_4 composition (almost 100% $Na_3Zr_4F_{19}$) was converted to ZrF_4 and liquid at 538°C. From the shape of the liquidus curve and from x-ray diffraction studies of large samples of slowly cooled mixtures, it appears that the ZrF_4 primary-phase field extends to about 56 mole % ZrF_4 in the NaF-ZrF_4 system.

Quenching and glass-devitrification experiments indicate that the liquidus-solidus temperature of the 47 mole % ZrF_4 composition is about 522°C, and the liquidus-solidus temperature of the 50 mole % ZrF_4 composition is about 511°C. Recently, a very careful thermal-analysis comparison of the 47 and 50 mole % ZrF_4 mixtures showed that the 47 mole % mixture melts and freezes sharply at 520°C and the 50 mole % mixture freezes sharply at 510°C. These results mean that the single phase which is always obtained on cooling 47 mole % ZrF_4 compositions is a congruently melting compound ($Na_9Zr_8F_{41}$), while the 50 mole % ZrF_4 composition is near a eutectic of $Na_3Zr_4F_{19}$ and $Na_9Zr_8F_{41}$.

A phase referred to as R-3 has appeared[2] in association with glass in compositions ranging

[1] C. J. Barton *et al.*, *ANP Quar. Prog. Rep. Dec. 10, 1953*, ORNL-1649, p 54.

[2] R. E. Thoma *et al.*, *ANP Quar. Prog. Rep. Mar. 10, 1954*, ORNL-1692, p 52-54.

from 45 to 57 mole % ZrF_4. This phase forms only when large quench samples are used, that is, under poor quenching conditions. Experiments with very small samples at various temperatures have failed to produce R-3. It was concluded from these experiments that R-3 does not have a stable existence in the binary system but is an easily crystallized metastable compound (probably $NaZrF_5$) that is produced by fairly rapid cooling below the equilibrium liquidus temperature.

Petrographic and x-ray diffraction examination of slowly cooled preparations led to the postulation of the existence of a weakly birefringent compound $Na_3Zr_2F_{11}$ and a series of solid solutions between it and $Na_9Zr_8F_{41}$. Petrographic examinations of samples of 43 and 45 mole % ZrF_4 compositions heated to 483°C and held for 20 hr, before quenching, definitely pointed to an immiscibility gap in this series between about 42 and 44 mole % ZrF_4.

Petrographic examinations of a large number of quenched samples with between 39 and 45 mole % ZrF_4 led to the conclusion that $Na_3Zr_2F_{11}$ is not stable at the liquidus temperature. In 47 to 42 mole % ZrF_4 compositions, the solid solution $Na_9Zr_8F_{41}$ is the primary phase. The liquidus temperatures of compositions with 47, 45, 43, and 42 mole % ZrF_4 are about 522, 520, 517, and 508°C, respectively. In 39 and 40 mole % ZrF_4 compositions, the primary phase is Na_2ZrF_6. The liquidus temperature for the 39 mole % ZrF_4 composition is above 513°C, and for the 40 mole % ZrF_4 composition it is near 510°C. For the 41 mole % composition the liquidus temperature is about 502°C, and this composition is near a eutectic between Na_2ZrF_6 and the $Na_9Zr_8F_{41}$ solid solution. Below about 488°C, $Na_3Zr_2F_{11}$ appears as fine-grained fibers. Slowly cooled compositions with about 40 mole % ZrF_4 usually undergo a reaction just after complete solidification that produces a fluff of very fine-grained material. According to x-ray diffraction results, this material is a mixture of $Na_3Zr_2F_{11}$ and $Na_9Zr_8F_{41}$. It is likely that the reaction is the solid-state conversion at about 488°C of the eutectic into these compounds. The formation of $Na_3Zr_2F_{11}$ in the solid state explains why it has always been found as fine grains.

A number of different forms of Na_2ZrF_6 have been observed, and quenching experiments have been conducted to establish the transition temperatures. This work is not yet complete, but the approximate temperatures are known. The phases which have been found and the optical properties and the approximate temperatures at which these phases are stable are given in Table 4.1. The temperature of transition from phase 5 to phase 4

TABLE 4.1. CRYSTAL MODIFICATIONS OF Na_2ZrF_6

PHASE	OPTICAL PROPERTIES	APPROXIMATE TEMPERATURE (°C)
1	Isotropic	545 to 620
2	Uniaxially positive, $O = 1.406$ $E = 1.408$	540 to 545
3	Uniaxially positive, $O = 1.376$ $E = 1.386$	505 to 540
4	Biaxially positive, $\gamma = 1.412$ $\alpha = 1.408$	Below 460
5	Biaxially negative, $\gamma = 1.419$ $\alpha = 1.412$	
6	Biaxially negative, $\gamma = 1.429$ $\alpha = 1.420$	

is not known, but it is below 460°C.

Phases 3 and 4 have been found in quenches of mixtures with 37 and 40 mole % ZrF_4 at the appropriate temperatures. The refractive indices were the same as for the 33 mole % ZrF_4 composition, and thus there appears to be little or no solid-solution range for these phases.

The phase diagram presented in Fig. 4.1 represents the data discussed here and in previous reports.[1-3] Thermal data obtained from cooling curves, together with visual observation of the Na_3ZrF_7 compound, were the chief sources of liquidus temperatures in the 0 to 30 mole % ZrF_4 region. The Na_3ZrF_7 compound was observed to melt rather sharply between 840 and 850°C to a clear liquid that permitted observation of turbidity on cooling to a temperature slightly above 850°C. The liquidus temperatures in the 60 to 100 mole % ZrF_4 region were obtained from thermal data.

$NaF-UF_4$

Eight samples covering the range in the $NaF-UF_4$ system from 18 to 67 mole % UF_4, chosen to fill insofar as possible the gaps in the knowledge of the system,[2] were mixed and hydrofluorinated to minimize oxide contamination. These slowly cooled specimens were examined by petrographic and x-ray techniques. The results of this examination, some of which were published previously, are shown in Table 4.2.

[3] R. E. Moore, C. J. Barton, and T. N. McVay, *ANP Quar. Prog. Rep. Sept. 10, 1953*, ORNL-1609, p 59.

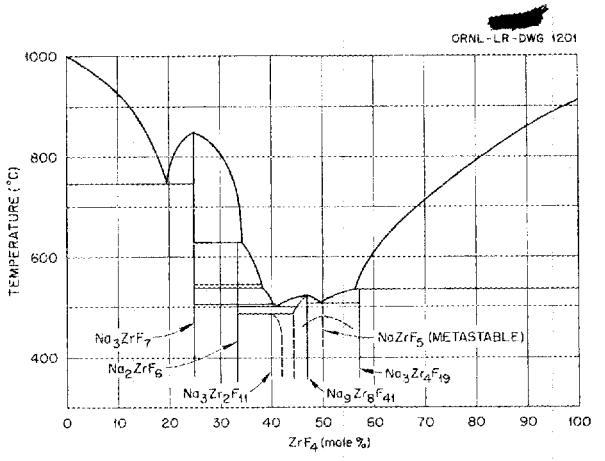

Fig. 4.1. Phase Diagram of the $NaF-ZrF_4$ System.

TABLE 4.2. PHASES PRESENT IN SLOWLY COOLED $NaF-UF_4$ MIXTURES

COMPOSITION (mole % UF_4)	PHASES IDENTIFIED BY PETROGRAPHIC AND X-RAY DIFFRACTION ANALYSES
18	β_3-Na_2UF_6, Na_3UF_7, NaF
22	β_3-Na_2UF_6, NaF
25	β_3-Na_2UF_6, Na_3UF_7, NaF (trace)
28	β_3-Na_2UF_6 (major), Na_3UF_7
30	β_3-Na_2UF_6 (major), Na_3UF_7
31.5	β_3-Na_2UF_6
33.3	β_3-Na_2UF_6
35	β_3-Na_2UF_6 (major), $NaUF_5$
37	β_3-Na_2UF_6 (major), $NaUF_5$
38.5	β_3-Na_2UF_6 (major), $NaUF_5$
40	β_3-Na_2UF_6, $NaUF_5$
43	β_3-Na_2UF_6, $NaUF_5$
46	β_3-Na_2UF_6, $NaUF_5$ (major)
48	$NaUF_5$, UF_4 (trace)
50	$NaUF_5$ (major), β_3-Na_2UF_6, UF_4, UO_2 (trace)
53	$NaUF_5$ (major), UF_4
67	$NaUF_5$, UF_4

Small portions of these specimens have been used with conventional techniques in quenching experiments. From 18 to 30 quenches have been made on portions of all specimens except the Na_2UF_6 composition, for which a total of about 80 attempts has been made. By quenching specimens from temperatures as high as 1022°C to as low as 399°C, it has been established that four crystalline forms of the Na_2UF_6 composition exist. These crystalline modifications are α (cubic), β_2 (hexagonal), β_3 (hexagonal), and γ (orthorhombic). In no case could the Na_2UF_6 be quenched completely to glass; the α and γ forms occurred in quenches from 637°C or higher. The γ form appears to be most prevalent in the more rapid quenches. The β_3 form has been observed as the major phase in large, slowly cooled melts and in most quenches from temperatures below 637°C. The β_2 form has been prepared in a practically pure state in the

temperature range of 612 to 589°C by using samples somewhat larger than those customarily used in quenching experiments.

In general, the quenching data indicate that $NaUF_5$ is the most uranium-rich compound in the $NaF-UF_4$ system. It is anticipated that a definitive diagram of this binary system will be prepared during the next quarter.

VISUAL OBSERVATION OF MELTING TEMPERATURES

R. J. Sheil C. J. Barton
Materials Chemistry Division

An apparatus has been constructed that permits visual observation of fused fluoride and chloride mixtures at high temperatures under an inert atmosphere. It consists of a 2½-in.-OD metal pipe threaded at the ends and mounted vertically. Glass disks gasketed with Teflon are fitted to the tube ends. Large nuts are used to compress the gaskets which form virtually gas-tight connections. Water-cooled copper coils are used to cool the furnace ends and to protect the Teflon gaskets. The inert gas, usually argon, is maintained at slightly above atmospheric pressure; a slow flow of gas enters near the bottom of the apparatus and leaves near the top.

Samples are placed in 20-ml nickel crucibles supported on a tripod near the center of the furnace. A bare chromel-alumel thermocouple junction is immersed in the fluoride sample. The thermocouple was checked at the sodium chloride melting point after several exposures to molten fluorides; it was found that the slight corrosion had not affected the emf output.

Visual observations have been confined thus far to a few compositions in the $NaF-ZrF_4$ and the $NaF-UF_4$ systems. However, the usefulness of the equipment for confirmation of liquidus and solidus temperatures has been demonstrated, and its use in phase studies will undoubtedly increase.

DIFFERENTIAL THERMAL ANALYSIS OF THE $NaF-ZrF_4$ SYSTEM

R. A. Bolomey
Materials Chemistry Division

A critical study of the differential thermal-analysis data collected for the $NaF-ZrF_4$ system shows that they are consistent with petrographic and x-ray analysis data obtained from quenching and devitrification experiments. A comprehensive report on the technique for differential thermal analysis is being prepared. The report will describe the theory of differential thermal analysis in a qualitative manner, the preparation of the samples, the experimental technique, the interpretation of the data, and the precision and accuracy of the method. Suggestions for further improvements of the method will be included.

FILTRATION ANALYSIS OF FLUORIDE SYSTEMS

R. J. Sheil C. J. Barton
R. E. Thoma
Materials Chemistry Division
G. D. White
Metallurgy Division

The filtration apparatus was diverted from phase studies to solubility determinations during this quarter because of the urgent need for data on the solubility of UF_3 in alkali fluorides and in $NaF-ZrF_4$ mixtures. A few experiments were made, however, to demonstrate the solubility of UF_4 in the NaF-RbF-LiF eutectic and to define the primary phase in some $NaF-ZrF_4$ mixtures.

$NaF-ZrF_4$

One filtration was carried out in the $NaF-ZrF_4$ system to supplement information obtained by other techniques. A mixture containing 63 mole % ZrF_4 was filtered at 552°C, and 79.5 wt % of the material filtered. The filtrate contained 55 mole % ZrF_4 and was predominantly $Na_3Zr_4F_{19}$ with a small amount of $Na_9Zr_8F_{41}$. The residue analyzed 78.5 mole % ZrF_4 and was predominantly ZrF_4 with some $Na_3Zr_4F_{19}$ and $Na_9Zr_8F_{41}$. These results, which demonstrate that ZrF_4 is the primary phase in the 63 mole % ZrF_4 composition, lend support to the revised diagram for the $NaF-ZrF_4$ system (Fig. 4.1).

$NaF-LiF-RbF-UF_4$

The solubility of UF_4 in the NaF-LiF-RbF eutectic at 500°C was determined by filtering a mixture of the following calculated composition (in mole %) 5.8 NaF–40.3 LiF–49.9 RbF–4.0 UF_4. A cooling curve obtained prior to the filtration showed a questionable thermal effect at 542°C and a definite break at 428°C, that is, slightly below the melting point of the ternary alkali fluoride eutectic (435°C). About 90% of the charge material

passed through the filter at 500°C. All the uranium was apparently in the form of Rb_3UF_7 complex. Petrographic examination showed that the filtrate contained about 10 to 20 wt % of this uranium compound and that the residue contained approximately 50 wt %. Chemical analyses of the separated phases gave the following compositions (in mole %):

	In Filtrate	In Residue
LiF	48.5	30.3
NaF	6.9	9.4
RbF	41.7	50.2
UF_4	2.8 (10.2 wt %)	10.1

The chemical analyses appear to confirm the petrographic finding that a $RbF\text{-}UF_4$ complex is the primary phase that separates from the $NaF\text{-}LiF\text{-}RbF\text{-}UF_4$ mixture. This result was not unexpected because phase studies of the alkali fluoride–UF_4 systems have shown that Rb_3UF_7 has the highest melting point and is the most stable of the UF_4 complexes that can be formed by the components present in the $NaF\text{-}LiF\text{-}RbF\text{-}UF_4$ system.

THERMAL ANALYSIS OF FLUORIDE SYSTEMS

L. M. Bratcher A. B. Wilkerson
Materials Chemistry Division
G. D. White T. N. McVay, Consultant
Metallurgy Division

Preliminary data on the $NaF\text{-}ZrF_4\text{-}UF_3$ and $NaF\text{-}ZrF_4\text{-}UF_4\text{-}UF_3$ systems disclose that conventional thermal-analysis techniques do not give a reliable indication of liquidus temperatures in these potentially useful systems. The apparatus developed for thermal analysis of chloride systems, which consists of a flanged stainless steel container which holds the samples in nickel crucibles, has been found useful for thermal analysis of these UF_3-bearing systems. An investigation of phase behavior in the $NaF\text{-}CrF_3$ system has been initiated because of the importance of CrF_3 in corrosion of Inconel and stainless steels by molten fluorides. Work on the $NaF\text{-}ThF_4$ system has been concluded, although the results obtained are not completely satisfactory; should this system become important other techniques will be required for establishing the phase behavior.

$LiF\text{-}UF_3$

Efforts to obtain data on mixtures in the $LiF\text{-}UF_3$ system were made rather early in the phase-study program, but the results were unsatisfactory because of the presence of UF_4 and UO_2 in the fused mixtures. Relatively pure $LiF\text{-}UF_3$ mixtures can be produced by adding 100% excess of uranium metal to a previously fused $LiF\text{-}UF_4$ mixture. The few data obtained for the relatively pure mixtures indicate that there is a eutectic containing about 25 mole % of UF_3 that melts at approximately 770°C. Petrographic examination of the fused mixtures showed only LiF and UF_3. It is thought that the $LiF\text{-}UF_3$ mixtures probably comprise a simple eutectic system.

$NaF\text{-}UF_3$

Data previously reported[4,5] indicated the existence of one eutectic and one compound in the $NaF\text{-}UF_3$ system. When a mixture containing 33 mole % UF_3 and 67 mole % NaF was prepared by fusing NaF with previously prepared UF_3, thermal effects were noted at 750, 695, 650, and 595°C. These data agree quite well with the earlier data, but the petrographic examination of the mixture showed the presence of a green, presumably oxidized, phase in addition to the lavender $NaF\text{-}UF_3$ complex. Further study of this system is planned.

$RbF\text{-}UF_3$

Very few compositions prepared in the $RbF\text{-}UF_3$ system were free of UO_2 and UF_4 complexes. The only compound which has been observed (either Rb_2UF_5 or Rb_3UF_6) is described as a brown-orange isotropic phase with a refractive index of 1.44. The 33.3 mole % UF_3 composition showed a thermal effect at 860°C. The method of preparing alkali fluoride–UF_3 mixtures by adding an excess of uranium metal to UF_4 mixtures is not suitable for the $RbF\text{-}UF_3$ system because the reduction of RbF by uranium gives volatile metallic rubidium.

$KF\text{-}LiF\text{-}UF_3$

A $KF\text{-}LiF\text{-}UF_3$ (48-48-4 mole %) mixture was prepared by reducing a previously fused $KF\text{-}LiF\text{-}UF_4$ mixture with 100% excess uranium metal. Thermal effects were noted on the cooling curve

[4] V. S. Coleman and W. C. Whitley, *ANP Quar. Prog. Rep. Sept. 10, 1952*, ORNL-1375, p 79.

[5] W. C. Whitley, V. S. Coleman, and C. J. Barton, *ANP Quar. Prog. Rep. Dec. 10, 1952*, ORNL-1439, p 109.

at 558, 540, and 487°C. It is probable, although not yet established, that the thermal effect at 558°C represents the true liquidus temperature for this composition. The fused melt contained about 15% of an orange, low-birefringent phase of refractive index 1.43 and colorless isotropic materials with the refractive indices of KF and LiF. These two alkali fluorides apparently do not form a complex comparable to the LiF-RbF complex.

RbF-LiF-UF_3

A RbF-LiF-UF_3 (56-40-4 mole %) mixture was prepared by mixing uranium metal and previously prepared UF_3 with the fused alkali fluorides. No thermal effect was observed above 475°C, the melting point of the RbF-LiF eutectic. Since the filtration experiments reported above indicate that the liquidus temperature for a similar composition is above 550°C, it is concluded that the first separation of a UF_3-containing phase from ternary mixtures in this region cannot be readily detected by conventional thermal-analysis techniques. Petrographic examination revealed that the melt contained a colorless birefringent phase, presumably a LiF-RbF complex, and a brownish isotropic phase that was probably a RbF-UF_3 complex.

NaF-ZrF_4-UF_4-UF_3

A series of samples with various amounts of the UF_4 was prepared in sealed nickel capsules in a mixture that contained initially NaF-ZrF_4-UF_4 (53.5-40-6.5 mole %) with sodium metal added to reduce the UF_3 to UF_4. When the capsules had been heated to maximum temperatures of about 900°C they were inverted so that the contents would mix. Duplicate cooling curves were obtained with each composition by reheating and remixing the contents. The data obtained are presented in Table 4.3. In the data, the dilution of the melt by the NaF produced in the reaction is disregarded.

The data seem to indicate a minimum melting point when a little more than one-half the uranium is reduced. Petrographic examination of the fused melts showed a regular gradation of properties in the series. Two phases were observed in the unreduced mixture, the $Na_9(Zr,U)_8F_{41}$ solid solution and a small amount of colorless Na_2ZrF_6. Four phases were observed in the reduced mixtures: UF_3, a yellow isotropic material, a yellow-green solid solution, and Na_2ZrF_6. With increasing degrees of reduction, the solid solution became increasingly yellow, and the isotropic yellow phase, free UF_3, and yellow-green Na_2ZrF_6 appeared in increasing amounts. This crystalline form of Na_2ZrF_6, usually referred to as "normal" Na_2ZrF_6, does not, according to present knowledge, dissolve tetravalent uranium.

NaF-ThF_4

Thermal analysis of the NaF-ThF_4 system has given data which are difficult to interpret. Petrographic examination of the fused melts has failed to clarify the situation; Na_2ThF_6 was the only crystalline phase that could be definitely identified. The further study that would be needed for clarification does not appear to be justified at this time, and therefore the available data are presented in the form of a tentative diagram (Fig. 4.2). Petrographic examination of some melts made recently indicated that the 50-50 composition is close to a pure compound and suggested that another crystal-

TABLE 4.3. THERMAL EFFECTS OBSERVED WITH NaF-ZrF_4-UF_4-UF_3 COMPOSITIONS

COMPOSITION (mole % UF_3, calculated)	THERMAL EFFECTS (°C)	
	First Cooling Curve	Second Cooling Curve
0	565, 530 (halt), 490	557, 528, 492
1.5	555, 535, 510	576,525
3.0	510, 500	507, 500 (halt)
4.5	507, 495	509, 495
5.5	540, 519 (halt)	550, 520
6.5	525, 487	525, 490

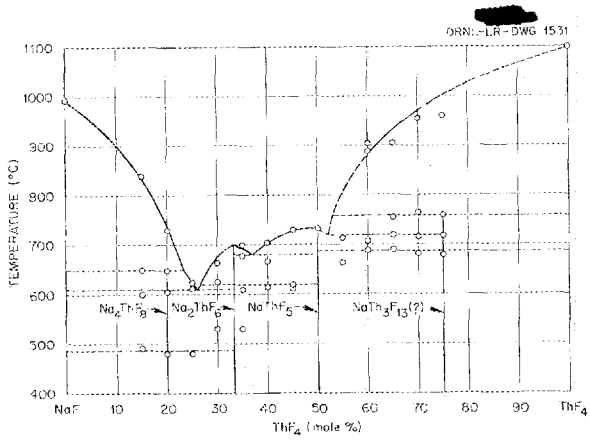

Fig. 4.2. Tentative Phase Diagram of the NaF-ThF_4 System.

line phase observed in the 25 and 30 mole % ThF_4 mixtures might be Na_4ThF_8. Zachariasen[6] reported the existence of this compound. These examinations also showed that more oxide was present in compositions formed by adding ThF_4 to the 50-50 mixture than in those formed by adding NaF. Therefore it seems probable that oxide and/or water in the ThF_4 is the major source of oxygen in the fused NaF-ThF_4 composition.

LiF-BeF_2-ThF_4-UF_4

Preliminary examination has been made of the LiF-BeF_2-ThF_4-UF_4 system which has been considered as a possible fuel for a breeder-power reactor.[7] Cooling curves obtained with two mixtures of LiF-BeF_2-ThF_4-UF_4 (48.6-48.6-2.7-0.1 mole %) showed thermal effects at 515, 392, and 325°C. The thermal effect at 515°C was slight but reproducible and probably represents the first separation of a ThF_4-containing phase. This separation should be confirmed by other techniques, such as filtration or quenching, if this composition continues to be of interest. It is possible that a composition with a higher LiF and a lower BeF_2 content might have a lower liquidus temperature, although presumably such a mixture would be less efficient as a moderator.

[6] W. H. Zachariasen, *J. Am. Chem. Soc.* 70, 2147 (1948).

[7] S. Peterson, *Reactor Chemistry*, ORNL CF-54-4-198 (May 12, 1954).

NaF-CrF_3

Mixtures containing 5 to 65% CrF_3 in the NaF-CrF_3 system have been examined. The thermal data do not serve to define the system uniquely. Petrographic examination indicates the existence of a compound which seems to be $NaCrF_4$. Two other crystalline materials have been observed but neither has the optical properties of the Na_3CrF_6 compound previously described.[8] Thermal effects are observed below the solidus temperature at 25 mole % CrF_3; it is possible that several crystalline modifications of Na_3CrF_6 exist.

THERMAL ANALYSIS OF CHLORIDE AND MIXED CHLORIDE-FLUORIDE SYSTEMS

A. B. Wilkerson C. J. Barton
Materials Chemistry Division
T. N. McVay, Consultant
Metallurgy Division

Studies of chloride systems have been continued at a somewhat diminished rate during the past quarter. The systems studied have included a few mixed chloride-fluoride compositions and some binary and ternary systems containing UCl_3.

UCl_3-UCl_4

Conflicting statements about the UCl_3-UCl_4 system are found in the literature. It was stated by Kraus[9] that the two compounds are only slightly soluble in each other in the liquid state, and he reported a liquidus break for only one composition. The group at Ames, Iowa,[10] stated that there is a eutectic in the system at 88 mole % UCl_4, with a melting point 14°C lower than that of the UCl_4. Five compositions in this system were prepared in sealed capsules, and thermal effects were noted on the cooling curves obtained after the mixtures had been heated to about 850°C and the capsules had been inverted to obtain mixing of the contents. Samples of UCl_3 and UCl_4 were also heated in sealed capsules. In addition, one UCl_4-UCl_3 (80-20 mole %) mixture was prepared in a nickel container at atmospheric pressure (helium), but it was not heated to such a high temperature as were the

[8] L. M. Bratcher and C. J. Barton, *ANP Quar. Prog. Rep. Dec. 10, 1952*, ORNL-1439, p 116.

[9] C. A. Kraus, *Phase Diagrams of Some Complex Salts of Uranium with Halides of the Alkali and Alkaline Earth Metals*, M-251 (July 1, 1943).

[10] J. J. Katz and E. Rabinowitch, *The Chemistry of Uranium*, p 488, McGraw-Hill, New York, 1951.

sealed capsules because of the high vapor pressure of UCl_4. The data are given in Table 4.4.

The thermal data give little indication of a eutectic but are not easily interpreted because of the anomalous thermal effects noted with the two components in the sealed capsules. In open containers under an inert atmosphere, only one break was noted on the UCl_3 cooling curve, at 840°C, and one with UCl_4, at 565°C. Both UCl_3 and UCl_4 were noted petrographically in the fused UCl_4 probably because of reduction of UCl_4 by the container, but this does not seem to account for all the thermal effects noted. Both UCl_3 and UCl_4 were found in all the mixtures, except for the 12% UCl_3 composition, in which no UCl_3 was visible under the microscope. It is possible that oxidation of the UCl_3 may have occurred before the petrographic examination could be completed.

UCl_4-UF_4

Only one composition was prepared in the UCl_4-UF_4 system, a 50-50 mixture corresponding to the compound UCl_2F_2 reported in the literature.[11] It gave a single thermal effect at 520°C with an indication of undercooling. Petrographic examination revealed three crystalline phases: UCl_4, UF_4, and a bright greenish-blue phase with refractive indices near 1.747. The latter was the principal phase and is believed to be the UCl_2F_2 compound. Other workers who have attempted to produce the compound by the fusion method[12] have also failed to obtain a pure product. A probable melting point of 460°C, based upon their work, was reported[13] for the compound.

UCl_3-UF_3

Five compositions in the UCl_3-UF_3 system have been prepared in sealed capsules. The thermal data are too meager to permit definite conclusions to be drawn, and petrographic examination of the fused melts was rather difficult. The 50-50 mole % mixture showed only one thermal effect, at 615°C, but it is not known whether the mixture was completely liquid above this temperature. The fused mixture was predominantly a single phase with optical properties different from those of the two components; this suggests the possibility of a compound such as $U_2Cl_3F_3$. Such a compound would be a novelty, since, insofar as is known here, no mixed chloride-fluoride compound of trivalent uranium has been reported.

KCl-UCl_4

The KCl-UCl_4 system, studied by Kraus,[9] has received considerable attention in this laboratory because thermal data obtained here[14-16] for a part of the system were at variance with the earlier work. The data, particularly the liquidus breaks in the 30 to 60 mole % UCl_4 region, have not been very reproducible. The reaction of UCl_4 with the nickel containers is responsible apparently for some of the difficulty. A crystalline growth, identified as $NiCl_2$, appears in the cooler part of the apparatus above the fused melt; apparently it is more volatile than the UCl_4 from these mixtures.

[11] J. W. Gates, Jr., G. H. Clewett, and H. A. Young, *Preparation of a New Mixed Halide of Tuballoy*, CD-454 (July 20, 1944); J. W. Gates, Jr., *et al.*, *A Mixed Tuballoy Tetrahalide*, CD-460 (Aug. 26, 1944).

TABLE 4.4. THERMAL EFFECTS ON COOLING CURVES FOR MIXTURES OF UCl_3 AND UCl_4

THEORETICAL COMPOSITION (mole % UCl_3)	THERMAL EFFECTS (°C)
100	835, 768, 520
80	797, 535, 488
60	798,[a] 540,[a] 495
40	762, 542, 497
20	622,[b] 545, 531, 497
20[c]	670, 555
12	720, 548, 500
0	602, 540,[a] 515, 498

[a] Indicates that undercooling occurred.

[b] Questionable thermal effect.

[c] Prepared at atmospheric pressure.

[12] J. C. Warf *et al.*, *Mixed Uranium Halides*, CC-1785 (Sept. 10, 1944); N. W. Gregory, *Compounds of Tuballoy Containing Two or More Different Halogen Atoms*, R.L. 4.6.905 (Jan. 8, 1945).

[13] J. J. Katz and E. Rabinowitch, *op. cit.*, p 542.

[14] R. J. Sheil and C. J. Barton, *ANP Quar. Prog. Rep. Mar. 10, 1953*, ORNL-1515, p 109.

[15] R. J. Sheil and C. J. Barton, *ANP Quar. Prog. Rep. June 10, 1953*, ORNL-1556, p 42.

[16] R. J. Sheil, S. A. Boyer, and C. J. Barton, *ANP Quar. Prog. Rep. Sept. 10, 1953*, ORNL-1609, p 58.

Petrographic examination of the fused melts indicated the probable existence of three compounds in this system, but only K_2UCl_6 has been prepared in sufficient purity to be readily identified. The likely compositions for the other two compounds are $KUCl_5$ and KU_2Cl_9, but since they were not produced free of the other crystalline phases in the system, it seems probable that they melt incongruently. The diagram shown in Fig. 4.3, which is based upon both petrographic and thermal studies of the system, is believed to give a reasonably accurate representation of the phase relationships. No further work on the system is planned at the present time.

RbCl-UCl_4

The RbCl-UCl_4 system, for which preliminary data have been reported,[17] has been studied considerably less than the KCl-UCl_4 system. Cooling curves with mixtures in the RbCl-UCl_4 system containing 5 to 65 mole % UCl_4 yielded very scattered and confusing data. Petrographic examination of several fused mixtures did not aid materially in the interpretation of the thermal data because none of the crystalline phases observed in the fused melts had been prepared in sufficient purity for definite identification. However, the available data seem to indicate that melting points and phase relationships in this system are not markedly different from those shown for the KCl-UCl_4 system in Fig. 4.3.

[17] C. J. Barton and S. A. Boyer, *ANP Quar. Prog. Rep. Dec. 10, 1953*, ORNL-1649, p 52.

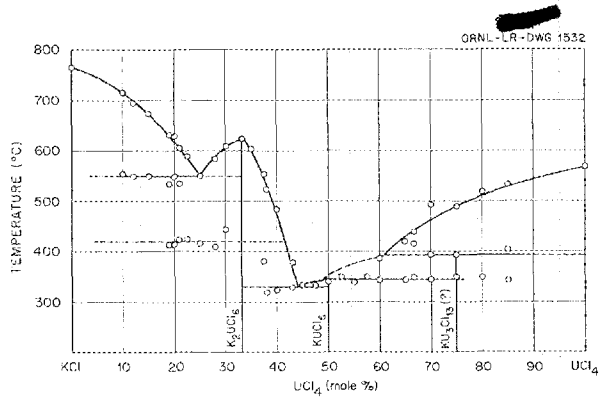

Fig. 4.3. Tentative Phase Diagram of KCl-UCl_4 System.

KCl-CuCl-UCl_3

A eutectic in the KCl-CuCl system that melts at 150°C was reported. A mixture corresponding to the reported eutectic composition (65 mole % CuCl) was prepared by using metallic copper to reduce the $CuCl_2$ in the CuCl. The resulting mixture, which showed a single thermal effect at 140°C, was colorless but contained some opaque inclusions in the crystalline material. No thermal effects were noted on the cooling curves when 2.5 or 5 mole % UCl_3 was added. Petrographic examination of the fused mixture was unsatisfactory, however, since it disclosed only a mass of very fine crystals with opaque material in the aggregates. It is not certain, therefore, that the UCl_3 dissolved in the fused KCl-CuCl mixture.

X-RAY DIFFRACTION STUDIES OF THE NaF-ZrF_4 SYSTEM

P. A. Agron M. A. Bredig
Chemistry Division

A high-temperature x-ray diffractometer is being utilized to further understanding of the phase transformations that occur in the NaF-ZrF_4 system. The equipment, which was originally developed[18] for the temperature range of 1500 to 2200°C, was modified to cover the 400 to 900°C range. In order to avoid decomposition of binary complexes by partial vaporization, the solid salt is enclosed in a 15-cc beryllium container. The walls were machined to a 10-mil thickness to allow free passage of the x-ray beams. This flanged container has been successfully gasketed to a stainless steel mounting with a combination of gold and copper rings. (In an initial attempt to use a gold gasket in contact with the beryllium, there was rapid deleterious alloying at about 500°C.) The sample, about 0.4 g of solid material, is held in a flat, nickel holder. This arrangement was successfully tested on the CsCl transition. A more detailed description of this equipment, which is useful only for the examination of solids, will be given at a future date.

In the region of 33 to 40 mole % ZrF_4, several polymorphic forms of Na_2ZrF_6 are indicated. At the 60% NaF–40% ZrF_4 composition the question of whether a solid solution in the cubic form (α)

[18] M. A. Bredig, *Chem. Div. Quar. Prog. Rep. Mar. 31, 1951*, ORNL-1053, p 114.

of Na_2ZrF_6 (as in the analogous Na_2UF_6 system[19]) or a new compound exists, or both, has yet to be settled. Nine separate samples from this composition range were heated successively over temperature intervals from 450 to 575°C. A period of 1 hr at a fixed temperature appeared to be sufficient for equilibrating the solid phases.

An analysis of the x-ray data obtained is presented in Table 4.5. The choice of temperatures was influenced by the results of differential thermal analyses and the quenching experiments described above. The data indicate that wide ranges of solid solutions exist in the regions examined. Diffuse scattering would have increased the background in the x-ray diffraction patterns if liquid was present along with the solid. It appears that one or two samples approximating 37 mole % ZrF_4 may have reached the liquidus region at 550°C, the highest temperature explored. Further experiments will be carried out before a phase diagram covering this region is drawn.

The phase B-1 was observed for the first time in a high-temperature x-ray pattern and appeared to be easily preserved even on slow cooling, as indicated for the compositions of 33.3, 33.9, and 35.0 mole % ZrF_4 (Table 4.5). The diffraction pattern of the (*X*) phase at elevated temperatures appears to be better developed than the pattern observed at room temperature with a quenched sample, "T-12". The agreement of the (*Z*) phase pattern with the pattern of a quenched "T-5" sample does not appear to be so good.

The x-ray pattern at 495°C for the 40 mole % ZrF_4 composition indicates the presence of B-1 and "Z5". The diffraction lines for the (40) phase are coincident with those of "Z5" and therefore cannot be positively identified if the (40) phase is present with an appreciable amount of "Z5". Also, the presence of three phases would indicate that equilibrium had not been established. At room temperature the pattern was that for the (40) phase, some low-temperature polymorphs of "Z6", and a small amount of the "Z5" phase. The petrographic examination[20] of this mixture at room temperature showed the presence of B-1 and the (40) phase, but the (40) phase here gave a slightly higher index of refraction than that observed on the original sample. The above observations would indicate that the (40) phase is not stable in the region of 495°C.

Some structural relationships among the compounds in the $NaF\text{-}ZrF_4$ binary system have been found to be similar to those in the $NaF\text{-}UF_4$ system. The structure of the compound $NaUF_5$ has been given by Zachariasen[19] as rhombohedral with 6 molecules per unit cell. The space group is $R3$ (C_{3i}^2). The positions of the cations are given in general positions, that is, $\pm(x\ y\ z)\ (y\ z\ x)\ (z\ x\ y)$, with the following parameter values:

	x	y	z
U	$^3/_{13}$	$^1/_{13}$	$^9/_{13}$
Na	$^6/_{13}$	$^2/_{13}$	$^5/_{13}$

There is a pseudocubic cell which contains 3.7 metal atoms and 9.2 fluorine atoms, and its structure closely resembles that of fluorite. The phase "Z5"[21] is isomorphous with $NaUF_5$. The relative intensities in the x-ray patterns of the uranium and the zirconium compounds are similar.

It has been noted[22] that in kilogram preparations of the $NaZrF_5$ and of compositions containing 47 mole % ZrF_4 the latter nonstoichiometric composition froze into a single glass-like phase, whereas the former invariably gave mixtures of the phases "Z5" and "E2".

For a discussion of the structure, a comparison of the directly measured density with the density derived from the x-ray data appeared necessary. Therefore the densities of 5 samples of the glass-like phase were measured,[23] and an average value of 4.11 ± 0.01 g/cc was found. Sampling from different portions of the melt gave no apparent difference in density value. It had also been noticed that no change in cell size of the "Z5" structure was apparent in the range from 43 to 52 mole % ZrF_4; however, some variations in intensity were observed. On the basis of 6 molecules per unit cell the calculated x-ray density is 4.04 g/cc. In order to resolve the discrepancy between the values 4.04 and 4.11, a structure model of "Z5" was built and examined. This model showed that it was possible to add another sodium cation at

[19] J. J. Katz and E. Rabinowitch, *op. cit.*, p 377-382.

[20] Sample examined by H. Insley, Consultant, Metallurgy Division.

[21] The "Z5" phase refers to the extensive solid solution range for the $NaZrF_5$ molecule.

[22] G. W. Watson, Materials Chemistry Division.

[23] S. I. Cohen, Reactor Experimental Engineering Division.

TABLE 4.5. HIGH-TEMPERATURE PHASES OF THE NaF-ZrF_4 BINARY SYSTEM

COMPOSITION (mole % ZrF_4)	TEMPERATURE AND PHASES FROM HIGH-TEMPERATURE X-RAY STUDY					
	Order of Heating Stages					
	a	b	c	d	e	f
33.3[a]	485°C: B-1[b] major	25°C: B-1 major	475°C: B-1	503°C: (X)[c]	575°C: sample expanded out of sample holder	
33.9	460 to 470°C: B-1 major, plus unidentified	490°C: B-1 major	25°C: B-1 major	530 to 535°C: (X)[c]	550 to 555°C: (Y)[d]	520°C: (Y)
35.0 (I)	480°C: B-1 major	25°C: B-1 major	480°C: B-1 major	575°C: (Z)[e] plus α[f]	475°C: unidentified	540°C: (Y)
35.0 (II)	485°C: B-1 plus "Z5"(?)	500 to 503°C: B-1 and (X)	505°C: (X)	540 to 550°C: (X) plus α	494°C: B-1 plus unidentified	
36.8	460°C: B-2[g] plus (40)[h]	495°C: B-1 plus unidentified	507°C: (X) plus unidentified	523°C: unidentified	550°C: unidentified	
37.9	~450°C: B-2 plus (40)	~500°C: B-1 plus "Z5"(?)	517°C: (X) plus unidentified	520°C: (X)	25°C: B-2, B-3,[i] and unidentified	
40.0	460°C: –(40) plus unidentified	495°C: B-1, "Z5", and (40)(?)	25°C: (40) major, "Z6", and "Z5"			

[a] Sampled from composition C, a large batch preparation of Na_2ZrF_6. Remaining samples were taken from the hydrofluorinated "X-mas tree" preparations.

[b] B-1 phase shown petrographically to be biaxially positive, R.I. $\simeq$ 1.41. Examined by G. D. White, Ceramics Department.

[c] (X) phase related to "T-12" phase quenched in this temperature region. Quenches of these compositions reported by R. E. Moore, Materials Chemistry Division.

[d] (Y) phases not identified.

[e] (Z) phase may be related to "T-5" phase; quenched phase identified petrographically.

[f] α phase corresponds with cubic Na_2ZrF_6.

[g] B-2 phase may be the polymorphic form of Na_2ZrF_6 just below B-1.

[h] The pattern of this (40) phase is similar to that obtained at room temperature with a 40 mole % ZrF_4 sample.

[i] B-2 and B-3 are two biaxial optically negative forms of "Z6" normally found at room temperature.

the (0 0 0) position and that it seemed feasible to also place an additional fluorine anion in the ↻ (0 0 ½) positions of the pseudocubic cell without causing a noticeable change in the cell size. The density calculated for this model was 4.16 g/cc at 53.8% NaF–46.2% ZrF_4. Maximum thermal stability of stoichiometrically odd compositions of solid solutions was noticed in other cases.[24,25] On further additions of NaF, the cell size appears to remain essentially constant. The structural model may explain this, if it is assumed that, below 46.2 mole % ZrF_4, substitutions of Na^+ for Zr^{4+} and vacancies in the anion positions occur and counterbalance each other with respect to cell size. (The introduction of the larger sodium cation may be offset by the removal of fluoride ions.) The "Z5" structure is ordered, and as more NaF is substituted into the unit cell the ordered arrangement is disrupted.

At 60% NaF–40% ZrF_4 on the NaF-rich side of a two-phase region the cations are in a disordered arrangement which gives a unit cell similar to what was referred to above as the pseudocubic cell in the "Z5" lattice. Here that unit cell contains, statistically speaking, 2.4 molecules of NaF and 1.6 molecules of ZrF_4. The petrographic observations[20] of this phase at room temperature have indicated some slight birefringence. Quenching experiments and high-temperature x-ray diffraction studies give some indication that perhaps both phases exist near this composition, in different temperature regions.

An attempt was made to evaluate the effect of changes in composition in the range between 46.2 and 50 mole % ZrF_4 upon the relative x-ray diffraction intensities. Factors were calculated for the "Z5" structures for both the 6 NaF–6 ZrF_4 (in molecules per unit cell) and the 7 NaF–6 ZrF_4 compositions by considering only the scattering by the cations. However, the omission of the contribution by the numerous anions may account for the lack of agreement between observed diffraction intensities and those calculated from structure factors. A more favorable situation is envisaged for a computation of the fluorite structure with the inclusion of both cation and anion scattering.

[24] W. Grahmann, *Z. anorg. Chem.* 81, 266 (1913).

[25] M. A. Bredig, *J. Phys. Chem.* 46, 747 (1942).

[26] L. G. Overholser, J. D. Redman, and C. F. Weaver, *ANP Quar. Prog. Rep. Mar. 10, 1954*, ORNL-1692, p 56.

CHEMICAL REACTIONS IN MOLTEN SALTS

F. F. Blankenship L. G. Overholser
W. R. Grimes
Materials Chemistry Division

Chemical Equilibria in Molten Fluorides

J. D. Redman C. F. Weaver
Materials Chemistry Division

Values for equilibrium constants at 600 and at 800°C for the reduction of UF_4 in molten $NaZrF_5$ by Cr° and Fe° were presented in the previous report.[26] No comparable study has been completed during the past quarter; however, a number of experiments have been made to answer questions suggested by the earlier work.

The solubility of FeF_2 in NaF-ZrF_4-UF_4 (50-46-4 mole %) is 0.7 and 7.5 wt % at 600 and 800°C, respectively. These values, which agree well with those found previously for $NaZrF_5$, show that small quantities of UF_4 have a negligible effect on the solubility of FeF_2.

Attempts to measure the solubility of FeF_3 in $NaZrF_5$ at 800°C in nickel equipment demonstrated that the reaction

$$2FeF_3 + Ni \longrightarrow NiF_2 + 2FeF_2$$

proceeded nearly to completion. Virtually all the iron appeared in the filtrate as FeF_2, along with about 60% of the stoichiometric quantity of NiF_2. Examination of the solid residue indicated clearly that the theoretical quantity of NiF_2 was formed but that solubility of this material at 800°C limited the quantity which appeared in the filtered liquid. The solubility of NiF_2 in $NaZrF_5$ at 800°C appears to be about 2.5 wt %.

Experiments at 800°C have shown that the reaction

$$2FeF_3 + Fe^\circ \longrightarrow 3FeF_2$$

proceeds essentially to completion in a short time; no trivalent iron was found in the filtrate. When the reaction

$$2FeF_3 + 3Cr^\circ \rightleftharpoons 3CrF_2 + 2Fe^\circ$$

was attempted, no FeF_3 and only 200 ppm (1%) of the original quantity of soluble iron which was added were detected in the filtrate. The Cr^{++} concentration which was found approximated the theoretical concentration.

Unsuccessful attempts have been made to measure the solubility of CrF_3 in $NaZrF_5$ and the NaF-ZrF_4-UF_4 mixture described above. The molten

salts were difficult to filter; a solid phase which clogged the filter or, as is somewhat less likely, a large increase in viscosity of the melt may have been responsible. The analyses of the few filtrates obtained were quite inconsistent. It does appear, however, that virtually all the Cr^{3+} is reduced to Cr^{++} by reaction with the nickel apparatus.

Some data on the reactions

$$Fe^{\circ} + 2CrF_3 \longrightarrow 2CrF_2 + FeF_2$$

and

$$Cr^{\circ} + 2CrF_3 \longrightarrow 3CrF_2$$

in molten $NaZrF_5$ at 600 and 800°C are shown in Table 4.6. The results obtained at 800°C indicate that in each case quantitative reduction to Cr^{++} occurs. It is not clear from these data what occurs at 600°C.

Preliminary attempts have been made to study the equilibrium

$$Fe + 2UF_4 \rightleftharpoons 2UF_3 + FeF_2$$

in molten $NaZrF_5$ by adding UF_3 and FeF_2 rather than Fe and UF_4 to the melt. Equilibrium concentrations of the soluble constituents agree qualitatively with those previously presented. More detailed study of this system will be conducted in the near future.

Preliminary attempts to determine the equilibrium concentrations of CrF_2 and UF_3 when Inconel turnings are used to reduce UF_4 in molten $NaZrF_5$ at 800°C have been made. The equilibrium concentrations are considerably lower than those found when pure chromium is used; the activity of chromium in Inconel is apparently considerably lower than unity.

Solubility of UF_3 in NaF-ZrF_4 Mixtures

G. M. Watson C. M. Blood
Materials Chemistry Division

The technique used in solubility experiments was, briefly, the following: About 3 kg of an appropriate NaF-ZrF_4-UF_4 mixture was prepared and purified by hydrogenation and hydrofluorination in the usual manner. The UF_4 was reduced to UF_3 by addition, under an inert atmosphere, of an excess of Zr° or U° to the melt at 800°C, followed by continuous sparging with purified hydrogen, usually overnight, to permit equilibration of the mixture. Samples of the mixture were then taken through filter sticks with the filtration medium consisting of sintered nickel. Equilibration times of at least 1 hr with continuous hydrogen sparging were permitted each time the temperature was changed.

The results obtained by filtration at seven temperatures in the range 600 to 900°C of a mixture containing 50 mole % NaF, 46.8 mole % ZrF_4, and 3.2 mole % UF_4 are shown in Fig. 4.4. Since the

TABLE 4.6. REACTION OF Fe° OR Cr° WITH CrF_3 IN MOLTEN $NaZrF_5$[a]

REDUCING AGENT USED[b]	TEMPERATURE (°C)	PRODUCTS OBSERVED IN FILTRATE				
		Fe (wt %)		Cr (wt %)		Ni (ppm)
		Fe^{++}	Total	Cr^{++}	Total	
Fe	800	0.38	0.37	1.50	1.02[c]	10
	800	0.41	0.38	1.45	1.01[c]	10
	600	0.07	0.18	0.79	0.53	335
	600	0.08	0.08	0.69	0.33	80
Cr	800			1.53[c]	1.51[c]	10
	800			1.55[c]	1.47[c]	10
	600			0.96	0.74[d]	90
	600			0.75	0.55[d]	10

[a] 1 wt % of Cr^{3+} added as CrF_3 to each sample.
[b] 5 wt % of reducing metal added to sample.
[c] Theoretical value.
[d] Low values may be due to low solubility of CrF_2 at 600°C.

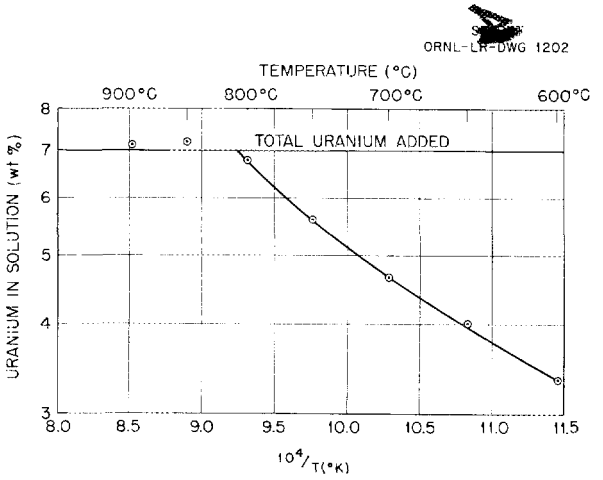

Fig. 4.4. Solubility of UF_3 in NaF-ZrF_4.

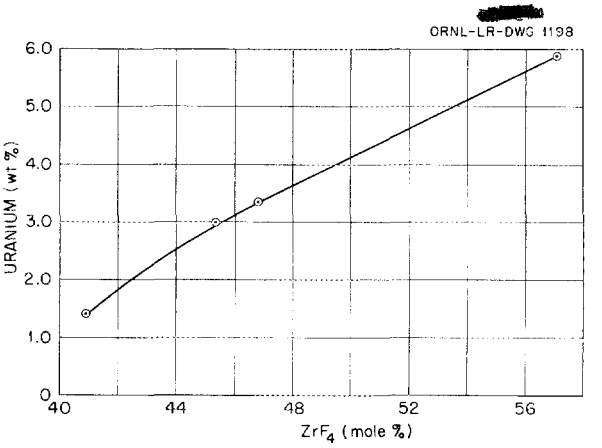

Fig. 4.5. Solubility of UF_3 at 600°C in NaF-ZrF_4.

mixture, as prepared, contained 7 wt % uranium, it is obvious from the analyses that all the uranium which was added was soluble above about 815°C. A composite sample of the residue which remained after removal of about 10% of the batch as samples contained 6.8 wt % uranium by analysis; it is apparent that the pretreatment and the considerable period at high temperatures affected the sample only slightly if at all. The accuracy of the data obtained is not sufficient to establish that the curvature of the line below 800°C in Fig. 4.4 is real. Heats of solution as calculated from the slope of this curve range from 8300 cal/mole at the higher temperatures to 5600 cal/mole at the lower temperatures.

Previous observations[27,28] indicated that the solubility of UF_3 increased with increasing ZrF_4 concentration in the concentration range near 50 mole % ZrF_4. Filtration at 600°C of five different preparations by the general technique described above has quantitatively confirmed these observations. The data obtained are shown in Fig. 4.5.

An increase in ZrF_4 concentration from 45 to 57 mole % apparently at least doubles the solubility of UF_3. Since the UF_3 dissolved by the 57 mole % ZrF_4 mixture agreed within experimental error with the amount added, the solubility of UF_3 in this mixture at 600°C must be equal to or greater than 5.9 wt % uranium.

[27] F. F. Blankenship *et al.*, *ANP Quar. Prog. Rep. Dec. 10, 1952*, ORNL-1439, p 119.

[28] J. D. Redman *et al.*, *ANP Quar. Prog. Rep. Mar. 10, 1953*, ORNL-1515, p 110.

The increase in solubility of UF_3 with increasing ZrF_4 concentration implies that UF_3 is not complexed strongly by free fluoride ion but that dissociation of UF_3 is aided by the presence of free ZrF_4. Whether disproportionation of UF_3 into UF_4 and U° is likely to become appreciable at a lower temperature in such melts is, as yet, unknown.

Some auxiliary experiments performed in smaller scale apparatus by other members of the ANP Chemistry Group (R. J. Sheil and C. J. Barton) have shown that a mixture prepared to contain 52.7 mole % NaF, 40.9 mole % ZrF_4, and 6.4 mole % UF_3 when filtered at 600°C yields a filtrate containing only 1.4 wt % uranium. The residue from this filtration comprised about 20% of the total sample and was predominantly UF_3 with some yellow crystals that were shown to be mainly $Na_9Zr_8F_{41}$ with opaque material which was almost certainly Zr° or ZrH_2. These data, which are in general agreement with those cited above, serve to demonstrate that UF_3 and not a complex uraniferous fluoride is the primary phase in the concentration range near 50 mole % ZrF_4.

Solubility of UF_3 in NaF-KF-LiF Mixtures

G. M. Watson C. M. Blood
Materials Chemistry Division

Two experiments were performed to determine the solubility of UF_3 in the NaF-KF-LiF eutectic. In both experiments, the UF_3 was obtained by reduction *in situ* of the dissolved UF_4 with uranium metal. The technique used in obtaining the filtrates

for solubility determinations was otherwise identical to that used in the corresponding experiments with $NaF\text{-}ZrF_4$ mixtures, as described above.

When a two-fold excess of metallic uranium was used, potassium metal was distilled from the reactor at temperatures of 800°C and above. When filter sticks were introduced into the melt, the filter media immediately became clogged. Filtrates weighing only 1 to 15 g could be obtained in contrast to the 50-g filtrates obtained in normal operations. At the end of the experiment, a metallic alloy was observed on the reactor walls and as a crust on the solidified melt.

The formation of potassium is explained when the equilibrium constant of the reaction

$$KF\ (solution) + \tfrac{1}{3}U\ (crystal) = K\ (vapor) + \tfrac{1}{3}UF_3\ (solution)$$

is calculated from published values of free energies of formation. At 800°C the equilibrium partial pressure of potassium, with the assumption of ideal solutions, may be estimated to be from 15 to 20 mm Hg.

The constituents of the metallic alloy were identified as nickel and uranium. The alloy formation may be rationalized from consideration of the U-Ni phase diagram,[29] which shows that eutectic melting of nickel and uranium can occur at about 738°C. The eutectic phases are UNi and U_6Ni.

In order to avoid or minimize side effects in the second experiment, only the stoichiometric quantity of uranium metal was added with 10% excess of zirconium metal. The mixture was heated to only 750°C. Much more satisfactory filtrates were obtained (an average of about 45 g above 600°C), and no metallic alloy was observed. The concentrations of uranium in the filtrates and in residues of both experiments are summarized in Table 4.7.

Petrographic examination of composite samples of the residue from each experiment failed to show the presence of tetravalent uranium but detected (in quantity) a bright-orange phase believed to be a $KF\text{-}UF_3$ compound. The tabulated results appear to show essentially constant uranium concentration at the temperatures studied. This effect would be shown if all the uranium were in the liquid phase throughout the temperature range. Unfortunately, the results are not consistent between experiments and the filtrate (or residue) analyses do not agree within experimental error with the amount of uranium added. It is obvious, however, that the solubility of UF_3 in the NaF-KF-LiF eutectic is higher than 15 wt % uranium.

[29] *The Reactor Handbook*, Vol. 3, p 495, Technical Information Service, AEC, 1953.

TABLE 4.7. SOLUBILITY OF UF_3 IN NaF-KF-LiF EUTECTIC

TEMPERATURE (°C)	SOLUBILITY OF UF_3 (wt % U)	
	R-153*	R-154**
800	15.4	
750	17.3	16.0
700	17.3	16.1
650	17.3	16.3
600	17.2	16.2
550		16.4
508		15.9
Residue	20.1	17.8

*22.0 wt % uranium added.
**18.6 wt % uranium added.

Solubility of UF_3 in NaF-RbF-LiF Mixtures

R. J. Sheil C. J. Barton
Materials Chemistry Division

The solubility of UF_3 in the NaF-RbF-LiF eutectic has been determined at three temperatures by equilibration of a melt to which sufficient UF_4 and excess uranium metal had been added to produce 4 mole % UF_3, filtration of a specimen at the desired temperature, and chemical analysis of the resulting solution. Because of the high RbF content of these mixtures, they are extremely hygroscopic; great care in handling the samples is necessary to obtain reliable values for UF_3 solubility.

The data obtained are shown in Table 4.8. The values obtained show that 597°C is probably above the liquidus temperature for this composition; 9 wt % of uranium is probably not the maximum that can be dissolved at this temperature. Petrographic examination of the filtrates indicated that no UF_4 or complex fluorides containing tetravalent uranium were present. The samples contained no free UF_3; no identification of the complex U^{3+} fluoride has yet been made.

TABLE 4.8. SOLUBILITY OF UF_3 IN NaF-RbF-LiF EUTECTIC

FILTRATION TEMPERATURE (°C)	FRACTION OF SAMPLE FILTERED (%)	SOLUBILITY OF UF_3 (wt % U)	FILTRATE COMPOSITION* (mole %)			
			LiF	RbF	NaF	UF_3
497	67	4.4	43.8	46.8	8.2	1.2
552	90	6.8	39.6	47.6	10.7	2.1
597	99	9.0	41.1	46.5	9.6	2.84

*Calculated from analyses for Li^+, Na^+, Rb^+, and total U.

Chlorination of UF_3

G. M. Watson C. M. Blood
Materials Chemistry Division

Analytical determinations of the UF_3 dissolved, with or without added UF_4, in fluoride melts gave values considerably lower than those anticipated from petrographic examination or from the stoichiometry of the preparation reactions. The description[30] of the preparation and the properties of UF_3Cl suggested that chlorination of the UF_3 to this compound and subsequent determinations of Cl^- in the product might be successfully used.

Attempts to chlorinate 1- to 2-g portions of a 200-mesh UF_3-UF_4 mixture contained in ceramic boats in a glass-tube reactor by exposure to dry Cl_2 at 350°C for various intervals of from 2½ to 20 hr yielded a green product of uniform appearance. Petrographic examination showed the product to be markedly birefringent and uniaxially (or possibly biaxially) negative, with refractive indices of 1.56 to 1.59. X-ray diffraction revealed no free UF_3 but did reveal an unknown diffraction pattern unrelated either to UF_3 or UF_4. Chemical analyses of samples chlorinated 2½ to 4½ hr indicated 5.7% total chlorine; since this is roughly one-half the expected value for chlorine, it appears that the chlorination was incomplete or that some hydrolysis and oxidation of the sample had occurred.

Attempts will be made to improve the contact between the powder and the Cl_2 by passage of the gas through the solid contained on a sintered-glass filter. If these attempts are successful, studies with UF_3-bearing fuel mixtures will be attempted.

[30] J. C. Warf and F. Edwards in *Chemical Research – General Chemistry Report for Period of March 10 to April 10, 1944*, CC-1496 (May 11, 1944); J. C. Warf *et al.*, *Mixed Uranium Halides*, CC-1785 (Sept. 10, 1944).

[31] V. S. Coleman, C. J. Barton, and T. N. McVay, *ANP Quar. Prog. Rep. Dec. 10, 1952*, ORNL-1439, p 117.

Preparation of $UF_3 \cdot 2ZrF_4$

F. P. Boody H. A. Friedman
Materials Chemistry Division

The compound $UF_3 \cdot 2ZrF_4$ was identified[31] in 1952 as one of the materials obtained on cooling ZrF_4-bearing melts containing large quantities of UF_3. Since large quantities of the compound had not been prepared, the preparation of a 3.5-kg batch was attempted to make available a quantity sufficient for measurement of vapor pressure and other physical properties. The method used was a modification of the standard hydrofluorination procedure which involved reduction of a UF_4-bearing mixture of proper composition with zirconium metal chips at 850°C. The product appeared homogeneous and was a dark reddish-brown in color. Only 655 g was filtered, since unavoidable cold spots in the transfer line permitted freezing of this relatively high-melting-point material (740°C). The compound material, unlike virtually all other melts observed here, appeared to expand slightly on freezing.

Petrographic examination of the product showed it to be approximately 99% homogeneous, red-orange, uniaxially positive $UF_3 \cdot 2ZrF_4$ and about 1% free UF_3. X-ray diffraction analysis confirmed the predominant phase to be $UF_3 \cdot 2ZrF_4$, with small amounts of free UF_3. On warming in air, the color of the product changes from orange-red to olive-green and the refractive index increases. Structurally the crystals do not appear to be altered by the color change, and no evidence of oxidation other than the color is visible.

Preparation of Various Fluorides

B. J. Sturm E. E. Ketchen
L. G. Overholser
Materials Chemistry Division

Several of the simple structural-metal fluorides,

as well as complexes of these materials with the alkali-metal fluorides, were prepared for corrosion experiments and some physical and chemical property testing. In an effort to prepare the structural-metal fluorides in a high state of purity, attempts were made to refine crude NiF_2 and CrF_3 by treatment with BrF_3. In a modification of the apparatus originally assembled by the ANP Analytical Group, the crude material was treated with BrF_3 at 350 to 400°C for 1 to 3 hr, and the product was outgassed by thorough pumping at about 350°C. Analyses of 10 samples indicated that considerable conversion of oxides and/or oxyfluorides was achieved by this procedure; however, the purity of the product was still not of the order desired.

Large quantities (1.5 to 2 kg) of K_3CrF_6 and of K_3FeF_6 were prepared by heating appropriate quantities of $2CrF_3 \cdot 7H_2O$ and $FeF_3 \cdot 3H_2O$ with KHF_2. Several batches of FeF_3, FeF_2, $FeCl_2$, NiF_2, $NiCl_2$, CrF_3, and CrF_2 were synthesized by methods previously described.

FUNDAMENTAL CHEMISTRY OF FUSED SALTS

EMF Measurements

L. E. Topol
Materials Chemistry Division

Measurements of decomposition potentials of KCl and of a variety of chlorides in solution in molten KCl at 850°C were attempted. Cathodes of platinum or nickel and anodes of carbon, nickel, zirconium, platinum, electrolytic chromium, Inconel, and stainless steel have been employed. Morganite (Al_2O_3) crucibles were used to contain the melt in each case.

The solutions were prepared by heating 2 moles of KCl with 1 mole of the desired anhydrous chloride to above the melting point of the mixture in a sealed, evacuated quartz tube. More dilute solutions were prepared by the addition of KCl to the materials so obtained. The data obtained are tabulated in Table 4.9. If the value of 0.90 volt for electrolysis of KCl with uranium anodes is combined with that of 3.15 volts for electrolysis of this material with inert anodes, E for the reaction

$$U + \frac{x}{2} Cl_2 \longrightarrow UCl_x$$

appears to be 2.25 volts. This value agrees well with the estimated E° (2.26 volts) for UCl_3. The value (1.27 volts) obtained by electrolysis of KCl with an anode of electrolytic chromium is less than that previously obtained (1.5 volts) with an anode of Cr° plated on gold wire.[32]

The potentials observed for electrolysis of KCl with Inconel electrodes suggest that Cr° is dissolved first and that, subsequently, Ni° is attacked; no dissolution of Fe° was detected. However, when the anode is a 300-series stainless steel, it appears that first iron, and then chromium, is dissolved.

Three possible reactions of $CrCl_2$,

(1) $3CrCl_2 \longrightarrow Cr^\circ + 2CrCl_3$, $E^\circ = 0.84$ volt,

(2) $CrCl_2 \longrightarrow Cr^\circ + Cl_2$, $E^\circ = 1.36$ volts,

(3) $CrCl_2 + Ni^\circ \longrightarrow NiCl_2 + Cr$, $E^\circ = 0.54$ volt,

may qualitatively explain the experimental observations on electrolysis of solutions of $CrCl_2$. It appears that with a nickel anode, reaction 3 occurs at both $CrCl_2$ concentrations tested. With the inert carbon anode, reaction 1 is controlling at high concentrations of $CrCl_2$, while reaction 2 is important in the dilute solutions.

The experimental electrolysis of $ZrCl_4$ solutions with nickel anodes checks well with E° values for reactions producing $ZrCl_3$, $ZrCl_2$, and Zr° with NiF_2, as described previously.[32] The values obtained with the graphite anodes may well be due to the reactions

(4) $ZrCl_4 \longrightarrow Zr^\circ + 2Cl_2$,

(5) $ZrO_2 + C \longrightarrow Zr^\circ + CO_2$,

for which the best estimates of E° are 1.9 and 1.24 volts, respectively. Attack on some of the graphite anodes indicates that reaction 5 occurs.

The electrochemical behavior of UCl_3 appears to be similar to that of $CrCl_2$. It is likely that the reactions

(6) $4UCl_3 \longrightarrow 3UCl_4 + U^\circ$, $E^\circ = 1.08$ volts,

(7) $2UCl_3 \longrightarrow 2U^\circ + 3Cl_2$, $E^\circ = 2.26$ volts,

(8) $2UCl_3 + Ni \longrightarrow 3NiCl_2 + 2U^\circ$, $E^\circ = 1.44$ volts,

[32] L. E. Topol, *ANP Quar. Prog. Rep. Mar. 10, 1954*, ORNL-1692, p 63.

TABLE 4.9. OBSERVED DECOMPOSITION POTENTIALS FOR REDUCIBLE CHLORIDES IN MOLTEN KCl AT 850°C

SOLUTE ADDED	CONCENTRATION OF SOLUTE (mole %)	ELECTRODES		BLANKETING ATMOSPHERE	POTENTIAL OBSERVED (volt)
		Cathode	Anode		
None		Pt	U	He	0.89
		Pt	U	H_2	0.90
		Ni	Zr	He	1.03
		Ni	Cr*	H_2	1.27
		Ni	Inconel	H_2	1.85, 2.03
		Ni	Inconel	He	1.85, 2.03
		Ni	Type 316 stainless steel	H_2	1.55, 1.85
		Ni	Type 347 stainless steel	H_2	1.43, 1.85
$CrCl_2$	33.3	Ni	C	H_2	0.88 to 0.92
	33.3	Ni	Ni	H_2	0.53 to 0.57
	2.0	Ni	C	He	1.30 to 1.43
	2.0	Ni	Ni	He	0.65 to 0.69
$ZrCl_4$	33.3	Ni	C	H_2	1.67 to 1.80
	33.3	Ni	Ni	H_2	0.50 to 0.57, 0.80, 1.01
	25.0	Ni	C	H_2	1.33, 1.80 to 1.90
	25.0	Ni	Ni	H_2	0.63, 0.94 to 1.06
UCl_3	100	Pt	Ni	H_2	0.80 to 0.84, 1.01 to 1.10
	100	Pt	Ni	He	0.80 to 0.87, 0.98
	33.3	Pt	C	H_2	0.78 to 0.85
	33.3	Pt	Ni	H_2	0.80 to 0.82
	33.3	Pt	Ni	He	0.83 to 0.85
	33.3	Ni	C	H_2	0.68 to 0.72
	33.3	Ni	Ni	H_2	0.78 to 0.82
	2.0	Pt	Ni	H_2	1.25 to 1.35
	2.0	Pt	Pt	He	2.10
	2.0	Pt	C	He	1.15, (2.08), 2.48 to 2.56
	1.0	Pt	Ni	He	1.36

*Electrolytically prepared.

are responsible for most of the effects observed. The agreement between values under He and H_2 suggests that UCl_4 is only slightly affected by H_2 in the dilute solutions with relatively poor contact efficiency used. When nickel cathodes were employed, an alloy of uranium and nickel resulted. The general constancy of the potential obtained with both pure UCl_3 and K_2UCl_5 seems to indicate some solubility of UCl_4 in UCl_3.

A zirconia crucible (fabricated by Titanium Alloys Division of National Lead) was heated at 750°C for 4 hr in a hydrogen atmosphere with a charge of NaF-KF-LiF-UF_3. The vessel proved to be somewhat porous; the only evidence of attack observed was a slight reaction to produce UO_2 at the crucible melt interface. It is hoped that vessels of this material may be useful for electrochemical studies of fluoride melts.

Physical Chemistry[33]

E. R. Van Artsdalen
Chemistry Division

The density and electrical conductivity of the molten system KCl-NaCl have been determined over the entire composition field from temperatures a little above the melting point of the individual mixtures to about 1000°C. Density can be expressed as a linear function of temperature, and the specific conductance can be expressed as a quadratic function of temperature. A plot of the molar volume vs the composition shows a slight positive deviation from linearity, with a maximum deviation of about 0.5% at 50 mole % KCl. Equivalent conductance, Λ, may be expressed in the form

$$\log \Lambda = C + A\frac{1000}{T} + 2302.6B \log \frac{1000}{T},$$

where T is in degrees Kelvin, C is a constant of integration, and A and B are the intercept and the slope, respectively, of the straight line which results from the graphical differentiation of log Λ vs $(1000/T)$. The possibility that this form of equation is general in nature and applicable to many molten salt systems is being investigated. A plot of equivalent conductance vs mole per cent KCl shows that the system is far from additive but that it resembles the molten KCl-LiCl system reported previously.[34] There is a very shallow minimum in equivalent conductance for the KCl-NaCl system at about 85 mole % KCl. The explanation for this is apparently the same as the one advanced in the case of the molten system KCl-LiCl.

An emf cell with transference has been designed for use with fused salts. With such a cell it is possible to make the potential measurements required for obtaining important information and cross-checks on transference numbers and activity coefficients of ions in melts. An initial study with the molten system $NaNO_3$-$AgNO_3$ indicated that useful results can be obtained by measurements of cells with transference. However, the attainment of good reproducibility poses a difficult problem.

Radiotracer techniques are being used for making measurements of the self-diffusion coefficient of individual ions in molten salts. This work has necessitated the development of new techniques for handling molten materials as well as for precision control of high-temperature furnaces over periods of several days. Measurements of the self-diffusion of sodium ions in molten sodium nitrate indicate that the diffusion coefficient is of the order of 1 or 2×10^{-5} sq cm sec^{-1} at temperatures a little above the melting point. This work is being pursued actively and is expected to yield important results applicable to transport processes.

A high-precision, adiabatic, heat-capacity calorimeter has been built for operation in the range up to about 1000°C. All preliminary tests have been completed and the calibration should be completed soon. It is anticipated that heats and free energies of formation can be determined with good accuracy for a number of important reactor materials. In addition, fundamental information should be obtained concerning the solid state as well as the molten state of salts.

CHEMICAL EFFECTS OF FISSION PRODUCTS

R. F. Newton
ANP Division

Other than the absorption of neutrons, the possible undesirable effects of fission products in a reactor are the decrease of heat transfer by separation of a solid phase on heat exchange surfaces and by change of viscosity or heat capacity of the molten mixture, and the acceleration of corrosion. Any such effects will be dependent on the quantities of fission products which accumulate.

Quantity of Fission Products

The fission products were calculated on the assumption that about 0.1 mole of uranium undergoes fission per kilogram of melt at a uniform rate during 1000 hr. The quantities given in Table 4.10 are for the end of the 1000-hr period. The yields for the various products were taken from the smooth curve of Siegel.[35] The quantities are as large as or larger than any which occur at earlier times and not greatly different than they would be if the fissions were spread over a greater time period.

Separation of Solid Phases

Of the elements listed, molybdenum, ruthenium, rhodium, and palladium are expected to separate

[33] For details of this work see *Chem. Div. Semiann. Prog. Rep. Dec. 20, 1953*, ORNL-1674, and *Chem. Div. Semiann. Prog. Rep. June 20, 1954* (to be published).

[34] E. R. Van Artsdalen, *ANP Quar. Prog. Rep. Dec. 10, 1953*, ORNL-1649, p 58.

[35] J. M. Siegel, *J. Am. Chem. Soc.* 68, 2411 (1946).

TABLE 4.10. FISSION-PRODUCT YIELD AT END OF 1000 hr

PRODUCT	YIELD*	PRODUCT	YIELD	PRODUCT	YIELD
Se	0.4	Cb	7.0	I	1.2
Br	0.25	Mo	18.6	Xe	18.4
Kr	3.5	Te	5.1	Cs	16.9
Rb	4.0	Ru	14.0	Ba	6.7
Sr	12.2	Rh	1.0	La	6.5
Y	5.3	Pd	1.3	Ce	26.0
Zr	24.8	Te	1.4	TRE**	53.3

*In atoms per 100 fissions occurring uniformly over 1000 hr.

**Total rare earths.

as the metals. Molybdenum and palladium alloy with nickel, and it is presumed that ruthenium and rhodium do likewise. If they form a solid solution with nickel or nickel alloy and slowly diffuse into the heat-exchanger wall, they will probably do no harm; if they deposit on the surface and remain there, they may reduce heat transfer because of roughening of the surface.

The possible separation of either simple or complex solid fluorides, because of their poor heat-transfer properties, would be much more serious than the deposition of metal. Rubidium may be dismissed immediately, since it is a desirable constituent of the fuel; chemically, cesium is also desirable. Zirconium likewise may already be present in the fuel, in which case the zirconium formed by fission will change the relative amount of zirconium in the fuel to a negligible extent. If zirconium is not an intentional constituent, it appears impossible that it could precipitate from a fluoride-based fuel not containing oxygen. Barium fluoride and sodium fluoride form a eutectic at 820°C that contains 35 mole % BaF_2. The extrapolated solubility of the eutectic is 14 mole % at 600°C. Corresponding data are not available for SrF_2, but an extrapolation from the eutectic of CaF_2-NaF gives a solubility of CaF_2 at 600°C of 12.3 mole %. Since the properties of strontium compounds are generally between those of calcium and barium, it is safe to assume a solubility of at least 10 mole % for the strontium compounds, that is, nearly 100 times the amount produced.

The only remaining substances worthy of consideration are the fluorides of yttrium and the rare earths. These substances are so similar chemically that they undoubtedly form a continuous series of solid solutions and can practically be treated as a single compound. From the phase diagrams of alkali-metal fluorides with LaF_3 and with YF_3, the lowest solubility (YF_3 in KF) extrapolated to 600°C is 8 mole %. Since the total of rare earths plus yttrium is of the order of 0.5 mole %, even here, there seems to be an ample factor of safety regarding the possibility of precipitation.

Effects on Viscosity and Heat Capacity

The replacement of one uranium atom by two atoms of fission products would be expected to increase the heat capacity per gram, but the density would be decreased at the same time, with very little change in the heat capacity per cubic centimeter. Similarly some fission products would increase the viscosity while others would decrease it. In any case, it is safe to predict that the changes will be no greater than about 1%.

Effects on Corrosion

It is apparent that the total number of equivalents of cationic fission products exceeds that of anionic fission products plus the fluoride made available by fission of the uranium (assuming the uranium as UF_4) only if molybdenum is included as one of the cationic elements. However, if the relative affinity of molybdenum and nickel for fluorine is considered (Glassner[36] gives free energies of formation of −56 and −63 kg-cal/gram-atom of fluorine for MoF_6 and NiF_2, respectively), it is evident that molyb-

[36] A. Glassner, *A Survey of the Free Energies of Formation of the Fluorides, Chlorides, and Oxides of the Elements to 2500°K*, ANL-5107 (Oct. 22, 1953).

denum will appear as the element along with ruthenium, rhodium, and palladium. In such cases, the fission of uranium occurring as UF_4 will be accompanied by the solution of a corresponding amount of nickel, chromium, or other wall constituent. The imbalance can be corrected by using a fuel in which one-half of the uranium which undergoes fission is UF_3. Since it is anticipated that about 20% of the uranium present will undergo fission, the change required to prevent solution of nickel because of this cation-anion imbalance is to have 10% or more of the uranium present as UF_3. From preliminary data available on the solubility of UF_3, it appears that even the zirconium-base fuels should be capable of dissolving this amount, while the alkali-metal-fluoride fuels possess a large margin of safety in this regard.

PURIFICATION AND PROPERTIES OF ALKALI HYDROXIDES

L. G. Overholser F. Kertesz
Materials Chemistry Division

Purification of Hydroxides

E. E. Ketchen L. G. Overholser
Materials Chemistry Division

Eight batches of NaOH were purified by filtering a 50-wt % aqueous solution through a fine sintered-glass filter to remove the Na_2CO_3 and then dehydrating at 400°C under vacuum. The product, as in the past, contained less than 0.1 wt % of H_2O and of Na_2CO_3. Four batches of commercial LiOH were dehydrated at 200°C under vacuum to yield material containing less than 0.1 wt % of H_2O and 0.2 wt % of Li_2CO_3. Approximately 5 lb of potassium, after being divided into ½-lb portions, was reacted with water, and the resulting solutions of KOH were dehydrated at 400°C under vacuum. The dehydrated KOH contained approximately 0.1 wt % of Na and less than 0.1 wt % of K_2CO_3 and of H_2O.

Reaction of Sodium Hydroxide with Metals

F. A. Knox H. J. Buttram
F. Kertesz
Materials Chemistry Division

The hydrogen equilibrium pressures developed in the sodium hydroxide–nickel reaction were further investigated with the use of the previously described quartz-jacketed nickel reaction tube which was connected to a manometer. It was planned that hydrogen would be added to the jacket to reduce the time necessary for establishment of the pressure equilibrium, but in practice this arrangement proved unsatisfactory. The hydrogen added to the jacket introduced an imbalance in the system and thus increased the pressure inside the reaction tube. It was also recognized that errors were introduced in the previous measurements by hydrogen being removed when the system was evacuated during heating up to 600°C, because the sodium hydroxide was thus subjected to heat and to lowering of the pressure. The current measurements are being made by evacuating the system at near the melting point of the hydroxide. The redetermined values, which seem to approximate steady-state conditions, were found to be higher than those reported previously. The redetermined values are given in Table 4.11. These data yield a straight line when log P_{H_2} is plotted against $1/T$ as indicated in Fig. 4.6.

In addition to these measurements of the hydrogen pressures developed during the reaction, an attempt was made to study the mechanism involved by determining the amount of metal dissolved. In the first series of experiments, nickel capsules containing hydrogen were sealed in quartz envelopes; in the second series, the capsules were unjacketed and the evolved gas was allowed to escape. The capsules were heated for periods which ranged from 2 to 256 hr.

It was found that the nickel concentration in the hydroxide in the capsules with the quartz jackets reached a plateau rather early and remained constant during the prolonged heating periods. It may be assumed that the nickel concentration reached an equilibrium value in the jacketed system. The nickel concentration continued to increase with time in the unjacketed capsules.

TABLE 4.11. HYDROGEN PRESSURE OVER NaOH IN NICKEL

TEMPERATURE (°C)	PRESSURE (mm Hg)
600	46
700	77
800	126
900	160
1000	205

Similar series of experiments with sodium hydroxide in copper capsules showed similar behavior. After 256 hr of exposure at 600°C, the copper concentration in the jacketed capsules was about 700 ppm, while it was as high as 8000 ppm in the unjacketed capsules. For the jacketed capsules the copper concentration rose to about 800 ppm at 700°C and 1100 ppm at 800°C. The unjacketed capsules that were heated at 800°C in a helium-filled dry box had relatively low copper concentrations, but the walls were covered with copper crystals. This is the first time that mass transfer of copper has been observed under these conditions. A larger percentage of the nickel impurity that originally existed in the copper capsule was found in the transferred metal than in the wall material of the capsule.

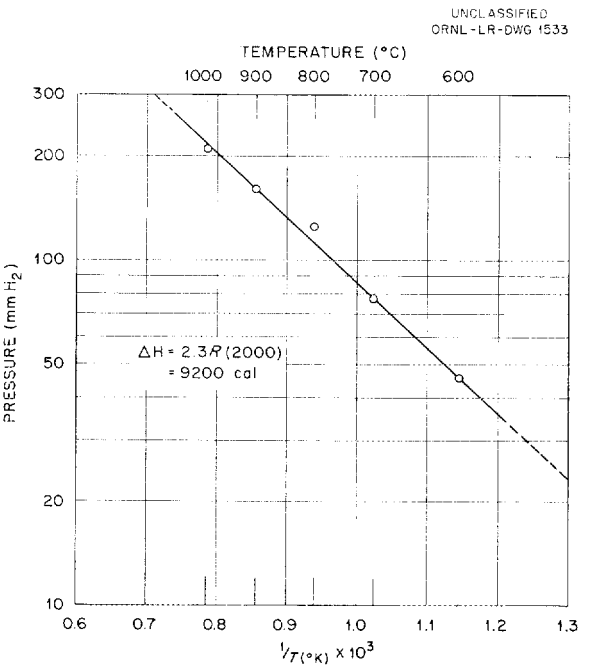

Fig. 4.6. Hydrogen Pressure over Sodium Hydroxide in Quartz-Jacketed Nickel Capsules.

PRODUCTION OF PURIFIED MOLTEN FLUORIDES

F. F. Blankenship G. J. Nessle
Materials Chemistry Division

Laboratory-Scale Production

C. M. Blood G. M. Watson
F. P. Boody H. A. Friedman
Materials Chemistry Division

A total of 28 batches of various molten fluorides was processed during the quarter; these materials were used for phase studies, for corrosion testing, for chemical separations research, and for studies in kinetics of high-temperature chemical reactions. The largest usage of these purified materials was in the studies of UF_3 solubility.

Interest has recently developed in the alkali fluoride eutectics as UF_3 solvents. Since there had previously been some difficulty in preparing the NaF-KF-LiF eutectic in a high state of purity by the hydrogenation-hydrofluorination technique without excessive corrosion of the apparatus, a study of the behavior of these materials during purification was attempted.

Two batches of the NaF-KF-LiF eutectic have been prepared successfully in apparatus which was assembled with special care to avoid leaks. The solid fluorides were admitted to the apparatus and dried at 350 to 380°C under flowing helium before elevation of the temperature. The fluorides were maintained under hydrogen during the heating to 800°C and HF was admitted only after this temperature was reached. One batch was treated for 100 min with HF and stripped with 500 liters of H_2; the other batch was treated with HF for 70 min and stripped with 600 liters of H_2. The HF concentration in the exit hydrogen from the first batch was 2.5×10^{-4} mole/liter and from the second, 1.8×10^{-4} mole/liter.

The color of the product was dead white in each case, and the product appeared to be quite homogeneous. Chemical analyses of the products have not been completed. Although there were deposits of metal around the thermocouple well, on the reactor walls, and as a partial plug in the gas-inlet tube that were shown spectrographically to consist of NaF, KF, and LiF, along with an alloy of nickel and iron, attack on the container seemed to compare favorably with that observed in processing NaF-ZrF_4 mixtures. Therefore it appears that the alkali-metal-fluoride melts can be prepared in a high state of purity by existing techniques if the procedure described above is followed.

Experimental Production

J. E. Eorgan C. R. Croft
J. Truitt J. P. Blakely
Materials Chemistry Division

A total of 162.7 kg of various fluoride compo-

sitions was prepared in the experimental production facility and dispensed to various requesters in the ANP program. The pilot-scale production facility which will somewhat more than double the present pilot-scale capacity is nearly completed and should be available for operations before June 1. The experimental production facility will then be adapted for safe operation with BeF_2.

Large-Scale Production

F. A. Doss R. Reid
R. G. Wiley
ANP Division
M. S. Freed
Pratt & Whitney Aircraft Division
F. L. Daley E. F. Joseph
E. L. Youngblood J. P. Blakely
Materials Chemistry Division

To meet the markedly increased demand for processed fluorides, the 250-lb production facility was placed on three-shift operation, and a total of 1358 kg of fluorides was processed. Most of this material was transferred to containers which ranged in size from 2 to 25 kg. Pratt & Whitney Aircraft Division received approximately 450 kg of this material, and, except for about 20 kg that was delivered to Battelle Memorial Institute, the remainder was dispensed to requesters in the ANP program at ORNL.

The increasing demands for purified fluorides necessitated, early in this calendar year, an increased output of ZrF_4 from the production plant operated by Y-12 personnel. With the available equipment, this production increase could be accomplished only by decreasing the hydrofluorination time of $ZrCl_4$ in the converter and by increasing the temperature of sublimation of the crude ZrF_4. The quality of the ZrF_4 was, accordingly, reduced; the iron content of the ZrF_4 increased from a mean of 250 to about 1000 ppm, while the nickel content rose from about 50 to about 200 ppm.

Although it is possible to prepare fluoride mixtures to rigorous specifications from this ZrF_4, use of this material has reduced the efficiency of the production facility to a level considerably below that obtained during 1953 when the ARE fuel solvent was being processed. For example, the gas-inlet tubes frequently become plugged by crystals of nickel and iron during the hydrogen-flushing operation. Since the amount of iron to be stripped (by reduction of FeF_2 with hydrogen) is much larger than that previously considered normal, the time required for the hydrogen stripping has increased from about 30 to nearly 100 hr, and hydrogen requirements have risen from 10,000 liters to nearly 25,000 liters per 250-lb batch of fluoride.

Since the anticipated demand for fluorides will probably preclude a slower production rate of ZrF_4 and since improved purity at the present production rate would require expansion of the facility, attempts are being made to obtain pure Na_2ZrF_6 from commercial sources. While ZrF_4 must be added to this material to reach the fuel compositions required, the amounts of ZrF_4 needed would be well within the capacity of the Y-12 Plant for ZrF_4 of acceptable purity.

It is anticipated that pure ZrF_4 (or its equivalent) will be available within the next six to eight weeks. Should no commercial concern be able to meet purity specifications (at a competitive price), it may prove more economical in the long run to use hafnium-free ZrF_4 for all fuel production without regard to intended use. This rather startling conclusion (based on price of production of about 3500 lb of hafnium-free material) is due, in part, to the better initial purity of the hafnium-free $ZrCl_4$ and, in part, to its higher bulk density which permits larger loadings of converters and sublimers and, accordingly, larger throughput of material in existing ZrF_4 production equipment.

Production of Enriched Fuel for In-Pile Loop

J. E. Eorgan
Materials Chemistry Division

To provide the fuel for an in-pile forced-convection loop (cf., Sec. 8, "Radiation Damage"), two batches of about 6 kg each of a mixture of 62.5 mole % NaF, 12.5 mole % ZrF_4, 25 mole % UF_4 were prepared from product-level UF_4 by Y-12 personnel with some technical assistance from the ANP Chemistry Group. Actual production of the material was accomplished during the interval March 15 to March 29, 1954.

5. CORROSION RESEARCH

W. D. Manly
Metallurgy Division
W. R. Grimes F. Kertesz
Materials Chemistry Division
H. W. Savage
ANP Division

The static and the seesaw corrosion testing facilities were used for further studies of Inconel, stainless steel, various cermets, and graphite exposed to fluoride mixtures or liquid metals. Chromium metal additions to fluoride mixtures with and without uranium contained in Inconel capsules have been shown to give some protection to the Inconel. Experiments conducted at various temperatures confirmed previous indications that the chromium content of a fluoride mixture contained in Inconel increases to a maximum and subsequently decreases with increasing temperature. The essentially linear relationship between chromium concentration of the fluoride mixture and the surface area of the exposed Inconel indicates that equilibrium concentrations are not attained when Inconel specimens are exposed to fluoride mixtures in graphite crucibles. Fluoride mixtures containing UF_3 were tested in Inconel capsules in the seesaw apparatus and, as in thermal-convection-loop tests, no evidence of attack on the Inconel was found. Experiments are under way to determine the effects of fission products on the corrosion of Inconel by fluoride mixtures.

Tests have shown that when Inconel and type 316 stainless steel are exposed in the same system to fluoride mixtures, the steel is inferior to Inconel in its resistivity to attack even when the steel is in the cold zone. Static tests confirmed the reported increase in corrosiveness of lithium metal when lithium nitride is added. Impregnation of the surfaces of steels with chromium did not improve the corrosion resistance of specimens tested in sodium and several liquid-metal alloys. Extensive tests of various cermets that are being considered for applications as bearing materials in contact with fluoride mixtures are under way. The corrosion resistance of cobalt-base bonded specimens has been found to be superior to that of nickel-base bonded specimens. Special tar-impregnated graphite crucibles showed better corrosion resistance in a fluoride mixture than in sodium. Reactor-grade (C-18) graphite exposed to sodium in a type 304 stainless steel container was unaltered, whereas a similarly exposed, tar-impregnated graphite was badly cracked and spalled.

Thermal-convection loops have been used for additional investigations of corrosive attack of fluoride mixtures and liquid metals on Inconel, a special Inconel-type alloy, stainless steel, Hastelloy B, and Inconel with stainless steel, nickel, or beryllium inserts. It has been shown that it is possible to greatly reduce the attack in Inconel loops when UF_3 is used with zirconium fluoride-base mixtures instead of the customary UF_4. One difficulty with these mixtures is the formation of layers on the hot-leg surface which may be uranium-Inconel alloys. Fluorides with mixtures of UF_3 and UF_4 are being investigated. Mass transfer of chromium was found to occur in thermal-convection loops with hot-leg temperatures as low as 1200°F. The amount of mass transfer increases with an increase either in operating temperature or in temperature difference between the hot and cold legs. When graphed, the values for depth of attack obtained in a loop operated for 5000 hr fell on a straight line with the values obtained in shorter times. The previously presented data which showed a rapid initial attack with a slower secondary attack after 250 hr were confirmed. The increase in depth of attack is about 4 mils for each 1000 hr of exposure. Reductions in depth of attack were obtained with loops of Hastelloy B and a special Inconel with a portion of the chromium replaced by molybdenum. In almost every loop constructed with combinations of Inconel and type 316 stainless steel, evidence of increased attack on the steel was observed. A reduction was usually noted in the attack on the Inconel but mass transfer was increased. Dissimilar-metal mass transfer was found with beryllium metal inserts in Inconel loops in which sodium was circulated at 1500°F. More mass transfer was found with a hot-leg insert, but it was present even with a cold-leg

insert. Two lithium-filled type 316 stainless steel thermal-convection loops operated for 1000 hr with hot-leg temperatures of 1445 and 1500°F, respectively. Only small amounts of mass transfer occurred, and at no time was there any indication of plugging. These results are in contrast to results obtained with previous loops of this type which would only operate in the neighborhood of 200 to 300 hr prior to plugging. The increased life was probably due to the higher purity of the lithium used and, especially, to a decrease in the lithium nitride content.

In the study of the corrosion and mass-transfer characteristics of materials in contact with liquid lead, it was found that quartz thermal-convection loops containing types 410 and 446 stainless steel specimens had a much longer life prior to plugging than similar loops containing pure iron and chromium or one of the 300-series stainless steels. Two possible explanations of these findings are being investigated. A tenacious oxide film might act as a diffusion barrier between the container material and the molten lead, or it may be that a thin film of sigma phase forms and acts as a diffusion barrier.

Studies are continuing on the identification of the compounds produced by hydroxide-metal reactions. Current research is concerned with the reaction of NaOH and nickel when hydrogen is allowed to escape from the system. In the past, color changes were observed when NaOH was heated to above 500°C. Present studies indicate that this is not due to a change in concentration of metallic ions from the container but that it must be due to the existence in thermal equilibrium of some species other than the expected sodium ions and hydroxyl ions. Additives such as oxygen, hydrogen, and water vapor have been studied. The interactions of these materials on hydroxides do not seem to be greatly altered by changing the cation from sodium to cesium, but they do seem to be associated with the anion.

FLUORIDE CORROSION OF INCONEL IN STATIC AND SEESAW TESTS

H. J. Buttram R. E. Meadows
J. M. Didlake F. Kertesz
Materials Chemistry Division

Effect of Chromium Addition to Fluoride Melt

An investigation was made of the effect of chromium additions to the fluoride mixtures NaF-ZrF_4-UF_4 (53.5-40.0-6.5 mole %) and NaF-ZrF_4 (53-47 mole %) on the fluoride corrosion of Inconel. In a series of seesaw tests the chromium was added as coarse powder and as slugs of three sizes with surface-area ratios of 1:2:4 to determine the effect of varying the surface area of the chromium. Inconel capsules which contained the fluoride mixtures with and without the chromium additions were tested. The capsules without chromium showed light attack to a depth of about 1 mil. A thin metallic layer was formed on the walls of a capsule tested with chromium powder added to the uranium-bearing mixture; no layer was found on a capsule containing chromium powder and the non-uranium-bearing mixture.

The weight losses of the solid chromium specimens which were added to the capsules were found to be independent of the size of the specimen used, but there was a marked difference between the weight losses caused by the two fluoride mixtures. The weight losses of the solid chromium specimens averaged 0.62 g in the uranium-bearing mixture and 0.11 g in the NaF-ZrF_4 mixture. It was obvious that the difference between the weight losses in the two types of mixtures, 0.51 g in this test, did not correspond to the amount of reduction according to the equation

$$2UF_4 + Cr^\circ \rightarrow CrF_2 + 2UF_3 \ .$$

A simple calculation shows that the weight lost by the chromium specimen would have been sufficient to reduce all the UF_4 contained in the 30-g charge. However, the chromium content gained by the fluoride mixture (about 2000 ppm) was much too small for the reduction of the UF_4. Also, an x-ray diffraction study of the solidified mixture revealed only the normal pattern of $Na_9Zr(U)_8F_{41}$ and none of the extraneous lines which would be expected if there were a high concentration of UF_3. Petrographic examination showed just a tinge of the yellow, reduced phase. The protective action exerted by the chromium was undoubtedly due to the higher activity of the pure metal in comparison with that of the chromium in the Inconel. Since the chromium content of the melt after the test was much lower than the amount lost by the specimen, the chromium must have been deposited and alloyed with the wall, especially at the cold end of the capsule.

Effect of Temperature

The effect of temperature on corrosion of Inconel in fluoride mixtures was examined previously to

establish the relationship between reaction temperature and chromium concentration in the melt. These studies suggested that the chromium concentration of the melt increased to a maximum and subsequently decreased with increasing temperature.

To check the validity of these rather surprising tentative conclusions, two series of tests were conducted. In each test both $NaZrF_5$ and NaF-ZrF_4-UF_4 (50-46-4 mole %) were used. Both series of tests were made under static, isothermal conditions for 100 hr; the test temperatures ranged from 600 to 1000°C. In one series of experiments the fluoride mixtures were contained in graphite capsules to which Inconel specimens were added. The second series of tests was made with the fluoride mixtures contained in Inconel capsules.

Metallographic examination of the Inconel specimens from the graphite capsules showed no attack after exposure at 600°C, while after exposure at 700°C, light to moderate subsurface-void formation to a depth of about 2 mils was observed. The attack was more marked at 800°C, and some of the voids were associated with carbide precipitation on the alloy. The depth of attack increased at 900°C, whereas at 1000°C a slight reduction in void formation was observed. Metallographic observation of the walls of the Inconel capsules used in the second series of tests showed considerable attack at the lower temperatures; at the higher temperatures the subsurface-void formation was light and scattered, but some areas of very deep intergranular penetration were observed. It is possible that this general decrease in number of subsurface voids at the higher temperatures is due to a much higher rate of diffusion of chromium under these circumstances and a consequent slight depletion in chromium concentration over a large region rather than to void formation.

The results of chemical analyses of the fluoride mixtures for chromium paralleled to some extent the metallographic observations. The chromium content of the fluoride mixtures in the Inconel capsules certainly did not increase in a regular fashion with temperature, as might be expected. While there appear to be slight tendencies toward maximums in the curves of chromium concentration vs temperature, it is likely that the differences observed are within the experimental errors of sampling and specimen analyses. For the samples tested in graphite capsules, however, the chromium content of the fluoride mixture increased with temperature up to 900°C, and a straight line was obtained when the logarithm of chromium concentration was plotted against the reciprocal of absolute temperature. The chromium values for the mixtures tested at 1000°C appear to be somewhat lower than the values for those tested at 900°C.

The appearance of the maximum values for the tests at 900°C, if it is real, is difficult to explain. The increase in chromium concentration with increasing temperature suggests that equilibrium is attained quite slowly at the lower temperatures and that some stage in the corrosion mechanism has a considerable activation energy. The difference between the behavior of specimens in graphite capsules and those in Inconel capsules may well be due to the formation of a carbide film which reduces the rate at which chromium is available to react with the melt. No effects attributable to the presence of uranium in the fluoride mixture could be observed in these tests.

Effect of Surface Area

In static, isothermal tests in which fluoride mixtures were contained in graphite capsules, two different sizes of Inconel specimens were used in identical quantities of fluoride mixture to establish the influence of ratio of corroding surface to fluoride volume on the quantity of chromium dissolved. Tests were conducted at temperatures from 600 to 1000°C at 100-deg intervals; the test time was 100 hr in each case.

The surface areas of the two sizes of Inconel specimen were in the ratio 1.88:1. Except for the tests at 600°C, in which the chromium concentrations were very similar for the two specimen sizes, the larger specimen gave higher chromium concentrations in the fluoride mixture. The ratio of chromium concentration in the fluoride mixtures ranged from a minimum value of 1.5 to a maximum of 2.1.

The essentially linear relationship between chromium concentration and surface area exposed cannot, at the chromium concentrations observed, be ascribed to prior surface oxidation of the specimens. It seems likely that equilibrium concentrations are not attained, possibly because of the formation of a carbide film on the specimens, and that the concentrations, which therefore are measurements of reaction rate, are controlled by area of surface exposed.

Effect of Reduced Phases in Fluoride Melt

The fuel containing trivalent uranium which gave low corrosion values in thermal-convection-loop tests has been tested in seesaw experiments. The UF_3 was obtained by adding metallic uranium in the melt of $NaF\text{-}ZrF_4\text{-}UF_4$ (53.5-40.0-6.5 mole %). After 100 hr of exposure in the seesaw apparatus, the unreduced control batch of the $NaF\text{-}ZrF_4\text{-}UF_4$ mixture showed intermittent, moderate, subsurface-void formation to a depth of 1 to 1.5 mils at the hot end of the capsule, whereas none of the batches containing UF_3 showed any measurable attack. Chemical analyses confirmed the metallographic observations; the chromium concentration of the unreduced control batch was higher than that of the mixtures containing reduced uranium compounds.

Effect of Fission Products

Preliminary experiments were run to determine the effect of fission products on the corrosive properties of $NaF\text{-}ZrF_4\text{-}UF_4$ on Inconel. The total amount of fission products per megawatt day of operation was taken as about 1.1 g or about 6.6 g for four days of operation at 1.5 Mw.

Most of the fission products would be present in amounts less than 10% of the uranium undergoing fission; so the maximum concentration of the product in highest abundance should be not more than about 1 ppm because the products will be diluted in about 1500 lb of the fuel. Such low concentrations are not expected to cause difficulty from the corrosion standpoint. Since it would be difficult to handle such small quantities in the regular corrosion tests which require only a total of 30 g of fluoride mixture, the concentrations of the simulated fission products were scaled up one-thousandfold.

In order to mock up a fuel containing fission-product elements, a number of arbitrary substitutions had to be made because some of the desired elements are not available. Zirconium was not included as a fission-product element because the mixture already contained a large amount of that element. The additions that were made to the $NaF\text{-}ZrF_4\text{-}UF_4$ mixture are shown in Table 5.1.

TABLE 5.1. MATERIALS ADDED TO SIMULATE FISSION-PRODUCT ELEMENTS IN A $NaF\text{-}ZrF_4\text{-}UF_4$ MIXTURE

MATERIAL	QUANTITY ADDED (meq/kg)	FISSION PRODUCT SIMULATED
Added Before Hydrofluorination of Mixture		
BaF_2	110	Ba
CsF	40	Cs
CeF_3	425	Rare earths
LaF_3	110	Rare earths
RbF	76	Rb
YF	122	Y
Added After Hydrofluorination of Mixture*		
$MoBr_3$	147	Br
Te	70	Te
RuF_4	157	Pt group
NaI	83	I

*These materials were added after hydrofluorination because they would have decomposed or volatilized during hydrofluorination.

Metallographic study of the Inconel-capsule walls after the 100-hr seesaw test showed heavy to very heavy subsurface-void formation 2 to 5 mils deep. In some cases the voids were so concentrated near the grain boundary that the attack appeared at first to be of an intergranular nature. Closer inspection revealed that the generally observed subsurface-void attack was present, and the voids showed a predominant tendency to form near or at the grain boundaries. Chemical analyses of the fluoride mixtures showed very high chromium concentrations that ranged from 0.23 to 0.25 wt % and thus confirmed the severe attack observed metallographically.

Tests are under way to determine the effects of the simulated fission-product materials individually in as small amounts as possible. Preliminary results show that after the usual 100-hr seesaw test, yttrium fluoride caused the greatest attack, with the maximum depth of subsurface-void formation being 3 mils, while molybdenum bromide caused the next greatest. Chemical results confirmed, in general, the metallographic observations. Tests are in progress to establish the exact amount of chromium removed from the Inconel by the various quantities of simulated fission products.

STATIC AND SEESAW TESTS OF VARIOUS MATERIALS IN FLUORIDE MIXTURES AND LIQUID METALS

E. E. Hoffman J. E. Pope
W. H. Cook L. R. Trotter
Metallurgy Division

Dissimilar Metals in NaF-ZrF_4-UF_4

A series of tests has been conducted to determine the effect of having dissimilar metals (type 316 stainless steel and Inconel) in contact with the fluoride mixture NaF-ZrF_4-UF_4 (50-46-4 mole %) in a dynamic system with a temperature differential. Each tube was one-half type 316 stainless steel and one-half Inconel and the joins were made by heliarc welding. The hot zone in the seesaw apparatus used for these tests was at 1500°F and the cold zone was at 1256°F. Both the type 316 stainless steel and the Inconel sections were tested in the hot zone for 100 and 300 hr. The results of these tests are presented in Table 5.2. The hot and cold zones and the welds joining the two materials were examined after each test. It may be concluded from the results of these tests that type 316 stainless steel is inferior to Inconel in resistivity to attack by molten fluorides even when the steel occupies the cold zone. The heaviest attack found was to a depth of 6 mils in the type 316 stainless steel tube adjacent to a weld; the Inconel tube adjacent to the opposite side of the weld was attacked to a depth of 1 mil (Fig. 5.1).

Molybdenum-Coated Inconel in NaF-ZrF_4-UF_4

Inconel specimens which were coated with molybdenum by the Crawford Fitting Company were tested in static lithium at 1500°F for 100 hr. Lithium was chosen as the corrodent in order to determine whether the molybdenum coating was continuous, because molybdenum is resistant to attack by molten lithium at this temperature and Inconel is heavily attacked. Examination of the as-received sample revealed a $\frac{1}{2}$- to $\frac{3}{4}$-mil molybdenum-rich surface layer. The molybdenum-rich phase penetrated the grain boundaries to a depth of $1\frac{1}{2}$ mils beneath the surface layer. Examination of the tested specimen showed very heavy intergranular attack to a depth of 35 mils; therefore the molybdenum surface layer was either not corrosion resistant or not continuous.

Stainless Steel in Lithium with Lithium Nitride Added

Static tests were made to confirm the reported increase in corrosiveness of lithium metal when lithium nitride is added. Type 316 stainless steel tubes were exposed at 1600°F for 100 hr to lithium metal with 0.1, 0.25, and 1% of lithium nitride added. The test temperature of 1600°F was chosen because lithium nitride has a melting point of approximately 1553°F. In all the tests the 35-mil walls of the type 316 stainless steel containers were completely penetrated intergranularly (Fig. 5.2). In standard tests under similar conditions, the maximum intergranular attack of type 316 stainless steel by lithium (without lithium nitride) is 5 mils or less.

Chromalloyed Steels in Liquid Metals

Seesaw tests of chromalloyed stainless steels in liquid sodium and in several liquid alloys were run to determine whether the chromium-rich layer improved the corrosion resistance of the base material. The surfaces of samples of type 304 stainless steel and type 1035 carbon steel were

TABLE 5.2. RESULTS OF SEESAW TESTS OF DISSIMILAR METALS WELDED TOGETHER AND EXPOSED TO $NaF-ZrF_4-UF_4$ (50-46-4 mole %)

MATERIAL	TEMPERATURE (°F)	EXPOSURE TIME (hr)	DEPTH OF ATTACK (mils)
Inconel (hot zone)	1500	100	0.3
Type 316 stainless steel (cold zone)	1256		2
Inconel (hot zone)	1500	300	0.5
Type 316 stainless steel (cold zone)	1256		1
Type 316 stainless steel (hot zone)	1500	100	2
Inconel (cold zone)	1256		0
Type 316 stainless steel (hot zone)	1500	300	2.5
Inconel (cold zone)	1256		0

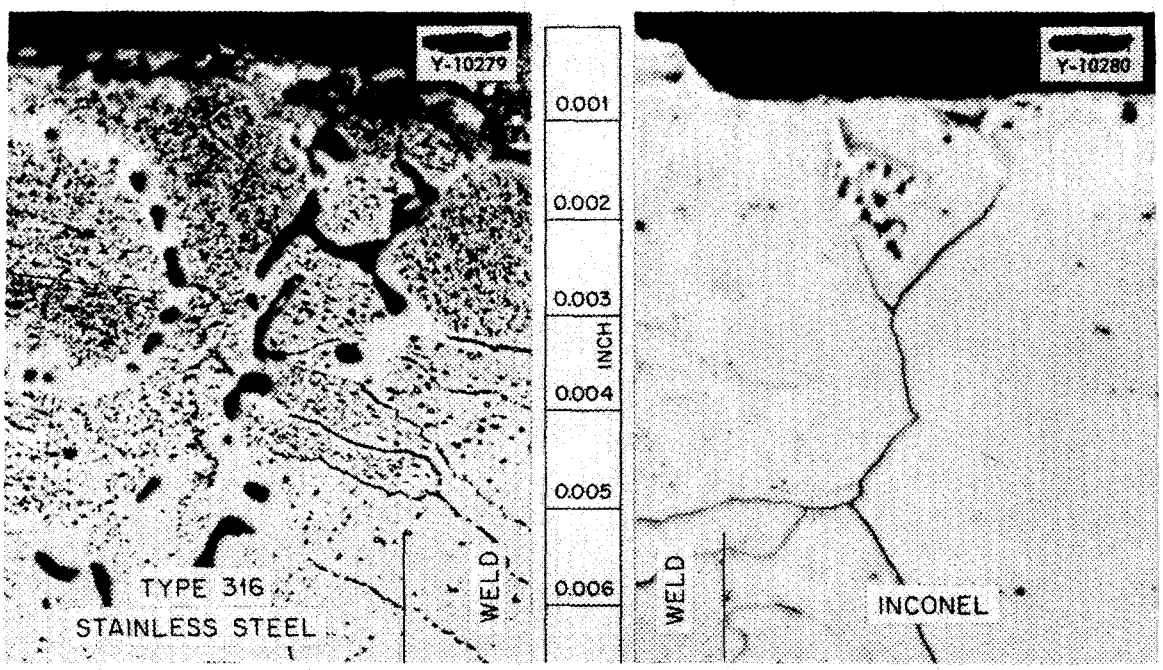

Fig. 5.1. Attack Adjacent to Weld Joining Type 316 Stainless Steel and Inconel After Exposure to $NaF-ZrF_4-UF_4$ (50-46-4 mole %) in Seesaw Apparatus for 100 hr. *During the test the temperature in the* weld zone was approximately 1382°F. 500X.

impregnated with chromium by the process which uses a reaction between a gaseous chromium compound and iron as a means of exchanging iron atoms for chromium atoms at the surface of the steel. The parts to be treated were packed in a powdered compound containing chromium, an energizer, and an inert material.

Both the type 304 stainless steel and the type 1035 carbon steel after being chromalloyed were tested for 100 hr with hot- and cold-zone temperatures of 1500 and 1220°F in sodium, 38% Pb–62% Sn, 82% Pb–18% Cd, 32% Cd–68% Sn, 60% Bi–40% Cd, and 45% Pb–55% Bi. In all cases the chromium-rich layer was found to have cracked, and

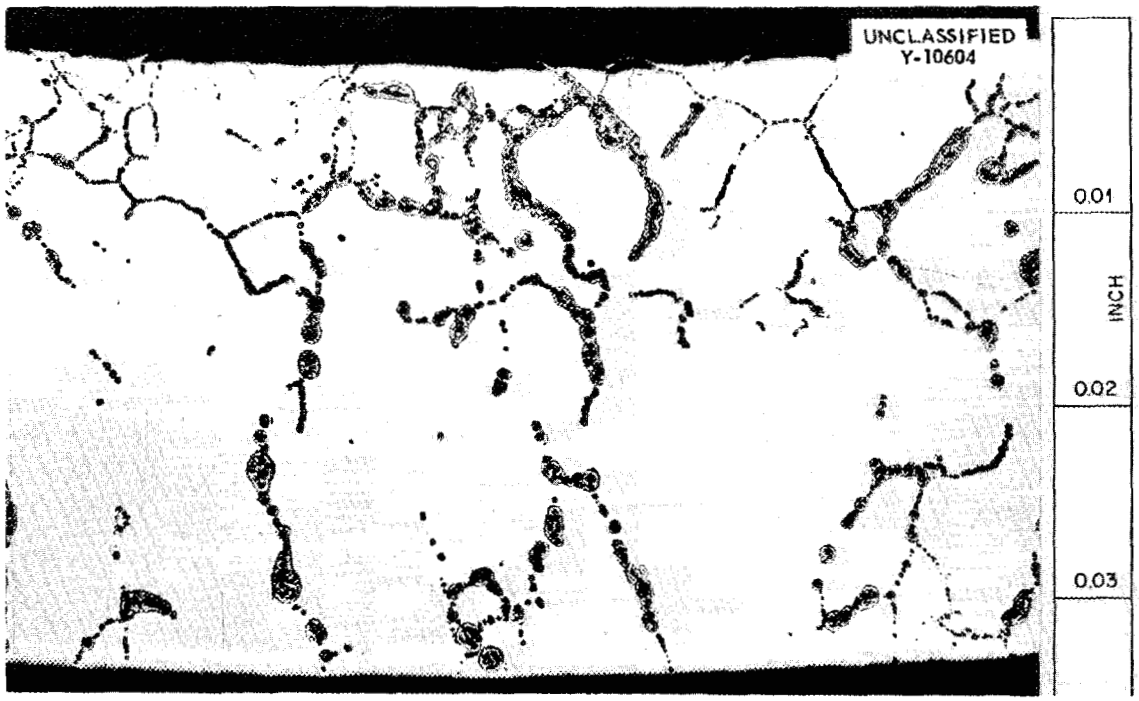

Fig. 5.2. Intergranular Penetration of Type 316 Stainless Steel Exposed at 1600°F for 100 hr to Static Lithium with 0.1% Lithium Nitride Added. Top edge exposed to liquid. 100X.

therefore the corrosion resistance of the base material was unimproved. Figure 5.3 shows photomicrographs of a chromalloyed type 304 stainless steel specimen before and after testing in 45% Pb–55% Bi.

Cermets in NaF-ZrF_4-UF_4

Various cermets that are being considered as bearing materials were exposed to NaF-ZrF_4-UF_4 (50-46-4 mole %) in seesaw apparatus. The specimens were restricted to the hot zone of Inconel tubes and were exposed to the fluoride mixture for 100 hr. During the tests the hot zones of the tubes were at 1500°F, and the cold zones were at approximately 1292°F. The results of the tests are presented in Table 5.3. Of the various cermets of titanium carbide with nickel binder, one specimen with 20% of binder and another with 30% of binder had the best resistance to attack. However, tests of duplicate specimens showed slightly heavier attack. This discrepancy may be due to variations in the specimens. Kennametal D4675 (tungsten carbide plus 2.5% cobalt) showed very good resistance, and additional tests are planned to confirm this result. Since Carboloy X3505, which is the same as Carboloy 608 except that it has no nickel binder, was not attacked, it appears that the nickel binder in Carboloy 608 (Cr_3C_2 plus 2% WC and 15% Ni) was attacked preferentially (Fig. 5.4).

A second group of cermet samples submitted by Kennametal Inc., and the Sintercast Corp. of America, was exposed under the same conditions. The exact compositions of one of the Kennametal samples and all the Sintercast samples are yet to be obtained from these firms. All these specimens had fair to good resistance to the fluoride mixture, as may be seen in Table 5.4. In general, the corrosion resistance of the cobalt-base bonded specimens was equal to or slightly superior to that of the nickel-base bonded specimens. In all cases the attack appeared to be along the titanium carbide particle surfaces that separate the particles from each other and from the binder. The corrosion along the surfaces of the titanium carbide particles might have been the attack of a fabrication reaction product between the titanium carbide and the binder. It has been reported that a finely dispersed reaction product is usually found in the metallic areas of cermets containing cobalt or nickel.[1]

[1] C. C. McBride, H. M. Greenhouse, and T. S. Shevlin, *J. Am. Ceram. Soc.* 35, 29-30 (1952).

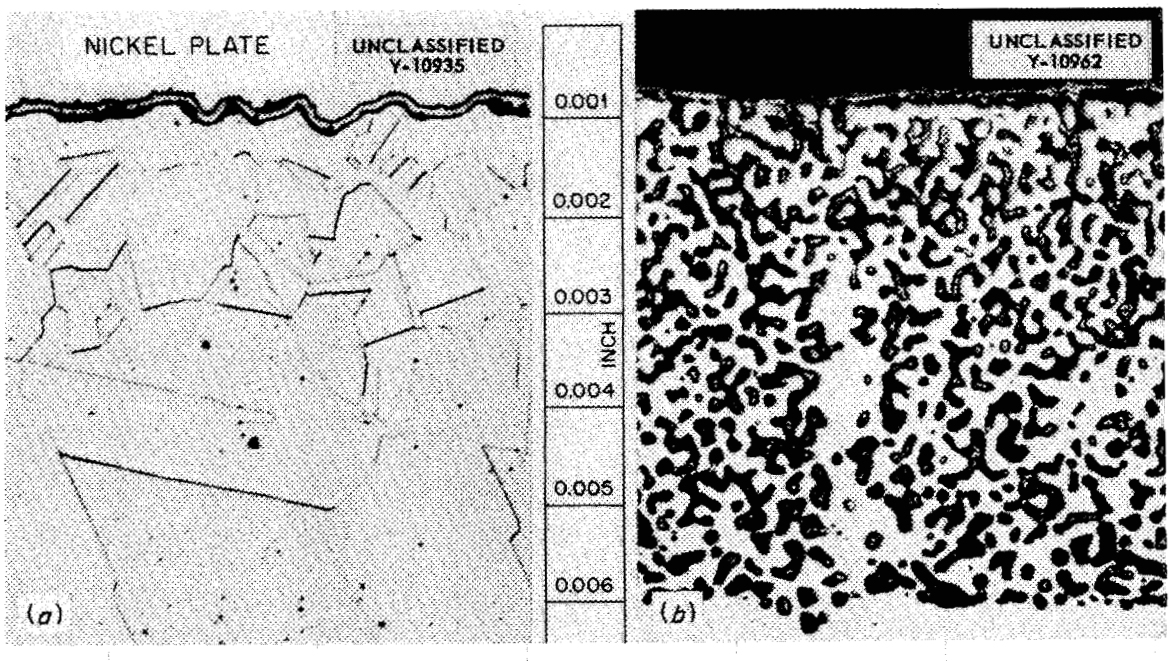

Fig. 5.3. Chromalloyed Type 304 Stainless Steel Before and After Exposure to 45% Pb–55% Bi in Seesaw Apparatus. (*a*) As received. Specimen nickel plated prior to examination to prevent rounding of edge during polishing. (*b*) After exposure. 500X.

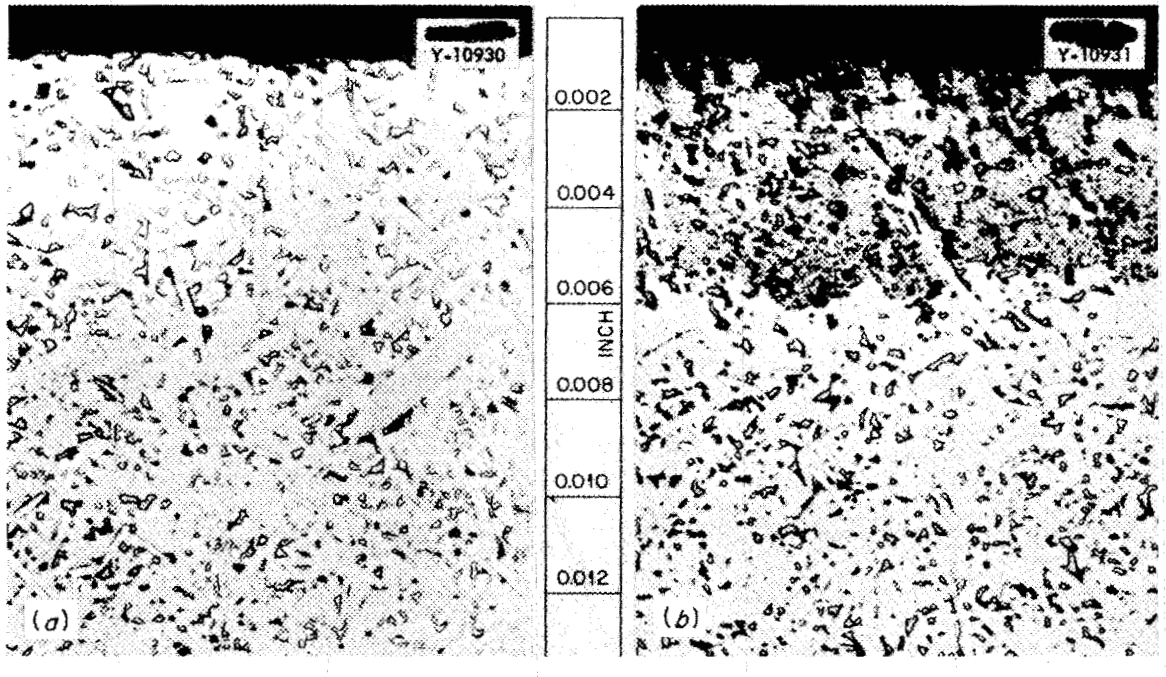

Fig. 5.4. Carboloy 608 (Cr_3C_2 plus 2% WC and 15% Ni) Before and After Exposure to NaF-ZrF_4-UF_4 (50-46-4 mole %) for 100 hr at 1500°F in Seesaw Apparatus. (*a*) As received. (*b*) After exposure. 250X.

TABLE 5.3. RESULTS OF SEESAW TESTS OF CERMETS EXPOSED TO $NaF-ZrF_4-UF_4$ (50-46-4 mole %) AT 1500°F FOR 100 hr

MATERIAL	COMPOSITION	METALLOGRAPHIC NOTES
Kentanium K-150-A	TiC + 10% Ni	Attacked to a depth of 4 mils
Kentanium K-151-A	TiC + 20% Ni	A zone of slightly affected material to a depth of 1 or 2 mils
Kentanium K-151-A	TiC + 20% Ni	Macroexamination revealed many blisters on the surface of the sample; attack extended to a depth of 6 mils
Kentanium K-152-B	TiC + 30% Ni	Attacked in only a few areas to a maximum depth of 2 mils; much less attack than on either K-150-A or K-151-A
Kentanium K-152-B	TiC + 30% Ni	Attacked somewhat erratically to a depth of 4 to 7 mils; did not resist attack so well as the other sample of K-152-B
Kentanium K-162-B	TiC + 25% Ni and 5% Mo	Macroexamination revealed a surface which had the appearance of a plated specimen with portions of the plating removed; attacked to a depth of 9 mils
Kennametal D4675	WC + 2.5% Co	Subsurface-void attack to a depth of 1 mil
Firth Sterling 27	TiC + 7% Cr_3C_2 and 50% Ni	Attacked to a depth of 2 to 5 mils
Carboloy 608	Cr_3C_2 + 2% WC and 15% Ni	Attacked to a depth of 4 mils
Carboloy X3505	Cr_3C_2 + 2% WC (no nickel binder)	No attack detected; both as-received and tested specimens very brittle and similar in appearance
Metamic LT-1 (not heat treated)	77% Cr–23% Al_2O_3	Completely penetrated
Metamic LT-1 (heat treated)	77% Cr–23% Al_2O_3	Completely penetrated

These limited tests indicate that corrosion resistance is low for the specimens with the greatest binder content, whether nickel or cobalt.

Titanium boride, zirconium boride, and molybdenum boride samples were also exposed to $NaF-ZrF_4-UF_4$ (53.5-40.0-6.5 mole %) at 1500°F for 100 hr in seesaw apparatus. The specimens were restricted to the hot zone of Inconel tubes. The results of the tests are presented in Table 5.5. The evidence of attack on the zirconium boride specimen may be seen in Fig. 5.5.

Graphite in $NaF-ZrF_4-UF_4$ and in Sodium

Special tar-impregnated graphite crucibles were exposed to $NaF-ZrF_4-UF_4$ (50-46-4 mole %) and to sodium at 1500°F for 100 hr in static tests. As can be seen in Fig. 5.6, the sodium completely penetrated the walls of the crucible and caused them to crack and crumble. The crucible containing the fluoride mixture had a weight loss of 0.012%, and the surface which was in contact with the fluoride had an etched appearance. The fluoride mixture did not penetrate the crucible walls.

Static tests were also run to compare the corrosion resistance in molten sodium at 1500°F for 100 hr of two types of graphite in type 304 stainless steel containers. The types of graphite tested were C-18 (reactor-grade) and a special tar-impregnated graphite that was impregnated and fired 16 times during its preparation. The purpose of the repeated impregnation and firing was to produce a high density and a tough skin that could possibly help to reduce penetration by various liquids. The C-18 graphite was practically unaltered by the test (Fig. 5.7a). The surface of the specimen had an etched appearance and the sharp corners had been rounded slightly. The tar-impregnated cylinder was cracked badly and had spalled, as may be seen in Fig. 5.7b.

TABLE 5.4. RESULTS OF SEESAW TESTS OF TITANIUM CARBIDE CERMETS EXPOSED TO $NaF\text{-}ZrF_4\text{-}UF_4$ (50-46-4 mole %) AT 1500°F FOR 100 hr

MATERIAL	COMPOSITION	METALLOGRAPHIC NOTES
Kentanium K-138-A	65% TiC–20% Co–15% $CbTiTaC_3$	Attack appeared to be on binder to a depth of 0.5 to 1 mil
Kentanium K-153-B	60% TiC–40% Ni	Attacked to a uniform depth of 3 mils; attack was along the TiC particle surfaces that separate the TiC particles from each other and from the binder
Kentanium K-161-B	TiC + Ni and Mo	No attack; tested surface slightly more irregular than as-received surface
Sintercast No. 1	TiC + Co	Attacked to a depth of 0.5 to 2 mils; many voids throughout specimen probably formed during fabrication
Sintercast No. 4	TiC + Co	Attacked to a depth of 1 mil; some TiC particles had a second phase within them
Sintercast No. 5	TiC + Ni	No attack; binder appeared to be firmly attached to the TiC particles throughout the specimen
Sintercast No. 8	TiC + Ni	Attacked to a depth of 2 mils; small section on corner of specimen not uniform; appeared to be binder without TiC particles and did not appear to be attacked
Sintercast No. 10	TiC + Ni	Attacked to a depth of 5 mils along the TiC particle surfaces; attack just enough to separate particles from the binder

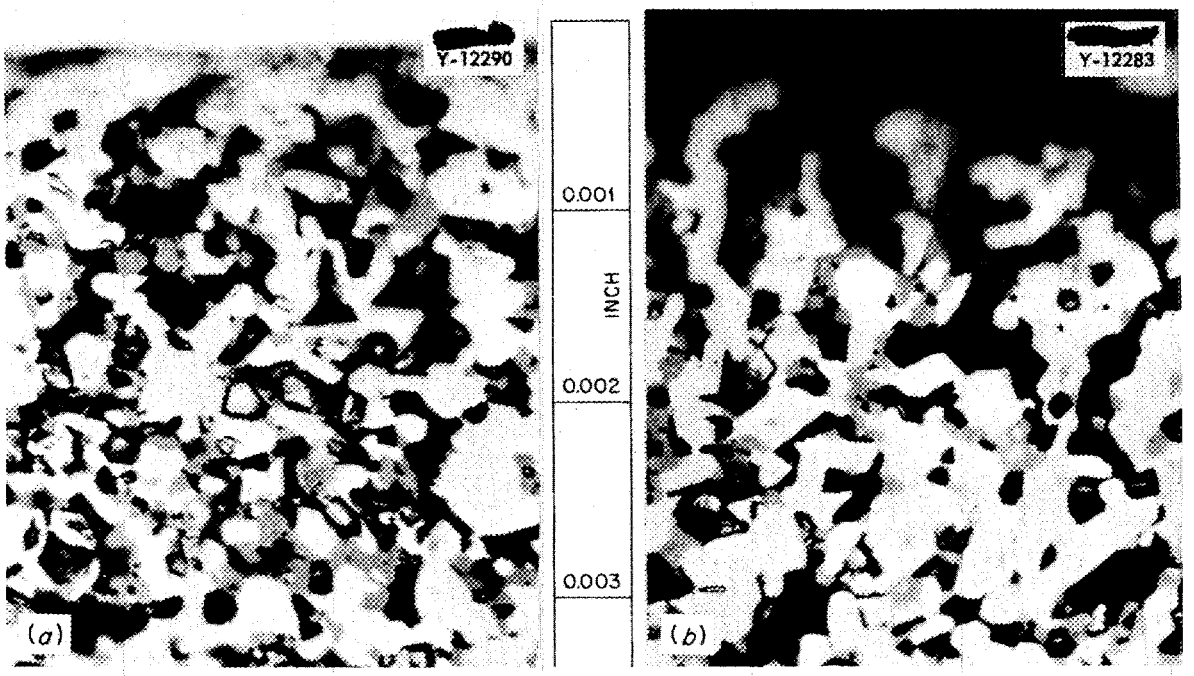

Fig. 5.5. Zirconium Boride Before and After Exposure to $NaF\text{-}ZrF_4\text{-}UF_4$ (53.5-40.0-6.5 mole %) for 100 hr at 1500°F in Seesaw Apparatus. (*a*) As received. (*b*) After exposure. 1000X.

TABLE 5.5. RESULTS OF SEESAW TESTS OF VARIOUS BORIDES EXPOSED TO $NaF-ZrF_4-UF_4$ (53.5-40.0-6.5 mole %) AT 1500°F FOR 100 hr

SAMPLE	DEPTH OF ATTACK (mils)	METALLOGRAPHIC NOTES
TiB_2	2	As-received sample had what appeared to be a pressing crack; tested sample had a cracked corner
ZrB_2	2	Irregular shaped dark and light grains; as-received sample cracked and porous
Mo_2B	16	Corrosion was definite and macroscopically visible in the polished metallographic sample; sample porous and very brittle

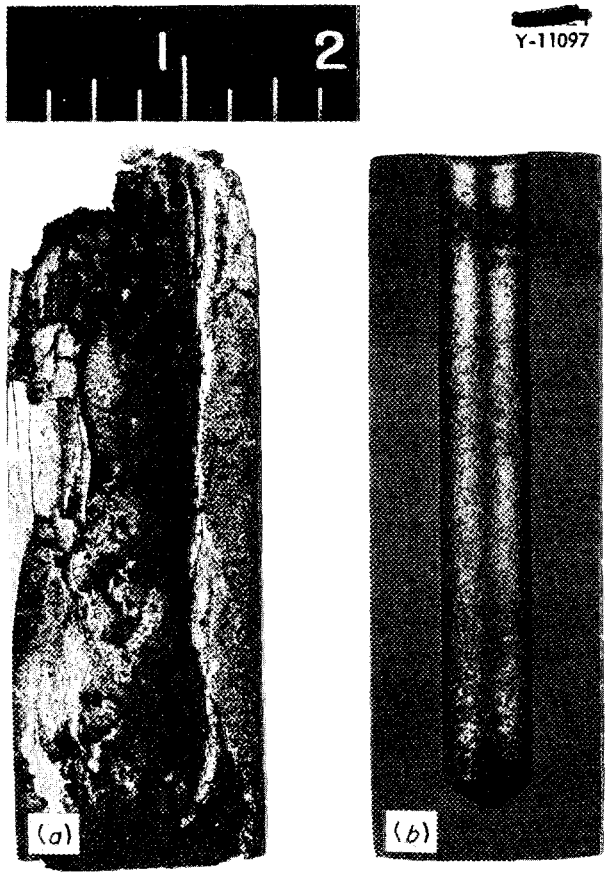

Fig. 5.6. Special Tar-Impregnated Graphite Crucibles After Static Tests in Sodium and in $NaF-ZrF_4-UF_4$ (50-46-4 mole %) at 1500°F for 100 hr. (a) Tested in sodium. (b) Tested in fluoride mixture.

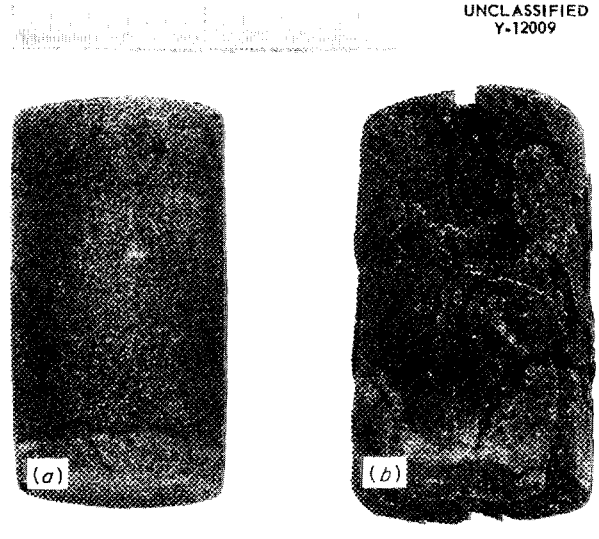

Fig. 5.7. C-18 Graphite and Tar-Impregnated Graphite After Exposure to Static Sodium in Type 304 Stainless Steel Containers at 1500°F for 100 hr. (a) C-18 graphite. (b) Tar-impregnated graphite.

FLUORIDE CORROSION OF INCONEL IN THERMAL-CONVECTION LOOPS

G. M. Adamson
Metallurgy Division

Effects of UF_3 and Mixtures of UF_3 and UF_4 in Fluoride Fuels

An extensive experimental program is under way to determine the effect on corrosion of Inconel thermal-convection loops by circulating fluoride

fuels containing UF_3 and mixtures of UF_3 and UF_4. It has been determined that fluoride fuels containing uranium as UF_3 are less corrosive to Inconel than UF_4-bearing fuels. However, UF_3 is not sufficiently soluble in the fluoride mixtures presently being considered for use in the Reflector-Moderated Reactor and mixtures of UF_3 and UF_4 are therefore being investigated. An effort is being made to determine the amount of UF_3 required to eliminate corrosive attack by a fluoride mixture containing UF_3 and UF_4. A few experiments have been completed with zirconium-base fluoride mixtures and tests with alkali-metal fluoride mixtures are planned.

The fluoride mixture NaF-ZrF_4-UF_3 was circulated for 500 hr in a standard Inconel thermal-convection loop with a hot-leg temperature of 1500°F (ΔT = 195°F). The uranium concentration was low, being only 2.8 wt %. Examination of the loop after 500 hr of operation showed no subsurface voids or intergranular type of attack. The hot-leg surface was partially covered by a thin, unidentified layer, but no change in the uranium analysis was found.

A mixture with a higher, but still low, uranium concentration was circulated in a second loop. The uranium concentration was 5.8 wt % and to obtain this high a concentration, a mixture of UF_3 and UF_4 was required. Estimates and analyses of the relative amounts of the two compounds have varied from 100% UF_3 to 100% UF_4. While a definite figure cannot be obtained, a reasonable value for the UF_3 seems to lie between one-half and three-fourths of the total uranium. This loop also showed no attack after 500 hr of operation with a hot-leg temperature of 1500°F. Layers were present in both the hot and the cold legs, but the layer in the hot leg was thicker than the layer in the cold leg (Fig. 5.8). The average uranium concentration of the fluoride mixture after circulation was 5.3 wt %, with none of the values as high as the value reported for the mixture before

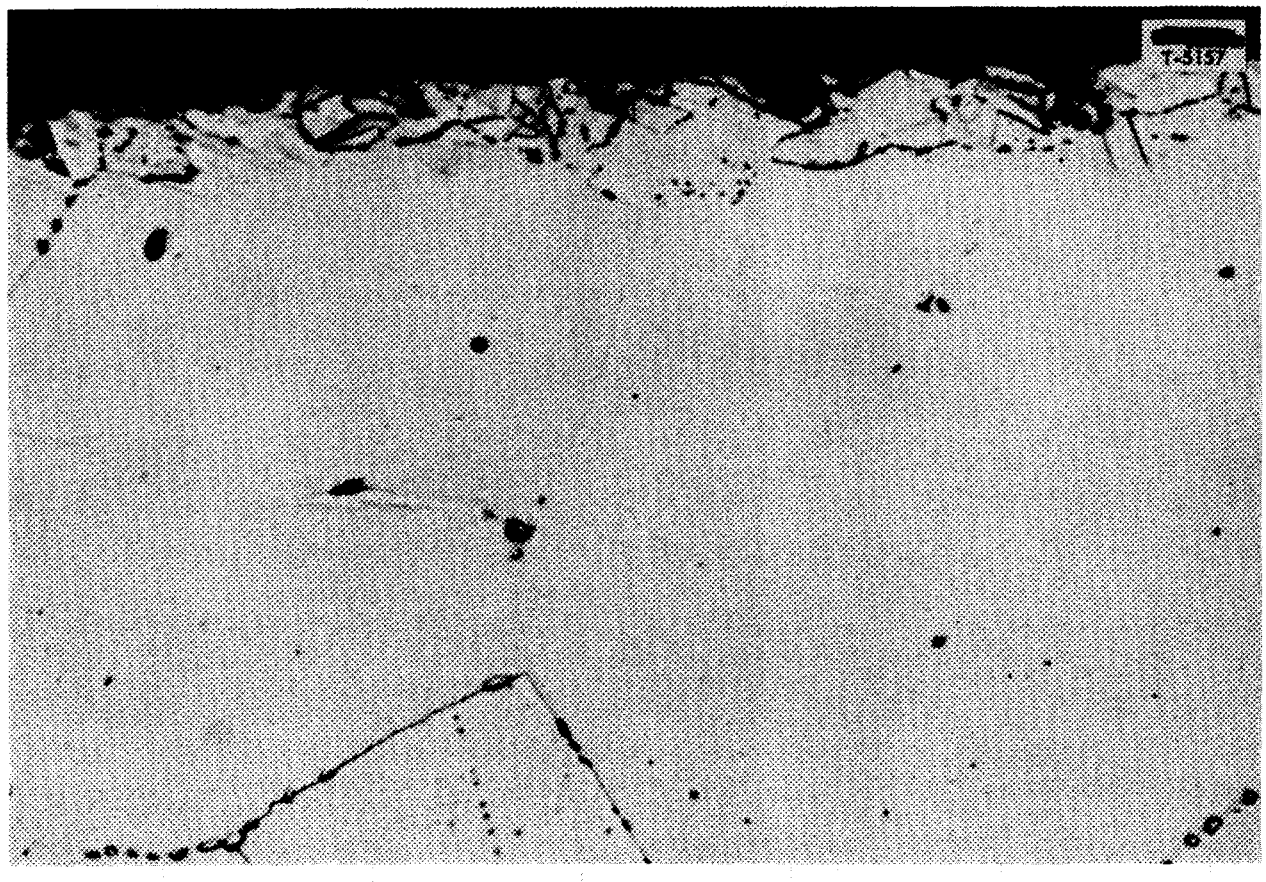

Fig. 5.8. Layer on Surface of Hot Leg of an Inconel Thermal-Convection Loop After Circulation for 500 hr at 1500°F of a NaF-ZrF_4 Mixture Containing UF_3 and UF_4. 1400X.

circulation. It is possible that the deposited material is a uranium-Inconel alloy formed by the dissociation of the UF_3 from the fluoride mixture. This is the main question that must be answered before a decision can be made as to whether these fluoride mixtures will be useful as reactor fuels circulating in Inconel.

An intermediate uranium mixture of 2.7 wt % UF_3 and 8.6 wt % UF_4 or a total uranium concentration of 8.7 wt % was circulated in another loop. These proportions were obtained by calculations, but the analytically determined uranium concentration of 8.63 wt % makes the calculated value appear to be reasonable. After 500 hr of circulation, a moderate concentration of subsurface voids with a maximum penetration of 4 mils was found. No layer was found in either the hot or the cold leg. The final analytical values have not been received.

Effect of Hydrogen Fluoride

Small additions of hydrogen fluoride gas were made to a batch of NaF-ZrF_4-UF_4 (50-46-4 mole %). Portions of this batch were then circulated for various times at 1500°F in Inconel thermal-convection loops in order to determine the effect of hydrogen fluoride on the corrosiveness of the fuel mixture. The data obtained are summarized in Table 5.6.

The doubling of the depth of penetration in loop 415 in comparison with that in loop 421 confirms the adverse effect of small amounts of hydrogen fluoride on the initial rate of attack. In comparison with the maximum penetration of 17 mils found in loop 417 after 2000 hr of operation, an estimate based on results obtained previously indicates that the maximum penetration in a loop operated for 2000 hr with the as-received fluoride mixture would be 12 mils. The effect of the hydrogen fluoride addition on maximum penetration appears to be about the same after 2000 hr of operation as after 500 hr of operation.

Effect of Temperature

The effects of temperature drop and of maximum hot-leg temperature on mass transfer in Inconel thermal-convection loops are being studied. The use of thermal-convection loops in the study of the effects of temperature gradients is not entirely satisfactory because the flow in a loop is a function of the density of the fluid and therefore the flow rate changes with changes in the temperature drop. The thermal-convection-loop results are of some value, however, because the flow rates are so low that the changes in flow rate are not so important as the direct changes in temperature drop.

Two series of loops in which the cold-leg temperature was varied while the hot-leg temperature was held at 1500°F were operated with NaF-ZrF_4-UF_4 (50-46-4 mole %) as the circulated fluid. The variation in the cold-leg temperature was accomplished by adding insulation or by blowing air on the cold leg. The data from these tests are presented in Table 5.7. The first, more rapid stage of attack is caused by impurities and therefore

TABLE 5.6. EFFECT OF HYDROGEN FLUORIDE ADDITIONS ON CORROSIVENESS OF NaF-ZrF_4-UF_4 IN INCONEL THERMAL-CONVECTION LOOPS

LOOP NO.	HYDROGEN FLUORIDE CONCENTRATION (moles/liter of purging gas)	ORIGINAL FLUORIDE-MIXTURE IMPURITY (ppm)		CIRCULATION TIME (hr)	MAXIMUM PENETRATION (mils)	HOT-LEG ATTACK
		Ni	Fe			
421	1.2×10^6*	<10	110	500	5	Intergranular, moderate to heavy
415	3.4×10^6			500	10	Intergranular, moderate to heavy
416	6×10^6	<10	345	1000	12	Heavy intergranular
417	6×10^6	<10	195	2000	17	Intergranular, moderate to heavy with large voids

*Normal concentration of hydrogen fluoride in as-received NaF-ZrF_4-UF_4 mixture.

would not be expected to be greatly influenced by the temperature drop. The differences found appear to take place in the mass-transfer portion of the attack which usually occurs after the first 250 to 500 hr of operation. Although no definite conclusions should be drawn from such meager data, the rate of mass transfer seems to vary quite markedly with changes in temperature drop.

A series of loops filled from one batch of NaF-ZrF_4-UF_4 was operated for 2000 hr in an effort to determine the effect on rate of mass transfer of variations in maximum hot-leg temperatures. The data obtained are presented in Table 5.8. The increases in depth of attack and incidence of cold-leg deposits indicate that the rate of mass transfer increases with increasing hot-leg temperatures.

Loops operated previously for 500 hr with maximum hot-leg temperatures of 1200°F showed maximum penetrations of 3 to 5 mils, and in a loop operated for 500 hr with a maximum hot-leg temperature of 1250°F the maximum penetration was 3 mils. The previously operated loops were not filled from the batch of fluoride mixture used for filling the loops listed in Table 5.8, but the small vari-

TABLE 5.7. EFFECT OF TEMPERATURE GRADIENT ON MASS TRANSFER IN INCONEL THERMAL-CONVECTION LOOPS CIRCULATING NaF-ZrF_4-UF_4

LOOP NO.	MAXIMUM ΔT (°F)	OPERATING TIME (hr)	MAXIMUM PENETRATION (mils)	HOT-LEG ATTACK
447	65	1000	5	Intergranular, light to moderate
448	195*	1000	10	General and intergranular, moderate to heavy; the deepest penetrations were scattered
446	220	1000	12	Intergranular, moderate to heavy
422	130	500	5	Intergranular, moderate to heavy
423	140	2000	6	Intergranular, moderate to heavy
442	195*	500	10	Intergranular, moderate to heavy

*Standard temperature drop.

TABLE 5.8. EFFECT OF VARIATIONS IN MAXIMUM HOT-LEG TEMPERATURE OF THERMAL-CONVECTION LOOPS OPERATED FOR 2000 hr

LOOP NO.	HOT-LEG TEMPERATURE (°F)	MAXIMUM PENETRATION (mils)	HOT-LEG CONDITION	COLD-LEG CONDITION
391*	1200	7	Very heavy general attack with small voids	No deposit
449	1250	6	Intergranular, moderate to heavy	No deposit
392	1400	8	Heavy general attack to 4 mils with occasional deeper intergranular penetrations	Intermittent metallic deposit
393	1600	13	Intergranular, moderate to heavy with large voids	Thin but continuous metallic deposit

*This run was terminated after 1313 hr when circulation was stopped for the second time by a power failure.

ations encountered in comparing different batches are not sufficient to invalidate the comparison between the previously operated loops and loops 391 and 449. The difference between the maximum penetration in loop 391 and the maximum penetration in the loops operated previously indicates that mass transfer takes place even at a hot-leg temperature as low as 1200°F.

Effect of Exposure Time

A maximum penetration of 27 mils was found in loop 344 which circulated NaF-ZrF_4-UF_4 (50-46-4 mole %) for 5000 hr at 1500°F. The fluoride mixture in this loop was from the same batch as that used for a series of tests reported previously. When graphed, the values for the depth of attack in 5000 hr fell surprisingly close to the straight line for the second stage of attack (after 250 hr), as shown in Fig. 6.6 of the previous report.[2] The average increase in depth of attack is about 4 mils for every 1000 hr of operation after the first 250 hr. A layer about ¼-in. thick of dendritic chromium metal crystals was found in the trap at the bottom of the cold leg of the loop operated for 5000 hr (Fig. 5.9).

Another series of experiments is under way to confirm the time curve and to provide samples from which a reaction rate may be obtained by determining the volume of the subsurface voids. The data obtained for the time study (tabulated in Table 5.9) confirm the data obtained previously,[2] including the change of slope of the curve at around 250 hr. However, the depth of attack found in the loop that operated for 1000 hr is out of line both with the other data obtained in this series of experiments and with the data from previous experiments.

[2]G. M. Adamson, *ANP Quar. Prog. Rep. Sept. 10, 1953*, ORNL-1609, p 79, esp. Fig. 6.6.

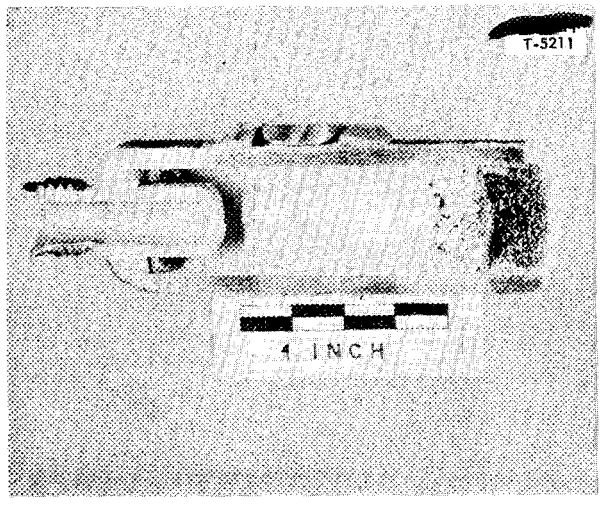

Fig. 5.9. Dendritic Chromium-Metal Crystals in Trap at Bottom of Cold Leg of an Inconel Thermal-Convection Loop That Circulated NaF-ZrF_4-UF_4 (50-46-4 mole %) for 500 hr at a Hot-Leg Temperature of 1500°F. 250X. Reduced 19.5%.

TABLE 5.9. EFFECT OF OPERATING TIME ON DEPTH OF ATTACK BY NaF-ZrF_4-UF_4 CIRCULATING IN INCONEL THERMAL-CONVECTION LOOPS AT A HOT-LEG TEMPERATURE OF 1500°F

LOOP NO.	OPERATING TIME (hr)	MAXIMUM PENETRATION (mils)	HOT-LEG ATTACK
431	10	2	Light with intermittent moderate areas
432	50	3	Moderate
433	100	4.5	Light to moderate
434	250	8	Moderate to heavy, primarily intergranular
435	500	8	Heavy, primarily intergranular
436	1000	14	Heavy, intergranular
445	1500	13	Heavy, intergranular

THERMAL-CONVECTION-LOOP TESTS OF VARIOUS MATERIALS

$NaF-ZrF_4-UF_4$ in Special Inconel

G. M. Adamson
Metallurgy Division

A special series of alloys with slight changes from the usual Inconel analysis were vacuum cast at ORNL and drawn into ½-in. tubing with a 0.065-in. wall by the Superior Tube Co. The first lot of tubing was made into a loop which circulated $NaF-ZrF_4-UF_4$ (50-46-4 mole %) for 500 hr at a hot-leg temperature of 1500°F. A portion of the chromium normally found in Inconel had been replaced in this special alloy by molybdenum. An analysis of the special alloy showed 6.0% Cr, 10.0% Fe, 74.4% Ni, and 9.8% Mo. Examination of the tubing after 500 hr showed light attack with a maximum penetration of 3.5 mils. Standard Inconel loops of commercial ½-in. tubing developed moderate to heavy attack 4 to 5 mils deep under the same conditions.[3] Although the attack on the special alloy was somewhat less than the attack on commercial Inconel, the special alloy was not as corrosion resistant as had been expected. Additional loops are to be operated for longer periods to study the effects of mass transfer.

$NaF-ZrF_4-UF_4$ in Hastelloy B

G. M. Adamson
Metallurgy Division

A loop of ½-in. Hastelloy B tubing was fabricated by seam welding and then solution annealed for 1 hr at 2150°F and aged 30 hr at 1950°F. The fluoride mixture $NaF-ZrF_4-UF_4$ (50-46-4 mole %) was then circulated in this loop for 500 hr at a hot-leg temperature of 1500°F. Examination of the tubing after 500 hr showed that the inner surface of the hot leg was rough and had light subsurface voids to a depth of 2 mils. The weld bead at the seam showed much less attack than the tubing (Fig. 5.10). The cold leg showed similar attack except that there were fewer subsurface voids.

$NaF-ZrF_4-UF_4$ in Stainless Steel

G. M. Adamson
Metallurgy Division

A second type 430 stainless steel loop[4] was operated with $NaF-ZrF_4-UF_4$ (50-46-4 mole %) for 500 hr at a hot-leg temperature of 1500°F. The hot leg developed very light, widely scattered subsurface voids to a maximum depth of 7 mils. A phase change of the stainless steel to what appeared to be martensite was noted in the vicinity of the voids. In an area up to 10 mils deep from the surface, the carbides had apparently gone back into solution and grain growth had occurred (Fig. 5.11). Particles of metal had deposited on the surface of the cold leg, and metallic crystals were found in the adhering fluorides. While the attack was less than that found in Inconel loops, more metallic crystals were visible. The attack was also slightly greater than that found in the first type 430 stainless steel loop.[4]

$NaF-ZrF_4-UF_4$ in Inconel with Stainless Steel or Nickel Inserts

G. M. Adamson
Metallurgy Division

Mass transfer of dissimilar metals was investigated in a series of loops with various combinations of Inconel and type 316 stainless steel. The fluoride mixture $NaF-ZrF_4-UF_4$ (50-46-4 mole %) was circulated in the loops for 500 hr at a hot-leg temperature of 1500°F.

Inconel loop 315 had a 6-in. insert of type 316 stainless steel in the upper portion of the hot leg.[5] The Inconel above the insert showed very light, widely scattered attack to a depth of 3 mils. The surface of the type 316 stainless steel insert was very rough and there was attack to a depth of 12 mils. There was a 0.3-mil-thick deposit on the Inconel cold leg.

In Inconel loop 430, the lower half of the hot leg was replaced with type 316 stainless steel. The Inconel showed moderate attack to a depth of 8 mils. At the welds the Inconel was rough but showed no other evidence of attack. The stainless steel had severe intergranular voids to a depth of 4 mils. There was no deposit and no attack in the cold leg.

Loop 429 was constructed with a hot leg of type 316 stainless steel and a cold leg of Inconel. The surface of the hot leg was very rough and showed severe intergranular penetrations to a depth of 4

[3] G. M. Adamson, *ANP Quar. Prog. Rep. Mar. 10, 1954*, ORNL-1692, p 71.

[4] G. M. Adamson, *ANP Quar. Prog. Rep. Dec. 10, 1953*, ORNL-1649, p 74.

[5] G. M. Adamson, *ANP Quar. Prog. Rep. Sept. 10, 1953*, ORNL-1609, p 77.

Fig. 5.10. Hot-Leg Surface and Weld Bead of a Hastelloy B Loop After Circulation of $NaF-ZrF_4-UF_4$ (50-46-4 mole %) for 500 hr at a Hot-Leg Temperature of 1500°F. 250X.

mils. At the welds the stainless steel was heavily attacked to a depth of 3 mils. At the lower weld the Inconel was unattacked, but at the upper weld there were many subsurface voids to a depth of 3 mils in the Inconel. A scattered metallic deposit was found on the Inconel cold leg.

In loop 428, the cold leg was type 316 stainless steel and the hot leg was Inconel. The Inconel hot leg showed heavy intergranular attack to a depth of 10 mils. At the welds the Inconel surface was rough and there was a light concentration of subsurface voids to a depth of 0.5 mil. The stainless steel at the welds showed severe but intermittent attack to a depth of 2 mils. The surface of the stainless steel cold leg was very rough with heavy intergranular attack to a depth of 2.5 mils. An all-Inconel loop (435) filled from the same batch of fluorides showed heavy hot-leg attack to a depth of 8 mils.

Fig. 5.11. Hot-Leg Surface of Type 430 Stainless Steel Loop After Circulation of $NaF-ZrF_4-UF_4$ (50-46-4 mole %) for 500 hr at a Hot-Leg Temperature of 1500°F. 250X. Reduced 35.5%.

In every loop tested, there was much deeper attack of the type 316 stainless steel insert, especially when it was in contact with Inconel in the hotter portion of the loop, than there would have been in an all-steel loop. The effect of the stainless steel on the Inconel is not so definite, but in most cases there seemed to be a reduction in the attack on the Inconel. Since the data showed rather large variations in wall thickness, the thicknesses are being rechecked, but it seems that considerable reductions in wall thickness occurred in all the type 316 stainless steel tubing.

A nickel insert was also placed in the cold leg of an Inconel loop. With this combination neither material seemed to be affected. This experiment confirms a previous experiment[6] in which a nickel hot-leg insert in an Inconel loop was also shown to have practically no effect.

Sodium in Inconel with Beryllium Inserts

G. M. Adamson
Metallurgy Division

Two Inconel loops were constructed with cylindrical hot-pressed beryllium inserts about 6 in. long. Both loops circulated sodium for 500 hr at a hot-leg temperature of 1500°F. In one loop the insert was in the upper portion of the hot leg. The outer surface of the insert, which was separated from the Inconel by a 0.020-in. annulus filled with slow-moving sodium, showed subsurface-void attack to a maximum depth of 14 mils. The inner surface of the insert did not have the void type of attack, but it was rough, and some even removal had probably occurred. The Inconel adjacent to the beryllium was rough, and there was a metallic-appearing deposit on the surface. A black scale was present in all sections of this loop, and metallic crystals were found both in the annulus and in the cold leg. These crystals were predominantly nickel and beryllium. The black scale produced a very complicated diffraction pattern which could not be identified.

In the other loop the beryllium insert was in the lower cold leg. No attack was found in the Inconel hot leg of this loop. A thin metallic deposit was visible on the surface of the Inconel below the insert but not on the surface above it. The insert showed some attack on both faces as surface roughness, intergranular penetrations, and voids to a maximum depth of 2 mils. Again, some even removal had probably occurred. No metallic crystals were found in this loop, but the same black scale was found in all sections. Three additional loops are now operating with similar hot-leg inserts. These loops are circulating sodium at 900, 1100, and 1300°F.

Lithium in Stainless Steel

E. E. Hoffman W. H. Cook
J. E. Pope L. R. Trotter
Metallurgy Division

Two lithium-filled type 316 stainless steel thermal-convection loops completed 1000 hr of operation. One loop operated with a hot-leg temperature of 1500°F and a cold-leg temperature of 1220°F. The other loop operated with a hot-leg temperature of 1445°F and a cold-leg temperature of 1337°F. At no time during the tests did the loops give any indication of plugging. There was very little difference in the appearance of the hot leg and the cold leg in either loop. There was no macroscopic evidence of mass-transferred crystals except at the bath-level line below the fill pipe where there was a fine ring of crystals in both loops. Metallographic examination of these loops is not yet complete.

FUNDAMENTAL CORROSION RESEARCH

G. P. Smith
Metallurgy Division

Mass Transfer in Liquid Lead

J. V. Cathcart
Metallurgy Division

The investigation of corrosion and mass transfer in liquid lead has revealed that small quartz thermal-convection loops containing types 410 and 446 stainless steel test specimens require from two to three times longer to plug than similar loops containing pure iron and chromium or one of the 300-series stainless steels.[7] An effort has been made to find an explanation for this phenomenon. As in previous experiments, all tests were con-

[6] G. M. Adamson, *ANP Quar. Prog. Rep. Mar. 10, 1954*, ORNL-1692, p 73.

[7] *ANP Quar. Prog. Rep. Sept. 10, 1953*, ORNL-1609, p 80; *ANP Quar. Prog. Rep. Mar. 10, 1953*, ORNL-1515, p 128; *ANP Quar. Prog. Rep. June 10, 1953*, ORNL-1556, p 64.

ducted in small quartz thermal-convection loops.[8]

Two possible explanations for the increased resistance to mass transfer of the 400-series stainless steels in liquid lead have been considered. First, the influence of the very thin oxide films on the specimens was investigated. It was thought possible that the oxide formed on the 400-series stainless steels possessed a structure which made it especially resistant to attack by liquid lead. In such an event a thin oxide film would present a barrier to the solution of material from the specimen walls and thus reduce the rate of mass transfer. It has been demonstrated[9] that relatively thick oxide films (approximately 1000 Å) greatly reduced mass transfer in loops containing types 304 and 347 stainless steel specimens.

An attempt was also made to remove completely the oxide film from type 446 stainless steel specimens mounted in a loop. A small quartz tube was sealed into the loop at the bottom of the bend in the cold leg and, before the loop was loaded, the specimens were heated to 950°C while hydrogen, which had been dried over magnesium perchlorate, was allowed to flow through the loop. After 1 hr of this treatment the side arm was sealed off with a hand torch, and the loop was immediately loaded with liquid lead. The loop plugged after 768 hr of operation with hot- and cold-leg temperatures of 805 and 525°C. The long time required for the plugging of this loop was taken as an indication that the presence of an oxide film on the specimens was not the correct explanation for the relatively high resistance to mass transfer in liquid lead exhibited by type 446 stainless steel. Of course, it is possible that the oxide on the test specimens was only partially reduced or that, even if it were completely reduced, enough oxide remained in the lead to reoxidize the surface of the test specimens. In such an event, the results of this test would be inconclusive; however, it is believed that the corrosion characteristics of type 446 stainless steel cannot be explained on the basis of the influence of thin oxide films on the surface of the test specimens.

The second approach made to the problem involved the assumption that a thin layer of sigma phase formed near the surface of the types 446 and 410 stainless steel hot-leg specimens and served as a barrier to solution of the specimens. The presence of such a layer has not yet been revealed either by metallographic examination of the test specimens or by an x-ray study of filings taken from the surface of a type 446 stainless steel hot-leg specimen. If this explanation is correct, however, only a very thin layer of sigma phase would be required to produce the increased resistance to mass transfer and it may not be surprising that such a layer has not been found.

In order to test the effect of sigma phase on resistance to mass transfer in iron-chromium-nickel alloys, a special alloy having a composition of 16% Ni–37% Cr–47% Fe was prepared. This alloy was chosen because its composition corresponds to that in the sigma-plus-austenite region of the nickel-chromium-iron phase diagram. Two sets of specimens were prepared; one set was annealed for 80 hr at 810°C to facilitate the precipitation of the sigma phase; the other set was annealed at 1200°C and water-quenched to leave only ferrite and austenite phases in the alloy.

Two loops containing sigma-phase (sigma and austenite) specimens of this alloy were operated. The first loop plugged after 456 hr of operation with hot- and cold-leg temperatures of 820 and 510°C. The second loop plugged after only 306 hr with hot- and cold-leg temperatures of 805 and 550°C. Metallographic examination of the second loop has not yet been completed, but a transverse section of the attacked region on the hot-leg specimen from the first loop is shown in Fig. 5.12. As may be seen, the attack was very irregular; thin filaments of the original metal extend into a lead matrix. Close examination revealed that each filament consisted of a core of sigma-phase material surrounded by a thin film of matrix metal. The sigma-phase regions of the test specimens appeared to have suffered much less attack than the austenitic regions.

The nonsigma-phase (ferrite and austenite) specimens of the alloy were also tested in two loops. The first loop plugged after 287 hr of operation with hot- and cold-leg temperatures of 810 and 520°C. The second loop plugged after 101 hr with hot- and cold-leg temperatures of 810 and 510°C. A transverse section of the hot-leg specimen from the first loop is shown in Fig. 5.13.

The lack of reproducibility in the plugging times for both the sigma- and nonsigma-phase loops can

[8] *ANP Quar. Prog. Rep. Dec. 10, 1952*, ORNL-1439, p 148.

[9] *ANP Quar. Prog. Rep. Dec. 10, 1953*, ORNL-1649, p 74.

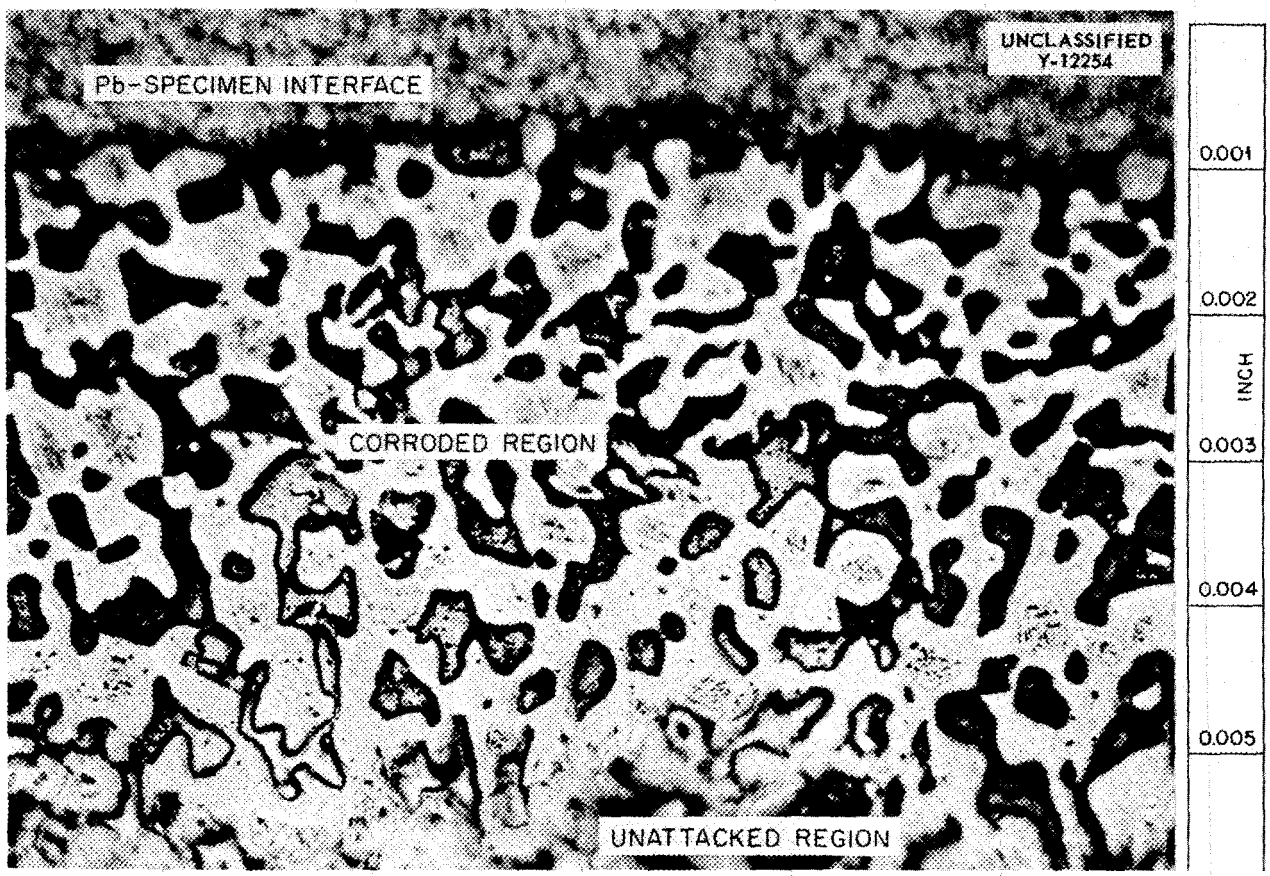

Fig. 5.12. Transverse Section of a Special Sigma-Phase Alloy (16% Ni–37% Cr–47% Fe) Specimen from the Hot Leg of a Quartz Thermal-Convection Loop Which Circulated Liquid Lead. 750X.

probably be accounted for in terms of differences in the degree of transformation which occurred during the heat treatments of the specimens. The hot-leg temperature during the operation of the loops was very close to the sigma-to-ferrite transformation temperature; thus it is not unlikely that an appreciable amount of sigma phase was either formed or destroyed during the operation of the loops and therefore produced the variation in plugging times which was observed.

The results obtained with the 16% Ni–37% Cr–47% Fe alloy indicate a definite increase in resistance to mass transfer for sigma-phase alloys in comparison with the nonsigma-phase alloys. However, no definite conclusions can be drawn as to the role of the sigma phase in the resistance to mass transfer exhibited by the 400-series stainless steels until a sigma-phase layer is actually observed in the test specimens from a loop containing one of these steels.

Products of Hydroxide-Metal Reactions

H. L. Yakel, Jr. G. P. Smith
Metallurgy Division

Studies are being made to identify the compounds produced by hydroxide-metal reaction and to determine their properties. Previous studies were concerned with the action of lithium and sodium hydroxides on nickel in the presence of oxidizing agents.[10] Current research is concerned with the reaction which occurs between sodium hydroxide and nickel when hydrogen is allowed to escape from the system.

Miller and Williams[11] have shown the existence

[10] L. D. Dyer, B. S. Borie, Jr., and G. P. Smith, *Alkali-Metal Nickel Oxides Containing Trivalent Nickel*, ORNL-1667 (Feb. 26, 1954).

[11] Reported by D. D. Williams and C. T. Ewing in *Sixth Progress Report on Thermal and Related Physical Properties of Molten Materials*, Naval Research Laboratory Problem No. 32C11-06 (1953) and preceding reports in this series.

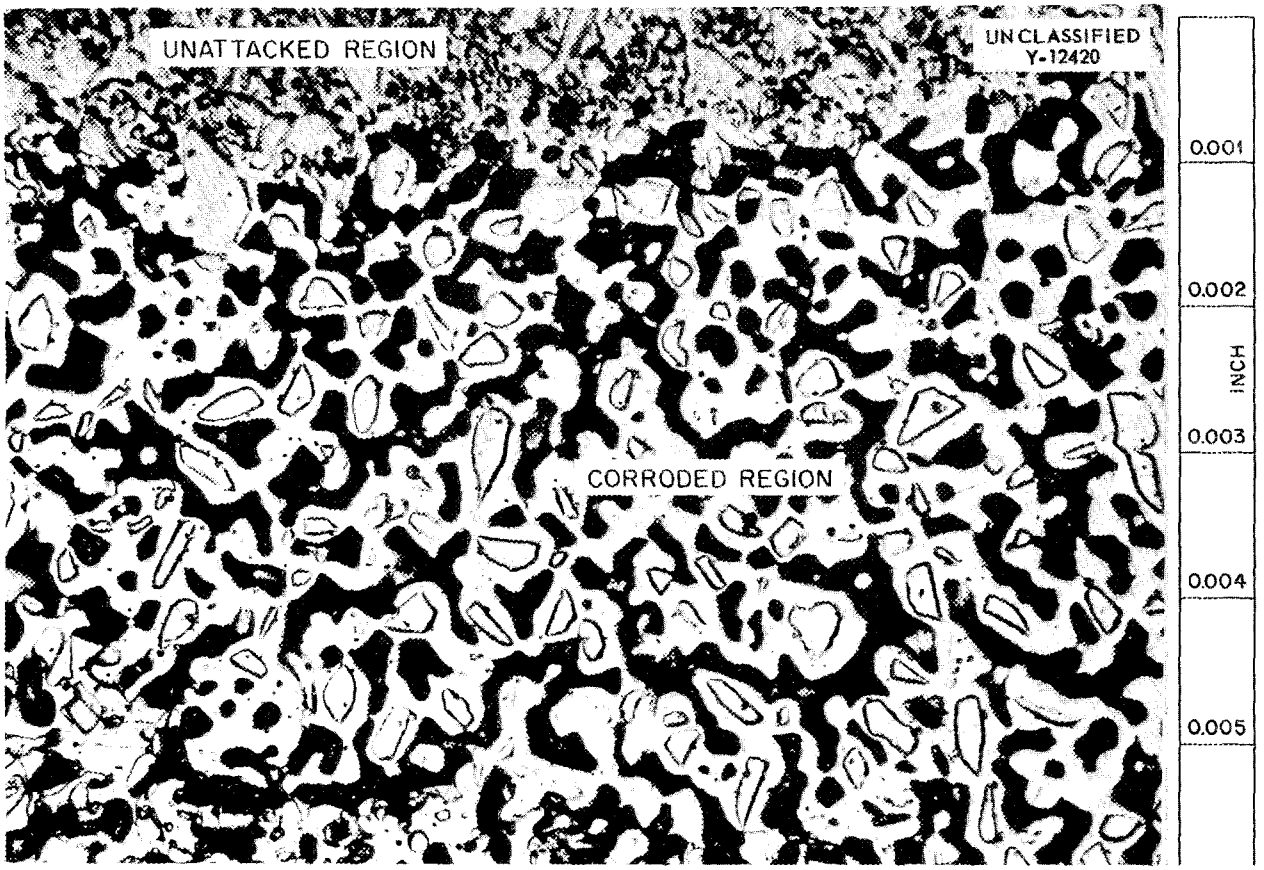

Fig. 5.13. Transverse Section of a Special Nonsigma-Phase Alloy (16% Ni–37% Cr–47% Fe) Specimen from the Hot Leg of a Quartz Thermal-Convection Loop Which Circulated Liquid Lead. 750X.

of an equilibrium of the type Ni + NaOH = H_2 + unknown products. They reported that when this equilibrium was displaced by evacuating at 900 to 1000°C until hydrogen evolution ceased, an "amorphous" product was obtained which had a gross composition corresponding to 1 mole of sodium oxide and 1 mole of nickelous oxide. Woltersdorf[12] found that mixtures of sodium oxide and nickelous oxide react at temperatures as low as 250°C to produce various crystalline sodium nickelate(II) compounds. He was able to establish that sodium orthonickelate(II) has the empirical formula Na_2NiO_2. Kruh[13] found that a mixture of NaOH and nickel heated to 700°C under flowing argon gave x-ray powder patterns which did not correspond to any patterns in the literature. Kertesz and Knox[14] induced a reaction between sodium hydroxide and nickel by slowly removing a relatively small amount of hydrogen gas. X-ray powder patterns of the resulting material did not show any identifiable lines.

During the past few months the reaction which takes place when hydrogen is rapidly evacuated from the NaOH-Ni system has been studied. The primary product of this reaction is a crystalline sodium divalent nickelate of an as yet undetermined formula.

In these studies the reaction chamber was a 1.27-cm-OD, 44-cm-long nickel tube (low-carbon grade). The tube was welded closed at the bottom end and fastened at the top end to the rest of the all-glass apparatus by means of a standard, ground ball joint. The nickel tube could be evacuated

[12] G. Woltersdorf, *Z. anorg. Chem.* 252, 126 (1943).

[13] Reported by R. F. Kruh, *Report for the Period April 1, 1953 through June 30, 1953*, p 5, University of Arkansas, Institute of Science and Technology, Fayetteville.

[14] F. Kertesz, private communication.

through either of two circuits by turning a stopcock. One circuit was relatively short and allowed fast pumping speeds. The other circuit contained a liquid-nitrogen cold trap. The pressure of the system was measured by means of a Pirani gage and an Octoil-S manometer similar to that described by Biondi.[15] This combination of instruments provided pressure measurements from 1 to 1000 μ with a precision of $\frac{1}{5}$ μ at the low-pressure extreme and 20 μ at the high-pressure extreme. The vacuum was produced by a Kinney CVM 3534 mechanical pump. Dry carbon-dioxide-free argon could be admitted to the apparatus when desired. The nickel reaction tube was heated by a tube furnace. Temperatures were measured with chromel-alumel thermocouples which were wired to the nickel tube. The method used for opening the reaction tubes at the end of an experiment did not make it practical to weld the thermocouples to the tube. Hence, the highest temperatures reported (950°C) may have been in error by as much as ±20°C.

The nickel reaction tube was loaded in air with about 10 g of cp-grade sodium hydroxide and then quickly attached to the apparatus. Dehydration of the hydroxide was accomplished by slowly heating it to about 400°C under a vacuum. The circuit containing the cold trap was used to remove the water evolved. The course of the dehydration was followed by observing pressure changes, and some observations were made that are described in the following section.

After the dehydration step the temperature was increased to a predetermined value while the gases evolved were pumped off through the short circuit. After reaction had proceeded as far as desired, the furnace was rapidly cooled. Dry carbon-dioxide-free argon was then admitted to the apparatus, and the reaction tube and its contents were removed to a dry box for examination.

Reactions were carried out over the temperature range of 770 to 950°C, and the reaction products were examined. At 770°C the pressure (assumed to be due to hydrogen) rose to a maximum of 200 μ and slowly decreased to 70 μ over a period of about 7 hr. The course of another reaction is shown in Fig. 5.14. It had been intended that this reaction would be carried out at 950°C. However, as may be seen from Fig. 5.14, the pressure passed through its maximum before 950°C was reached. The shaded area connects the extremes of pressure fluctuations.

[15] M. A. Biondi, *Rev. Sci. Instr.* 24, 989 (1953).

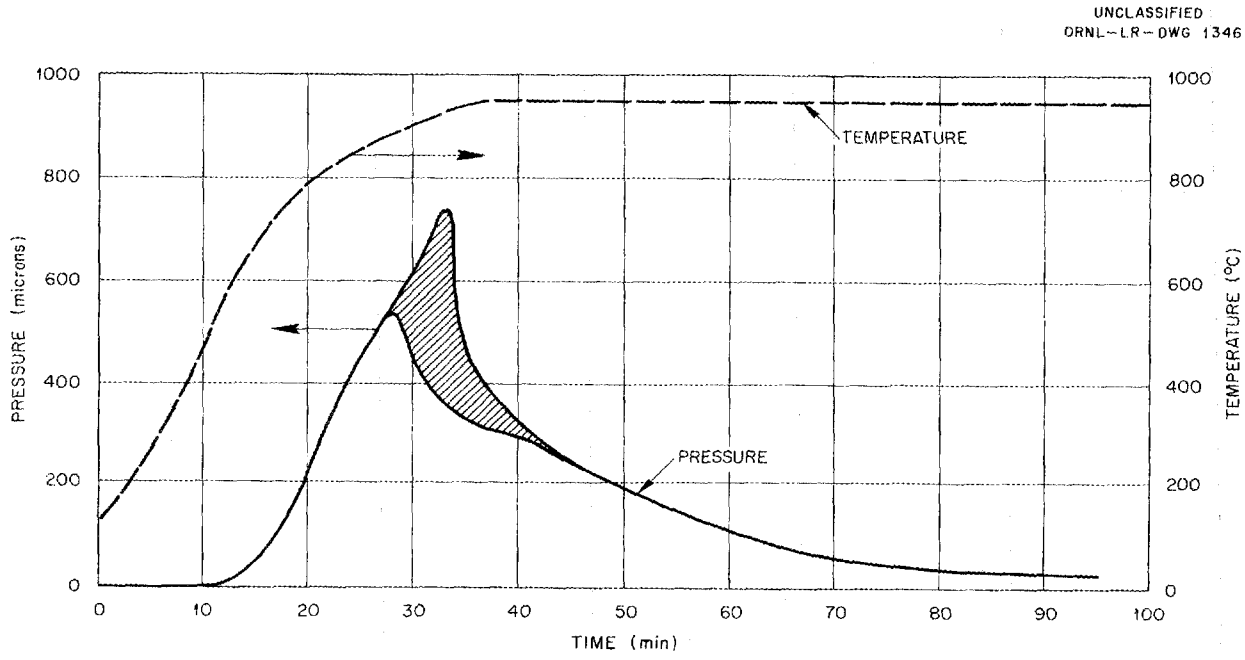

Fig. 5.14. Gas Evolution in the Reaction of Nickel with Sodium Hydroxide in a Continuously Evacuated System.

In Fig. 5.14, an area A taken under the curve for any time interval Δt is proportional to n, the number of moles of gas evolved during the time interval Δt. The pumping speed s is defined to be $s = dV/dt$, where dV is the increment of gas volume passing through a given cross section of tubing in the time interval dt. By applying the ideal gas law in its usual form it is seen that

$$dn = \frac{sP}{RT}\,dt \quad .$$

If s is constant over the pressure range under consideration,

$$n = \frac{s}{RT}\int_{t_i}^{t_f} P\,dt = \frac{sA}{RT} \quad ,$$

and therefore

$$n \sim A \quad .$$

For the pressure range represented in Fig. 5.14, the pumping speed varies by about 20% for the Kinney CVM 3534 pump.

Application of this analysis to Fig. 5.14 shows that the reaction NaOH + Ni = nickelate + H_2 cannot be said to cease at any definite time under the experimental conditions. The effect which the accumulation of the reaction product has on the diffusion of sodium hydroxide to the nickel wall is undoubtedly the reason for this.

The nickel tubes containing the reaction products were opened in a helium-filled dry box. Microscopic examination showed that the reaction products consisted of fibers and a powder, which were subsequently separated.

The fibers, when very thin, were transparent green. They showed no recognizable crystal faces and were frequently bent or partially split along the fiber axis. They dissolved readily in 1 *N* hydrochloric acid, had an oxidizing power of less than 0.88 meq/g (probably due to cobalt and manganese impurity), and reacted with moisture and carbon dioxide in the air to form a crust of sodium carbonate monohydrate. The chemical data suggest that the compound is a sodium nickelate(II).

A single fiber was sealed in a glass capillary in the dry box immediately after the nickel reaction tube was open. This fiber, which was found to be a single crystal, was used for preliminary structure determination work. Rotation, Weissenberg, and precession photographs of the single-crystal fiber show orthorhombic symmetry (Laue symmetry *mmm*). Unit cell dimensions were measured from all three types of photograph, and the suitably averaged results are:

$$a = 8.28_4\ \text{Å} \pm 0.011\ \text{Å} \quad ,$$
$$b = 10.14_9\ \text{Å} \pm 0.008\ \text{Å} \quad ,$$
$$c = 2.81_5\ \text{Å} \pm 0.008\ \text{Å} \quad ,$$
$$V = 236.67 \times 10^{-24}\ \text{cc} \quad .$$

The extinctions observed in the single-crystal diffraction pattern are consistent with the three space groups *Amam*, *Ama2*, and $Ama2_1$. Piezoelectric or pyroelectric experiments might distinguish between the centrosymmetric space group *Amam* and the other noncentrosymmetric possibilities, but these experiments have not been performed because of the lack of experimental equipment. A statistical averaging of the observed intensities may also permit a distinction to be made between the possible space groups.

If the compound is assumed to consist only of Na^+, Ni^{2+}, and O^{2-}, chemical analysis for sodium and nickel of alcohol-washed products gives a composition which cannot exist. If, on the other hand, it is assumed that nickelous hydroxide is present, the chemical analysis is quantitively satisfied by a mixture of Na_2NiO_2 with 40 wt % $Ni(OH)_2$. Such a mixture would be plausible. It is not unlikely that sodium orthonickelate(II) is the original product of the reaction, that it reacts with atmospheric water to form nickelous hydroxide and sodium hydroxide, and that the sodium hydroxide is removed by the alcohol washing.

Dehydration of Sodium Hydroxide

G. P. Smith
Metallurgy Division

It is well known that sodium hydroxide can be dehydrated by heating to 400°C under a vaccum. However, the details of this process have not previously been reported. In studies of the reaction of sodium hydroxide with nickel, as described above, it was possible to measure the evolution of water during the course of dehydration. It was found that virtually all the water evolution occurred near the melting points of sodium hydroxide monohydrate and sodium hydroxide. This result is not surprising in view of the enhanced diffusion rates in the liquid as compared with the solid. However, the quantitative extent of this effect is greater than might have been predicted.

Figure 5.15 is a plot of pressure and temperature vs time during one of four similar dehydrations. As was shown in the preceding section, an area under the pressure-time curve for a specified time interval is proportional to the amount of gas evolved during that time interval. Hence, most of the water was evolved within the relatively narrow limits of two peaks or bands, the first of which corresponds to the melting of sodium hydroxide monohydrate and the second of which corresponds to the melting of sodium hydroxide. The shaded area on the second peak connects the upper and lower limits of rapid pressure fluctuations which were probably caused by the bursting of water-vapor bubbles.

Color Changes in Fused Hydroxides

C. R. Boston M. E. Steidlitz
Metallurgy Division

Color changes observed in fused hydroxides indicate the existence of species in thermal equilibrium other than the expected sodium ions and hydroxyl ions. Several years ago it was noted in this laboratory that colorless fused sodium hydroxide in a nickel container under an atmosphere of hydrogen turned green when heated to above 500°C and again became colorless when cooled to below 500°C. This color change was at first thought to be due to a changing concentration of nickel ions with changing temperature. Subsequently it was found that the same color change took place when the hydroxide was contained in silver. These observations indicated that the color was not due to the presence of heavy-metal ions. This qualitative study of color changes has been greatly extended.

The experimental method used consisted of placing the hydroxide in a crucible which was contained in a quartz tube which could be evacuated with a mechanical pump and to which various atmospheres could be admitted. The crucible of hydroxide was heated by a small pot-type furnace in which the hydroxide could be observed. The gases were either dried by passing them through a liquid-nitrogen cold trap or they were saturated with water vapor by bubbling them through water. In most of the experiments the crucibles used were pure sintered aluminum oxide (Morganite) to ensure the absence of heavy-metal ions. Morganite is very slowly and uniformly attacked by fused hydroxides. However, of the various ceramic crucibles available, Morganite was by far the most resistant to corrosion. In a few tests, nickel crucibles were used. The lithium, sodium, and potassium hydroxides used were cp grade. The rubidium and cesium hydroxides were supplied by L. G. Overholser of the ORNL Materials Chemistry Division.

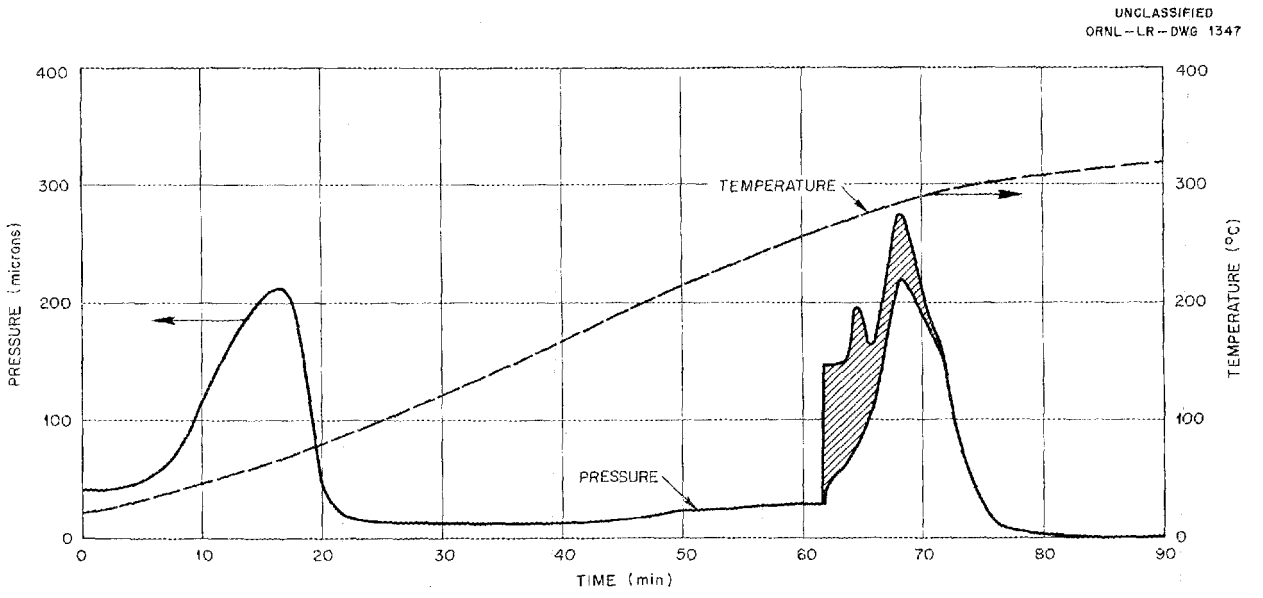

Fig. 5.15. Water Evolution During the Dehydration of Sodium Hydroxide at a Slow Heating Rate.

A series of experiments was conducted in which the hydroxides were heated to approximately 600°C under specified atmospheres. At 600°C the initial atmosphere was evacuated and various atmospheres were successively admitted and evacuated. Finally the hydroxide was cooled to room temperature. During each step the color changes were noted.

The colors of the hydroxides (contained in Morganite) which developed on standing in specified atmospheres at 600°C are shown in Table 5.10. For each combination of fused hydroxide and atmosphere which was studied, the hydroxide was colorless below approximately 500°C and distinctly colored at 600°C. The colorless-colored transition was reversible with changing temperature. When the system was evacuated or filled with a specified gas, the color changed sometimes with startling abruptness after a brief induction period.

Lithium hydroxide did not lend itself well to testing because of its tendency to decompose with the evolution of water. Sodium hydroxide, after being heated for a long period in either air or vacuum, changed in color from yellow to a deep red-orange. This color, however, disappeared promptly on cooling or when the atmosphere was changed.

Several experiments were conducted with sodium hydroxide contained in nickel crucibles. The colors found were the same as those observed with a Morganite container except when an atmosphere of air was used. In this instance, reaction with the nickel quickly turned the hydroxide black.

Experiments were performed in which various sodium compounds were added to sodium hydroxide and the mixtures were heated under a vacuum to a temperature of about 400°C. These additives were of commercial purity. Metallic sodium and sodium hydride additions gave, at first, a blue color which, in time, turned to green. Sodium peroxide additions imparted an orange color. With sodium oxide additions the hydroxide was yellow. It should be noted that these colors were formed at a temperature at which the pure hydroxide would have been colorless. All the colors were retained upon cooling the hydroxide to below its melting point.

The results of these experiments are still too incomplete and too qualitative to permit specific conclusions as to the species giving rise to the various colors. Nevertheless, a number of tentative speculations can be made. First, various simple atmospheres such as oxygen, hydrogen, and water vapor can interact with the fused alkali-metal hydroxide to produce different chemical species which can be characterized, at least to a limited extent, by their color. These interactions do not seem to be greatly altered by progressively changing the cation from sodium to cesium. Hence, they seem to be associated with the anion. The extent of interaction is rapidly established and thereafter seems to change only very slowly with time at constant temperature. The extent of interaction seems to increase markedly with increasing temperature.

It is significant that these hydroxide-gas interactions take place in the absence of free metal. It is well known that the atmosphere plays a dominant role in controlling the mass transfer of nickel. It is not entirely unlikely, then, that the chemical reactions that cause mass transfer do not take place directly between nickel and the hydroxyl ion, as is generally believed, but rather between nickel

TABLE 5.10. COLORS OF HYDROXIDES IN VARIOUS ATMOSPHERES AT 600°C

HYDROXIDE	COLOR IN SPECIFIED ATMOSPHERE				
	Air	Vacuum	H_2	He	Water Vapor in H_2 or He
LiOH	Yellow				
NaOH	Yellow, orange	Yellow, orange	Green	Yellow	Colorless
KOH	Yellow	Yellow	Green		
RbOH	Yellow	Yellow	Green		
CsOH	Yellow	Yellow	Green		

and a chemical species whose concentration is dependent on an interaction between the hydroxyl ion and the atmosphere.

Preliminary measurements have been made of the electrical conductivity of fused sodium hydroxide contained in silver exposed to the air at temperatures up to 550°C. The results are in fair agreement with those reported by Arndt and Ploetz[16] who give data up to 450°C. It is interesting to note that the conductivity was found to rise rapidly over the temperature range for which a color change is first noted.

[16] K. Arndt and G. Ploetz, *Z. physik. Chem.* 110, 237 (1924).

6. METALLURGY

W. D. Manly
Metallurgy Division

The studies of the mechanical properties of Inconel in contact with the fused fluorides have shown that material stressed under uniaxial conditions has a much longer rupture life than material tested under multiaxial conditions. Since in any ANP type of reactor the material will be under multiaxial stresses, the testing of alloys for this service should be performed by using tube-burst tests. The uniaxial test conditions are much easier to control and will give a much better insight into the effect of environments, but for obtaining actual design data, the tube-burst tests or other multiaxial-stress tests are preferred. It has been found that the load-carrying abilities of Inconel, as well as the corrosion, are also quite dependent on the ratio of surface area to volume of fluoride mixture. As the ratio of surface area of container material to volume of fluoride mixture decreases, the rupture life for a given stress is also decreased.

Investigations of materials suitable for high-conductivity fins have been primarily concerned with the protection of copper from oxidation and with the prevention of diffusion between the cladding material and the copper. This work has shown that copper clad with types 310, 446, or 430 stainless steel or with Inconel is quite satisfactory in the unstressed condition if a suitable diffusion barrier is provided. In oxidation tests of the clad material under the stress, however, it was found that high stresses greatly increase the oxidation of the material. Additional tests will be made at lower stresses and for longer times.

In the search for container materials for fluid fuels, Hastelloys B and C were found to have very poor extrusion characteristics. A comparison with the results of extrusion experiments with nickel-molybdenum special alloys indicates that the difficulty in extruding Hastelloy B was probably caused by the impurities in the material and the poor melting practice used in its preparation, rather than poor lubrication during extrusion. The work-hardening characteristics of columbium were determined.

Sheets of high-boron-content material will be required for shielding between the moderator and the heat exchanger and between the heat exchanger and the pressure shell of the Reflector-Moderated Reactor. Powder compacts of boron carbide blended with copper and with silver powders were hot pressed, and boron densities which approached the density required were obtained. It is thought that the required density can be obtained by warm-pressing compacts of boron carbide and copper.

High-temperature oxidation-resistance tests of several brazing alloys at 1500 and 1700°F for 200 and 500 hr have shown that the majority of the nickel and nickel-chromium-base alloys are suitable for service in an oxidizing atmosphere at 1500°F and that several of the alloys retain this resistance at 1700°F.

A new semiautomatic heliarc-welding process for production of tube-to-header joints is described and its use in the construction of a prototype sodium-to-air radiator is illustrated. The fabrication of a radiator with high-conductivity fins requires a brazing alloy that has good strength at 1600°F and flowability at approximately 1900°F. Coast Metals alloy No. 52, which will suitably wet stainless steels and flow in dry-hydrogen atmospheres, has been found to be satisfactory for this use. In addition to having a suitable alloy, the furnace temperature must be very carefully controlled so that there will be a minimum of thermal variation over the assembly. To test the brazing alloys and to check the controls of the furnace, a prototype radiator with high-conductivity fins was constructed. The successful fabrication of this prototype radiator indicates that such complicated configurations can be constructed.

An assembly consisting of a beryllium plate canned in an Inconel assembly in which the beryllium will be heated by electrical resistance and cooled by sodium passing through holes in the beryllium plate was fabricated. This unit will be used for determining the effect of thermal stresses and thermal cycling on beryllium metal and for studying the compatibility of sodium and beryllium.

STRESS-RUPTURE TESTS OF INCONEL

R. B. Oliver D. A. Douglas
J. W. Woods
Metallurgy Division

The previous report[1] presented results for a series of stress-rupture tests of tubular Inconel specimens under multiaxial stress in contact with $NaF-ZrF_4-UF_4$ (50-46-4 mole %). Some additional data which compare time to rupture for multiaxially stressed tubular specimens with that for uniaxially stressed flat specimens in the same fluoride mixture are presented in Fig. 6.1. The previous results were for specimens tested with the fluoride mixture inside the tube and purified argon gas outside. Metallographic examination of the tubes after rupture did not show the void formation which characterizes the type of corrosive attack found on the straight tension tests. The surface appeared uneven, but there was no evidence of intergranular attack. With the fluoride mixture inside the tube, there is a ratio of about ten units of surface area to one of volume. It was thought that the change in the corrosion rate could be

[1] R. B. Oliver, D. A. Douglas, and J. W. Woods, *ANP Quar. Prog. Rep. Mar. 10, 1954*, ORNL-1692, p 84.

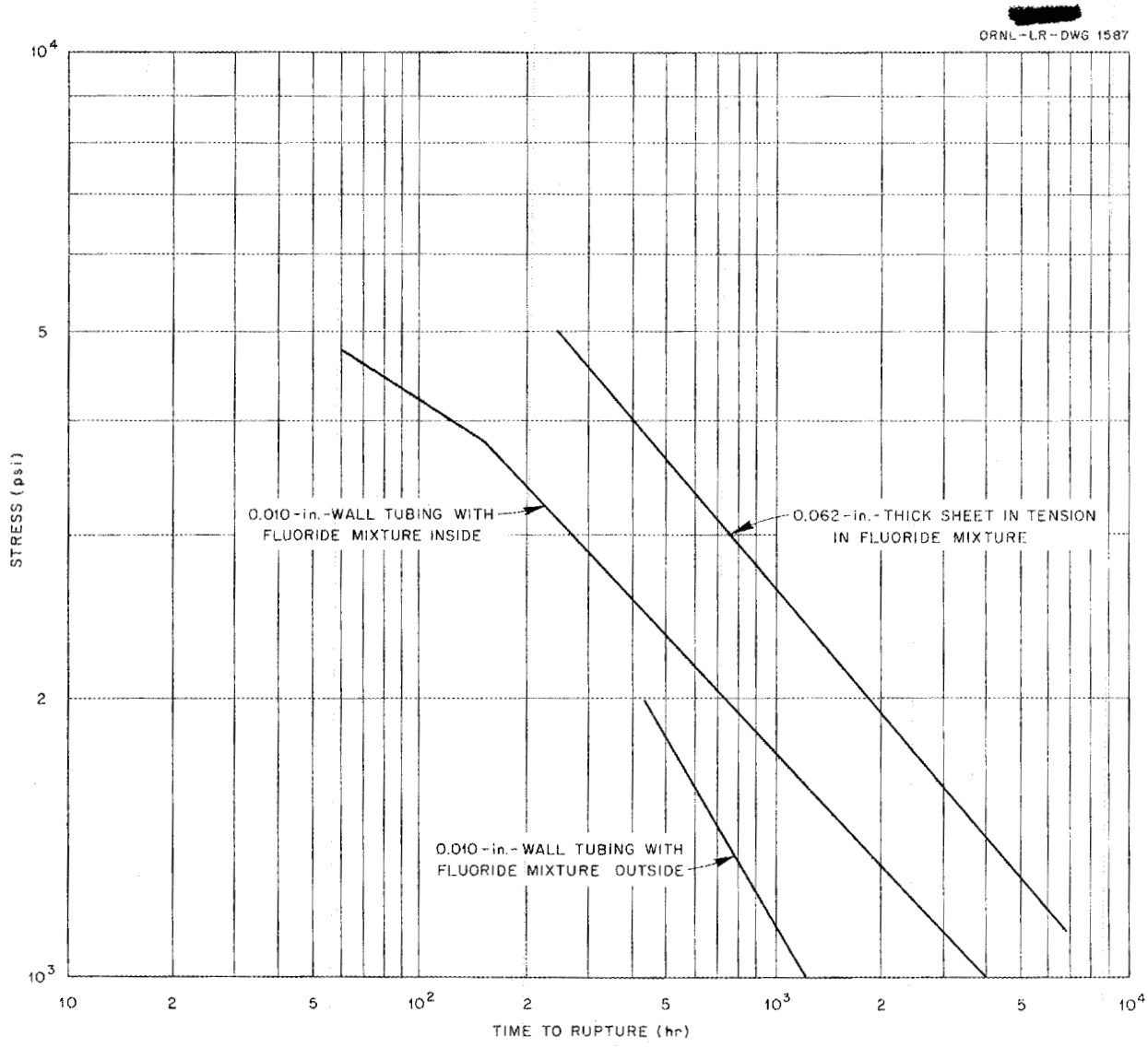

Fig. 6.1. Stress vs Time to Rupture for Inconel Sheet and Inconel Tubing in $NaF-ZrF_4-UF_4$ (50-46-4 mole %) at 1500°F.

explained on the basis that the surface-to-volume ratio was too high to sustain the corrosive attack. With this point in mind, tests were run with the fluoride mixture outside the tube and argon inside, with a resulting ratio of one unit of surface area to eight units of volume. The types of corrosive attack on these specimens are illustrated in Figs. 6.2 and 6.3. The attack shown in Fig. 6.3, which is similar to that found in uniaxial tests, differs radically from the attack found when the fluoride

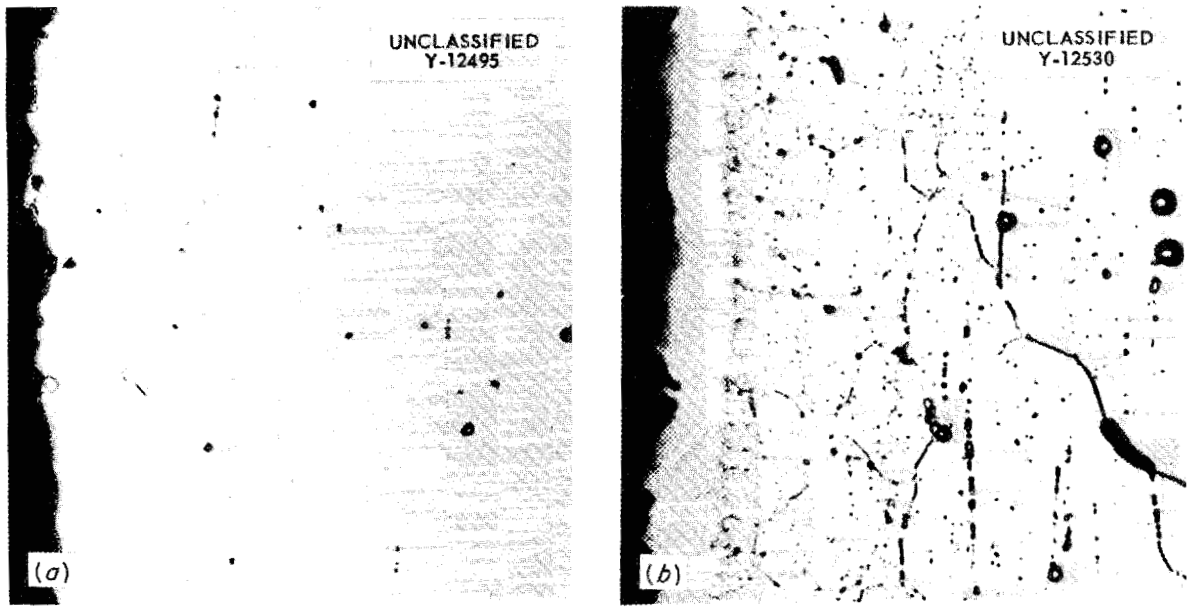

Fig. 6.2. Inconel Tubing After Exposure to NaF-ZrF_4-UF_4 at 1500°F in Stress-Rupture Test in Which the Fluoride Mixture Was Inside the Tube and the Resulting Surface-to-Volume Ratio Was 10 to 1. (*a*) Unetched. (*b*) Etched. 250X.

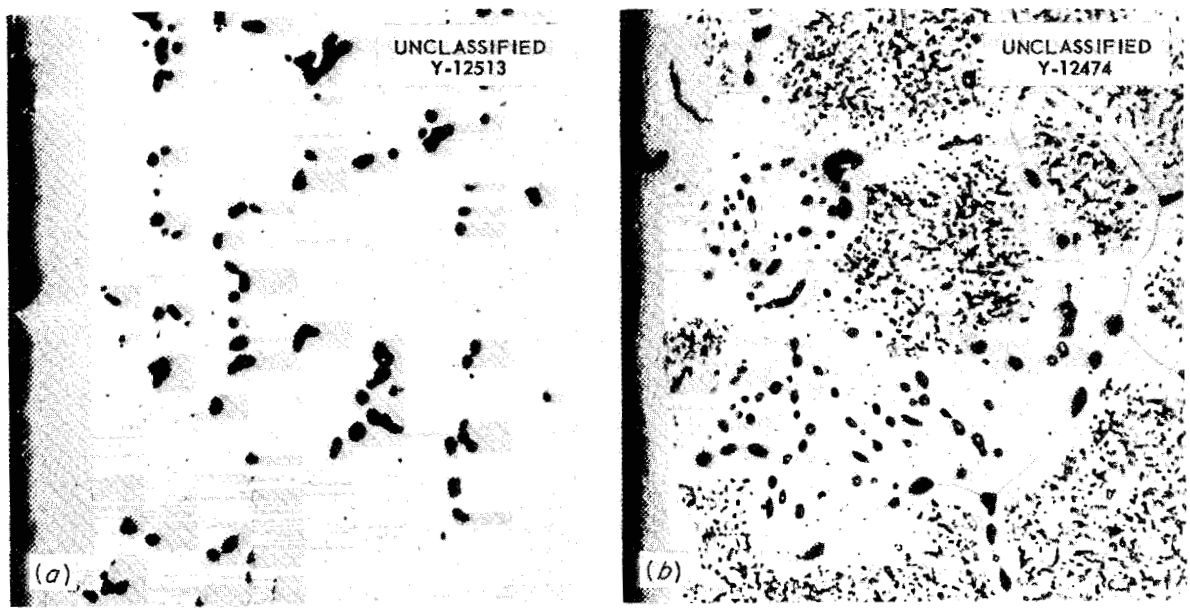

Fig. 6.3. Inconel Tubing After Exposure to NaF-ZrF_4-UF_4 at 1500°F in Stress-Rupture Test in Which the Fluoride Mixture Was Outside the Tube and the Resulting Surface-to-Volume Ratio Was 1 to 8. (*a*) Unetched. (*b*) Etched. 250X.

mixture was inside the tube (Fig. 6.2). It is therefore concluded that the surface-to-volume ratio is as important in stress-rupture tests as it is in corrosion tests. It appears that under these test conditions a certain minimum volume of fluoride mixture in relation to the surface area is required for corrosion to proceed. Since stress-rupture tests in fluoride mixtures are being run at a number of testing laboratories, some of which will be in support of the efforts of ORNL, it seems imperative that the best surface-to-volume ratio for reproducibility be determined. Otherwise, a comparison of the data from the various laboratories may lead to confusion or erroneous conclusions.

Another variable which should be considered in analyzing tube-burst data is the wall thickness of the specimen being tested. The data presented in Fig. 6.1 are for tubular specimens with 0.010-in.-thick walls. Naturally, corrosive attack will have more effect on this type of specimen than on a thick-walled tube. Specimens with wall thicknesses of 0.020, 0.040, and 0.060 in. are being tested so that the effect of this variable can be studied. It is expected that all the tubular specimens will fail in shorter times than will corresponding specimens tested in straight tension. One reason for this prediction is that in the tube-burst test there is a tangential-to-axial stress ratio of 2 to 1. It is generally recognized that this stress distribution will result in the minimum ductility for any given material. No strain measurements are made during the tube-burst test; however, after-test measurements do not show measurable deformation that would be evidence of the brittle behavior of Inconel in this type of test. The lowered ductility of the multiaxially stressed specimen is believed to be the prime reason for its early failure.

Since the available data from tube-burst tests indicate that multiaxial stresses reduce rupture life in comparison with rupture life under the uniaxial stresses used in the more conventional straight-tension tests, it appears that more emphasis should be placed on the tube-burst tests. Information on the behavior of Inconel tubing under multiaxial stress will be particularly pertinent to ANP-type reactor design.

HIGH-CONDUCTIVITY METALS FOR RADIATOR FINS

E. S. Bomar H. Inouye
J. H. Coobs R. W. Johnson
Metallurgy Division

Investigations of fin material have been primarily concerned with the protection of copper from oxidation and with the prevention of diffusion between copper and the cladding material. The materials that were found to be satisfactory as cladding were types 310, 446, and 430 stainless steel and Inconel, provided a suitable diffusion barrier was placed between the cladding and the copper. Since the purpose of the investigation was to develop a high-thermal-conductivity fin, a large ratio of copper to cladding was obviously desirable. With the roll-cladding techniques employed, the minimum clad that could be applied successfully was about 2 mils thick, although clads as thin as 1 mil have been made successfully by other methods. The minimum cladding thickness is apparently dependent only on ability to fabricate the composite. Under the conditions that the fin material will be used it must be assumed that there will be stresses. Therefore tensile-strength tests of the composites under oxidizing conditions are being made.

A few exploratory tests were made on 8-mil-thick type 310 stainless-steel-clad copper composites; the cladding was 2 mils thick on each side of the copper. The composites made by the General Plate Company were tested in the as-received condition. The results of a few tests are presented in Table 6.1. Additional tests at different stresses and temperatures are contemplated. No definite conclusions can be made at this time, but it is evident that low stresses caused failures that were not evident in tests under no-load conditions.

SPECIAL MATERIALS RESEARCH

E. S. Bomar H. Inouye
J. H. Coobs R. W. Johnson
Metallurgy Division

Hastelloys B and C

Seven rod extrusions of as-cast Hastelloys B and C were made to determine the optimum temperatures and the general fabrication characteristics

of these alloys. The extrusion data are presented in Table 6.2. These extrusions were successful in that they demonstrated that the material could be extruded. However, in nearly every instance the extruded rod cracked at the leading edge, and in one instance the extrusion shattered. At the present stage of investigation it is thought that the cracking of the leading edge is due to intermittent welding of the alloy to the die ("rattlesnaking") because of insufficient lubrication. Fractures of a different kind occurred near the center of the extruded rod that probably resulted from faults in the billets – the melts were made in air. Shattering is believed to be caused by low-melting phases in the grain boundaries.

These extrusion difficulties may be solved by (1) making the melts in vacuum and thus minimizing atmosphere contamination and probably the low-melting constituents, since purification might also be accomplished, (2) changing the die shape to cause more working in the leading edge, (3) canning the billet in such a manner that the alloy

TABLE 6.1. TENSILE STRENGTH TESTS OF TYPE 310 STAINLESS-STEEL-CLAD COPPER AT 1500°F IN AIR

STRESS (psi)	TEST DURATION (hr)	ELONGATION (% in 2½ in.)	REMARKS
500	500	5	Surface blistery but otherwise sound
1000	500	20	Stringers of oxide on surface; a few nodules of copper oxide
1500	500	47.5	Numerous copper oxide nodules on surface; areas oxidized throughout; considered to be a failure
1800	336	50	Sample ruptured
2000	96	39	Sample ruptured

TABLE 6.2. EXTRUSION DATA ON HASTELLOYS B AND C

Die: CHW* preheated to 572°F, 45-deg cone
Lubrication: glass wool in container
Ram sleeve: 3⅛ in., preheated to 692°F
Billet: 3½ in. long, 3 in. OD, heated in Houghton's No. 1550 salt bath

BILLET	EXTRUSION TEMPERATURE (°F)	HEATING TIME (hr)	EXTRUDED SIZE (in.)	RAM PRESSURE (tons)	
				Start	Run
Hastelloy B	2300	¾	1½	548	400
	2300	1¼	1¼	550	420
	2100	17½	1½	560	390
	2100	20	1¼	615	450
Hastelloy C	2100	18	1½	530	390
	2100	20½	1¼	565	460
	2100	4	1	570	450

*Manufactured by Latrobe Electric Steel Company.

is placed where lubrication is known to be adequate, that is, by using a dummy in front of the billet.

The short billets ($3\frac{1}{2}$ in.) were extruded at high velocities, and in many instances the tools were broken when the ram struck the die. This difficulty in stopping the ram movement at a precise moment was prevented by using a brass dummy block behind the billet so that the ram could be allowed to move until the press stopped.

Nickel-Molybdenum Alloys

Two vacuum melts of nominal composition 24% Mo–76% Ni and 20% Mo–80% Ni have been made. Attempts to extrude the 24% Mo–76% Ni alloy at 2350°F at reductions of 13 to 1 and 9 to 1 failed because of tool breakage. In the attempt at extrusion at a ratio of 9 to 1, the die insert fractured. A solid die was made, and attempts to extrude the 20% Mo–80% Ni alloy with the new die failed because of mandrel breakage. A straight mandrel and a 25-deg cone die were used. The extruded material that was obtained before the mechanical failures occurred had good surfaces and no evidence of "rattlesnaking."

Stainless-Steel-Clad Molybdenum and Columbium

Molybdenum tubing (0.620-in.-OD, 0.098-in.-wall) was clad on the outside with 0.065-in.-thick type 321 stainless steel. The composite tube was successfully bent 105 deg on a 3-in. radius at temperatures around 400°F and made into the shape of a conventional thermal-convection loop. Attempts to weld the molybdenum were unsuccessful because of porosity and extreme brittleness. Another complicating problem was that, at the temperatures required to fuse the molybdenum, the cladding melted and alloyed in the weld. These difficulties were circumvented by assembling the loop with threaded molybdenum joints and welding the stainless steel cladding. Two such loops were made. Type 310 stainless-steel-clad columbium tubing has been bent into the shape of a conventional thermal-convection loop, but the joint has not yet been welded. The bending was accomplished at room temperature by using Cerrobend inside the tube.

Columbium

Fansteel columbium sheet 0.250 in. thick was reduced to 0.193 in. in thickness and annealed in vacuum to an ASTM grain size of 6 to 7. The work-hardening characteristics were determined by making Tukon hardness measurements at various stages of reduction up to 89.6% in thickness. The results of these tests are given in Table 6.3. The data show that hardening in cold-worked columbium does not increase rapidly, and therefore the metal may be severely deformed without danger of fracture. A similar investigation[2] showed somewhat higher hardness values for the same reduction.

TABLE 6.3. WORK-HARDENING CHARACTERISTICS OF COLUMBIUM SHEET AT VARIOUS STAGES OF REDUCTION OF THICKNESS

THICKNESS (in.)	REDUCTION IN THICKNESS (%)	HARDNESS (VPN)
0.193	Annealed	72.4
0.170	11.9	98.2
0.152	21.2	100.2
0.135	30.0	108.3
0.115	40.3	111.1
0.095	50.2	115.5
0.077	60.1	123
0.058	70.0	127
0.040	79.3	134
0.025	87.0	144
0.020	89.6	150

Boron Carbide

Thin high-boron-content shielding is required for the heat exchanger of the Reflector-Moderated Reactor. This shield will be in two $\frac{1}{8}$-in.-thick layers, one inside and one outside the heat exchanger, and it should have as high a boron content as practical. A concentration of 1.5 g/cc of boron, equivalent to B_4C compacted to 80% density, would be sufficient.

The temperature of the shield, which will be about 1500°F, severely limits the choice of bonding materials for use in consolidating the

[2] W. O. Alexander, *Observations on the Fabricating Properties of Columbium Sheet*, BR-627 (July 12, 1945).

boron carbide. Iron and nickel both react with B_4C to form eutectics and brittle intermetallic phases, but they have been used to bond B_4C by hot-pressing or high-temperature sintering. Copper and silver are more attractive since they do not react with boron carbide and would therefore retain their strength and conductivity after being formed into a composite. However, silver is somewhat objectionable because of its relatively high cross section and associated gamma activity.

Hirsch[3] has reported fabricating strong compacts of boron bonded with 15 vol % of copper or of silver with boron densities as high as 1.52 g/cc by warm-pressing at 500°C with 50-tsi pressure. In the hope of producing satisfactory compacts by duplicating this work with high-grade B_4C, compositions containing 15 vol % of copper or 20 vol % of silver were prepared. Fine, annealed electrolytic copper and precipitated silver powders were used with blends of various particle-size fractions of B_4C. These mixtures were then pressed at 350°C with 40-tsi pressure, and the density was determined from the measured volume.

The maximum boron density obtained from these compositions thus far is about 1.25 g/cc for high-grade B_4C bonded with 20 vol % of silver. Densities attainable by using sized fractions of metallurgical-grade B_4C are 1.1 g/cc of boron with 20 vol % of copper binder and about 1.2 g/cc with 20 vol % of silver binder. By using compositions of high-grade B_4C (>80% boron) with copper and by pressing at 500°C, it should be possible to obtain compacts with boron densities at least as high as 1.3 g/cc. This density is somewhat lower than desired but may still be considered. The attainment of higher densities will require one of three alternatives:

1. the use of metallic boron bonded with copper by warm-pressing, as reported by Hirsch,
2. the high-temperature hot-pressing of B_4C, with or without iron or other reactive bonding agent,
3. the high-temperature sintering, at 1900 to 2000°C, of carefully prepared B_4C-Fe compositions, for which boron densities as high as 1.45 g/cc have been reported.[4]

A more complete investigation of the warm-pressing technique is to be made. For this investigation, 15 to 20 vol % of copper in B_4C will be pressed at 500°C with 40- to 50-tsi pressure. A new die of high-alloy steel will be required for satisfactory service at this temperature.

In addition to the problem of fabricating a satisfactory shield, the possible effects of boron diffusion must be studied. Since the shield will be in contact with Inconel at operating temperatures of 1500°F, extensive diffusion of boron may occur. Samples of Inconel coated with Al_2O_3 are being obtained for compatibility tests with boron-containing compacts.

[3]H. Hirsch, *J. Met. Ceram.*, TID-67, p 7 (May 1949).

[4]Knolls Atomic Power Laboratory, *Report of Metallurgy Section for December 1952 and January and February 1953*, KAPL-894.

WELDING AND BRAZING

P. Patriarca, G. M. Slaughter, B. McDowell, C. E. Shubert, K. W. Reber, J. M. Cisar
Metallurgy Division

Brazing Alloy Development

The extent and rate of high-temperature oxidation of brazing alloys during service are among the important factors which will determine the useful life of ANP radiators. Inconel T joints brazed with 15 different high-temperature brazing alloys were subjected to static air at 1500 and 1700°F for periods of 200 and 500 hr. The results of these tests, as determined by metallographic examination (100X magnification) in the as-polished condition, are presented in Table 6.4. It appears that the majority of the nickel and nickel-chromium-base alloys are suitable for service in an oxidizing atmosphere at 1500°F, and several are suitable at 1700°F. However, since G-E alloy No. 81 has shown considerable promise for tube-to-fin joints and as a backup for tube-to-header joints, its unexpected behavior at 1700°F is being investigated further. It was encouraging to find that the Coast Metals alloy No. 52 was very oxidation resistant, since its favorable flow point makes this alloy useful for joining high-conductivity fin materials.

A prototype sodium-to-air radiator utilizing Inconel-clad-copper high-conductivity fins was fabricated by a combination heliarc-welding and dry-hydrogen-brazing technique. The assembly, shown in Fig. 6.4, contains 180 heliarc-welded tube-to-header joints and approximately 4300 brazed tube-to-fin joints. As an added precaution against undesirable stress concentrations and leaks during service, the tube-to-header joints were back brazed.

TABLE 6.4. OXIDATION RESISTANCE OF DRY-HYDROGEN-BRAZED T JOINTS

BRAZING ALLOY	COMPOSITION (wt %)	BRAZING TEMPERATURE (°F)	OXIDATION IN STATIC AIR[a]			
			At 1500°F		At 1700°F	
			For 200 hr	For 500 hr	For 200 hr	For 500 hr
Commercial Alloys						
Nicrobraz	70 Ni–14 Cr–6 Fe–5 B–4 Si–1 C	2150	Slight	Slight	Slight	Slight
Low-melting-point Nicrobraz	80 Ni–6 Fe–5 Cr–5 Si–3 B–1 C	1920	Slight	Slight	Slight	Slight
Coast Metals alloy No. 52	89 Ni–5 Si–4 B–2 Fe	1840	Very slight	Slight	Slight	Slight
Mond Nickel Co. alloy	64 Ag–33 Pd–3 Mn	2150	Severe internal oxidation	Severe internal oxidation	Complete	
Copper	100 Cu	2050	Complete			
Experimental Nickel-Base Alloys						
GE alloy No. 81	66 Ni–19 Cr–10 Si–4 Fe–1 Mn	2150	Very slight	Slight	Severe[b]	Severe[b]
Ni-Ge	75 Ni–25 Ge	2150	Slight	Slight	Moderate	Moderate
Ni-Ge-Cr	65 Ni–25 Ge–10 Cr	2140	Very slight	Slight	Moderate[b]	Severe
Electroless Ni-P	88 Ni–12 P	1740	Very slight	Slight		
	80 Ni–10 P–10 Cr	1830	Very slight	Slight		
	68 Ni–32 Sn	2150	Slight	Moderate	Severe	Complete
	40 Ni–60 Mn	1920	Complete			
Precious-Metal-Base Alloys						
Au-Ni	82 Au–18 Ni	1830	Very slight	Slight	Moderate	Moderate
Au-Cu	80 Au–20 Cu	1740	Moderate	Complete		
Pd-Al	92 Pd–8 Al	2020	Very slight	Very slight	Very slight	Slight

[a] Very slight, less than 1 mil of penetration.
Slight, 1 to 2 mils of penetration.
Moderate, 2 to 5 mils of penetration.
Severe, greater than 5 mils of penetration.
Complete, fillet completely destroyed.

[b] Void formation caused by internal oxidation at braze alloy fillet–Inconel interface.

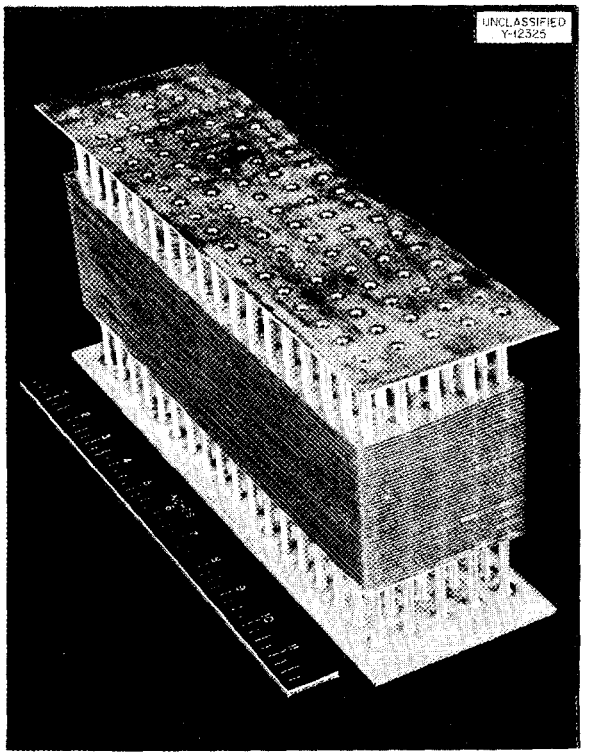

Fig. 6.4. Sodium-to-Air Radiator.

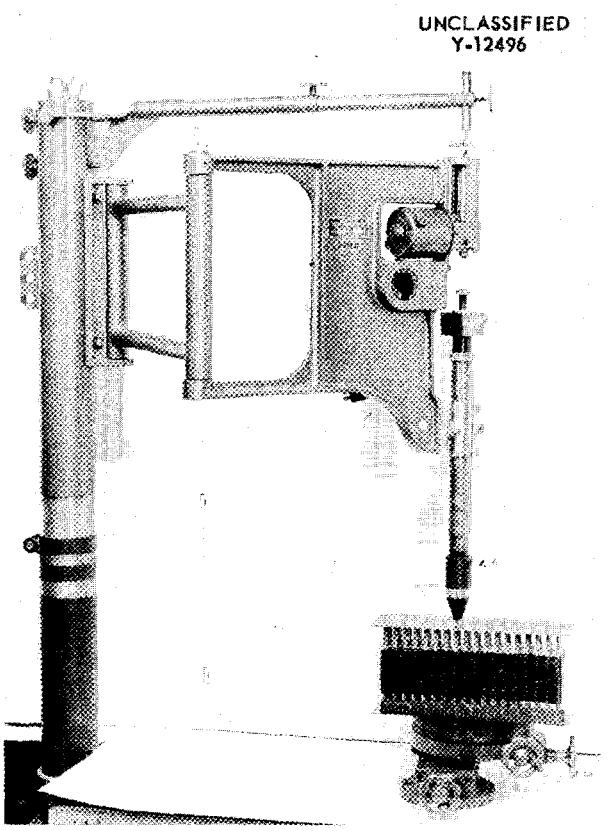

Fig. 6.5. Semiautomatic Tube-to-Header Welding Machine.

All tube-to-header joints were heliarc welded by a semiautomatic process. In this process, a commercially available heliarc torch is rotated around the tube periphery by a variable-speed motor-driven offset-cam mechanism which can be adjusted to any desired diameter of swing. A photograph of this equipment is shown in Fig. 6.5.

Preliminary experiments were conducted on typical tube-to-header samples to investigate the effects of arc current and welding speed upon weld size, hole constriction, and weld penetration. It was shown in these tests that welds comparable to those produced manually by a skilled operator[5] could be made semiautomatically. For example, satisfactory welds having a penetration of at least one tube-wall thickness could be made at a weld time of 7 sec over a welding current range from 40 to 50 amp. The hole constriction resulting from welds made over this current range did not exceed 5%.

As would be expected, welds made at other welding speeds required corresponding changes in the welding variables. Further experiments are now being conducted to study more thoroughly the relationships between the joint parameters and the welding variables. Since it is expected that the maximum weld penetration will be dependent to a significant extent on the radius of electrode swing, experiments will be conducted to determine this effect.

The fabrication of a radiator containing high-conductivity fins requires close control of the furnace temperatures during brazing to assure a minimum of thermal variations over the assembly. Experiments were conducted which indicated that the large Globar pit furnace available in the Welding Laboratory would permit a temperature control of ±5°F over the assembly at 1870°F and hence would be satisfactory for this fabrication. Coast Metals alloy No. 52 (Table 6.4) was se-

[5]P. Patriarca, G. M. Slaughter, and J. M. Cisar, *ANP Quar. Prog. Rep. Dec. 10, 1953*, ORNL-1649, p 86, Fig. 7.3.

lected as the brazing material because of its superior oxidation resistance and its relatively low flow point of 1840°F.

A preheat temperature of 1520°F was utilized in this dry-hydrogen-brazing operation to permit an equalization of temperatures over the assembly before brazing began. The preheat portion of the thermal cycle aided fillet formation by minimizing selective flowing of the brazing alloy to the fins. Boron diffusion from this alloy was not a problem during preheating because very little sintering occurs at this temperature. It also appears that the fin distortion on the assembly was kept to a minimum as a result of the preheating and the careful temperature control during brazing.

Good flowability of the alloy on both the tube-to-fin and tube-to-header joints was obtained during brazing for 30 min at 1870°F. Since the copper exposed by the fin-punching operation can be protected adequately by the brazing alloy, it is believed that the oxidation resistance of the tube-to-fin joints should be satisfactory.

Beryllium Test Assembly

An Inconel assembly for determining the effects of thermal stresses and thermal cycling on beryllium was fabricated. This unit, which will be used to evaluate the temperature distributions in the beryllium, as well as the compatibility of sodium and beryllium, consists of 46 tube-to-header joints and extensive manifold welding. The beryllium block is enclosed in the center section of the assembly shown in Fig. 6.6. All joints were manually heliarc welded by qualified operators and were leak-tight to helium.

Since heating will be achieved by the electric resistance heating of sodium, it was necessary to fabricate two laminated-copper bus bars and to join these to the Inconel assembly. A silver-copper eutectic brazing alloy was used to join the copper laminations into a solid electrical connection. However, since this silver brazing alloy will not wet Inconel satisfactorily in the available dry-hydrogen atmosphere at the brazing temperature of 1510°F, it was necessary to copper-braze nickel sheets to the Inconel cans before subsequent joining of the bus bars to the test assembly with the silver-copper eutectic alloy.

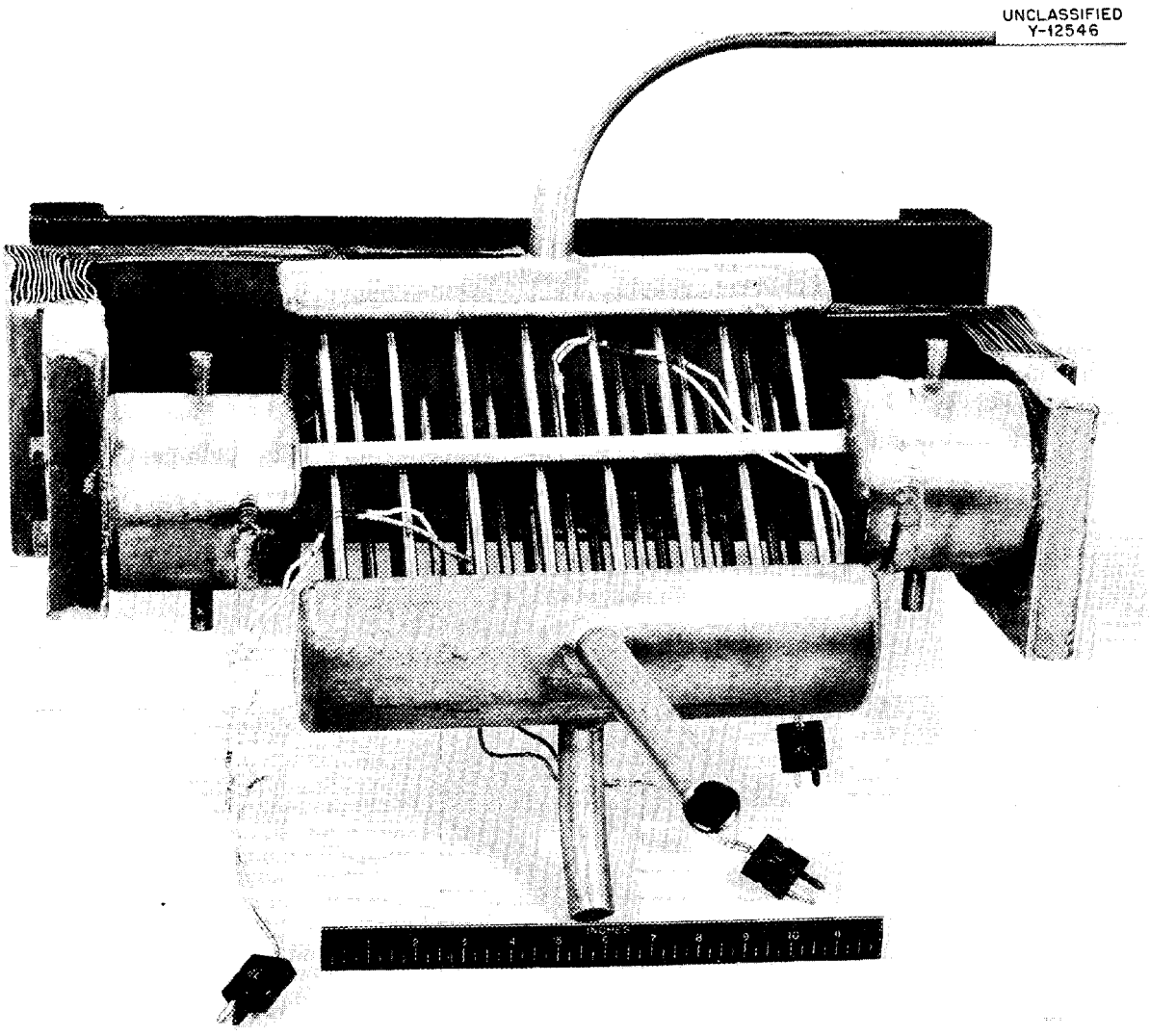

Fig. 6.6. Beryllium Test Assembly.

7. HEAT TRANSFER AND PHYSICAL PROPERTIES

H. F. Poppendiek
Reactor Experimental Engineering Division

The enthalpies and heat capacities of the ARE fuel NaF-ZrF_4-UF_4 (53.5-40.0-6.5 mole %) were determined; the heat capacity in the solid state over the temperature range 260 to 490°C was found to be 0.19 cal/g·°C, and the heat capacity in the liquid state over the temperature range 590 to 920°C was found to be 0.23 cal/g·°C. Enthalpy and heat-capacity measurements for K_3CrF_6 in the solid state were also obtained. Density and viscosity measurements were made for molten RbF-LiF (57-43 mole %); the viscosity varied from about 8 centipoises (cp) at 550°C to about 3 cp at 750°C. The thermal conductivity of molten RbF-LiF (57-43 mole %) was determined to be about 1.2 Btu/hr·sq ft (°F/ft). The thermal conductivity of solid NaF-KF-LiF (11.5-42.0-46.5 mole %) was found to be about 3 Btu/hr·sq ft (°F/ft). Electrical-conductivity measurements of molten NaOH were obtained over the temperature range 625 to 1490°F.

Additional forced-convection heat-transfer measurements of molten NaF-KF-LiF were made at higher Reynolds numbers than had previously been obtained. Some thermal-conductivity information on K_3CrF_6, a wall-deposit material, was obtained. A Lucite model of the circulating-fuel reflector-moderated reactor has been fabricated and will be used to study the hydrodynamic structure in that system. The results of a mathematical analysis of convection are presented for the case of forced flow between parallel plates which are ducting fluids with volume heat sources; this analysis is useful in estimating the temperature structure in the flow annuli of reflector-moderated reactor cores. A study has been initiated to investigate the heat-transfer and fluid-flow characteristics of a NaOH-moderated circulating-fuel reactor system.

PHYSICAL PROPERTIES MEASUREMENTS

Heat Capacity

W. D. Powers G. C. Blalock
Reactor Experimental Engineering Division

The following enthalpy and heat-capacity measurements were made with Bunsen ice calorimeters:

NaF-ZrF_4-UF_4 (53.5-40.0-6.5 mole %)
Solid (260 to 490°C)

$$H_T - H_{0°C} = -4.1 + 0.19T$$
$$C_p = 0.19 \pm 0.02$$

Liquid (590 to 920°C)

$$H_T - H_{0°C} = 34 + 0.23(5)T$$
$$C_p = 0.23(5) \pm 0.03$$

K_3CrF_6
Solid (50 to 830°C)

$$H_T - H_{0°C} = -4 + 0.22(8)T$$
$$C_p = 0.22(8) \pm 0.006$$

NaF-KF-LiF (11.5-42.0-46.5 mole %)
Solid (60 to 455°C)

$$H_T - H_{0°C} = -2.6 + 0.27T + 0.98 \times 10^{-4}T^2$$
$$C_p = 0.27 + 1.96 \times 10^{-4}T$$

In these expressions H is the enthalpy in cal/g, C_p is the heat capacity in cal/g·°C, and T is the temperature in °C. The enthalpy of K_3CrF_6 (an insoluble deposit material) is shown in Fig. 7.1. The enthalpy and heat-capacity data for NaF-KF-LiF (11.5-42.0-46.5 mole %) in the solid state correspond to a much greater temperature range than was previously reported. A copper calorimeter has been constructed that will be used to supplement the Bunsen ice calorimeters now in use. The heat content of the sample will be measured by the temperature rise of the copper housing.

Density and Viscosity

S. I. Cohen T. N. Jones
Reactor Experimental Engineering Division

Density and viscosity measurements were made on two fluoride mixtures. The viscosities of RbF-LiF (57-43 mole %) were determined with modified Brookfield and capillary viscometers, and the values varied from about 8.0 cp at 550°C to about 3 cp at 750°C. The density measurements of RbF-LiF in the molten state are represented by the relation

$$\rho = 3.39 - 0.00085T ,$$

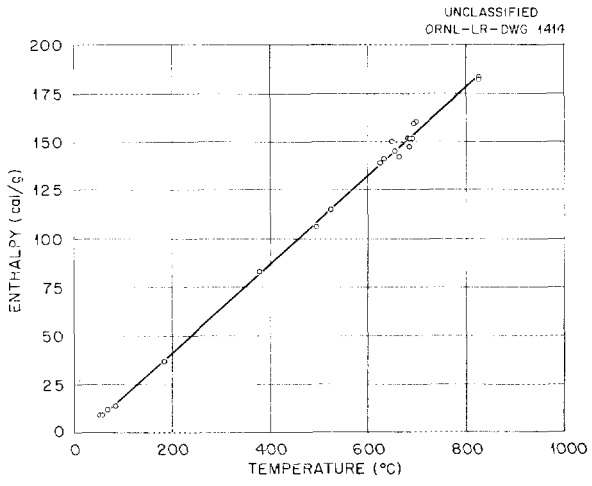

Fig. 7.1. Enthalpy-Temperature Relationship for K_3CrF_6.

where ρ is in g/cc and the temperature range is $500°C < T < 700°C$.

The density and viscosity values[1] for NaF-KF-LiF (11.5-42.0-46.5 mole %) that were determined in the early stages of the ANP Project were checked, and the recent determinations were in substantial agreement with the early ones. The viscosities for the mixture vary from about 8 cp at 500°C to about 3 cp at 750°C, and the molten densities are represented by the relation

$$\rho = 2.53 - 0.00073T \ , \qquad 600°C < T < 900°C \ .$$

A report[2] published recently lists all the density measurements that have been made on molten fluoride mixtures for the ANP Project and includes a correlation of the data that can be used to predict densities of molten fluoride mixtures of known composition.

Thermal Conductivity

W. D. Powers S. J. Claiborne
R. M. Burnett
Reactor Experimental Engineering Division

The Deem-type apparatus has been used to measure the thermal conductivity of RbF-LiF (57-43 mole %). The conductivity was determined to be 1.2 Btu/hr·sq ft (°F/ft) at an average sample temperature of about 1050°F.

A flat-plate method for determining the thermal conductivities of solid salts has been developed in which the salt is cast in the form of a slab. The heat that is passed through the sample is measured by the rise in temperature of the water that circulates through the cooling plate. The temperature drop through the sample is also measured. The conductivity may be calculated easily from this information and the physical dimensions of the slab. The preliminary thermal conductivity value obtained for NaF-KF-LiF (11.5-42.0-46.5 mole %) by using this method was about 3 Btu/hr·sq ft (°F/ft).

Additional thermal-conductivity measurements have been made on solids by using the transient cooling or heating technique. An improved method of casting nonporous spheres has been developed which involves cooling the mold from the bottom at a very slow rate. Improved methods of cooling and heating the spheres have also been developed. The preliminary thermal-conductivity value obtained by using this method on NaF-KF-LiF (11.5-42.0-46.5 mole %) in the solid state was about 2.7 Btu/hr·sq ft (°F/ft).

Electrical Conductivity

N. D. Greene
Reactor Experimental Engineering Division

A preliminary determination of the electrical conductivity of molten NaOH at temperatures of up to 1500°F has been made with the platinum conductivity cell. This determination has extended the temperature range of the electrical-conductivity measurements of NaOH to approximately 650°F higher than the maximum temperature reported in the literature. The experimental conductivity data are shown in Fig. 7.2, together with the published measurements[3] for low temperatures.

Checks on the platinum conductivity cell have been made by studying three molten salts for which conductivity values have been published. The salts investigated, together with the deviation between ORNL and literature values and the tem-

[1] ANP Physical Properties Group, *Physical Property Charts for Some Reactor Fuels, Coolants, and Miscellaneous Materials*, 3d ed., ORNL CF-53-3-261 (Mar. 20, 1953).

[2] S. I. Cohen and T. N. Jones, *A Summary of Density Measurements on Molten Fluoride Mixtures and a Correlation Useful for Predicting Densities of Fluoride Mixtures of Known Composition*, ORNL-1702 (May 14, 1954).

[3] *International Critical Tables*, vol 6, p 149.

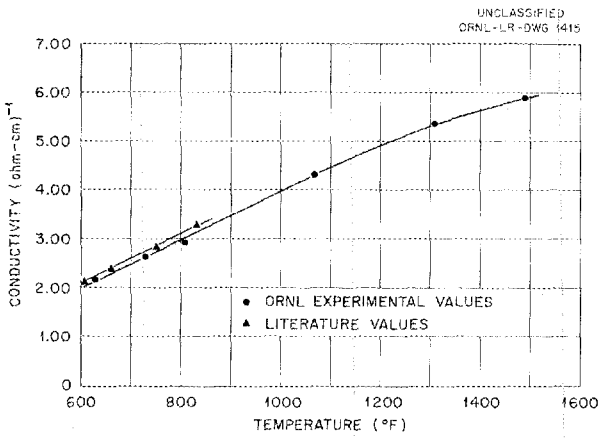

Fig. 7.2. Electrical Conductivity of Molten NaOH.

perature ranges, are listed in the following:

	Mean Deviation (%)	Temperature Range (°F)
NaOH	+2.7	625 to 835
$LiNO_3$	+4.4	534 to 862
KNO_3	−3.3	875 to 900

The measurements are difficult to make because of polarization within the cell, and therefore some alternate method of measurement has been sought. It is felt that a hemispherical graphite crucible in which it would be possible to position leads so that both current and potential measurements would be obtained simultaneously might be useful. Since the potential measurement would be independent of the degree of polarization at the current-carrying electrode and an alternating current would be used, it is estimated that good accuracy would be obtained. An attempt to verify the results of the measurements made with the platinum conductivity cell will be made with this alternate method during the coming quarter. The conductivities at various pertinent temperatures of some of the salts which are of interest to the ANP Project will also be determined.

Vapor Pressures

R. E. Moore C. J. Barton
Materials Chemistry Division

In an attempt to resolve some anomalies, observed in another laboratory,[4] in vapor pressures of some $NaF-ZrF_4$ mixtures, the method and apparatus of Rodebush and Dixon[5] have been applied to a $NaF-ZrF_4$ mixture containing 75 mole % ZrF_4. Preliminary values obtained for this material are 37, 54, 66, 74, 83, 115, and 152 mm Hg at 769, 786, 796, 805, 816, 828, and 844°C, respectively. A straight line through these values on a log P vs $1/T$ plot intersects the plot of vapor pressure of ZrF_4 at 762°C. Since the primary phase at 75 mole % ZrF_4 in this system is ZrF_4, the intersection should correspond to the liquidus temperature for the mixture, which thermal-analysis data indicate to be 755°C. The difference between the two temperatures is only slightly larger than the expected error of either method.

It was discovered that there was a consistent temperature error in the vapor pressure data given in a previous report[6] for the 50 mole % NaF–50 mole % ZrF_4 mixture. Therefore the correct pressures are lower than those given before. The corrected equation for this composition is

$$\log P\,(\text{mm Hg}) = -\frac{7425}{T(^\circ\text{K})} + 7.889 \ .$$

FUSED-SALT HEAT TRANSFER

H. W. Hoffman J. Lones
Reactor Experimental Engineering Division

Previous NaF-KF-LiF heat-transfer experiments made in systems in which no tube-wall deposits were formed were limited to rather low Reynolds numbers because of the temperature limitations inherent in the use of nickel tubes. It had been observed that molten fluorides could be contained in type 316 stainless steel for short periods of time without serious corrosion results or the formation of the insoluble fluoride deposits, such as K_3CrF_6, that are found in Inconel systems. Therefore in order to get data at higher Reynolds numbers it was decided to conduct a heat-transfer experiment of short duration in type 316 stainless steel tubes. The results of the experiment are shown in Fig. 7.3. As was to be expected when there was no wall deposit, the data fell on the curve for normal turbulent-flow for ordinary fluids, that is, the curve expressed by $j = 0.023\ Re^{-0.2}$. The

[4] H. R. Nelson and R. W. Dayton, *Progress Report for January 1954*, BMI-902 (Feb. 1954).

[5] W. H. Rodebush and A. L. Dixon, *Phys. Rev.* **26**, 851 (1925).

[6] R. E. Traber, Jr., R. E. Moore, and C. J. Barton, *ANP Quar. Prog. Rep. Dec. 10, 1953*, ORNL-1649, p 99.

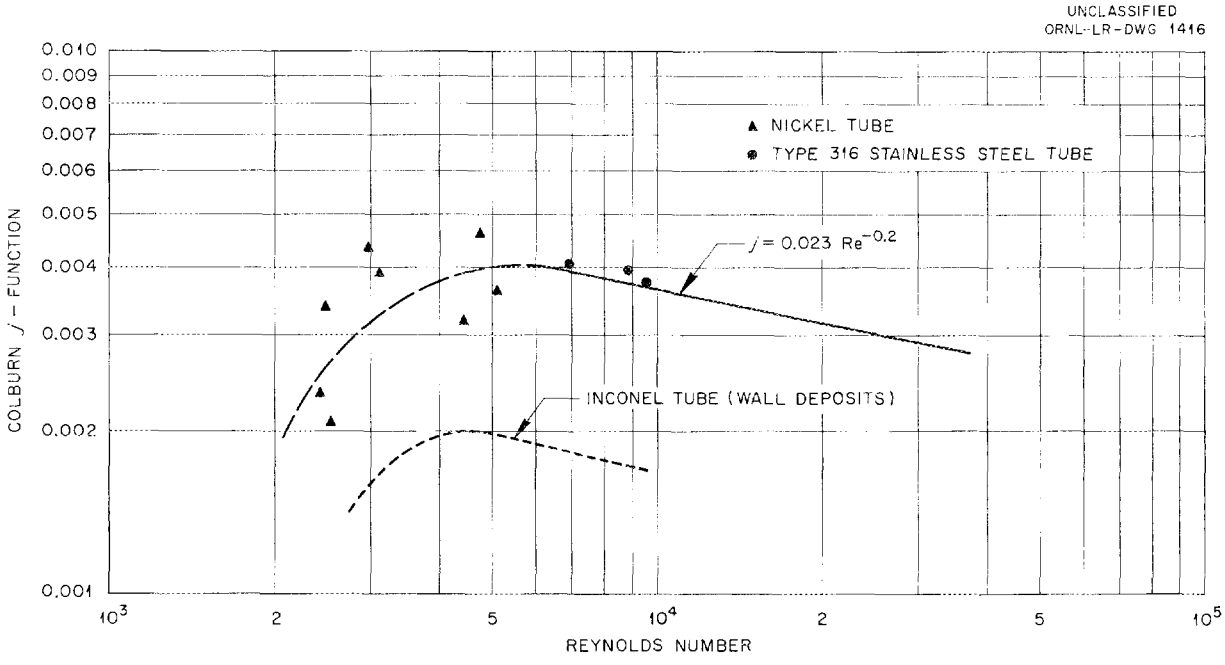

Fig. 7.3. Colburn j-Function vs Reynolds Number for Molten NaF-KF-LiF.

previously obtained nickel-tube and Inconel-tube data are also shown in Fig. 7.3.

Some preliminary determinations show the thermal conductivity of K_3CrF_6 to be about 0.13 Btu/hr·sq ft (°F/ft) for the temperature range 100 to 200°F. The salt was hydrostatically molded into the shape of a cylinder, approximately ½ in. in diameter and 4 in. in length. The density of the molded salt was 96% of the theoretical value. The cylinder was heated to a uniform temperature and then suddenly exposed to a cool air stream where it was transiently cooled. The thermal conductivity was calculated from the time-temperature measurements obtained in this experiment.

REACTOR HYDRODYNAMICS

J. O. Bradfute L. D. Palmer
G. M. Winn
Reactor Experimental Engineering Division

A Lucite model of the reflector-moderated reactor core has been fabricated. The fluid velocity distribution in the variable-cross-section flow annulus is to be determined by photographing tiny particles which will be dispersed throughout the flowing water. An improved method of increasing the light output of the Strobolume (the flashing light source) has been devised. The timing unit for the Strobolume has nearly been completed.

An investigation was made of a technique[7] for visual observation of the nature of fluid flow in transparent duct systems. It was found that the features which determined the average velocity profile, as well as the velocity fluctuations, under turbulent flow conditions could be observed. A beam of ultraviolet light was flashed through a region of the flowing fluid (containing suspended phosphorescent particles) for which the velocity profile was to be observed. The beam of phosphorescent particles generated in the flowing fluid by the ultraviolet light was slowly distorted by the flow into a curve which exactly described the fluid velocity profile. It is believed that this technique can be used to visualize flow characteristics in reactor cores.

HEAT-REMOVAL STUDY OF BSF REACTOR

D. C. Hamilton F. E. Lynch
Reactor Experimental Engineering Division

A study has been initiated for determining the heat-removal rate that can be provided by free convection in a bulk-shielding-facility type of reactor.

[7] L. D. Palmer and G. M. Winn, *A Feasibility Study of Flow Visualization Using a Phosphorescent Particle Method*, ORNL CF-54-4-205 (Apr. 30, 1954).

The problem divides naturally into two cases depending on whether or not nucleate boiling is permitted. When boiling is not permitted, the limiting fuel-plate temperature will be equal to the saturation temperature. If nucleate boiling is permitted, the exit temperature of the water may not exceed the saturation temperature.

The analysis is somewhat similar to an analysis performed on a thermal convection harp.[8] There are two distinct regions in the flow circuit of the reactor, the reactor region and the jet or stack region. The reactor region presents a problem in flow and heat transfer between parallel plates with a known but not uniform wall-heat-flux distribution. At lower reactor powers, the flow is superposed free-and-forced viscous convection. At higher powers, the Reynolds modulus may approach the lower limit for isothermal turbulent flow; in either case, the heat-transfer and friction data are not available in the literature. The manner of mixing of the jet with the surrounding pool will determine the contribution of the jet to the flow through the reactor. An accurate consideration of the jet contribution will be difficult.

HEAT TRANSFER IN CIRCULATING-FUEL REFLECTOR-MODERATED REACTOR

H. F. Poppendiek L. D. Palmer
G. M. Winn
Reactor Experimental Engineering Division

A heat-transfer analysis[9] was made for the case of forced convection between parallel plates of infinite extent, which are ducting fluids that contain uniform volume-heat sources, with heat transferred uniformly to or from the fluids through the parallel plates. The laminar and turbulent flow data in terms of dimensionless wall-fluid temperature differences are plotted in Fig. 7.4 as a function of Reynolds moduli for the case of no wall-heat transfer. If it is desired to obtain the solution for the composite case, that is, a flow system with wall-heat transfer as well as volume-heat sources, the data given in Fig. 7.4 must be superposed on the known data for the case of wall-heat transfer with no volume-heat sources. It will be noted that the data shown in Fig. 7.4 pertain to liquid metals as well as to ordinary fluids and may also be used to estimate heat transfer in annulus systems such as the reflector-moderated reactor for which inner-to-outer radius ratios do not differ significantly from unity.

A series of experiments was conducted recently to determine the influence of electrical-current flow on the hydrodynamic characteristics of a liquid flowing in a tube under both laminar and turbulent flow conditions. This problem arises in convection experiments in which the volume heat sources are generated electrically. No influence of the electrical-current flow on the hydrodynamic structure has yet been detected.

HEAT TRANSFER IN NaOH-MODERATED CIRCULATING-FUEL REACTOR

J. O. Bradfute H. F. Poppendiek
Reactor Experimental Engineering Division

A study has been initiated to determine the feasibility of a NaOH-moderated circulating-fuel reactor in terms of heat transfer and fluid flow. In such a reactor, the molten sodium hydroxide would be the moderator as well as the coolant necessary to reduce the high wall temperatures in the fuel region. Because of the corrosion difficulty that arises when NaOH is used with the typical structural materials of reactor systems that operate at temperatures above 1000°F, it is further necessary to cool the fuel-tube wall sufficiently (by forced circulation of the NaOH) to yield a NaOH-wall interface temperature of below 1000°F. Therefore it is necessary to know whether this cooling can be accomplished with NaOH with reasonable pumping powers and pressure drops. Some preliminary heat- and momentum-transfer analyses have been made for the case in which fuel circulates through tubes that are force-cooled by molten NaOH which circulates in a direction parallel to that of the fuel; the number of tubes was varied in the analyses. The preliminary results suggest that the pumping powers and pressure drops are not prohibitively high. Further calculations on multitube, as well as annulus and channel, systems are being made.

[8] D. C. Hamilton, F. E. Lynch, and L. D. Palmer, *The Nature of the Flow of Ordinary Fluids in a Thermal Convection Harp*, ORNL-1624 (Feb. 23, 1954).

[9] H. F. Poppendiek and L. D. Palmer, *Forced Convection Heat Transfer Between Parallel Plates and in Annuli with Volume Heat Sources Within the Fluids*, ORNL-1701 (May 11, 1954).

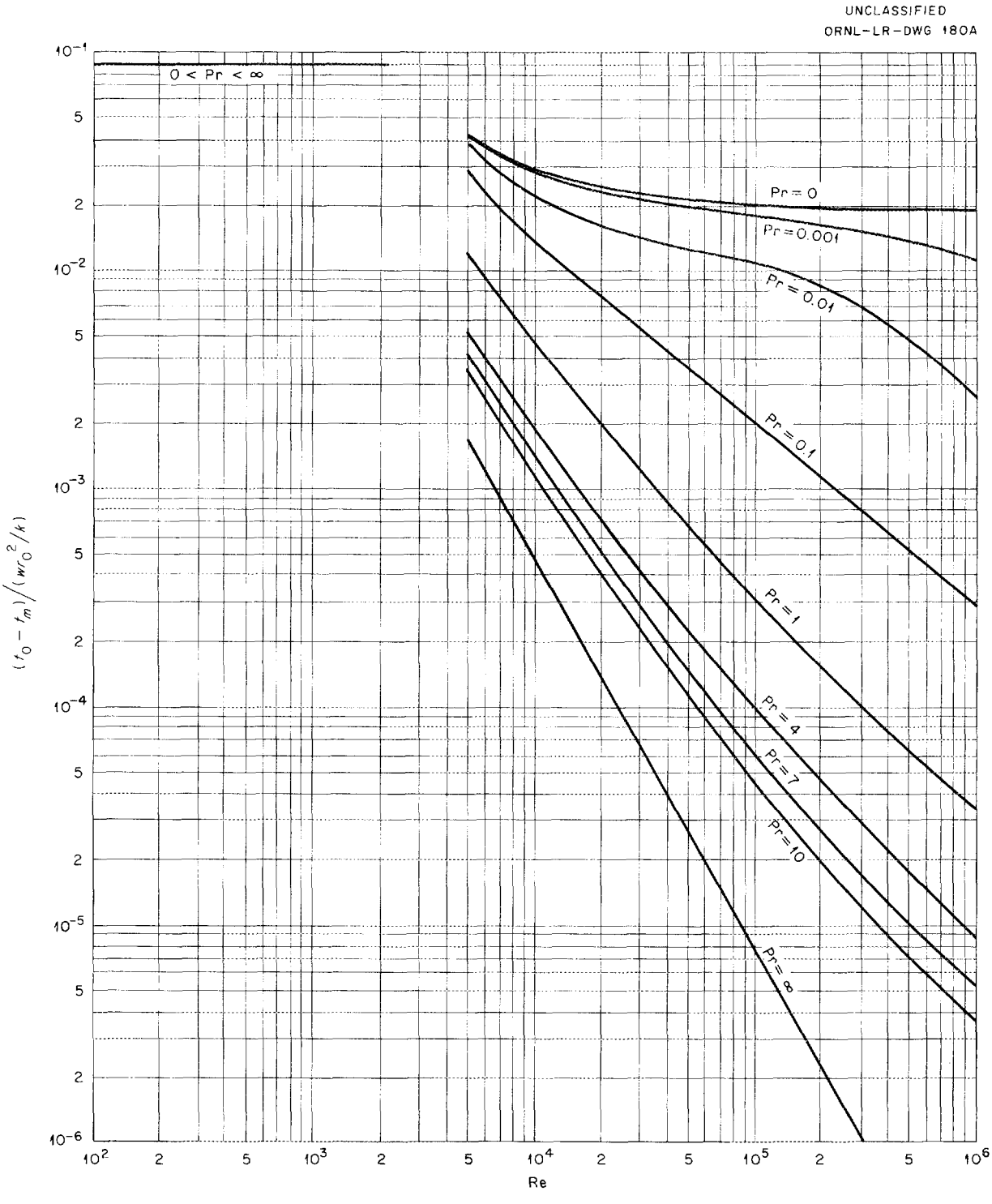

Fig. 7.4. Dimensionless Differences Between Wall and Mixed-Mean Fluid Temperatures as Functions of Reynolds and Prandtl Moduli for a Parallel Plate System (Walls Insulated).

8. RADIATION DAMAGE

J. B. Trice
Solid State Division
A. J. Miller
ANP Division

The program of irradiating fused-salt fuels in the MTR continued with mixtures containing UF_3- and UF_4-bearing fuels. The fuel-Inconel interface temperature is being maintained at more nearly 1500°F than in previous tests with UF_4 fuels. A re-examination was made of a group of Inconel capsules from the earlier runs along with a study of the temperature control system used and the thermal histories. It was concluded that in most capsules the interface temperature was in the region of 100°F higher than the desired 1500°F and that 2 to 4 mils of intergranular corrosion occurred. Excessive grain growth and deep penetration of the Inconel occurred only in a few capsules and those capsules had been heated to much higher temperatures.

The first in-pile circulating fuel loop was installed in a horizontal beam hole of the LITR but difficulties developed before start-up of the reactor which caused the loop to be removed for inspection. Development continued on smaller loops for insertion in LITR and MTR beryllium A-pieces.

Creep-test equipment was revised to permit creep testing in the MTR, and development of in-pile stress-corrosion equipment continued. Metallographic studies were made for Pratt & Whitney Aircraft Division on sandwich-type UO_2–type 347 stainless steel fuel elements irradiated in the MTR.

RADIATION STABILITY OF FLUORIDE FUELS

G. W. Keilholtz
J. G. Morgan
H. E. Robertson
C. C. Webster
M. T. Robinson
W. R. Willis
W. E. Browning
M. F. Osborne
Solid State Division

As previously reported,[1] some of the Inconel capsules containing fluoride fuel which were irradiated in the MTR were found to have developed large Inconel grains and deep intergranular cracks. Since such corrosion effects indicated excessive heating, a re-examination of the thermal conditions that had been imposed on the capsules during the irradiations was undertaken. Temperature control had been based on data from several thermocouples welded to the outside surface of the capsule and was aimed at maintaining this outside temperature at a level that would provide a 1500°F fuel-Inconel interface temperature.

In order to evaluate the accuracy of the control method, a series of tests was made to determine the relationship between the temperature of the outside surface of the capsule as indicated by a thermocouple to the actual wall temperature in an equivalent portion of the capsule that was unperturbed by the presence of a thermocouple. The indicated temperature could have low values because of the thermocouple junction being raised slightly above the surface of the capsule and because of conduction of heat by the cooling air stream from the very small amount of uninsulated exposed wire. A review was also made of the chart temperature records of the experiments to detect runs in which the temperature had risen to experimentally undesirable magnitudes.

A bench-test apparatus used to mock up the conditions of the MTR capsule tests is shown schematically in Fig. 8.1. The electrically heated test section which simulates the capsule consists of a 1-in. section of an actual Inconel fuel capsule. The annulus for cooling air corresponds to that used in the reactor, and the pyrex portion serves as a sight glass to permit accurate temperature measurements with an optical pyrometer at a point 180 deg from the thermocouple being tested.

Typical data from one of the 30 thermocouples tested are shown for three different airflow rates in Fig. 8.2, in which T_S is the unperturbed surface temperature determined with the pyrometer at any position along the length of the capsule. On each of the three curves the temperature indicated by the thermocouple T_I is shown at its contact position. For airflow rates of 189, 220, and 250 fps, it can be seen that the thermocouple readings are low by 75, 88, and 105°F. The maximum difference between T_S and T_I for 30 thermocouples was 200°F

[1] G. W. Keilholtz *et al.*, *ANP Quar. Prog. Rep. Mar. 10, 1954*, ORNL-1692, p 102.

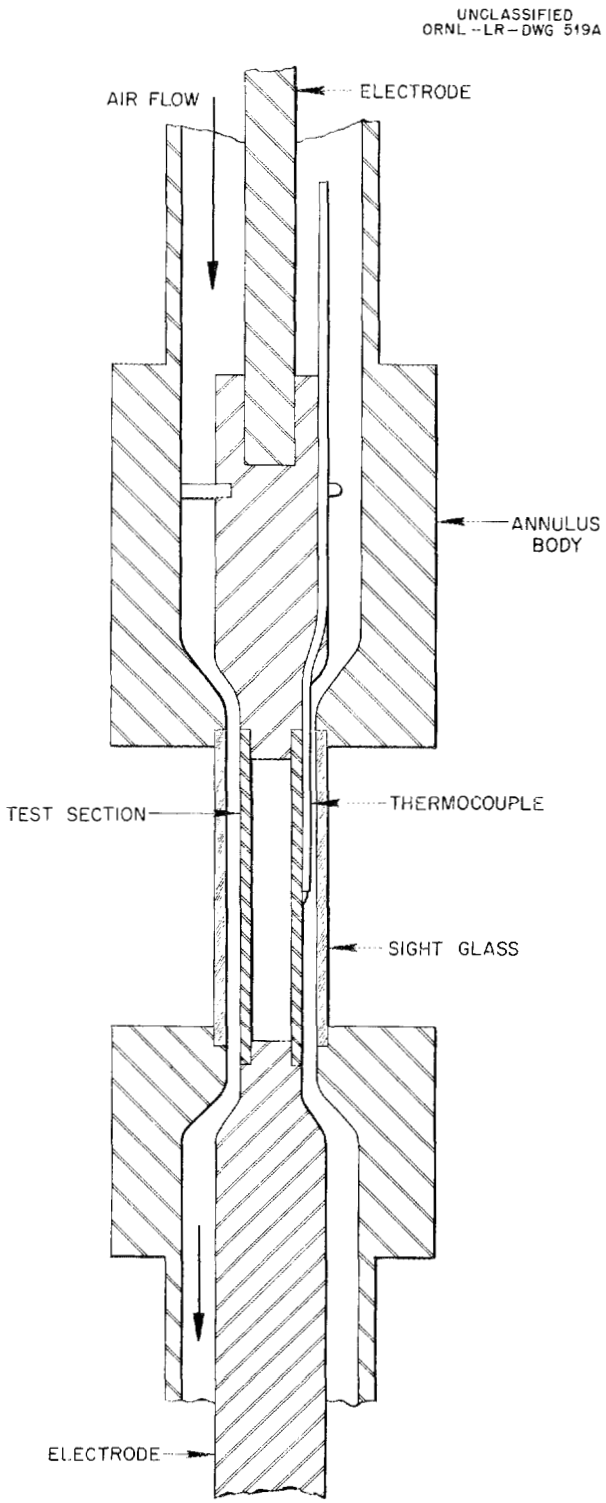

Fig. 8.1. Thermocouple Test Apparatus.

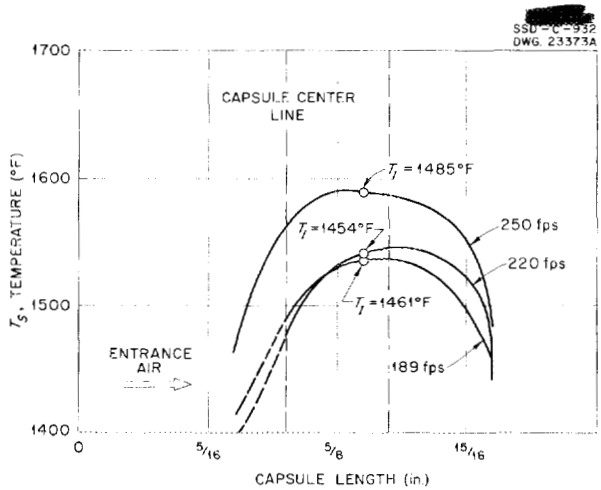

Fig. 8.2. Temperature Measurements on MTR Capsule Mock-up.

and the average difference at the medium airflow rates used in the reactor was 100°F.

This error, together with several others of lesser magnitude, led to the conclusion that the temperature-control system employed in the reactor experiments tended to produce fuel-Inconel interface temperatures averaging 1620°F and never higher than 1750°F at the hottest point of the capsule rather than the desired 1500°F. These findings are in agreement with calculations made by H. F. Poppendiek prior to the test experiments.

Temperature record charts of the 13 MTR capsules irradiated so far in the MTR were examined. In every instance of deep intergranular corrosion and abnormally large grains, the temperature pattern for the fuel-Inconel interface was found to be either too high or too unsteady. For the cases in which the capsule temperature-time profile was within the limits originally set for the experiment, depth of attack (2 to 4 mils) and grain growth were not grossly different from those observed in bench tests at 1500°F. The pattern of corrosion was, however, still intergranular rather than that consisting of subsurface voids as in the case in out-of-pile tests.

An additional aid to interpretation of results from the in-pile capsule tests was afforded by a study of the effect of high temperatures on the grain structure of Inconel. Samples of capsule material were subjected to temperatures of 1800 to 2350°F for various periods of time. Metallographic exami-

nations of these samples are now being made. Preliminary results indicate that large grains may be found in Inconel which has been heated for periods of time of less than 8 min duration at temperatures of the order of 2100°F.

The Inconel capsules presently being irradiated in the MTR contain both UF_3- and UF_4-bearing fuel mixtures. The recent indications in out-of-pile tests that the use of UF_3 might result in less corrosion suggested in-pile testing of UF_3-bearing mixtures. Temperatures of the capsules are being carefully controlled so that the Inconel-fuel interface temperature will remain approximately 1500°F throughout each test.

LITR FLUORIDE-FUEL LOOP

W. E. Brundage
C. D. Baumann
F. M. Blacksher
C. Ellis
M. T. Morgan
A. S. Olson
W. W. Parkinson
O. Sisman
R. M. Carroll
Solid State Division

The design of fluoride-fuel loops for use in the LITR horizontal-beam facility was described in previous reports.[2] The fabrication of components for three of these loops was completed. The first loop was inserted in the LITR but was removed before start-up of the reactor because of a leak in the fuel system. All fuel material was retained within the loop apparatus. Examination to determine the cause of the breakdown is in progress.

Development continued on in-pile pumps for loops to be operated in the horizontal-beam facilities of the LITR and MTR (cf., Sec. 2, "Experimental Reactor Engineering"). Several models are being constructed. A smaller uranium investment and less dilution of fission products would be attained by using such pumps in place of the present pumps which are operated at the reactor face.

IN-PILE STRESS CORROSION AND CREEP

W. W. Davis
N. E. Hinkle
J. C. Wilson
J. C. Zukas
Solid State Division

Since intergranular corrosion of Inconel by molten fused salts of the type $NaF\text{-}ZrF_4\text{-}UF_4$ has been observed in bench tests in which a strain was introduced into the Inconel, it is conceivable that thermal stress may be associated with the intergranular type of attack seen in in-pile tests. To investigate this possibility, an in-pile stress-corrosion apparatus for the Inconel-fused salt systems was designed. Several prototypes of this apparatus are being bench tested.

Creep tests of Inconel in the ORNL Graphite Reactor and in the LITR under conditions pertinent to ANP reactor designs have been reported previously. Apparatus for tests in the higher flux of the MTR is being built. Much of the mechanical assembly is completed and the unit is almost ready for wiring. It is planned to use Bourdon tube extensometers rather than thermal-expansion (bimetal) units since the former are in a more advanced stage of evolution.

REMOTE METALLOGRAPHY

A. E. Richt
E. Schwartz
W. Parsley
R. Ramsey
M. J. Feldman
Solid State Division

Solid, sandwich-type, UO_2–type 347 stainless steel fuel elements irradiated in the MTR were submitted to the Laboratory by Pratt & Whitney Aircraft Division for metallographic examination. These studies, which were at first intended to yield information of interest only to the supercritical-water-cycle aircraft reactor, are also related to certain power-package reactor designs because of the similarity between the two types of fuel elements both in materials and in required operating conditions. Both reactors have operating pressures of the order of 5000 psi, temperatures in the range of 300 to 700°F, and high power generation rates. Both fuel element prototypes are made as solid sandwich-type elements clad with stainless steel or Inconel.

A typical Pratt & Whitney fuel element test is run with the element immersed in water in a sealed capsule at one of a series of fixed temperatures ranging from 100 to 700°F and with pressures of 3000 to 5000 psi. The power density of the fuel runs was as high as several thousand watts per cubic centimeter in the MTR. Results from the five capsules examined so far provide information about the effects of temperature and irradiation on core density changes, bonding of core to cladding, core hardness, and corrosion of the stainless steel

[2] W. E. Brundage *et al.*, *ANP Quar. Prog. Rep. Mar. 10, 1954*, ORNL-1692, p 105.

cladding. No measurable core density changes have been found and general corrosive attack on the cladding is absent. Hardness measurements taken on the core indicate a dependence between particle size and hardness change. Cores with particles less than 3 μ in diameter show greater hardness changes than do those in the 15- to 44-μ range. In general, it can be said that hardness changes, expressed in DPH units, as great as ratios of 2 to 3 occur for irradiation periods of several hundreds of hours and for test temperatures as high as 700°F. Cracking of the core in bending tests (1.5-in. radius bend) was found only in the less than 3-μ core samples. It is expected that this work will be completed during the next several months.

9. ANALYTICAL STUDIES OF REACTOR MATERIALS

C. D. Susano
Analytical Chemistry Division
J. M. Warde
Metallurgy Division
R. Baldock
Stable Isotope Research and Production Division

Research and development in analytical chemistry for the ANP Project was concentrated on the problem of separating UF_3 from UF_4 in $NaZrF_5$-base fuels and fuel solvents. Methods were investigated for the conversion of the fluorides to chloride salts and the simultaneous extraction of the chlorides into nonaqueous solutions. Boron trichloride in a solution of dioxane appeared to be promising for this purpose, since UCl_4 is soluble in dioxane, whereas UCl_3 is essentially insoluble. The separation is also feasible in the presence of chromium chlorides. Chromium dichloride is soluble in dioxane in contrast to $CrCl_3$, which is insoluble. However, the conversion reaction was found to proceed slowly.

A method was devised for the determination of oxygen in $NaZrF_5$-base fuels and fuel solvents in which the oxides react with anhydrous hydrogen fluoride to produce water, quantitatively; the water materially increases the conductivity of the hydrofluoric acid. It has been calculated that the conductivity of anhydrous hydrogen fluoride is doubled by the addition of 1 ppm of water. In the study of the oxidation of trivalent uranium by hexavalent uranium it was shown that the competitive oxidation with hydrogen ion could not be completely eliminated. Stability tests of trivalent uranium in hydrochloric acid solutions were conducted. Although evaluation of the data is not complete, potentiometric measurements indicated that the transition in color from purple to green, which is considered to be evidence of oxidation, is not accompanied by corresponding changes in potential. A 1% aqueous solution of the tetrasodium salt of ethylenediaminetetraacetric acid effectively removed a film of calcium metasilicate from Inconel. No evidence of corrosion was found by chemical tests. The sulfur content of natural gas was determined to be 0.5 mg/cu ft of gas.

Petrographic examination of NaF-ZrF_4-UF_4 fuels reduced with metallic zirconium, with metallic uranium, or with hydrogen has shown that the predominant phase in the reduction complexes obtained is always a solid solution of reduced U^{4+} in $Na_9Zr_8F_{41}$. In the RbF-UF_3 system, there appears to be a compound, 3 RbF-UF_3, which is tan and isotropic, with an $n = 1.438$. The NaF-UF_3 system contains a compound of unknown composition which is lavender and uniaxially positive, with refractive indices of approximately 1.552. Examinations of melts in the NaF-CrF_3 system were made, and four compounds were observed.

ANALYTICAL CHEMISTRY OF REACTOR MATERIALS

J. C. White
Analytical Chemistry Division

Oxidation States of Chromium and Uranium in $NaZrF_5$-Base Fuels

A. S. Meyer, Jr. D. L. Manning
W. J. Ross
Analytical Chemistry Division

In extensive studies, covered in previous reports,[1] no solvent has been discovered that will selectively dissolve UF_3 or UF_4 from $NaZrF_5$-base fuels. Certain organic solvents preferentially dissolved UCl_4 from UCl_3, but the equilibrium of the reaction

$$U^{IV} + Cr^{II} \longrightarrow U^{III} + Cr^{III}$$

could conceivably be altered during the conversion of the metallic fuel components by the method of fusing the sample with $NaAlCl_4$. Therefore, an attempt is being made to dissolve the UCl_4 into an organic solvent during the conversion of the fuel to the chloride salts.

Dioxane, which has been reported to dissolve UCl_4 from UCl_3,[1] was selected as the most promising solvent. It may offer an additional advantage in that aliphatic ethers are reported[2] to

[1] J. C. White *et al.*, *ANP Quar. Prog. Rep. Mar. 10, 1954*, ORNL-1692, p 107 ff.

[2] N. V. Sidgwick, *The Chemical Elements and Their Compounds*, Vol. II, p 1024, Oxford University Press, Oxford, 1950.

dissolve $CrCl_2$ from $CrCl_3$ to yield stable solutions which are void of reducing power. Thus, if the chlorination of the sample could be carried out in the presence of dioxane, UCl_4 and $CrCl_2$ would be dissolved, while UCl_3 and $CrCl_3$ would remain in the residue. It is hoped that the rate of reaction between the solid chlorides is negligibly slow at room temperature.

Preliminary tests were carried out by stirring 25-mg samples of UF_3, UF_4, $NaZrF_5$, and $NaZrF_5$-UF_4 in solutions of aluminum chloride in dioxane for periods of 4 to 24 hr. Visual observations and qualitative tests showed no evidence of dissolution of any of these samples. Similar negative results were obtained when the tests were repeated with solutions of aluminum chloride in ethyl ether, tetrahydrofuran, and benzene, respectively.

Thermodynamic calculations indicated that BCl_3 is superior to $AlCl_3$ as the reagent for the metathetical chlorination of the fluorides of uranium, chromium, and zirconium. In qualitative tests, 25-mg samples of UF_4 and $NaZrF_5$-UF_4 fuel were not completely dissolved after 16 hr of stirring in a solution of dioxane that had been saturated with BCl_3. When UF_4 was stirred with liquid BCl_3 at 0°C, there was no apparent dissolution of the sample. Analysis of the residue for chloride indicated that the reaction

$$4UF_4 + 3BCl_3 \longrightarrow 4UCl_4 + 3BF_3$$

was only about 20% complete. Since the free-energy change of this reaction is −110 kcal, it appears that a slow reaction rate is responsible for the incomplete dissolution of the samples. Attempts were made to increase the rate of reaction by treating the UF_4 and the fuel samples with BBr_3 at reflux temperatures of 91°C. Quantitative results of these experiments are not yet available, but portions of the unreacted samples were visible after refluxing for 3 hr. The reaction appeared to be accelerated by addition of $AlCl_3$ to the BBr_3.

When 60 mg of UF_4 was stirred at room temperature for 6 hr with 60 ml of dioxane, which had been saturated with BCl_3, about 25% of the salt dissolved to form a green solution. The concentration of uranium in solution did not increase significantly when aluminum chloride was added and the stirring was continued for 90 min. No tests of the solubilities of CrF_2 and CrF_3 have yet been carried out.

Since this method is the only approach which appears to offer possibilities of the separation of tetravalent uranium from a fuel containing another element for which the oxidation potential is near that of the $U^{3+} \longrightarrow U^{4+}$ couple, efforts will be made to accelerate the reaction to rates suitable for analytical applications. Because ethereal solutions of BCl_3 are decomposed by heating, it will probably be necessary to find a catalyst for the chlorination reaction. Experiments are also being carried out to determine whether UCl_4 may be sublimed by heating the fuels in an atmosphere of BCl_3.

Determination of Oxygen in $NaZrF_5$-Base Fuels

A. S. Meyer, Jr. J. M. Peele
Analytical Chemistry Division

Studies have been made to determine whether microgram quantities of oxygen in $NaZrF_5$-base fuels can be determined by measuring the water generated by the reaction of the metallic oxides with anhydrous hydrofluoric acid. Calculations of the free energies for the reactions of the type

$$M_2O_3 + 6HF\ (liquid) \longrightarrow 2MF_3 + 3H_2O\ (liquid)$$

have been carried out for the oxides which might be present in $NaZrF_5$-base fuels. These calculations indicate that the reaction is quantitative for the following oxides: ZrO_2, Cr_2O_3, Fe_2O_3, UO_2, NiO, and Na_2O.

The conductivity of hydrogen fluoride is known to be very sensitive to traces of water. Literature values[3] for the equivalent conductivity of water in hydrogen fluoride were used for calculations which showed that the conductivity of anhydrous hydrofluoric acid is doubled by the addition of 1 ppm of water.

An apparatus is being constructed with which it will be possible to measure the changes in conductivity of hydrofluoric acid that result from the water produced by the fluorination reaction of oxides in the fuel samples. The apparatus includes a drying still, a reaction vessel, and a fluorothene conductivity cell. Provisions can be made for carrying out the reaction with liquid hydrofluoric acid at room temperature or with the gaseous reagent at elevated temperatures.

[3] J. H. Simons, *Fluorine Chemistry*, Vol. I, p 240, Academic Press, New York, 1950.

Oxidation of Trivalent Uranium by Hexavalent Uranium

A. S. Meyer, Jr. D. L. Manning
Analytical Chemistry Division

Experiments were continued on the oxidation of trivalent uranium by the uranyl ion UO_2^{++} according to the reaction

$$2U^{3+} + UO_2^{++} + 4H^+ \longrightarrow 3U^{4+} + 2H_2O \ .$$

In previous tests[1] the extent of the reaction was determined by measuring polarographically the concentration of the unreacted uranyl ion. This measurement can also be made by titrating the U^{4+} formed with the ceric ion Ce^{4+}. Several tests were conducted in which known amounts of UCl_3 were added to 100 ml of 0.01 *N* uranyl acetate under varying conditions of acidity and temperature. After dissolution of the UCl_3, the concentration of the U^{4+} was determined by titrating with 0.1 *N* Ce^{4+}. The end point was obtained potentiometrically. The solutions were swept thoroughly with helium and titrated under an inert-gas blanket.

Quantitative oxidation with the uranyl ion was not achieved in any of the tests. Indeed, when solutions more acidic than 1 *N* were used as solvent media, evolution of hydrogen was observed. The reaction is favored, however, when the uranium is added as the chloride instead of as the fluoride. This is probably due to the greater dissolution rate for UCl_3 in acid (several minutes) as compared with the slow dissolution rate (several hours) for UF_3 in this medium.

Efforts to eliminate the competitive reaction for the oxidation of trivalent uranium in aqueous solutions,

$$2U^{3+} + H^+ \longrightarrow U^{4+} + \tfrac{1}{2}H_2 \ ,$$

have to date been unsuccessful. Future work will involve investigation of possible nonaqueous systems for the oxidation by uranyl ion.

Stability of Trivalent Uranium in Hydrochloric Acid Solutions

A. S. Meyer, Jr. W. J. Ross
D. L. Manning
Analytical Chemistry Division

Katz and Rabinowitch[4] stated that the stability of UCl_3 is greater in hydrochloric acid than in water and reported a "characteristic" purple color for the trivalent ion. An investigation of the stability of trivalent uranium in hydrochloric acid media was made to ascertain the feasibility of titrating U^{3+}. The potential of a solution of UCl_3 in 1.0 *N* HCl at 0°C was followed with a platinum, calomel electrode system. The initial potential upon dissolution was +250 mv vs S.C.E., and the potential decreased only 15 mv in 10 min. No evidence of a purple color was observed in this experiment; the solution turned green upon dissolution.

The experiments were repeated with concentrated hydrochloric acid at both 0 and −20°C. In both cases, instantaneous formation of a purple-colored solution occurred, and the purple color remained for 10 to 20 min before it changed to green. The purple color remained longest in the solution tested at the lower temperature. The initial potential in all tests was of the order of +150 mv, and the potential did not change appreciably during the transition in color from purple to green. The potential was essentially constant at +150 mv for 30 min. The constancy of the potential of these solutions contradicts the usually accepted hypothesis that the change in color from purple to green represents oxidation to the U^{4+} state. Some quantitative data were obtained on the concentrations of tri- and tetravalent uranium in these solutions by titration with ceric ion. In 0.1 *N* HCl solutions, two distinct breaks in the potential curve were noted, while only one break was observed in concentrated acid solutions. The data have not yet been thoroughly evaluated. The anomaly of the change in color of the solutions without an accompanying change in potential will be investigated.

Removal of Film from Inconel Tubing

J. C. White
Analytical Chemistry Division

The tetrasodium salt of ethylenediaminetetraacetic acid was tested as a possible reagent for removing a film, probably calcium metasilicate, which was found to be deposited upon the walls of Inconel tubing following a wash with a detergent Conklene. A 1% solution of the reagent in water, heated to 75 to 80°C, effectively removed the film from a specimen of Inconel in a few minutes. The metal had a bright finish after it was rinsed with water. Chemical analysis of the reagent solution

[4] J. J. Katz and E. Rabinowitch, *The Chemistry of Uranium*, p 458, McGraw-Hill, New York, 1951.

after contact for 60 hr at 75°C with Inconel showed less than 1 ppm of chromium and nickel.

Determination of Sulfur in Natural Gas

G. Goldberg
Analytical Chemistry Division

A determination was made of the sulfur content of the natural fuel gas received at the Y-12 Plant because it is planned to use natural gas as a source of heat in future corrosion tests. The Referee[5] method was used in which the gas is burned in an ammonia-rich atmosphere and the condensable gases are collected in a tower filled with glass balls and ammonium carbonate. The reaction is

$$SO_2 + 2NH_3 + H_2O \longrightarrow (NH_4)_2SO_3 .$$

The solution of ammonium sulfite is oxidized to sulfate, and the sulfur is determined as barium sulfate. The sulfur content was found to be 0.5 mg/cu ft of gas, which is equivalent to 0.8 grain per 100 cu ft. This concentration is essentially the same as the sulfur concentration (1 grain of sulfur per 100 cu ft) of the propane which is received at the Y-12 Plant.

PETROGRAPHIC INVESTIGATIONS OF FLUORIDE FUELS

G. D. White T. N. McVay, Consultant
Metallurgy Division

With the shift in emphasis to reduced fuels, more effort was devoted to the determination of the optical properties of compounds containing UF_3. In NaF-ZrF_4-UF_4 fuels reduced with metallic zirconium, with metallic uranium, or with hydrogen, the predominant phase in the reduction complexes obtained is always a solid solution of reduced U^{4+} in $Na_9Zr_8F_{41}$. The color of this complex varies from greenish-yellow, to greenish-tan, to a brilliant yellow. The optic figure remains the same as that for unreduced solid solution, but there is a definite lowering of the refractive indices. Evidently the amount of optic change in the crystal depends upon the amount of reduction. In addition to the reduced solid solution, minor amounts of $UF_3 \cdot 2ZrF_4$, which is orange, uniaxially positive, and has refractive indices of approximately 1.55, and an olive-drab phase, which is pleochroic with refractive indices of about 1.54, are found. The composition of the olive-drab phase is unknown. Sometimes a trace of an isotropic yellow phase with $n = 1.44$ is present.

In the RbF-UF_3 system, there appears to be a compound, $3RbF \cdot UF_3$, which is tan and isotropic, with an $n = 1.438$. The NaF-UF_3 system contains a compound which is lavender and uniaxially positive, with refractive indices of approximately 1.552. The composition of this compound is not known.

Examinations of melts in the NaF-CrF_3 system were made and four compounds were observed. The compound Na_3CrF_6 was previously reported as isotropic and green, with $n = 1.411$. In compositions with high CrF_3 content, two phases were present. The predominant phase was pleochroic, with the fast direction yellow-green and the slow direction blue-green, uniaxially positive, with $O = 1.452$ and $E = 1.460$, and polysynthetically twinned. A second phase that was present in smaller amounts was green and biaxially negative, with a small optic angle and high dispersion. It had a moderate birefringence, and its refractive indices were near 1.52. A third phase was present in melts with compositions near 50% NaF–50% CrF_3. It was yellow-green and uniaxially negative, with $O = 1.444$, and it had an estimated birefringence of 0.008.

The optical properties of the several compounds that have been synthesized were compiled and published in an ORNL report.[6]

SUMMARY OF SERVICE ANALYSES

J. C. White W. F. Vaughan
C. R. Williams
Analytical Chemistry Division

Analyses of samples from corrosion tests of the $NaZrF_5$-base fuel continued to be the major portion of the work in the service laboratory. Samples of fuel preparations containing mixtures of UF_3 and UF_4 were received. In addition to the determinations for the corrosion products iron, nickel, and chromium, the concentrations of UF_3 and UF_4 were determined. The method[7] for hydrogen evolution

[5] L. M. Dennis and M. L. Nichols, *Gas Analysis*, p 359, MacMillan, New York, 1929.

[6] T. N. McVay and G. D. White, *The Optical Properties of Some Inorganic Fluoride and Chloride Compounds*, ORNL-1712 (May 5, 1954).

[7] D. L. Manning, W. K. Miller, and R. Rowan, Jr., *Methods of Determination of Uranium Trifluoride*, ORNL-1279 (Apr. 25, 1952).

has been used for the determination of UF_3, and following the determination of total uranium, the content of UF_4 is calculated from the difference in concentration between total uranium and UF_3. Samples from corrosion tests of prospective future fuels which consist of fluorides of sodium, lithium, and potassium or rubidium were also analyzed.

During this quarter the laboratory received 1163 samples and reported 1060 which involved 9357 determinations (Table 9.1).

TABLE 9.1. SUMMARY OF SERVICE ANALYSES REPORTED

	NUMBER OF SAMPLES	NUMBER OF DETERMINATIONS
Reactor Chemistry	610	4435
Experimental Engineering	370	4116
Fuel Production	64	671
Miscellaneous	16	135
	1060	9357

Part III

SHIELDING RESEARCH

10. LID TANK FACILITY

C. L. Storrs
GE-ANP
G. T. Chapman J. M. Miller D. K. Trubey
Physics Division
J. B. Dee
Pratt & Whitney Aircraft Division

The Lid Tank Facility (LTF) has been used primarily for studying special attenuation problems which arise in aircraft shield design. One of these studies which is of interest for crew-shield design has been the penetration of slant-incident neutrons through a hydrogenous shield. In another study, comparison was obtained of secondary (neutron-induced) gamma-ray production in lead and in bismuth.

SLANT PENETRATIONS OF NEUTRONS THROUGH WATER

G. T. Chapman
Physics Division

The experiments for determining the slant penetration of fission neutrons through water have been continued at the LTF. In a previous experiment[1] the neutron flux at the end of the duct was low and it was possible to make measurements with only small amounts of water between the detector and the duct. For the present work, a new duct, larger in diameter and shorter in length (Fig. 10.1), was used, and the flux was increased to the extent that measurements could be made 45 cm from the end of the duct. The distribution of the fast-neutron dose around the end of the duct is plotted in Fig. 10.2.

The dose was integrated along planes at different slant thicknesses (t_s) of water and at angles (α_i) of 0, 30, and 60 deg to the incident flux. The results are given in Fig. 10.3. Owing to the large size of the source, the distance to the integration plane is not well defined at other than 0 deg, and therefore the relative magnitudes of the curves are in some doubt; however, the slopes are probably significant.

The observed relaxation length for the 0- and 30-deg measurements was 7.2 cm. For the incident angle of 60 deg, the relaxation length increased from 7.8 to 12.5 cm as the slant thickness increased. This increase in relaxation length is presumably due to the "short-circuiting" effect, that is, the scattering of neutrons in a direction which permits them to penetrate the shield along a nearly normal path rather than along a slant path.

[1] C. L. Storrs *et al.*, *ANP Quar. Prog. Rep. Dec. 10, 1953*, ORNL-1649, p 120.

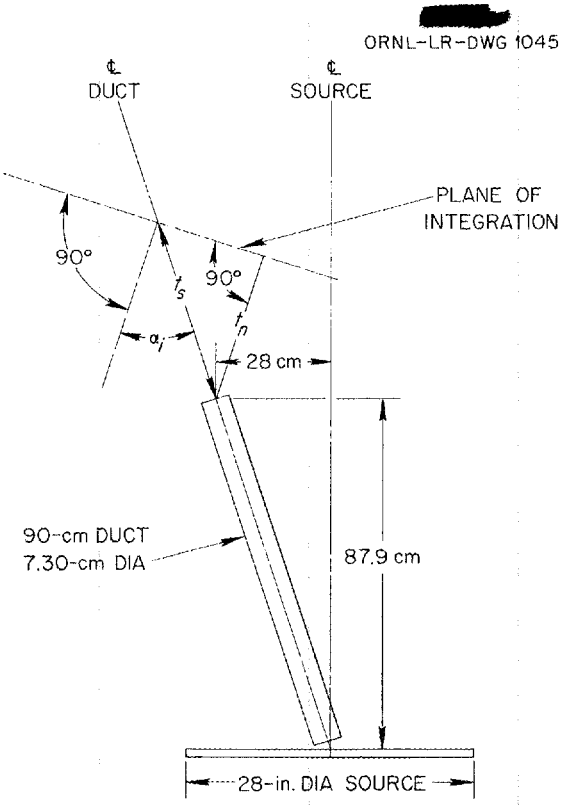

Fig. 10.1. Duct Arrangement for Slab Penetration Experiment.

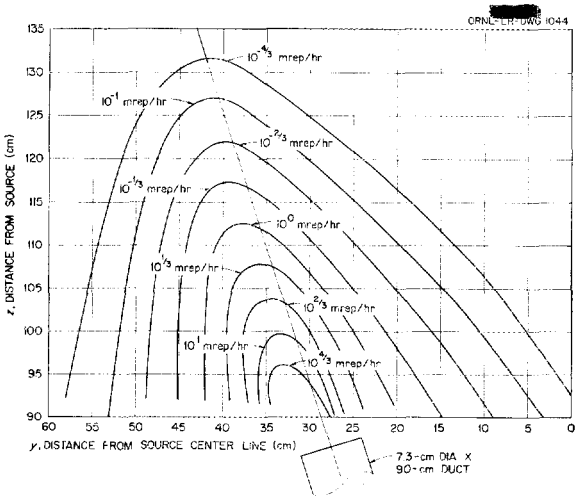

Fig. 10.2. Fast-Neutron Dose Distribution Beyond End of Duct.

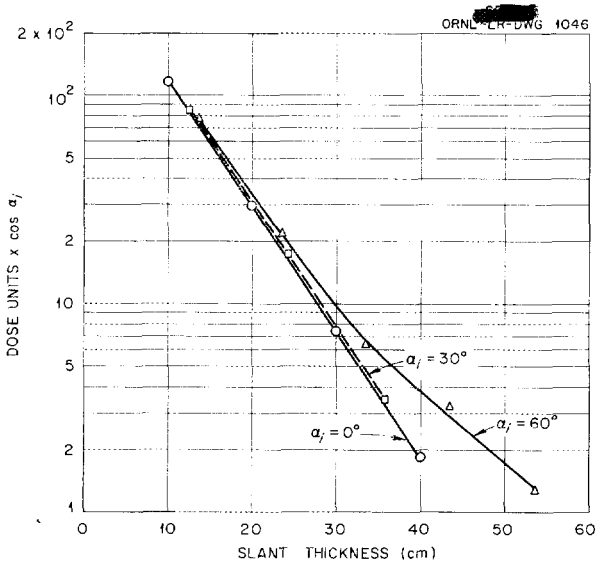

Fig. 10.3. Slant Penetration of Fast Neutrons in Water.

SECONDARY GAMMA-RAY STUDY

D. K. Trubey
Physics Division

A study of secondary gamma-ray production in materials considered for use as gamma-ray shields has been undertaken at the LTF. Measurements have been made behind 6 in. of lead or bismuth placed in borated water (1.1 wt % boron) at various distances from the fission source plate (Fig. 10.4). The 6-in. thicknesses of metal amounted to 145 g/sq cm for the bismuth and 161 g/sq cm for the lead. The borated water was contained in a 36-in.-long aluminum tank placed adjacent to the source. The detector used primarily was a 1-in. anthracene scintillation crystal and a photomultiplier tube.

The gamma-dose measurements taken in the plain water behind the borated-water tank in which the lead or bismuth slabs were placed at various distances (d) from the source are shown in Figs. 10.5 and 10.6. It can be noted that the dose becomes less sensitive to slab position as d increases. In both Figs. 10.5 and 10.6, curves showing the gamma dose in plain water in the Lid Tank and in plain water behind the borated-water tank have been added for comparison. The slopes of these two curves differ because the 2.2-Mev hydrogen-capture gammas produced in the plain water are attenuated more rapidly than the harder-source gammas predominant in the water behind the borated-water tank. In Fig. 10.5 the effects of lead placed 3.2 and 8.4 cm from the source in plain water are also shown.

A comparison of the dose measurements behind lead and bismuth as a function of the position of the metal, with the detector placed 120 cm from the source, is shown in Fig. 10.7. Measurements at any other detector position would be similar. The difference in the two curves for d = 47.6 cm is

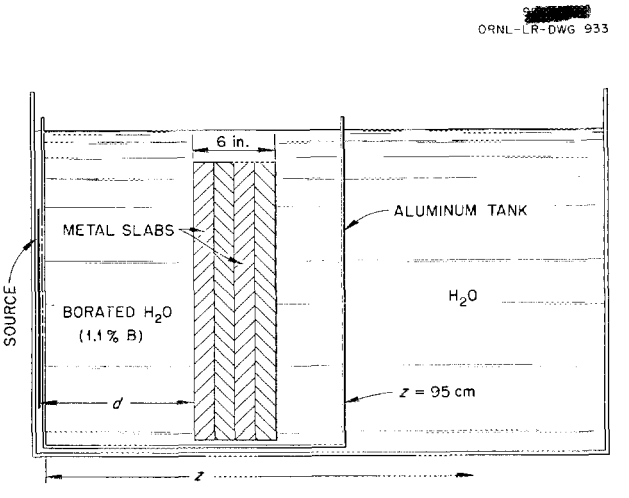

Fig. 10.4. Arrangement for Measuring Secondary Gamma-Ray Production in Materials Considered for Use as Gamma-Ray Shields.

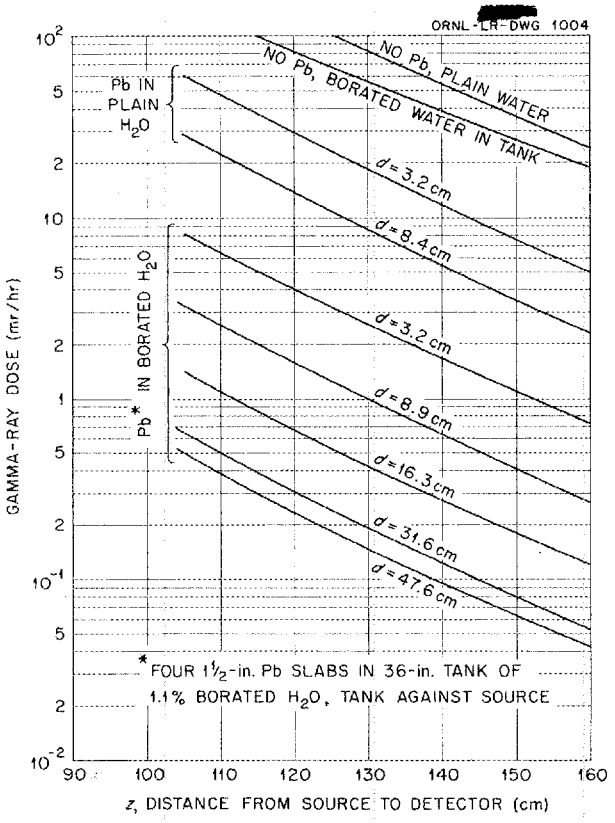

Fig. 10.5. Effect of Lead on Gamma Dose as a Function of Distance in Water from Fission Source.

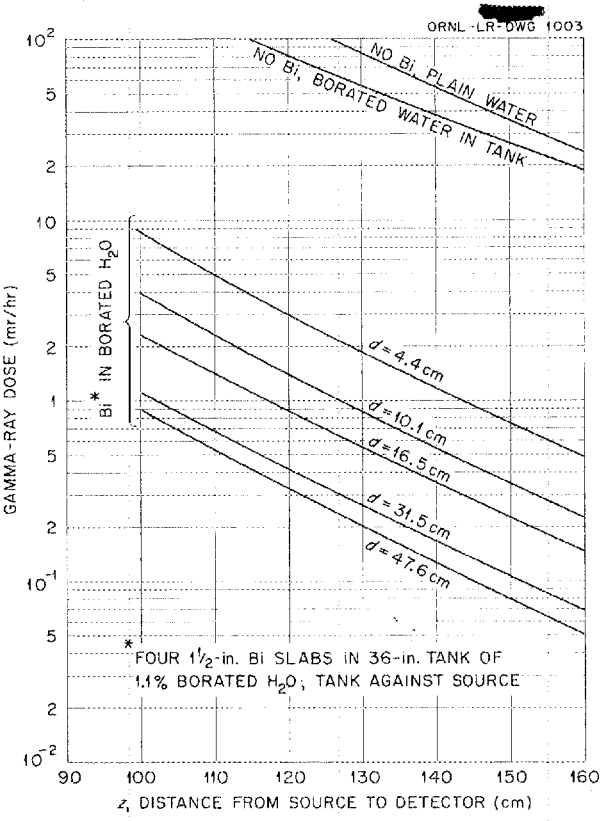

Fig. 10.6. Effect of Bismuth on Gamma Dose as a Function of Distance in Water from Fission Source.

presumably due to the difference in the densities of the two metals. The fact that the curves become flat for $d > 47$ cm indicates that the slabs placed at greater distances from the source were in such a small neutron flux that the secondary gamma production had become almost negligible. The gamma-ray dose behind the slabs at $d = 47.6$ cm is therefore considered to be caused by source gamma rays, including those originating in the water near the source because of hydrogen capture of thermal neutrons. The source dose can be subtracted from the dose behind the slabs at other positions to determine the secondary gamma-ray dose at a given distance from the source. The resulting secondary doses for lead and bismuth are given in Figs. 10.8 and 10.9, respectively, as a function of distance from the front face of the slabs, since it was considered that the origin of these gamma rays was associated with the position of the slabs.

A comparison of the doses from secondary gamma-ray production in lead and in bismuth is presented in Fig. 10.10, in which the dose at 100 cm from the front face of the metal is plotted as a function of the metal position. The experimental accuracy does not justify concluding that the slopes are different. Normalized thermal-neutron and fast-neutron curves (measurements made in plain water) have been included in Fig. 10.10 to show that the secondary-gamma dose curve has a slope characteristic of neutron curves.

From this experiment little difference between lead and bismuth secondary gamma-ray production can be seen. The data are to be extended in the near future with the hope that it will be possible to obtain a more complete understanding of the phenomena.

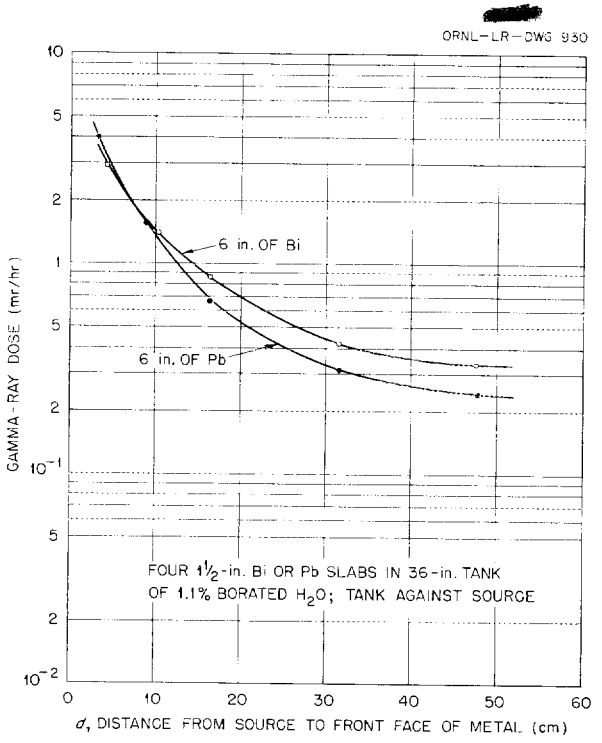

Fig. 10.7. Gamma-Ray Dose 120 cm from Source as a Function of Position of Metal.

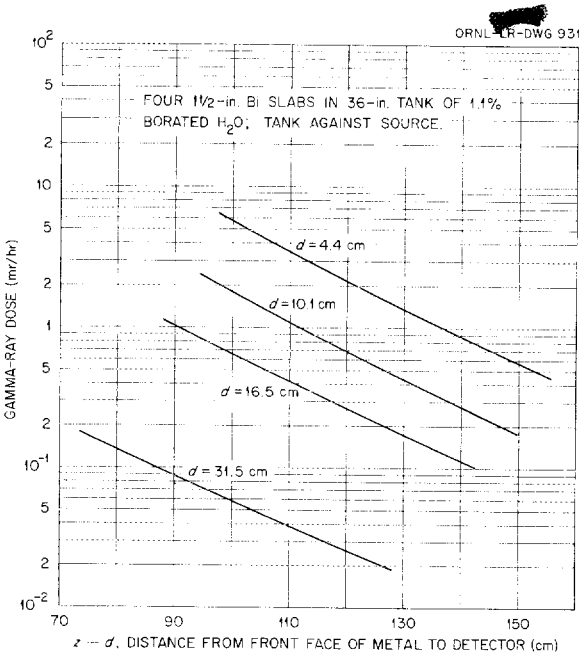

Fig. 10.9. Dose from Secondary Gamma-Rays (Source Gamma-Rays Substracted) as a Function of Distance from Bismuth Slabs.

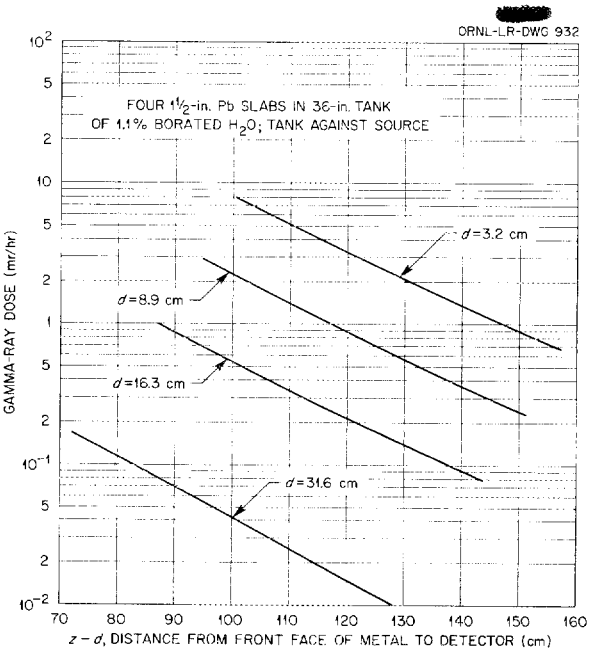

Fig. 10.8. Dose from Secondary Gamma-Rays (Source Gamma-Rays Substracted) as a Function of Distance from Lead Slabs.

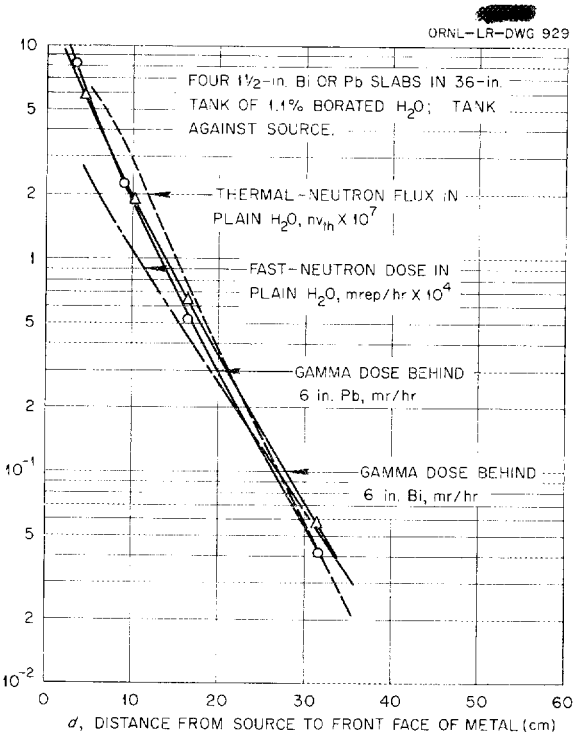

Fig. 10.10. Dose from Secondary Gamma-Rays (Source Gamma-Rays Substracted) 100 cm from Front Face of Metal as a Function of Position of Metal.

11. BULK SHIELDING FACILITY

R. G. Cochran F. C. Maienschein
G. M. Estabrook H. E. Hunderford
J. D. Flynn E. B. Johnson
M. P. Haydon T. A. Love
K. M. Henry R. W. Peelle
Physics Division

The Bulk Shielding Facility (BSF) reactor has been used for determining the power and power distribution of loadings similar to those used in the new Tower Shielding Facility (TSF) reactor. The search for a better fast-neutron spectrometer continues, but no substantial progress has been made. Calculations of gamma-ray dose in a standard divided-shield design have been extended to include crew-shield penetration.

GAMMA-RAY AIR-SCATTERING CALCULATIONS

F. C. Maienschein
Physics Division

Calculations of the dose received from air-scattered gamma rays at the outside edge of the crew compartment of an aircraft divided shield were reported previously.[1] These calculations have now been extended to determine the dose inside the crew compartment. The NDA method[2] was used for calculations of the gamma-ray penetration through the crew shield, and in this case the ANP-53 crew shield[3] was replaced by a simple cylinder of about the same dimensions.

A further calculation was made of the penetration of the direct (unscattered) gamma radiation reaching the crew position through the rear of the crew shield. The buildup factors used were those reported by Fano.[4]

Results of the air-scattering calculation indicate that although the skew-beam flux at the outside of the crew shield is extremely small compared with the radial-beam flux, the dose inside the crew compartment from the skew-beam flux is comparable to the total radial-beam dose. This result was expected, since the skew-beam gamma rays, having scattered through smaller angles on the average than the radial-beam gamma rays, are of higher energy and thus penetrate the crew shield more readily.

The total dose inside the crew compartment from air-scattered gamma rays, as calculated by this method, is somewhat lower than that calculated by the ANP-53 method[3] (Table 11.1); however, the agreement is good if it is considered that for the ANP-53 calculations it was assumed that all the gamma rays were of 3-Mev energy and that all were radially emitted from the reactor shield. The calculations would be in poorer agreement if the correction (unknown) for difference in leakage ratios between the two reactors were applied.

For the direct beam, the large increase shown by this calculation in comparison with the value obtained by the ANP-53 calculation is caused primarily by the gamma radiation that escapes around the edges of the shadow shield. The gamma-ray spectral measurements at the BSF show that a large number of low-energy (<2-Mev) gamma rays emerge from the reactor shield in such a direction that they may strike the crew shield without scattering. Unfortunately, the spectrometer background at such positions was so large that little value can be placed on the absolute magnitude of the dose. In general, for all results from these calculations, the shapes of the curves obtained are considerably more reliable than the absolute magnitudes.

The contributions to the total scattered dose of various regions outside the reactor and crew shields are shown in Figs. 11.1 and 11.2. The effect of the shadow shield is shown in Fig. 11.2, which is shaded proportionally to the dose contribution from each region. Furthermore it is shown in that figure

---

[1] J. L. Meem *et al.*, *ANP Quar. Prog. Rep. June 10, 1953*, ORNL-1556, p 109; F. Bly and F. C. Maienschein, *A Calculation of the Gamma Radiation Reaching the ANP-53 Crew Shield*, ORNL CF-53-5-117 (May 23, 1953).

[2] H. Goldstein, *Reactor Handbook*, Vol. 1, p 831, Technical Information Service, U. S. Atomic Energy Commission, 1953.

[3] *Report of the Shielding Board for the Aircraft Nuclear Propulsion Program*, ANP-53 (Oct. 16, 1950).

[4] U. Fano, *Nucleonics* 11, 55 (1953).

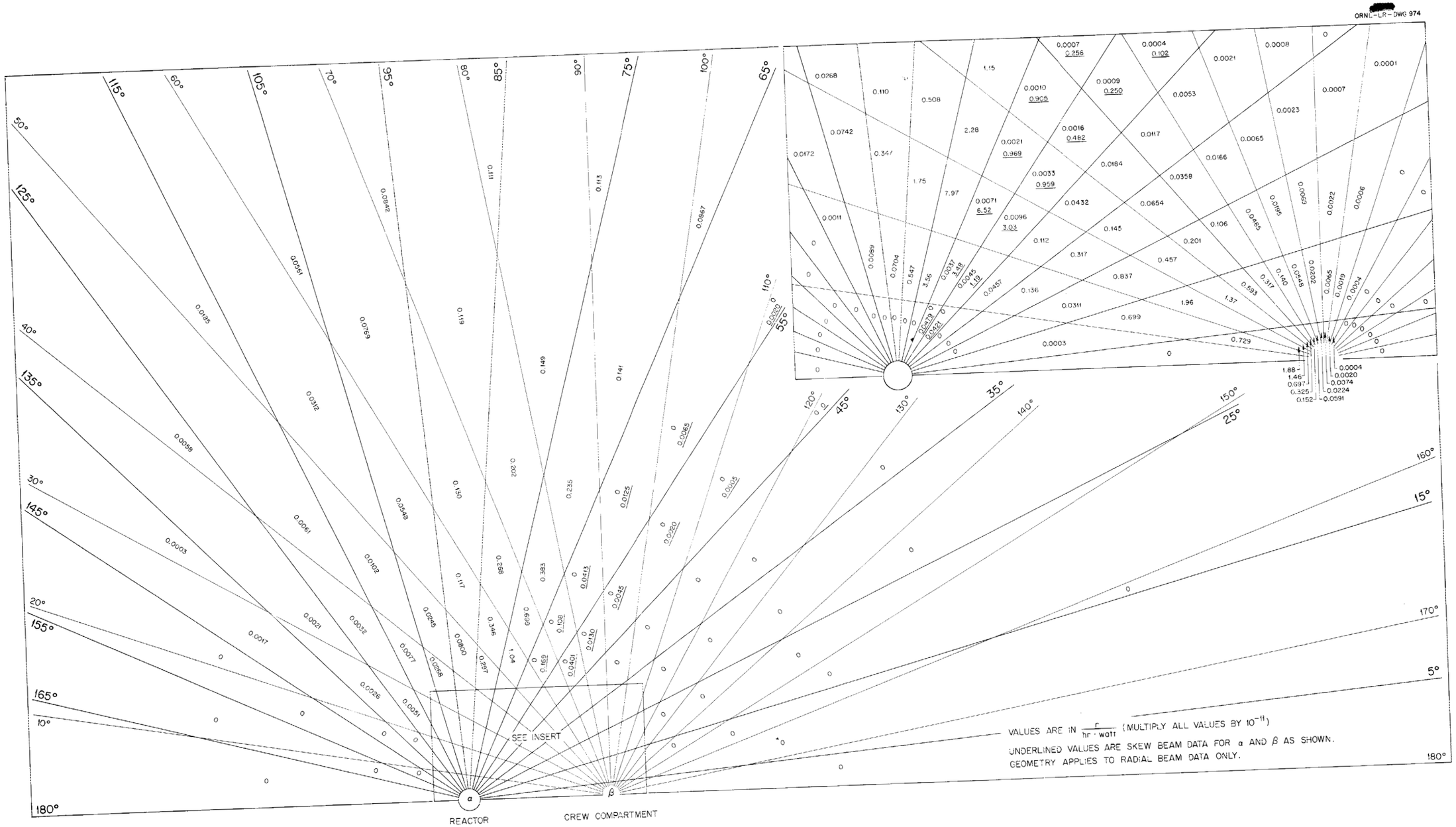

Fig. 11.1. Gamma-Ray Dose Inside Crew Shield Resulting from Air Scattering from Individual Cells – Radial and Skew Emission.

TABLE 11.1. GAMMA-RAY FLUX AND DOSE AT THE CREW COMPARTMENT

METHOD	FLUX OUTSIDE CREW COMPARTMENT, Φ/P (photons/sec/watt)	DOSE INSIDE CREW COMPARTMENT, D (r/hr/watt)
Radial scattered	4.5	0.36×10^{-9}
Skew scattered	0.016	0.19×10^{-9}
Direct	16.0	130×10^{-9}
ANP-53 scattered*		1.2×10^{-9}
ANP-53 direct*		1.2×10^{-9}
Skyshine**		1.14×10^{-9}

*No correction made for reactor leakage.

**H. E. Hungerford, *The Skyshine Experiments at the Bulk Shielding Facility*, ORNL-1611 (to be issued).

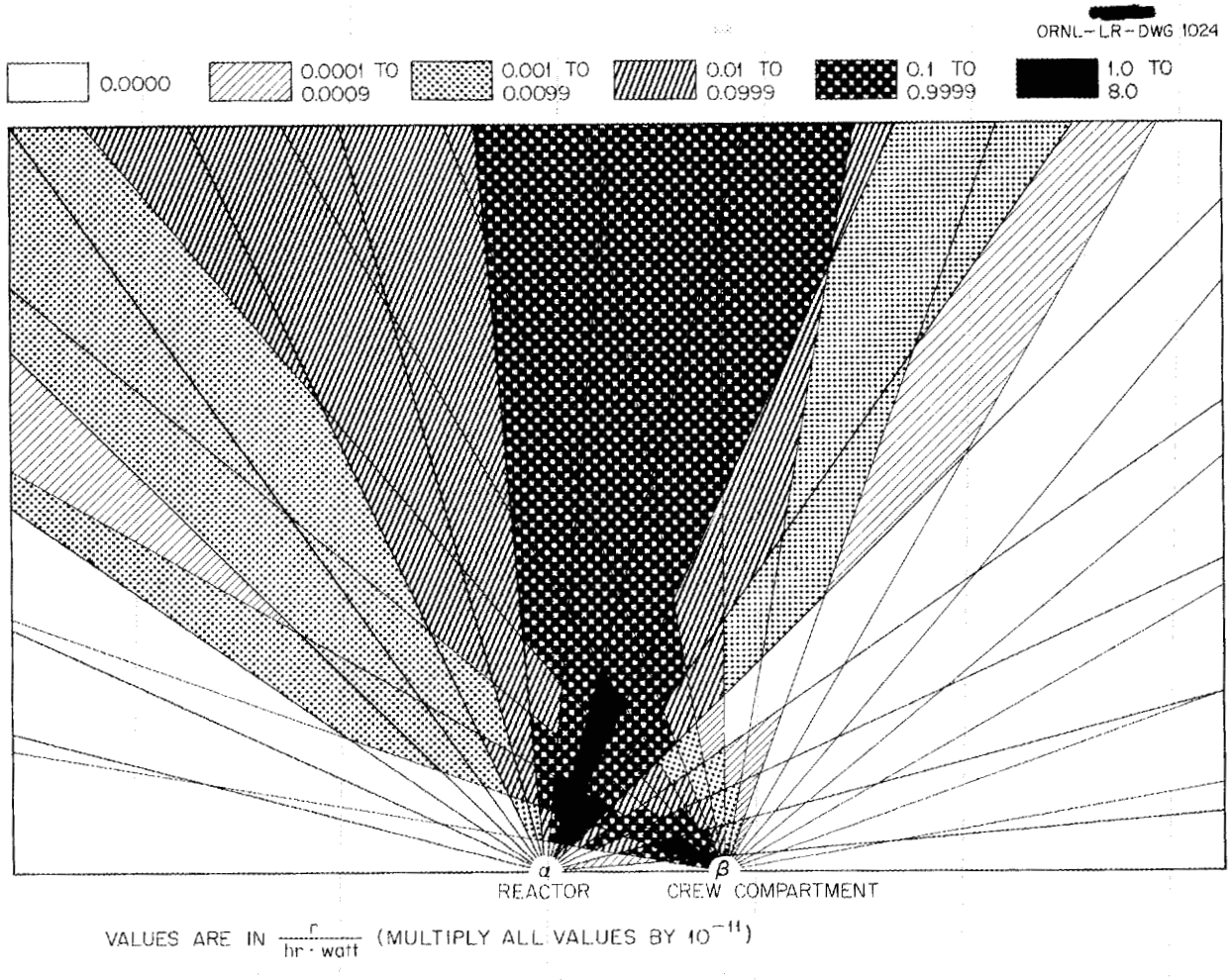

Fig. 11.2. Gamma-Ray Dose Inside Crew Shield from Air Scattering.

that air-scattering from regions far from the aircraft makes an important contribution to the dose in the crew compartment. In all cases, only the penetration through the side wall of the crew shield has been given, since the front- and rear-wall contributions were negligible. Complete calculations were carried out for the front wall for both radial and skew emission in order to prove that these contributions were actually small.

The dependence of the scattered dose (for all angles) upon the prescatter energy is shown in Fig. 11.3, and the dependence on the postscatter energy in Fig. 11.4. It is interesting to note that the average energy for the skew-emission dose is higher than that for the radial-emission dose.

The scattered dose is presented as a function of the source angle in Fig. 11.5 and as a function of the receiver angle in Fig. 11.6. The distribution around the reactor shield (Fig. 11.5) clearly shows the peak in the forward direction which is due to the relatively favorable geometry for radiation starting forward. After a drop of a factor of about 300 out to 55 deg, the dose contribution rises rapidly at the edge of the shadow shield and again falls off because of geometry. It thus appears obvious that the shadow shield should extend to larger angles. It should, of course, be thinner with increasing values of α. It also appears that the ANP-53 crew shield was considerably overshielded in the rear. This was recognized at the time it was designed,

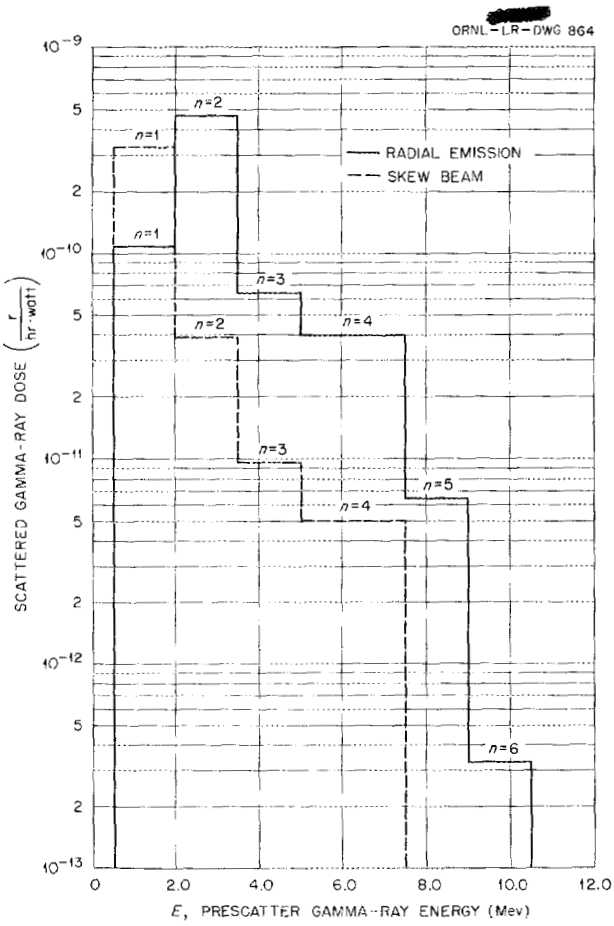

Fig. 11.3. Scattered Gamma-Ray Dose as a Function of Prescatter Energy.

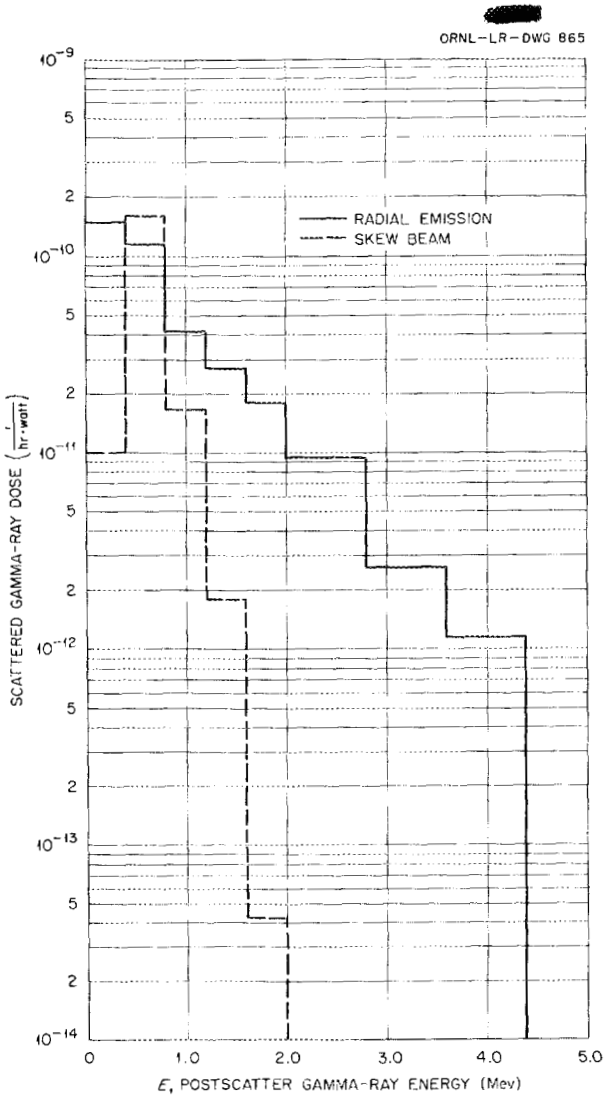

Fig. 11.4. Scattered Gamma-Ray Dose as a Function of Postscatter Energy.

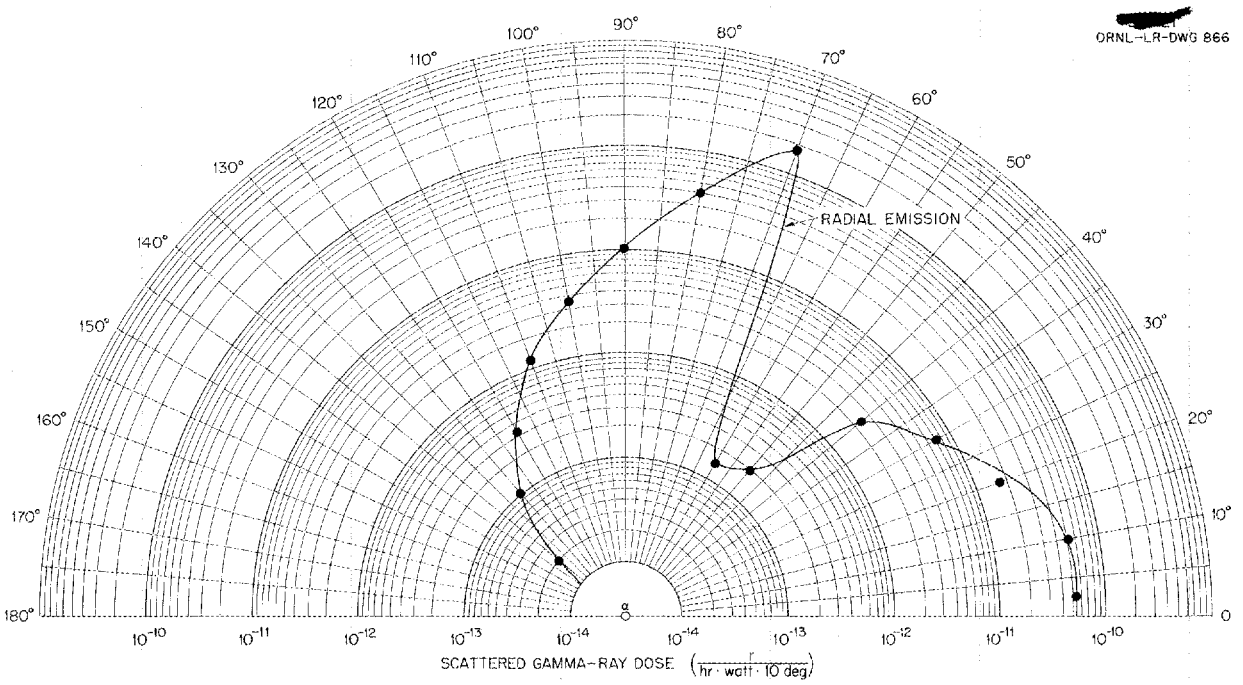

Fig. 11.5. Scattered Gamma-Ray Dose as a Function of Source Angle.

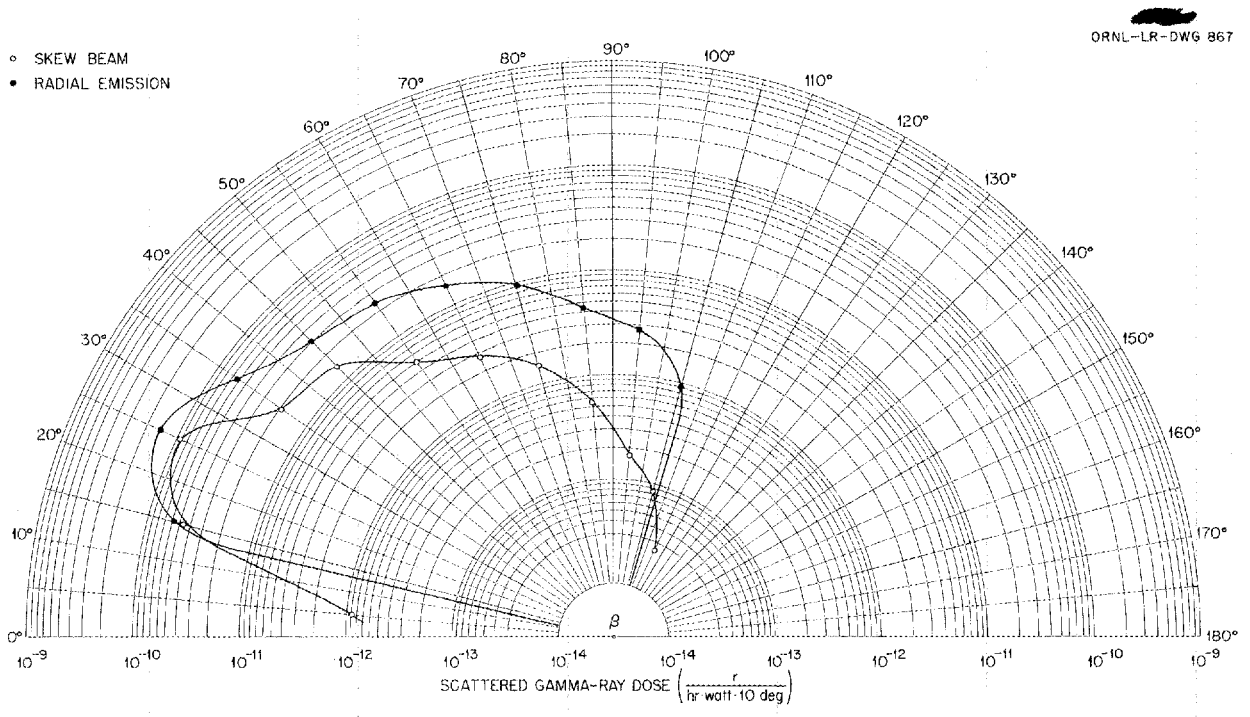

Fig. 11.6. Scattered Gamma-Ray Dose as a Function of Receiver Angle.

but the excess shielding was supposed to compensate somewhat for the presence of ducts in the rear hemisphere of the reactor shield.

The distribution of the dose inside the crew shield as a function of the angle around the crew-compartment midpoint (Fig. 11.6) shows a larger contribution from scattered gamma rays from the rear of the crew-shield side wall, as would be expected because the crew compartment was taken to be a long cylinder with walls of uniform thickness. The variations observed in this case are not nearly so large as those for the source angle.

The direct dose as a function of the energy of the gamma rays emerging from the reactor shield is shown in Fig. 11.7. The dependence of the dose upon the energy is determined by the large angle at which the major contribution to the direct dose occurs, as shown in Fig. 11.8 in which the direct dose as a function of the source angle α is presented. Figure 11.8 again shows the extreme importance of the radiation escaping around the edges of the shadow shield. The detailed calculations of the gamma radiation reaching the crew compartment will be published in a separate report.[5]

THERMAL-NEUTRON-FLUX PERTURBATION BY GOLD FOILS IN WATER

E. B. Johnson
Physics Division

It is well known that when a detector that is not infinitely thin is introduced into a neutron flux, the flux is perturbed. The magnitude of the perturbation depends upon the absorption cross section of the detector and its physical dimensions and upon the properties of the medium into which it is introduced. It is customary at the BSF to use the flux of the ORNL Standard Graphite Pile[6] as the reference flux for the calibration of foils and counters. However, when a foil is used for thermal-neutron-flux measurements in water, the flux perturbation caused by the presence of the foil is different since the slowing-down properties of water differ from those of graphite. Klema and Ritchie[7] arrived at a semiempirical correction for this effect for the 25-sq cm 5-mil-thick indium foils normally used for flux measurements in water. The presence of these foils results in a 22% depression of the flux from its unperturbed value. Frequently it would have been desirable to use gold foils for flux determinations in water, but no value for the flux depression has been available. Therefore an experiment has been completed at the BSF that was designed for measuring this effect.

Thermal-neutron-flux measurements were made with both the indium and the gold (1-sq cm, 5-mil-thick) foils at five positions along the north-south center line of the reactor. The perturbation factor of 1.22 was applied, as usual, to the indium-foil data, but no such correction was made on the gold-foil data. The results are shown in Fig. 11.9. If it is assumed that a probable error of $\pm 2\%$ is associated with each measurement, there is no discernible difference between the thermal-neutron-flux measurements made with indium foils using the perturbation correction and those with gold foils using no correction. While it is recognized that the presence of any absorbing material must result in a local depression of the flux, it seems that this effect is within the probable errors of measurement for small gold foils in a water medium. It should be pointed out that such would not necessarily be the case if gold foils of larger dimensions were used. These results substantiate those obtained by P. M. Uthe[8] from a similar experiment performed in the water tank at the thermal column of the ORNL Graphite Reactor.

REACTOR POWER CALIBRATION TECHNIQUES[9]

E. B. Johnson G. M. Estabrook
R. G. Cochran
Physics Division

Correlation of shielding data from the TSF with those from the BSF requires that the power determinations for the two reactors be made by comparable methods. Power determinations at the BSF have been based on thermal-neutron-flux measurements obtained by inserting foils between the

[5] F. C. Maienschein, F. Bly, and T. A. Love, *Sources and Attenuation of Gamma Radiation from a Divided Aircraft Shield*, ORNL-1714 (to be published).

[6] E. D. Klema, R. H. Ritchie, and G. McCammon, *Recalibration of the X-10 Standard Graphite Pile*, ORNL-1398 (Nov. 11, 1952).

[7] E. D. Klema and R. H. Ritchie, *Preliminary Results on the Determination of Thermal Neutron Flux in Water*, ORNL CF-51-4-103 (Apr. 24, 1951).

[8] P. M. Uthe, private communication.

[9] E. B. Johnson *et al.*, *Power Calibration Techniques for BSR*, ORNL-1723 (to be published).

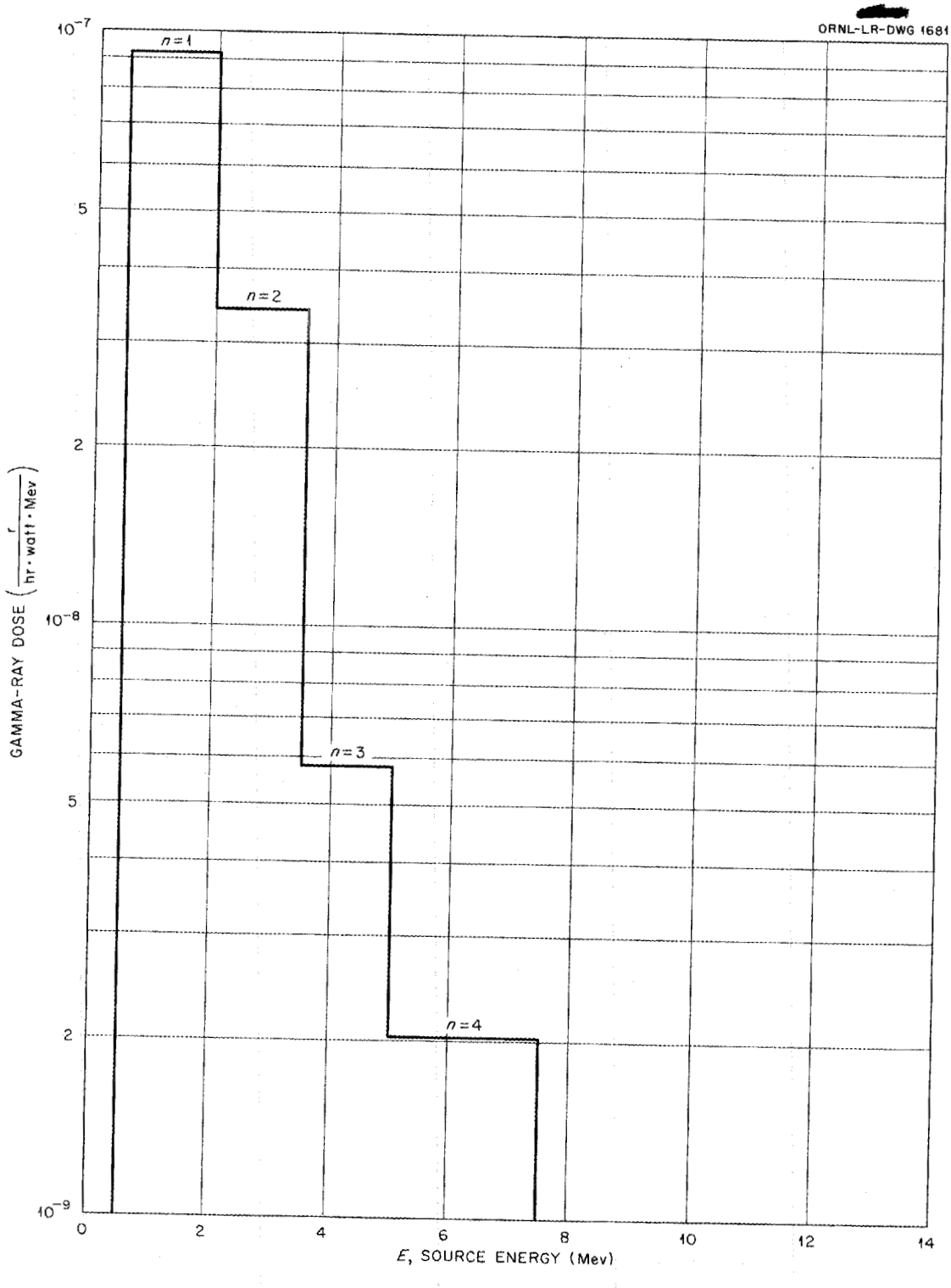

Fig. 11.7. Direct Gamma-Ray Dose as a Function of Source Energy.

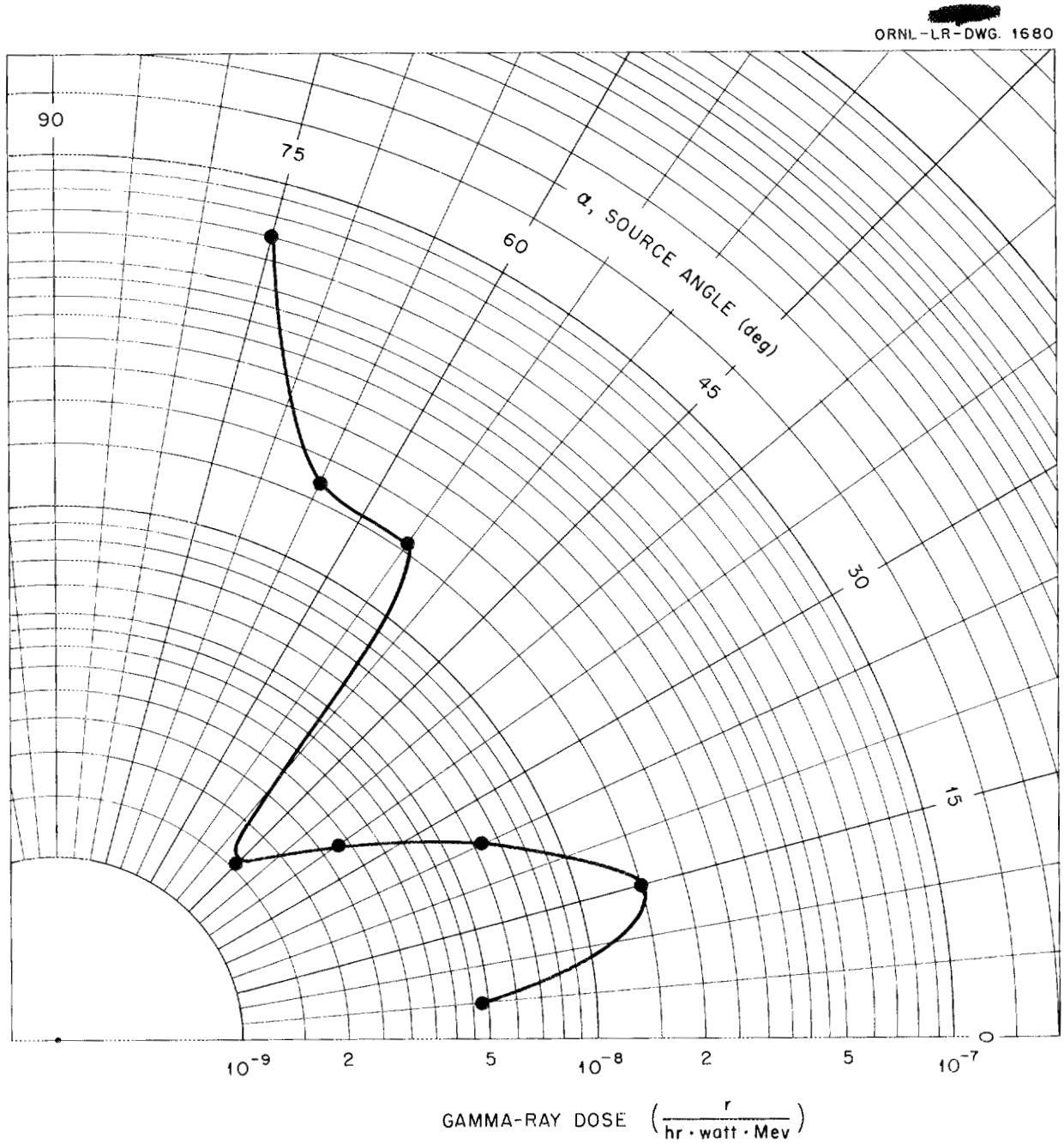

Fig. 11.8. Direct Gamma-Ray Dose as a Function of Source Angle.

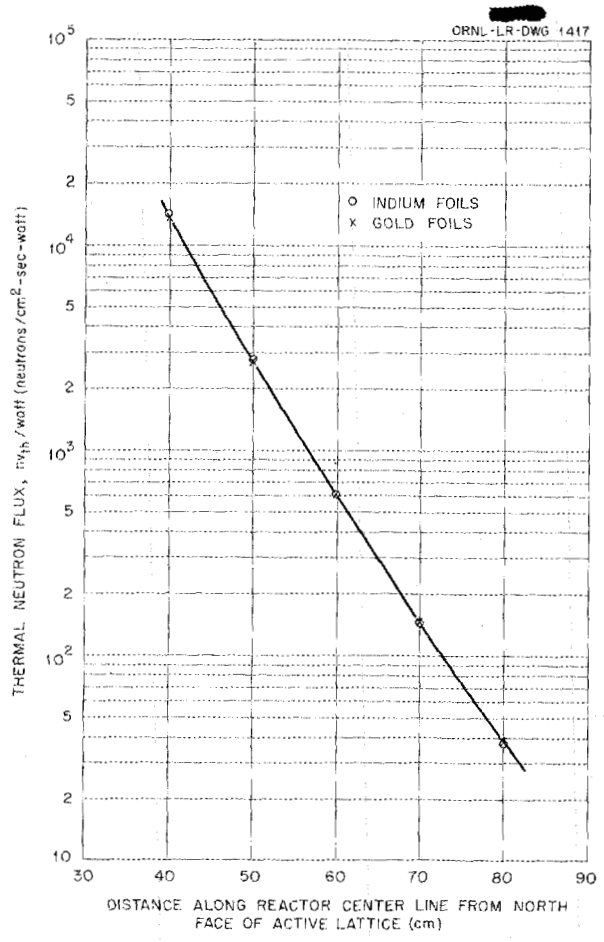

Fig. 11.9. Comparison of Indium- and Gold-Foil Measurements in Water Surrounding BSF Reactor.

plates of the fuel elements in the reactor lattice.[10] However, the Tower Shielding fuel elements have lead-shielded tops which make foil insertion impossible, and, in addition, the reactor control chambers are located directly over the lattice.

It has been planned to make the flux measurements in the TSF reactor by inserting cobalt wires down the center of the fuel elements. However, this technique will yield only a total flux rather than the thermal flux needed for power-calibration calculations. Therefore, a method for obtaining reactor power directly from total-flux measurements was needed. In the method used at the BSF for power calibration, the total and epicadmium activities of detectors placed throughout the reactor lattice are obtained. The thermal-neutron flux obtained by this method is used to calculate the reactor power, since the fission rate and therefore the power level of an enriched-fuel reactor depend primarily on the thermal-neutron flux. The relation between the thermal-neutron flux as measured with foils and the power produced as indicated by strategically placed thermocouples has been very carefully determined.[11] It was found that the power of the reactor can be expressed as

$$(1) \qquad P = 4.264 \times 10^{-11} G \bar{\phi}_{th} ,$$

where P is the power in watts and G is the mass of U^{235} in the volume over which $\bar{\phi}_{th}$ is the average thermal flux. The constant contains the fission cross section, energy release per fission, fast-fission factor, and conversion factors.

Various methods have been investigated at the BSF for simplifying and adapting the currently used power-calibration procedure for use with the TSF reactor. The reactor power was calculated for each of three loadings by using both total flux and thermal flux as measured with small cobalt foils. Loading 20B (Fig. 11.10) had a slab reflector of beryllium oxide on all four sides, whereas loadings 22A (Fig. 11.11) and 24B (Fig. 11.12) were completely water reflected. The resulting data indicate that there is a constant ratio (within 1%) between the power calculated from thermal flux and that calculated from total flux. This indicates that if the constant in Eq. 1 is changed to 3.86×10^{-11}, the average flux in the equation can be considered to be the total flux as measured with cobalt detectors. Flux measurements made by using cobalt wires have been obtained for the BSF reactor but the calculations have not yet been completed.

[10] J. L. Meem and E. B. Johnson, *Determination of the Power of the Shield Testing Reactor – I. Neutron Flux Measurements in the Water-Reflected Reactor*, ORNL-1027 (Aug. 13, 1951); E. B. Johnson and J. L. Meem, *Determination of the Power of the Bulk Shielding Reactor – II. Neutron Flux Measurements in Several Beryllium Oxide-Reflected Critical Assemblies*, ORNL-1438 (May 7, 1953).

[11] J. L. Meem, L. B. Holland, and G. McCammon, *Determination of the Power of the Bulk Shielding Reactor – III. Measurement of the Energy Released per Fission*, ORNL-1537 (Feb. 15, 1954).

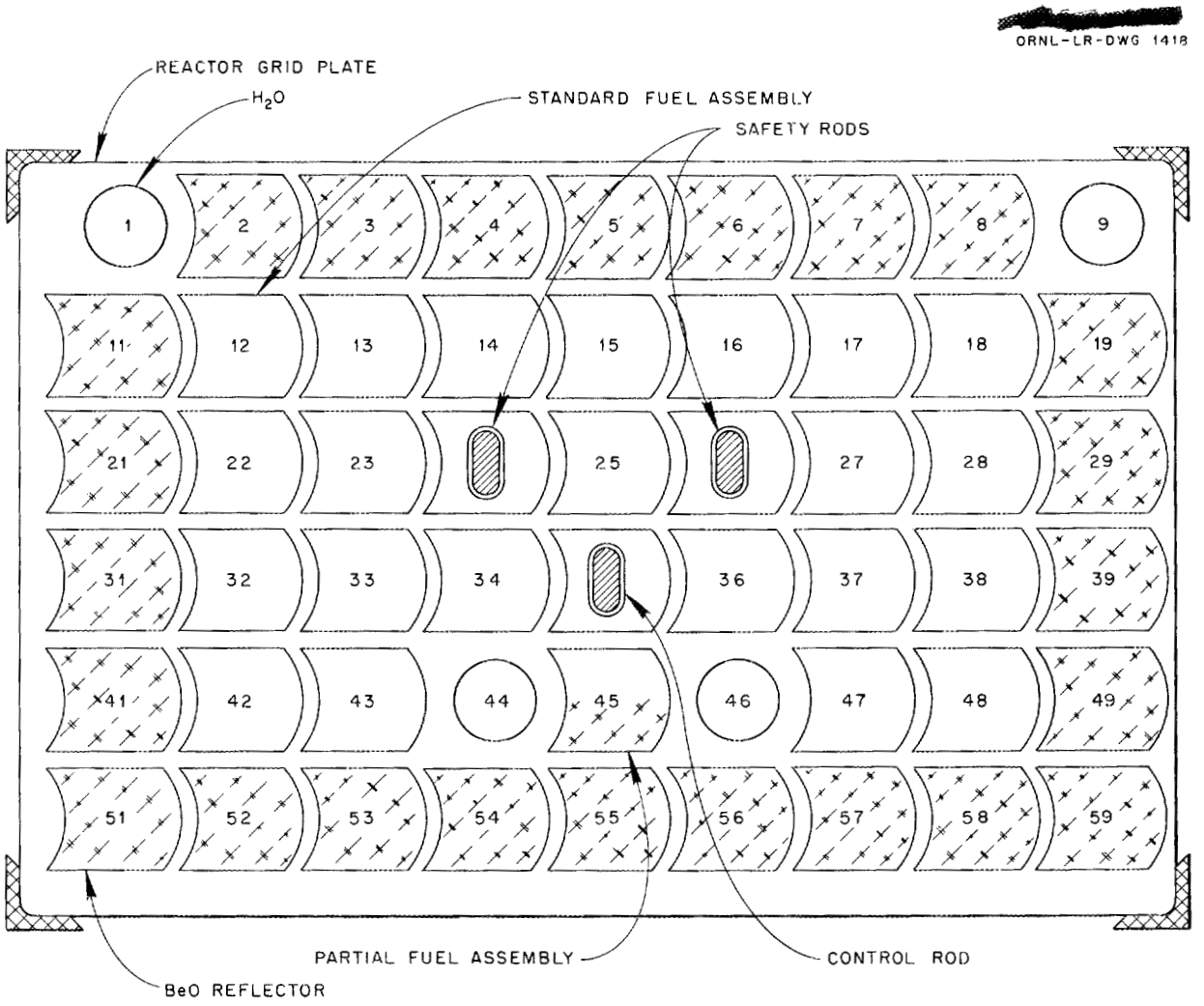

Fig. 11.10. BSF Reactor Loading 20B.

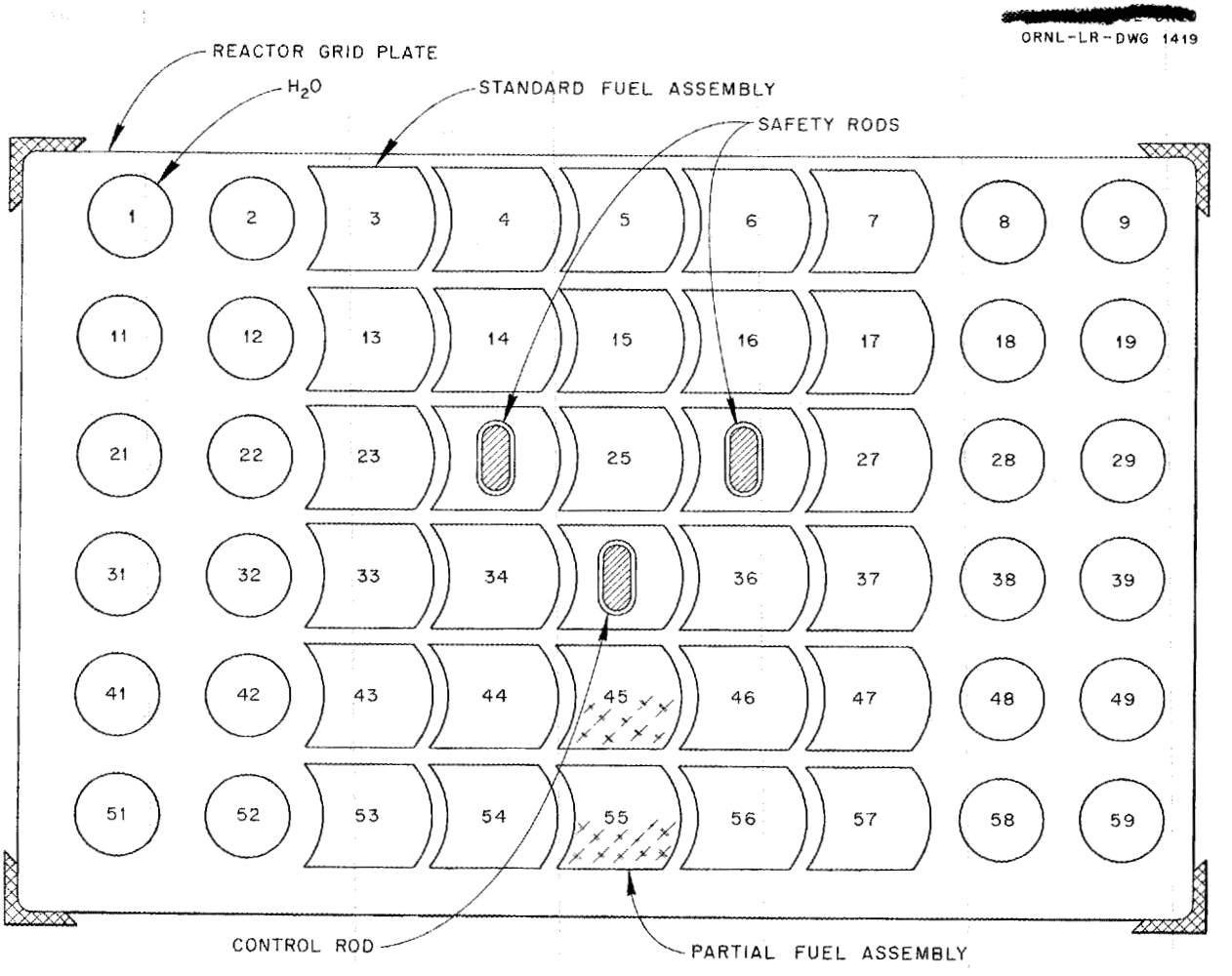

Fig. 11.11. BSF Reactor Loading 22A.

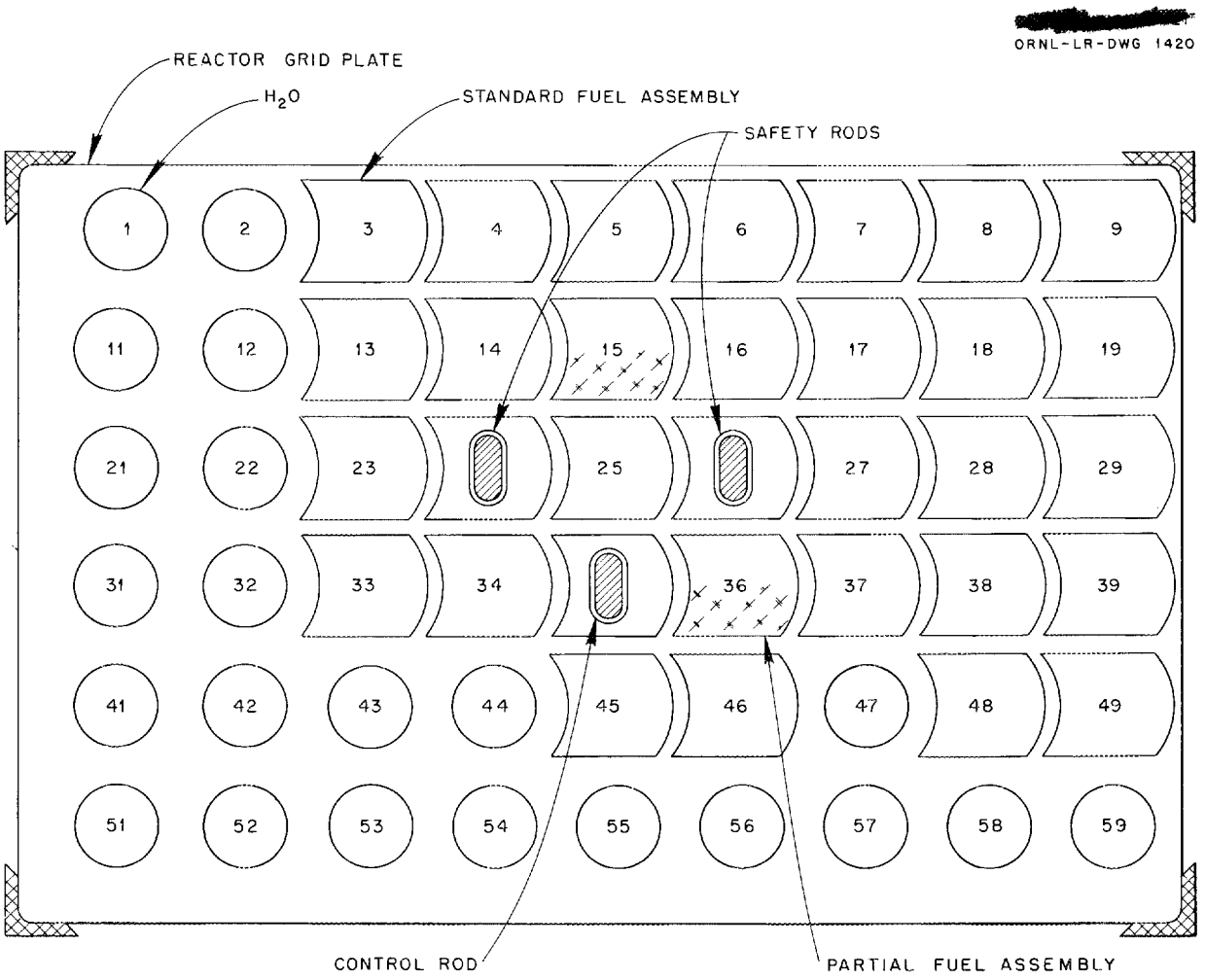

Fig. 11.12. BSF Reactor Loading 24B.

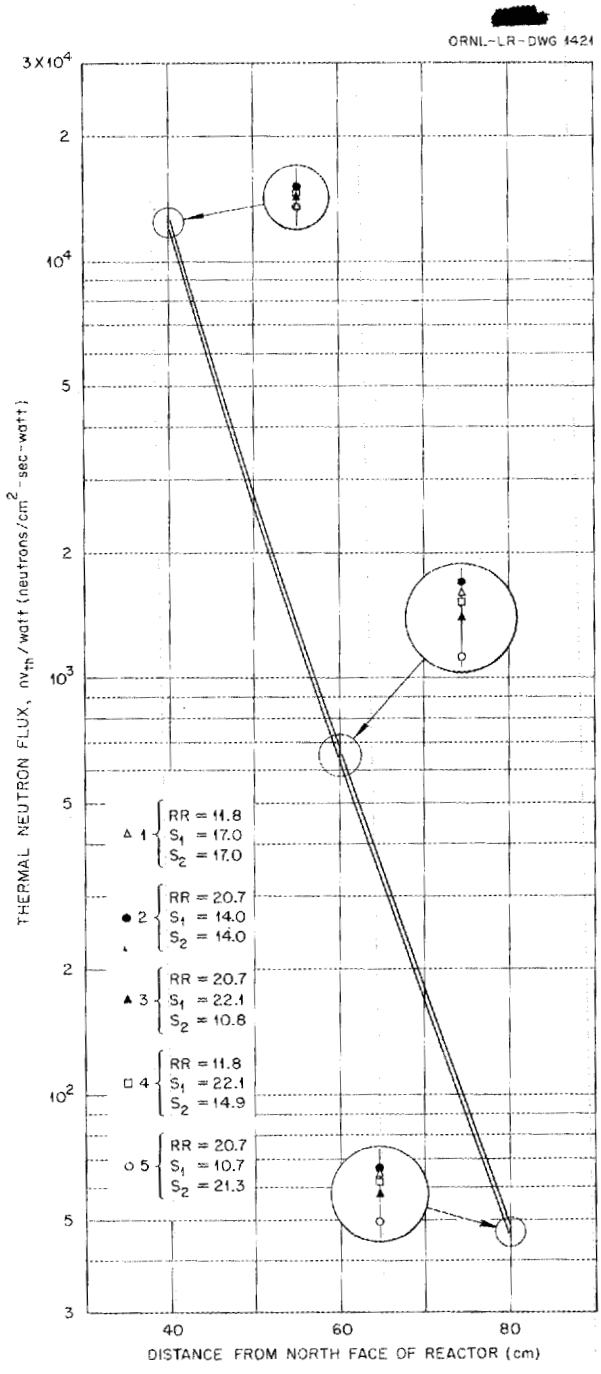

Fig. 11.13. Comparison of Effects of Various Control-Rod Settings on Leakage Flux of BSF Reactor.

LEAKAGE-FLUX CHANGES DUE TO CONTROL-ROD SETTINGS

J. D. Flynn R. G. Cochran
Physics Division

An experiment was performed at the BSF to determine the effect of the leakage flux of changes in setting of the regulating rod and the safety rods in order to obtain better correlation between successive shielding measurements. At positions close to the reactor face, some effect would be expected; however, at large distances from the reactor, there should be no effect. The data (Fig. 11.13) indicate that there was no appreciable effect on the thermal flux at distances of 40 to 80 cm.

In another experiment, the effect of changing the quantity of U^{235} in a reactor loading was investigated. A 110-g element was replaced with a 140-g element on the side of the reactor opposite to the side at which the measurement was made, and it was found that the leakage flux was insensitive to the quantity of uranium.

12. TOWER SHIELDING FACILITY

C. E. Clifford
T. V. Blosser
D. L. Gilliland[1]
L. B. Holland
J. L. Hull
F. N. Watson

Physics Division

Construction at the Tower Shielding Facility (TSF) was completed May 1 (Fig. 12.1), and the facility is now operating on a schedule of four days per week. Critical experiments with the reactor were started early in March, and installation of the detector tank and experimental instrumentation was completely by the end of March. Since that time, experimental operation of the facility has been continued intermittently to permit final adjustments and modifications of all equipment.

EXPERIMENTAL PROGRAM

Preliminary measurements have been taken for the differential shielding experiments in a small water tank (5 × 5 × 5 ft) which is known as the detector tank. For these measurements the reactor was in the 47-ton hemispherical water tank. The relaxation length for the air-scattered neutron radiation entering the sides and front of the detector tank is 5.3 cm, which is to be compared to the 4.5-cm relaxation length obtained in the BSF Skyshine experiments[2] and the 5-cm relaxation length used in the 1953 Summer Shielding Session.[3]

Neutron- and gamma-dose measurements in the reactor tank have been made with the 3-in. fission counter, the 900-cc ion chamber, and the three-chamber BF_3 counter. These measurements are in qualitative agreement with those taken at the BSF with a similar reactor loading.[4]

The first of a series of measurements for determining the background from ground-scattered radiation has been completed with the reactor and detector tanks 4 ft above the ground. The separation distances of the tanks were 35, 65, and 100 ft. Since the power of the reactor is not absolutely established, the data from this experiment will be reported first in terms of radiation intensity relative to a nominal power, which is expected to be within 30% of the actual power.

OPERATION OF THE REACTOR

The reactor was loaded to criticality on March 12. This loading consisted of 26 fuel elements, the minimum number required for criticality. Since that time, another loading (30 fuel elements in a 5 by 6 array) has been checked by a critical experiment and is now being used for the preliminary measurements. Both these loadings were run earlier in the BSF reactor with TSF reactor fuel elements, and the power distribution of the 5 by 6 element array was determined with BSF reactor elements. The two TSF reactor loadings are comparable in shim-rod and regulating-rod positions to those used at the BSF.

During the experiments the reactor was run at power levels of 1 to 10 watts at the 200-ft elevation and at approximately 4 kw at just above the pool level. The instruments and controls performed satisfactorily under both conditions.

Use has been made of the remote visual-indicator system to observe operation and to position the reactor and the crew compartment. The ease with which it is possible to position the large loads by remote control with this system has exceeded expectations.

A system of slack-line limit switches has been installed on the large hoists to prevent damage to the hoist gear mechanism such as that experienced during the run-in period. The operation of the switches is satisfactory, but, to add assurance, the cables will be kept taut by additional counterweights that will be added to the floating sheave blocks.

---

[1] On loan from General Electric Company.

[2] H. E. Hungerford, *The Skyshine Experiments at the Bulk Shielding Facility*, ORNL-1611 (to be issued).

[3] *Report of the 1953 Summer Shielding Session*, ORNL-1575 (to be issued).

[4] R. G. Cochran, J. L. Meem, T. E. Cole, and E. B. Johnson, *Reactivity Measurements with the Bulk Shielding Reactor*, ORNL-1682 (to be issued).

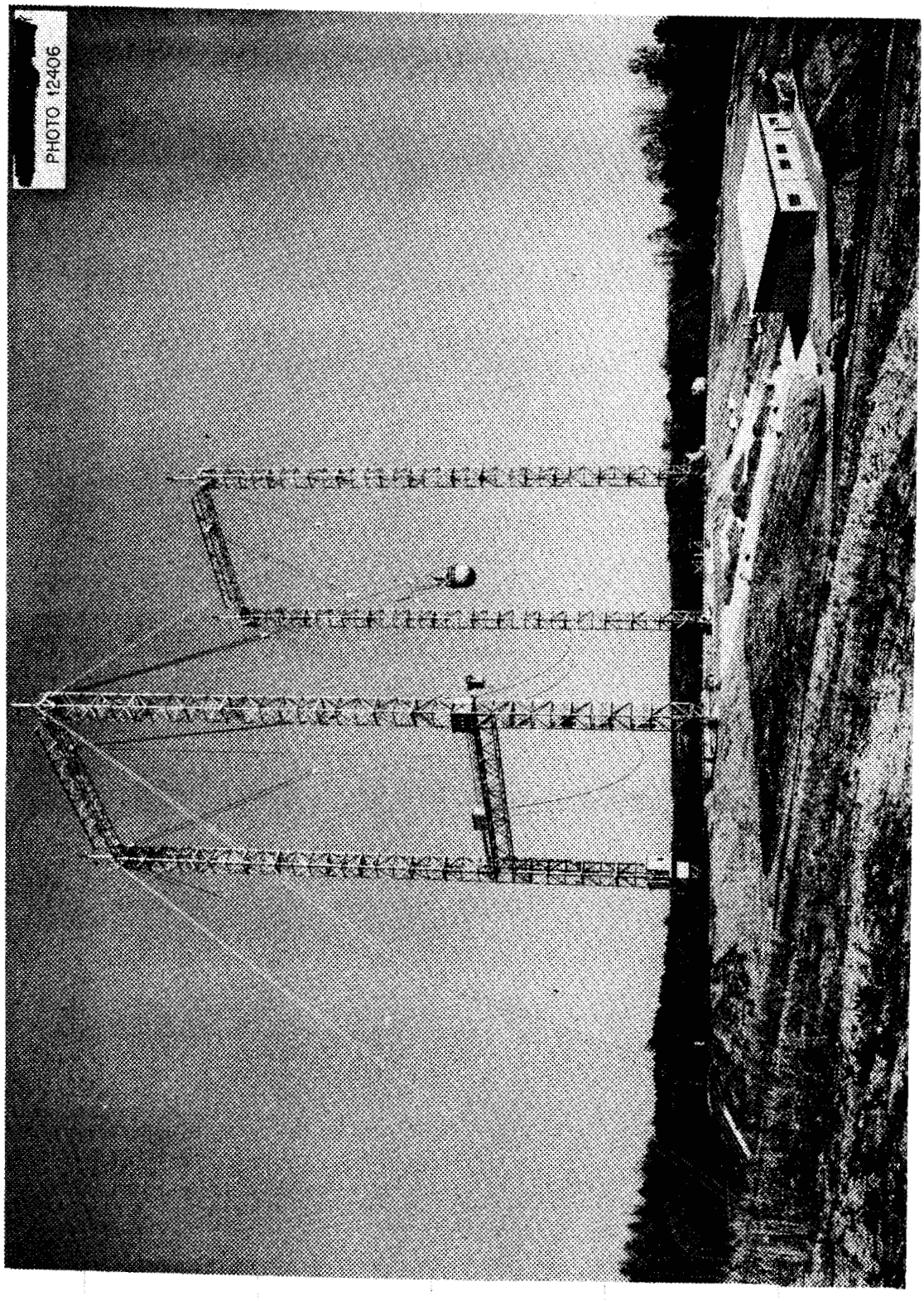

Fig. 12.1. Completed Tower Shielding Facility.

Part IV

APPENDIX

13. LIST OF REPORTS ISSUED DURING THE QUARTER

REPORT NO.	TITLE OF REPORT	AUTHOR(s)	DATE ISSUED
	I. Aircraft Reactor Experiment		
CF-54-3-65	ARE Design Data Supplement	W. B. Cottrell	3-2-54
CF-54-4-218	ARE Instrumentation List	R. G. Affel	4-7-54
CF-54-5-51	Analysis of Critical Experiments	C. B. Mills	5-12-54
	II. Reflector-Moderated Reactor		
CF-54-2-185	Effects of Reactor Design Conditions on Aircraft Gross Weight	H. J. Stumpf B. M. Wilner	5-21-54
CF-54-4-6	The Kinetics of the Circulating-Fuel Reactor	W. K. Ergen	5-5-54
CF-54-4-53	Reflector-Moderated Critical Assembly Experimental Program	D. Scott B. L. Greenstreet	4-8-54
CF-54-4-221	Radiation Damage Elastomers, Lubricants, Fabrics, and Plastics for Use in Nuclear-Powered Aircraft	H. J. Stumpf B. M. Wilner	4-15-54
CF-54-5-1	The Xenon Problem in the ART	J. L. Meem	5-3-54
CF-54-5-196	Temperature Gradient and Thermal Stresses in Heat-Generating Bodies	F. A. Field	5-21-54
	III. Experimental Engineering		
CF-54-3-37	50-Mw Design – Canned Be	C. B. Mills	3-9-54
CF-54-3-194	Cross Sections	C. B. Mills	3-8-54
CF-54-4-195	Discussions and Results of the Dielectric Heating Test	A. L. Southern	4-27-54
ORNL-1688	Sodium Plumbing	W. B. Cottrell L. A. Mann	8-14-53
ORNL-1716	Turbulent Heat Transfer from a Molten Fluoride Salt Mixture to Sodium-Potassium Alloy in a Double-Tube Heat Exchanger	D. F. Salmon	To be issued
	IV. Chemistry		
CF-54-4-47	Data on the BeF_2-NaF System	E. Orban	4-27-54
CF-54-5-40	Effects of Fission Products in Performance of a Reactor Using Fluorides as Solvent for Fuel	R. F. Newton	5-7-54
CF-54-5-47	Measurement of the Stability of Lithium Hydride	E. Orban	5-26-54
CF-54-5-189	Analysis of Salt Mixtures	F. F. Blankenship	5-25-54
CF-54-6-6	Fused Salt Compositions	C. J. Barton	6-2-54
	V. Metallurgy		
CF-54-3-15	Metallographic Examination of Forced Circulation Loop No. 2	G. M. Adamson	3-3-54
CF-54-3-193	High Flow Velocity and High Temperature Gradient Loops	W. D. Manly	3-18-54

REPORT NO.	TITLE OF REPORT	AUTHOR(s)	DATE ISSUED
CF-54-4-162	Status of Columbium, Beryllium, and Lithium	W. D. Manly	4-6-54
CF-54-4-224	Report of Literature Survey of Beryllium	J. W. Woods	4-13-54
CF-54-5-88	Heat Exchanger Fabrication	E. E. Hoffman P. Patriarca	5-17-54
CF-54-5-91	Free Energies of Formation of Oxides and Fluorides	J. M. Cisar	5-5-54
ORNL-1667	Alkali-Metal Nickel Oxides Containing Trivalent Nickel	L. D. Dyer B. S. Borie, Jr. G. P. Smith	2-26-54
	VI. Heat Transfer and Physical Properties		
CF-54-4-205	A Feasibility Study of Flow Visualization Using a Phosphorescent Particle Method	L. D. Palmer G. M. Winn	4-30-54
CF-54-5-159	Effect of Oil Contamination on the Boiling Heat Transfer Characteristics of Heat Exchangers and Solid Fuel-Plate Reactors	M. W. Rosenthal R. L. Miller	5-19-54
CF-54-5-160	Heat Capacities of Composition No. 12, No. 44, and of K_3CrF_6	W. D. Powers G. C. Blalock	5-20-54
ORNL-1701	Forced Convection Heat Transfer Between Parallel Plates and in Annuli with Volume Heat Sources within the Fluids	H. F. Poppendiek L. D. Palmer	5-11-54
ORNL-1702	A Summary of Density Measurements on Molten Fluoride Mixtures and a Correlation Useful for Predicting Densities of Fluoride Mixtures of Known Composition	S. I. Cohen T. N. Jones	5-14-54
	VII. Analytical Studies of Reactor Materials		
CF-54-4-96	Data on Aircraft Fuel Samples	R. Baldock	4-14-54
ORNL-1712	The Optical Properties of Some Inorganic Fluoride and Chloride Compounds	T. N. McVay G. D. White	5-5-54
	VIII. Radiation Damage		
CF-54-5-41	Metallographic Analysis of Pratt and Whitney Capsules 1-4, 1-6, and 1-7	M. J. Feldman A. E. Richt	5-5-54
CF-54-6-4	Release of Xenon from Fluoride Fuels: Proposal for an Experimental Program	M. T. Robinson	6-2-54
	IX. Shielding		
CF-54-5-201	Secondary Gamma Ray Study	D. K. Trubey	5-26-54
CF-54-5-219	Slant Penetration of Neutrons Through Water	G. T. Chapman	5-28-54
ORNL-1682	Reactivity Measurements with the Bulk Shielding Reactor	R. G. Cockran *et al.*	To be issued

REPORT NO.	TITLE OF REPORT	AUTHOR(s)	DATE ISSUED
ORNL-1714	Sources and Attenuation of Gamma Radiation from a Divided Aircraft Shield	F. C. Maienschein F. Bly T. A. Love	To be issued
ORNL-1723	Power Calibration Techniques for BSR	E. B. Johnson *et al.*	To be issued
	X. Miscellaneous		
ORNL-1686	Quantities and Reactions of Solid Surfaces	E. P. Carter	4-7-54
ORNL-1692	Aircraft Nuclear Propulsion Project Quarterly Progress Report for Period Ending March 10, 1954	A. W. Savolainen	4-15-54